



# **Progress in Mathematical Physics**

Volume 48

## *Editors-in-Chief*

Anne Boutet de Monvel, *Université Paris VII Denis Diderot, France*

Gerald Kaiser, *The Virginia Center for Signals and Waves, Austin Texas, USA*

## *Editorial Board*

Sir M. Berry, *University of Bristol, UK*

C. Berenstein, *University of Maryland, College Park, USA*

P. Blanchard, *University of Bielefeld, Germany*

A.S. Fokas, *University of Cambridge, UK*

D. Sternheimer, *Université de Bourgogne, Dijon, France*

C. Tracy, *University of California, Davis, USA*

# **Quantum Decoherence**

**Poincaré Seminar 2005**

Bertrand Duplantier  
Jean-Michel Raimond  
Vincent Rivasseau  
Editors

Birkhäuser Verlag  
Basel • Boston • Berlin

Editors:

Bertrand Duplantier  
Service de Physique Théorique  
Orme des Merisiers  
CEA - Saclay  
91191 Gif-sur-Yvette Cedex  
France  
e-mail: bertrand.duplantier@cea.fr

Vincent Rivasseau  
Laboratoire de Physique Théorique  
Université Paris XI  
91405 Orsay Cedex  
France  
e-mail: Vincent.Rivasseau@th.u-psud.fr

Jean-Michel Raimond  
Laboratoire Kastler Brossel  
Département de Physique  
de l'Ecole Normale Supérieure  
24, rue Lhomond  
75231 Paris Cedex 05  
France  
e-mail: jmr@lkb.ens.fr

2000 Mathematics Subject Classification 81P68, 81Q50, 81Q99, 81T99, 94Bxx

Library of Congress Control Number: 2006934500

Bibliographic information published by Die Deutsche Bibliothek  
Die Deutsche Bibliothek lists this publication in the Deutsche Nationalbibliografie; detailed bibliographic data is available in the Internet at <<http://dnb.ddb.de>>.

ISBN 978-3-7643-7807-3 Birkhäuser Verlag, Basel – Boston – Berlin

This work is subject to copyright. All rights are reserved, whether the whole or part of the material is concerned, specifically the rights of translation, reprinting, re-use of illustrations, broadcasting, reproduction on microfilms or in other ways, and storage in data banks. For any kind of use whatsoever, permission from the copyright owner must be obtained.

© 2007 Birkhäuser Verlag, P.O. Box 133, CH-4010 Basel, Switzerland

Part of Springer Science+Business Media

Printed on acid-free paper produced of chlorine-free pulp. TCF ∞

Printed in Germany

ISBN-10: 3-7643-7807-7

ISBN-13: 978-3-7643-7807-3

e-ISBN-10: 3-7643-7807-5

e-ISBN-13: 978-3-7643-7808-0

9 8 7 6 5 4 3 2 1

[www.birkhauser.ch](http://www.birkhauser.ch)

# Contents

Foreword	ix
Wojciech Hubert ZUREK	
<i>Decoherence and the Transition from Quantum to Classical – Revisited</i>	1
Introduction . . . . .	2
Decoherence in Quantum Information Processing . . . . .	5
Correlations and Measurements . . . . .	7
The Question of Preferred Basis: What Was Measured? . . . . .	8
Missing Information and Decoherence . . . . .	9
Quantum Discord – A Measure of Quantumness . . . . .	11
Decoherence: How Long Does It Take? . . . . .	12
Experiments on Decoherence . . . . .	16
Classical Limit of Quantum Dynamic . . . . .	16
The Predictability Sieve . . . . .	20
Quantum Chaos and Phase Space Aspects of Quantum – Classical Correspondence . . . . .	21
Quantum Theory of Classical Reality . . . . .	24
The Existential Interpretation . . . . .	26
Further Reading . . . . .	27
Jean-Michel RAIMOND and Serge HAROCHE	
<i>Monitoring the Decoherence of Mesoscopic Quantum Superpositions in a Cavity</i>	33
1 Introduction . . . . .	33
2 A quantum field at the boundary of quantum and classical worlds	36
2.1 A quantum cavity mode . . . . .	36
2.2 Coherent states . . . . .	38
2.3 Schrödinger cat states . . . . .	41
2.4 A pictorial representation of field states . . . . .	44
2.5 Field mode relaxation . . . . .	47
3 Cat state generation and decoherence studies . . . . .	51
3.1 The atom/cavity system . . . . .	51
3.2 Dispersive cat generation . . . . .	56

3.3	Decoherence of cavity cats . . . . .	60
3.4	Probing the cat with a quantum mouse . . . . .	65
4	The future of cavity cats . . . . .	69
4.1	Generation of large cats by resonant atom-field interaction	70
4.2	Imaging Schrödinger cats: a direct determination of the cavity field Wigner function . . . . .	77
4.3	Towards non-local cats . . . . .	78
5	Conclusion . . . . .	80
	References . . . . .	81

## Julia KEMPE

	<i>Approaches to Quantum Error Correction</i>	85
1	Introduction . . . . .	86
2	The subtleties of quantum errors . . . . .	86
3	What is a quantum computer? . . . . .	88
4	What is a quantum error? . . . . .	89
5	The first error correction mechanisms . . . . .	92
6	Quantum Error Correcting Codes . . . . .	96
7	Fault-tolerant computation . . . . .	99
7.1	Guidelines of fault-tolerance . . . . .	100
7.2	Fault-tolerant error correction . . . . .	100
7.3	Fault-tolerant computation . . . . .	102
8	Concatenated coding and the threshold . . . . .	103
9	Error avoidance and Decoherence Free Subsystems . . . . .	105
10	Conclusion and Epilogue . . . . .	106
A	Further Reading . . . . .	107
B	How to model decoherence . . . . .	108
B.1	Hamiltonian Picture . . . . .	109
B.2	Operator Sum Picture . . . . .	110
B.3	Markovian Picture . . . . .	112
C	The Error-model . . . . .	114
D	Stabilizer Codes . . . . .	115
E	Noise model for Decoherence-Free Subsystems . . . . .	117
	References . . . . .	119

## Grégoire ITHIER, François NGUYEN, Eddy COLLIN, Nicolas BOULANT, Phil J. MEESON, Philippe JOYEZ, Denis VION and Daniel ESTÈVE

	<i>Decoherence of a Quantum Bit Circuit</i>	125
1	Why solid state quantum bit circuits? . . . . .	125
2	Towards quantum machines . . . . .	126
2.1	Criteria required for qubits . . . . .	126
2.2	Qubit implementation: Atoms and ions versus electrical circuits . . . . .	127
2.3	Solid state electrical qubit circuits . . . . .	127

- 3 Qubits based on semiconductor structures . . . . . 127
  - 3.1 Kane’s proposal: nuclear spins of P impurities in silicon . . 128
  - 3.2 Charge states in quantum dots . . . . . 129
  - 3.3 Electron spins in quantum dots . . . . . 129
  - 3.4 Flying qubits . . . . . 130
- 4 Superconducting qubit circuits . . . . . 130
  - 4.1 Hamiltonian of Josephson circuits . . . . . 130
  - 4.2 The Cooper pair box . . . . . 132
  - 4.3 How to maintain quantum coherence? . . . . . 133
  - 4.4 Qubit-environment coupling Hamiltonian . . . . . 133
  - 4.5 Relaxation . . . . . 133
  - 4.6 Decoherence= relaxation + dephasing . . . . . 134
  - 4.7 The optimal working point strategy . . . . . 134
- 5 The quantronium circuit . . . . . 135
  - 5.1 Relaxation and dephasing in the quantronium . . . . . 135
  - 5.2 Readout of the quantronium . . . . . 137
- 6 Coherent control of the qubit . . . . . 138
  - 6.1 NMR-like control of a qubit . . . . . 138
- 7 Probing qubit coherence . . . . . 140
  - 7.1 Relaxation . . . . . 140
  - 7.2 Decoherence during free evolution . . . . . 141
  - 7.3 Decoherence during driven evolution . . . . . 143
- 8 Qubit coupling schemes . . . . . 144
  - 8.1 First experimental results . . . . . 144
  - 8.2 Tunable versus fixed couplings . . . . . 144
  - 8.3 Control of the interaction mediated by a fixed Hamiltonian 146
- 9 Conclusions and perspectives . . . . . 146
  - References . . . . . 147

H. Dieter ZEH

- Roots and Fruits of Decoherence* . . . . . 151
- 1 Definition of concepts . . . . . 151
- 2 Roots in nuclear physics . . . . . 153
- 3 The quantum-to-classical transition . . . . . 155
- 4 Quantum mechanics without observables . . . . . 158
- 5 Rules versus tools . . . . . 162
- 6 Nonlocality . . . . . 163
- 7 Information loss (paradox?) . . . . . 166
- 8 Dynamics of entanglement . . . . . 168
- 9 Irreversibility . . . . . 171
- 10 Concluding remarks . . . . . 174
  - References . . . . . 174

## Erich JOOS

	<i>Dynamical Consequences of Strong Entanglement</i>	177
1	Introduction . . . . .	177
2	The quantum Zeno effect . . . . .	178
3	Interference, Motion and Measurement in Quantum Theory . . . .	179
4	Measurement as a Dynamical Process: Decoherence . . . . .	182
5	Strong Decoherence of a Two-State System . . . . .	183
6	Strong Decoherence of Many-State Systems . . . . .	186
	6.1 Macroscopic objects . . . . .	186
	6.2 Rate equations . . . . .	189
7	Summary . . . . .	191
	References . . . . .	192

# Foreword

This book is the sixth in a series of lectures of the *Séminaire Poincaré*, which is directed towards a large audience of physicists and of mathematicians.

The goal of this seminar is to provide up-to-date information about general topics of great interest in physics. Both the theoretical and experimental aspects are covered, with some historical background. Inspired by the Bourbaki seminar in mathematics in its organization, hence nicknamed “Bourbaphi”, the Poincaré Seminar is held twice a year at the Institut Henri Poincaré in Paris, with contributions prepared in advance. Particular care is devoted to the pedagogical nature of the presentations so as to fulfill the goal of being readable by a large audience of scientists.

This volume contains the eighth such Seminar, held in 2005. It is devoted to Quantum Decoherence. A broad perspective on the subject is provided by the contributions of W.H. Zurek (introductory), H.D. Zeh and E. Joos (historical), together with clear (precise) up-to-date presentations of the recent experiments on decoherence both in the mesoscopic systems of atomic physics, by J.M. Raimond and S. Haroche, and in the “quantronic” or condensed matter context, by D. Esteve et al. Finally the question of quantum codes and error corrections is discussed in the contribution of J. Kempe.

We hope that the publication of this series will serve the community of physicists and mathematicians at graduate student or professional level.

We thank the Commissariat à l'Énergie Atomique (Division des Sciences de la Matière), the Centre National de la Recherche Scientifique (Sciences Physique et Mathématiques), and the Daniel Iagolnitzer Foundation for sponsoring the Seminar. Special thanks are due to Chantal Delongas for the preparation of the manuscript.

Bertrand Duplantier  
Jean-Michel Raimond  
Vincent Rivasseau

## Decoherence and the Transition from Quantum to Classical – Revisited

Wojciech Hubert Zurek

**Abstract.** The environment surrounding a quantum system can, in effect, monitor some of the systems observables. As a result, the eigenstates of these observables continuously decohere and can behave like classical states.

This paper has a somewhat unusual origin and, as a consequence, an unusual structure. It is built on the principle embraced by families who outgrow their dwellings and decide to add a few rooms to their existing structures instead of starting from scratch. These additions usually “show,” but the whole can still be quite pleasing to the eye, combining the old and the new in a functional way. What follows is such a “remodeling” of the paper I wrote a dozen years ago for *Physics Today* (1991). The old text (with some modifications) is interwoven with the new text, but the additions are set off in boxes throughout this article and serve as a commentary on new developments as they relate to the original. The references appear together at the end.

In 1991, the study of decoherence was still a rather new subject, but already at that time, I had developed a feeling that most implications about the system’s “immersion” in the environment had been discovered in the preceding 10 years, so a review was in order. While writing it, I had, however, come to suspect that the small gaps in the landscape of the border territory between the quantum and the classical were actually not that small after all and that they presented excellent opportunities for further advances.

Indeed, I am surprised and gratified by how much the field has evolved over the last decade. The role of decoherence was recognized by a wide spectrum of practicing physicists as well as, beyond physics proper, by material scientists and philosophers. The study of the predictability sieve, investigations of the interface between chaotic dynamics and decoherence, and most recently, the tantalizing glimpses of the information-theoretic nature of the quantum have elucidated our understanding of theubert Universe.

Not all of the new developments are reported in this review: Some of the most recent (and, conceivably, most far-reaching) are still too “fresh”, and, hence,



The only “failure” of quantum theory is its inability to provide a natural framework for our prejudices about the workings of the Universe. States of quantum systems evolve according to the deterministic, linear Schrödinger equation

$$i\hbar \frac{d}{dt} |\psi\rangle = H|\psi\rangle . \quad (1)$$

That is, just as in classical mechanics, given the initial state of the system and its Hamiltonian  $H$ , one can, at least in principle, compute the state at an arbitrary time. This deterministic evolution of  $|\psi\rangle$  has been verified in carefully controlled experiments. Moreover, there is no indication of a border between quantum and classical at which Equation (1) would fail (see cartoon on the opener to this article).

There is, however, a very poorly controlled experiment with results so tangible and immediate that it has enormous power to convince: Our perceptions are often difficult to reconcile with the predictions of Equation (1). Why? Given almost any initial condition, the Universe described by  $|\psi\rangle$  evolves into a state containing many alternatives that are never seen to coexist in our world. Moreover, while the ultimate evidence for the choice of one alternative resides in our elusive “consciousness,” there is every indication that the choice occurs much before consciousness ever gets involved and that, once made, it is irrevocable. Thus, at the root of our unease with quantum theory is the clash between the principle of superposition – the basic tenet of the theory reflected in the linearity of Equation (1) – and everyday classical reality in which this principle appears to be violated.

The problem of measurement has a long and fascinating history. The first widely accepted explanation of how a single outcome emerges from the multitude of potentialities was the Copenhagen Interpretation proposed by Niels Bohr (1928), who insisted that a classical apparatus is necessary to carry out measurements. Thus, quantum theory was not to be universal. The key feature of the Copenhagen Interpretation is the dividing line between quantum and classical. Bohr emphasized that the border must be mobile so that even the “ultimate apparatus” – the human nervous system – could in principle be measured and analyzed as a quantum object, provided that a suitable classical device could be found to carry out the task.

In the absence of a crisp criterion to distinguish between quantum and classical, an identification of the classical with the macroscopic has often been tentatively accepted. The inadequacy of this approach has become apparent as a result of relatively recent developments: A cryogenic version of the Weber bar – a gravity-wave detector – must be treated as a quantum harmonic oscillator even though it may weigh a ton (Braginsky et al. 1980, Caves et al. 1980). Nonclassical squeezed states can describe oscillations of suitably prepared electromagnetic fields with macroscopic numbers of photons (Teich and Saleh 1990). Finally, quantum states associated with the currents of superconducting Josephson junctions involve macroscopic numbers of electrons, but still they can tunnel between the minima of the effective potential corresponding to the opposite sense of rotation (Leggett et al. 1987, Caldeira and Leggett 1983a, Tesche 1986).

If macroscopic systems cannot be always safely placed on the classical side of the boundary, then might there be no boundary at all? The Many Worlds Interpretation (or more accurately, the Many Universes Interpretation), developed by Hugh Everett III with encouragement from John Archibald Wheeler in the 1950s, claims to do away with the boundary (Everett 1957, Wheeler 1957). In this interpretation, the entire universe is described by quantum theory. Superpositions evolve forever according to the Schrödinger equation. Each time a suitable interaction takes place between any two quantum systems, the wave function of the universe splits, developing ever more “branches.”

Initially, Everett’s work went almost unnoticed. It was taken out of mothballs over a decade later by Bryce DeWitt (1970) and DeWitt and Neill Graham (1973), who managed to upgrade its status from “virtually unknown” to “very controversial.” The Many Worlds Interpretation is a natural choice for quantum cosmology, which describes the whole Universe by means of a state vector. There is nothing more macroscopic than the Universe. It can have no a priori classical subsystems. There can be no observer “on the outside.” In this universal setting, classicality must be an emergent property of the selected observables or systems.

At first glance, the Many Worlds and Copenhagen Interpretations have little in common. The Copenhagen Interpretation demands an a priori “classical domain” with a border that enforces a classical “embargo” by letting through just one potential outcome. The Many Worlds Interpretation aims to abolish the need for the border altogether. Every potential outcome is accommodated by the ever-proliferating branches of the wave function of the Universe. The similarity between the difficulties faced by these two viewpoints becomes apparent, nevertheless, when we ask the obvious question, “Why do I, the observer, perceive only one of the outcomes?” Quantum theory, with its freedom to rotate bases in Hilbert space, does not even clearly define which states of the Universe correspond to the “branches.” Yet, our perception of a reality with alternatives – not a coherent superposition of alternatives – demands an explanation of when, where, and how it is decided what the observer actually records. Considered in this context, the Many Worlds Interpretation in its original version does not really abolish the border but pushes it all the way to the boundary between the physical Universe and consciousness. Needless to say, this is a very uncomfortable place to do physics.

In spite of the profound nature of the difficulties, recent years have seen a growing consensus that progress is being made in dealing with the measurement problem, which is the usual euphemism for the collection of interpretational conundrums described above. The key (and uncontroversial) fact has been known almost since the inception of quantum theory, but its significance for the transition from quantum to classical is being recognized only now: Macroscopic systems are never isolated from their environments. Therefore – as H. Dieter Zeh emphasized (1970) – they should not be expected to follow Schrödinger’s equation, which is applicable only to a closed system. As a result, systems usually regarded as classical suffer (or benefit) from the natural loss of quantum coherence, which “leaks out” into the environment (Zurek 1981, 1982). The resulting decoherence cannot

be ignored when one addresses the problem of the reduction of the quantum mechanical wavepacket: Decoherence imposes, in effect, the required “embargo” on the potential outcomes by allowing the observer to maintain only records of the alternatives sanctioned by decoherence and to be aware of only one of the branches – one of the “decoherent histories” in the nomenclature of Murray Gell-Mann and James Hartle (1990) and Hartle (1991).

The aim of this paper is to explain the physics and thinking behind decoherence and environment-induced superselection. The reader should be warned that this writer is not a disinterested witness to this development (Wigner 1983, Joos and Zeh 1985, Haake and Walls 1986, Milburn and Holmes 1986, Albrecht 1991, Hu et al. 1992), but rather, one of the proponents. I shall, nevertheless, attempt to paint a fairly honest picture and point out the difficulties as well as the accomplishments.

## Decoherence in Quantum Information Processing

Much of what was written in the introduction remains valid today. One important development is the increase in experimental evidence for the validity of the quantum principle of superposition in various contexts including spectacular double-slit experiments that demonstrate interference of fullerenes (Arndt et al. 1999), the study of superpositions in Josephson junctions (Mooij et al. 1999, Friedman et al. 2000), and the implementation of Schrödinger “kittens” in atom interferometry (Chapman et al. 1995, Pfau et al. 1994), ion traps (Monroe et al. 1996) and microwave cavities (Brune et al. 1996). In addition to confirming the superposition principle and other exotic aspects of quantum theory (such as entanglement) in novel settings, some of these experiments allow – as we shall see later – for a controlled investigation of decoherence.

The other important change that influenced the perception of the quantum-to-classical “border territory” is the explosion of interest in quantum information and computation. Although quantum computers were already being discussed in the 1980s, the nature of the interest has changed since Peter Shor invented his factoring algorithm. Impressive theoretical advances, including the discovery of quantum error correction and resilient quantum computation, quickly followed, accompanied by increasingly bold experimental forays. The superposition principle, once the cause of trouble for the interpretation of quantum theory, has become the central article of faith in the emerging science of quantum information processing. This last development is discussed elsewhere in this volume, so I shall not dwell on it here.

The application of quantum physics to information processing has also transformed the nature of interest in the process of decoherence: At the time of my original review (1991), decoherence was a solution to the interpretation problem – a mechanism to impose an effective classicality on de facto quantum systems. In quantum information processing, decoherence plays two roles. Above all, it is

a threat to the quantumness of quantum information. It invalidates the quantum superposition principle and thus turns quantum computers into (at best) classical computers, negating the potential power offered by the quantumness of the algorithms. But decoherence is also a necessary (although, until recently, tacitly taken for granted) ingredient in quantum information processing, which must, after all, end in a “measurement.”

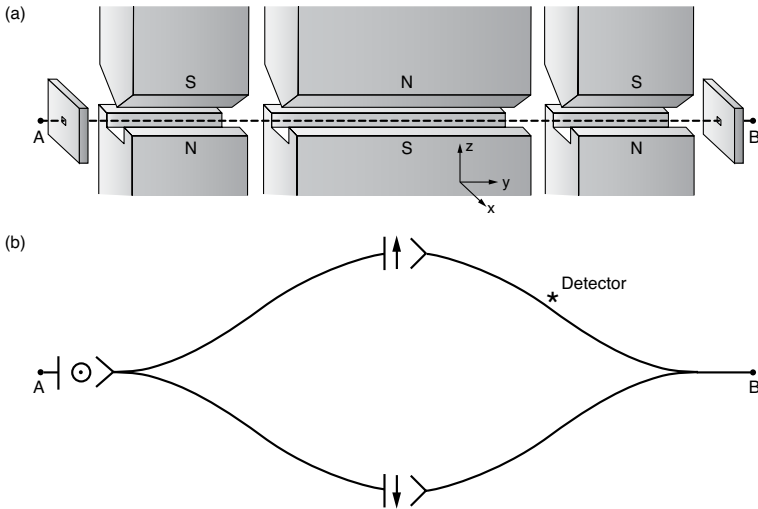


FIGURE 1. A Reversible Stern-Gerlach Apparatus.

The “gedanken” reversible Stern-Gerlach apparatus in (a) splits a beam of atoms into two branches that are correlated with the component of the spin of the atoms (b) and then recombines the branches before the atoms leave the device. Eugene Wigner (1963) used this gedanken experiment to show that a correlation between the spin and the location of an atom can be reversibly undone. The introduction of a one-bit (two-state) quantum detector that changes its state when the atom passes nearby prevents the reversal: The detector inherits the correlation between the spin and the trajectory, so the Stern-Gerlach apparatus can no longer undo the correlation. (This illustration was adapted with permission from Zurek 1981.)

The role of a measurement is to convert quantum states and quantum correlations (with their characteristic indefiniteness and malleability) into classical, definite outcomes. Decoherence leads to the environment-induced superselection (einselection) that justifies the existence of the preferred pointer states. It enables

one to draw an effective border between the quantum and the classical in straightforward terms, which do not appeal to the “collapse of the wavepacket” or any other such *deus ex machina*.

## Correlations and Measurements

A convenient starting point for the discussion of the measurement problem and, more generally, of the emergence of classical behavior from quantum dynamics is the analysis of quantum measurements due to John von Neumann (1932). In contrast to Bohr, who assumed at the outset that the apparatus must be classical (thereby forfeiting claim of quantum theory to universal validity), von Neumann analyzed the case of a quantum apparatus. I shall reproduce his analysis for the simplest case: a measurement on a two-state system  $\mathcal{S}$  (which can be thought of as an atom with spin 1/2) in which a quantum two-state (one bit) detector records the result.

The Hilbert space  $\mathcal{H}_S$  of the system is spanned by the orthonormal states  $|\uparrow\rangle$  and  $|\downarrow\rangle$ , while the states  $|d_\uparrow\rangle$  and  $|d_\downarrow\rangle$  span the  $\mathcal{H}_D$  of the detector. A two-dimensional  $\mathcal{H}_D$  is the absolute minimum needed to record the possible outcomes. One can devise a quantum detector (see Figure 1) that “clicks” only when the spin is in the state  $|\uparrow\rangle$ , that is,

$$|\uparrow\rangle|d_\downarrow\rangle \rightarrow |\uparrow\rangle|d_\uparrow\rangle, \quad (2)$$

and remains unperturbed otherwise.

I shall assume that, before the interaction, the system was in a pure state  $\psi_S$  given by

$$|\psi_S\rangle = \alpha|\uparrow\rangle + \beta|\downarrow\rangle, \quad (3)$$

with the complex coefficients satisfying  $|\alpha|^2 + |\beta|^2 = 1$ . The composite system starts as

$$|\Phi^i\rangle = |\psi_S\rangle|d_\downarrow\rangle, \quad (4)$$

Interaction results in the evolution of  $|\Phi^i\rangle$  into a correlated state  $|\Phi^c\rangle$ :

$$|\Phi^i\rangle = (\alpha|\uparrow\rangle + \beta|\downarrow\rangle) \otimes |d_\downarrow\rangle \Rightarrow \alpha|\uparrow\rangle|d_\uparrow\rangle + \beta|\downarrow\rangle|d_\downarrow\rangle = |\Phi^c\rangle. \quad (5)$$

This essential and uncontroversial first stage of the measurement process can be accomplished by means of a Schrödinger equation with an appropriate interaction. It might be tempting to halt the discussion of measurements with Equation (5). After all, the correlated state vector  $|\Phi^c\rangle$  implies that, if the detector is seen in the state  $|d_\uparrow\rangle$ , the system is guaranteed to be found in the state  $|\uparrow\rangle$ . Why ask for anything more?

The reason for dissatisfaction with  $|\Phi^c\rangle$  as a description of a completed measurement is simple and fundamental: In the real world, even when we do not know the outcome of a measurement, we do know the possible alternatives, and we can safely act as if only one of those alternatives has occurred. As we shall see in the next section, such an assumption is not only unsafe but also simply wrong for a system described by  $|\Phi^c\rangle$ .

How then can an observer (who has not yet consulted the detector) express his ignorance about the outcome without giving up his certainty about the “menu” of the possibilities? Quantum theory provides the right formal tool for the occasion: A density matrix can be used to describe the probability distribution over the alternative outcomes.

Von Neumann was well aware of these difficulties. Indeed, he postulated (1932) that, in addition to the unitary evolution given by Equation (1), there should be an ad hoc “process 1”—a nonunitary reduction of the state vector—that would take the pure, correlated state  $|\Phi^c\rangle$  into an appropriate mixture: This process makes the outcomes independent of one another by taking the pure-state density matrix:

$$\begin{aligned} \rho^c = |\Phi^c\rangle\langle\Phi^c| &= |\alpha|^2 |\uparrow\rangle\langle\uparrow| |d_\uparrow\rangle\langle d_\uparrow| + \alpha\beta^* |\uparrow\rangle\langle\downarrow| |d_\uparrow\rangle\langle d_\downarrow| \\ &\quad + \alpha^*\beta |\downarrow\rangle\langle\uparrow| |d_\downarrow\rangle\langle d_\uparrow| + |\beta|^2 |\downarrow\rangle\langle\downarrow| |d_\downarrow\rangle\langle d_\downarrow|, \end{aligned} \quad (6)$$

and canceling the off-diagonal terms that express purely quantum correlations (entanglement) so that the reduced density matrix with only classical correlations emerges:

$$\rho^r = |\alpha|^2 |\uparrow\rangle\langle\uparrow| |d_\uparrow\rangle\langle d_\uparrow| + |\beta|^2 |\downarrow\rangle\langle\downarrow| |d_\downarrow\rangle\langle d_\downarrow|. \quad (7)$$

Why is the reduced  $\rho^r$  easier to interpret as a description of a completed measurement than  $\rho^c$ ? After all, both  $\rho^r$  and  $\rho^c$  contain identical diagonal elements. Therefore, both outcomes are still potentially present. So what – if anything – was gained at the substantial price of introducing a nonunitary process 1?

## The Question of Preferred Basis: What Was Measured?

The key advantage of  $\rho^r$  over  $\rho^c$  is that its coefficients may be interpreted as classical probabilities. The density matrix  $\rho^r$  can be used to describe the alternative states of a composite spin-detector system that has classical correlations. Von Neumann’s process 1 serves a similar purpose to Bohr’s “border” even though process 1 leaves all the alternatives in place. When the off-diagonal terms are absent, one can nevertheless safely maintain that the apparatus, as well as the system, is each separately in a definite but unknown state, and that the correlation between them still exists in the preferred basis defined by the states appearing on the diagonal. By the same token, the identities of two halves of a split coin placed in two sealed envelopes may be unknown but are classically correlated. Holding one unopened envelope, we can be sure that the half it contains is either “heads” or “tails” (and not some superposition of the two) and that the second envelope contains the matching alternative.

By contrast, it is impossible to interpret  $\rho^c$  as representing such “classical ignorance.” In particular, even the set of the alternative outcomes is not decided by  $\rho^c$ ! This circumstance can be illustrated in a dramatic fashion by choosing  $\alpha = -\beta = 1/\sqrt{2}$  so that the density matrix  $\rho^c$  is a projection operator constructed

from the correlated state

$$|\Phi^c\rangle = (|\uparrow\rangle|d_\uparrow - \downarrow\rangle|d_\downarrow\rangle)\sqrt{2}. \quad (8)$$

This state is invariant under the rotations of the basis. For instance, instead of the eigenstates of  $|\uparrow\rangle$  and  $|\downarrow\rangle$  of  $\hat{\sigma}_z$  one can rewrite  $|\Phi^c\rangle$  in terms of the eigenstates of  $\hat{\sigma}_x$ :

$$|\odot\rangle = (|\uparrow\rangle + |\downarrow\rangle)\sqrt{2}, \quad (9a)$$

$$|\otimes\rangle = (|\uparrow\rangle - |\downarrow\rangle)\sqrt{2}. \quad (9b)$$

This representation immediately yields

$$|\Phi^c\rangle = (|\odot\rangle|d_\odot\rangle - |\otimes\rangle|d_\otimes\rangle)/\sqrt{2}, \quad (10)$$

where

$$|d_\odot\rangle = |d_\downarrow\rangle - |d_\uparrow\rangle/\sqrt{2} \quad \text{and} \quad |d_\otimes\rangle = |d_\uparrow\rangle + |d_\downarrow\rangle/\sqrt{2}, \quad (11)$$

are, as a consequence of the superposition principle, perfectly “legal” states in the Hilbert space of the quantum detector. Therefore, the density matrix

$$\rho^c = |\Phi^c\rangle\langle\Phi^c|$$

could have many (in fact, infinitely many) different states of the subsystems on the diagonal.

This freedom to choose a basis should not come as a surprise. Except for the notation, the state vector  $|\Phi^c\rangle$  is the same as the wave function of a pair of maximally correlated (or entangled) spin-1/2 systems in David Bohm’s version (1951) of the Einstein-Podolsky-Rosen (EPR) paradox (Einstein et al. 1935). And the experiments that show that such nonseparable quantum correlations violate Bell’s inequalities (Bell 1964) are demonstrating the following key point: The states of the two spins in a system described by  $|\Phi^c\rangle$  are not just unknown, but rather they cannot exist before the “real” measurement (Aspect et al. 1981, 1982). We conclude that when a detector is quantum, a superposition of records exists and is a record of a superposition of outcomes – a very nonclassical state of affairs.

## Missing Information and Decoherence

Unitary evolution condemns every closed quantum system to “purity.” Yet, if the outcomes of a measurement are to become independent events, with consequences that can be explored separately, a way must be found to dispose of the excess information. In the previous sections, quantum correlation was analyzed from the point of view of its role in acquiring information. Here, I shall discuss the flip side of the story: Quantum correlations can also disperse information throughout the degrees of freedom that are, in effect, inaccessible to the observer. Interaction with the degrees of freedom external to the system – which we shall summarily refer to as the environment – offers such a possibility.

Reduction of the state vector,  $\rho^c \Rightarrow \rho^r$ , decreases the information available to the observer about the composite system  $\mathcal{SD}$ . The information loss is needed if

the outcomes are to become classical and thereby available as initial conditions to predict the future. The effect of this loss is to increase the entropy  $\mathcal{H} = -\text{Tr}\rho \ln \rho$  by an amount

$$\Delta\mathcal{H} = \mathcal{H}(\rho^r) - \mathcal{H}(\rho^c) = (|\alpha|^2 \ln |\alpha|^2 + |\beta|^2 \ln |\beta|^2) . \quad (12)$$

Entropy must increase because the initial state described by  $\rho^c$  was pure,  $\mathcal{H}(\rho^c) = 0$ , and the reduced state is mixed. Information gain – the objective of the measurement – is accomplished only when the observer interacts and becomes correlated with the detector in the already precollapsed state  $\rho^r$ .

To illustrate the process of the environment-induced decoherence, consider a system  $\mathcal{S}$ , a detector  $\mathcal{D}$ , and an environment  $\mathcal{E}$ . The environment is also a quantum system. Following the first step of the measurement process – establishment of a correlation as shown in Equation (5) – the environment similarly interacts and becomes correlated with the apparatus:

$$|\Phi^c\rangle|\mathcal{E}\rangle = (\alpha|\uparrow\rangle|d_\uparrow\rangle + \beta|\downarrow\rangle|d_\downarrow\rangle)|\mathcal{E}_0\rangle \Rightarrow \alpha|\uparrow\rangle|d_\uparrow\rangle|\mathcal{E}_\uparrow\rangle + \beta|\downarrow\rangle|d_\downarrow\rangle|\mathcal{E}_\downarrow\rangle = |\Psi\rangle . \quad (13)$$

The final state of the combined  $\mathcal{SDE}$  “von Neumann chain” of correlated systems extends the correlation beyond the  $\mathcal{SD}$  pair. When the states of the environment  $\mathcal{E}_i$  corresponding to the states  $|d_\uparrow\rangle$  and  $|d_\downarrow\rangle$  of the detector are orthogonal,  $\langle\mathcal{E}_i|\mathcal{E}_{i'}\rangle = \delta_{ii'}$ , the density matrix for the detector-system combination is obtained by ignoring (tracing over) the information in the uncontrolled (and unknown) degrees of freedom

$$\begin{aligned} \rho_{\mathcal{DS}} &= \text{Tr}_{\mathcal{E}}|\Psi\rangle\langle\Psi| = \sum_i \langle\mathcal{E}_i|\Psi\rangle\langle\Psi|\mathcal{E}_{i'}\rangle \\ &= |\alpha|^2 |\uparrow\rangle\langle\uparrow| |d_\uparrow\rangle\langle d_\uparrow| + |\beta|^2 |\downarrow\rangle\langle\downarrow| |d_\downarrow\rangle\langle d_\downarrow| = \rho^r . \end{aligned} \quad (14)$$

The resulting  $\rho^r$  is precisely the reduced density matrix that von Neumann called for. Now, in contrast to the situation described by Equations (9)–(11), a superposition of the records of the detector states is no longer a record of a superposition of the state of the system. A preferred basis of the detector, sometimes called the “pointer basis” for obvious reasons, has emerged. Moreover, we have obtained it – or so it appears – without having to appeal to von Neumann’s nonunitary process 1 or anything else beyond the ordinary, unitary Schrödinger evolution. The preferred basis of the detector – or for that matter, of any open quantum system – is selected by the dynamics.

Not all aspects of this process are completely clear. It is, however, certain that the detector-environment interaction Hamiltonian plays a decisive role. In particular, when the interaction with the environment dominates, eigenspaces of any observable  $\Lambda$  that commutes with the interaction Hamiltonian,

$$[\Lambda, H_{int}] = 0 . \quad (15)$$

invariably end up on the diagonal of the reduced density matrix (Zurek 1981, 1982). This commutation relation has a simple physical implication: It guarantees that the pointer observable  $\Lambda$  will be a constant of motion, a conserved quantity under

the evolution generated by the interaction Hamiltonian. Thus, when a system is in an eigenstate of  $\Lambda$ , interaction with the environment will leave it unperturbed.

In the real world, the spreading of quantum correlations is practically inevitable. For example, when in the course of measuring the state of a spin-1/2 atom (see Figure 1b), a photon had scattered from the atom while it was traveling along one of its two alternative routes, this interaction would have resulted in a correlation with the environment and would have necessarily led to a loss of quantum coherence. The density matrix of the  $SD$  pair would have lost its off-diagonal terms. Moreover, given that it is impossible to catch up with the photon, such loss of coherence would have been irreversible. As we shall see later, irreversibility could also arise from more familiar, statistical causes: Environments are notorious for having large numbers of interacting degrees of freedom, making extraction of lost information as difficult as reversing trajectories in the Boltzmann gas.

## Quantum Discord – A Measure of Quantumness

The contrast between the density matrices in Equations (6) and (7) is stark and obvious. In particular, the entanglement between the system and the detector in  $\rho^c$  is obviously quantum – classical systems cannot be entangled. The argument against the “ignorance” interpretation of  $\rho^c$  still stands. Yet we would like to have a quantitative measure of how much is classical (or how much is quantum) about the correlations of a state represented by a general density matrix. Such a measure of the quantumness of correlation was devised recently (Zurek 2000, Ollivier and Zurek 2002). It is known as quantum discord. Of the several closely related definitions of discord, we shall select one that is easiest to explain. It is based on mutual information – an information-theoretic measure of how much easier it is to describe the state of a pair of objects ( $\mathcal{S}, \mathcal{D}$ ) jointly rather than separately. One formula for mutual information  $\mathcal{I}(\mathcal{S} : \mathcal{D})$  is simply

$$\mathcal{I}(\mathcal{S} : \mathcal{D}) = \mathcal{H}(\mathcal{S}) + \mathcal{H}(\mathcal{D}) - \mathcal{H}(\mathcal{S}, \mathcal{D}) ,$$

where  $\mathcal{H}(\mathcal{S})$  and  $\mathcal{H}(\mathcal{D})$  are the entropies of  $\mathcal{S}$  and  $\mathcal{D}$ , respectively, and  $\mathcal{H}(\mathcal{S}, \mathcal{D})$  is the joint entropy of the two. When  $\mathcal{S}$  and  $\mathcal{D}$  are not correlated (statistically independent),

$$\mathcal{H}(\mathcal{S}, \mathcal{D}) = \mathcal{H}(\mathcal{S}) + \mathcal{H}(\mathcal{D}) ,$$

and  $\mathcal{I}(\mathcal{S} : \mathcal{D}) = 0$ . By contrast, when there is a perfect classical correlation between them (for example, two copies of the same book),  $\mathcal{H}(\mathcal{S}, \mathcal{D}) = \mathcal{H}(\mathcal{S}) = \mathcal{H}(\mathcal{D}) = \mathcal{I}(\mathcal{S} : \mathcal{D})$ . Perfect classical correlation implies that, when we find out all about one of them, we also know everything about the other, and the conditional entropy  $\mathcal{H}(\mathcal{S}|\mathcal{D})$  (a measure of the uncertainty about  $\mathcal{S}$  after the state of  $\mathcal{D}$  is found out) disappears. Indeed, classically, the joint entropy  $\mathcal{H}(\mathcal{S}, \mathcal{D})$  can always be decomposed into, say,  $\mathcal{H}(\mathcal{D})$ , which measures the information missing about  $\mathcal{D}$ , and the conditional entropy  $\mathcal{H}(\mathcal{S}|\mathcal{D})$ . Information is still missing about  $\mathcal{S}$  even after the state of  $\mathcal{D}$  has been determined:  $\mathcal{H}(\mathcal{S}, \mathcal{D}) = \mathcal{H}(\mathcal{D}) + \mathcal{H}(\mathcal{S}|\mathcal{D})$ . This expression for

the joint entropy suggests an obvious rewrite of the preceding definition of mutual information into a classically identical form, namely,

$$\mathcal{J}(S : D) = H(S) + H(D) - (H(D) + H(S|D)) .$$

Here, we have abstained from the obvious (and perfectly justified from the classical viewpoint) cancellation in order to emphasize the central feature of quantumness: In quantum physics, the state collapses into one of the eigenstates of the measured observable. Hence, a state of the object is redefined by a measurement. Thus, the joint entropy can be defined in terms of the conditional entropy only after the measurement used to access, say,  $\mathcal{D}$ , has been specified. In that case,

$$\mathcal{H}_{|d_k\rangle} = (H(D) + H(S|D))_{|d_k\rangle} .$$

This type of joint entropy expresses the ignorance about the pair  $(S, D)$  after the observable with the eigenstates  $\{|d_k\rangle\}$  has been measured on  $\mathcal{D}$ . Of course,  $\mathcal{H}_{|d_k\rangle}(S, D)$  is not the only way to define the entropy of the pair. One can also compute a basis-independent joint entropy  $\mathcal{H}(S, D)$ , the von Neumann entropy of the pair. Since these two definitions of joint entropy do not coincide in the quantum case, we can define a basis-dependent quantum discord

$$\delta_{|d_k\rangle}(S|D) = I - \mathcal{J} = (H(D) + H(S|D))_{|d_k\rangle} + \mathcal{H}(S, D)$$

as the measure of the extent by which the underlying density matrix describing  $\mathcal{S}$  and  $\mathcal{D}$  is perturbed by a measurement of the observable with the eigenstates  $\{|d_k\rangle\}$ . States of classical objects – or classical correlations – are “objective”: They exist independent of measurements. Hence, when there is a basis  $\{|\hat{d}_k\rangle\}$  such that the minimum discord evaluated for this basis disappears,

$$\hat{\delta}(S|D) = \min_{|d_k\rangle} \{ \mathcal{H}(S|D) - (H(D) + H(S|D))_{|d_k\rangle} \} = 0 ,$$

the correlation can be regarded as effectively classical (or more precisely, as “classically accessible through  $\mathcal{D}$ ”). One can then show that there is a set of probabilities associated with the basis  $\{|d_k\rangle\}$  that can be treated as classical. It is straightforward to see that, when  $\mathcal{S}$  and  $\mathcal{D}$  are entangled (for example,  $\rho^c = |\phi^c\rangle\langle\phi^c|$ ), then  $\hat{\delta} > 0$  in all bases. By contrast, if we consider  $\rho^r$ , discord disappears in the basis  $\{|d_\uparrow\rangle, |d_\downarrow\rangle\}$  so that the underlying correlation is effectively classical.

It is important to emphasize that quantum discord is not just another measure of entanglement but a genuine measure of the quantumness of correlations. In situations involving measurements and decoherence, quantumness disappears for the preferred set of states that are effectively classical and thus serves as an indicator of the pointer basis, which as we shall see, emerges as a result of decoherence and einselection.

## Decoherence: How Long Does It Take?

A tractable model of the environment is afforded by a collection of harmonic oscillators (Feynman and Vernon 1963, Dekker 1981, Caldeira and Leggett 1983a,

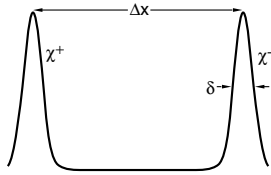


FIGURE 2. A “Schrödinger Cat” State or a Coherent Superposition. This cat state  $\varphi(x)$ , the coherent superposition of two Gaussian wavepackets of Equation (18), could describe a particle in a superposition of locations inside a Stern-Gerlach apparatus (see Figure 1) or the state that develops in the course of a double-slit experiment. The phase between the two components has been chosen to be zero.

1983b, 1985, Joos and Zeh 1985, Hu et al. 1992) or, equivalently, by a quantum field (Unruh and Zurek 1989). If a particle is present, excitations of the field will scatter off the particle. The resulting “ripples” will constitute a record of its position, shape, orientation, and so on, and most important, its instantaneous location and hence its trajectory.

A boat traveling on a quiet lake or a stone that fell into water will leave such an imprint on the water surface. Our eyesight relies on the perturbation left by the objects on the preexisting state of the electromagnetic field. Hence, it is hardly surprising that an imprint is left whenever two quantum systems interact, even when “nobody is looking,” and even when the lake is stormy and full of preexisting waves, and the field is full of excitations – that is, when the environment starts in equilibrium at some finite temperature. “Messy” initial states of the environment make it difficult to decipher the record, but do not preclude its existence.

A specific example of decoherence – a particle at position  $x$  interacting with a scalar field  $\phi$  (which can be regarded as a collection of harmonic oscillators) through the Hamiltonian

$$H_{int} = \epsilon x d\phi/dt \quad (16)$$

where  $\epsilon$  is the strength of the coupling, has been extensively studied by many, including the investigators just referenced. The conclusion is easily formulated in the so-called “high-temperature limit,” in which only thermal-excitation effects of the field  $\phi$  are taken into account and the effect of zero-point vacuum fluctuations is neglected. In this case, the density matrix  $\rho(x, x')$  of the particle in the position representation evolves according to the master equation

$$\dot{\rho} = \underbrace{-\frac{i}{\hbar}[H, \rho]}_{\dot{\rho} = -\text{FORCE} = \Delta V} - \underbrace{\gamma(x - x') \left( \frac{\partial}{\partial x} - \frac{\partial}{\partial x'} \right)}_{\dot{\rho} = -\gamma p} - \underbrace{\frac{2m\gamma k_B T}{\hbar^2} (x - x')^2 \rho}_{\text{Classical Phase Space}}, \quad (17)$$

where  $H$  is the particle's Hamiltonian (although with the potential  $V(x)$  adjusted because of  $H_{int}$ ),  $\gamma$  is the relaxation rate,  $k_B$  is the Boltzmann constant, and  $T$  is the temperature of the field. Equation (17) is obtained by first solving exactly the Schrödinger equation for a particle plus the field and then tracing over the degrees of freedom of the field. I will not analyze Equation (17) in detail but just point out that it naturally separates into three distinct terms, each of them responsible for a different aspect of the effectively classical behavior. The first term – the von Neumann equation (which can be derived from the Schrödinger equation) – generates reversible classical evolution of the expectation value of any observable that has a classical counterpart regardless of the form of  $\rho$  (Ehrenfest's theorem). The second term causes dissipation. The relaxation rate  $\gamma = \eta/2m$  is proportional to the viscosity  $\eta = \epsilon^2/2$  due to the interaction with the scalar field. That interaction causes a decrease in the average momentum and loss of energy. The last term also has a classical counterpart: It is responsible for fluctuations or random “kicks” that lead to Brownian motion. We shall see this in more detail in the next section.

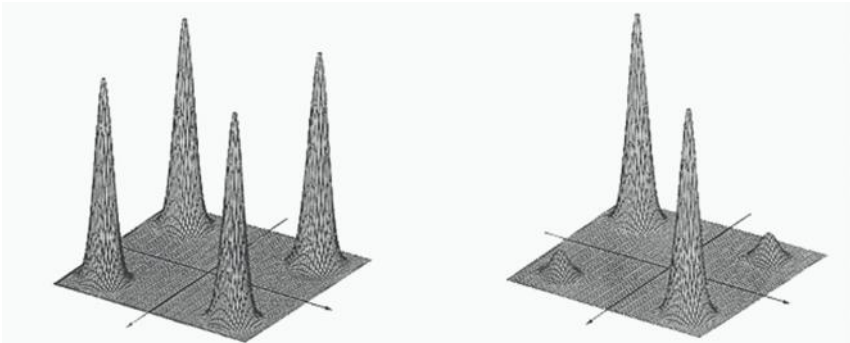


FIGURE 3. Evolution of the Density Matrix for the Schrödinger Cat State in Figure 2. (a) This plot shows the density matrix for the cat state in Figure 2 in the position representation  $\rho(x, x') = \varphi(x)\varphi^*(x')$ . The peaks near the diagonal (green) correspond to the two possible locations of the particle. The peaks away from the diagonal (red) are due to quantum coherence. Their existence and size demonstrate that the particle is not in either of the two approximate locations but in a coherent superposition of them. (b) Environment-induced decoherence causes decay of the off-diagonal terms of  $\rho(x, x')$ . Here, the density matrix in (a) has partially decohered. Further decoherence would result in a density matrix with diagonal peaks only. It can then be regarded as a classical probability distribution with an equal probability of finding the particle in either of the locations corresponding to the Gaussian wave packets.

For our purposes, the effect of the last term on quantum superpositions is of greatest interest. I shall show that it destroys quantum coherence, eliminating off-diagonal terms responsible for quantum correlations between spatially separated pieces of the wavepacket. It is therefore responsible for the classical structure of the phase space, as it converts superpositions into mixtures of localized wave packets which, in the classical limit, turn into the familiar points in phase space. This effect is best illustrated by an example. Consider the “cat” state shown in Figure 2, where the wave function of a particle is given by a coherent superposition of two Gaussians:  $\varphi(x) = (\chi^+(x) + \chi^-(x))/2^{\frac{1}{2}}$  and the Gaussians are

$$\chi^\pm(x) = \langle x|\pm\rangle \exp\left[-\frac{(x \pm \frac{\Delta x}{2})^2}{4\delta^2}\right]. \quad (18)$$

For the case of wide separation ( $\Delta x \gg \delta$ ), the corresponding density matrix  $\rho(x, x') = \varphi(x)\varphi^*(x')$  has four peaks: Two on the diagonal defined by  $x = x'$ , and two off the diagonal for which  $x$  and  $x'$  are very different (see Figure 3). Quantum coherence is due to the off-diagonal peaks. As those peaks disappear, position emerges as an approximate preferred basis.

The last term of Equation (17), which is proportional to  $(x - x')^2$ , has little effect on the diagonal peaks. By contrast, it has a large effect on the off-diagonal peaks for which  $(x - x')^2$  is approximately the square of the separation  $(\Delta x)^2$ . In particular, it causes the off-diagonal peaks to decay at the rate  $\frac{d}{dt}(\rho^\pm) \sim 2\gamma mk_B T / \hbar^2 (\Delta x)^2 \rho^\pm = \tau_D^{-1} \rho^\pm$ . It follows that quantum coherence will disappear on a decoherence time scale (Zurek 1984);

$$\tau_D \simeq \gamma^{-1} \left(\frac{\lambda_{dB}}{\Delta x}\right)^2 = \tau_R \left(\frac{\hbar}{\Delta x \sqrt{2mk_B T}}\right)^2 \quad (19)$$

where  $\lambda_{dB} = \hbar/(2mk_B T)^{-\frac{1}{2}}$  is the thermal de Broglie wavelength. For macroscopic objects, the decoherence time  $\tau_D$  is typically much less than the relaxation time  $\tau_R = \gamma^{-1}$ . For a system at temperature  $T = 300$  kelvins with mass  $m = 1$  gram and separation  $\Delta x = 1$  centimeter, the ratio of the two time scales is  $\tau_D/\tau_R \sim 10^{-40}$ ! Thus, even if the relaxation rate were of the order of the age of the Universe,  $\sim 10^{17}$  seconds, quantum coherence would be destroyed in  $\tau_D \sim 10^{-23}$  second.

For microscopic systems and, occasionally, even for very macroscopic ones, the decoherence times are relatively long. For an electron ( $m_e = 10^{-27}$  grams),  $\tau_D$  can be much larger than the other relevant time scales on atomic and larger energy and distance scales. For a massive Weber bar, tiny  $\Delta x$  ( $\sim 10^{-17}$  centimeter) and cryogenic temperatures suppress decoherence. Nevertheless, the macroscopic nature of the object is certainly crucial in facilitating the transition from quantum to classical.

## Experiments on Decoherence

A great deal of work on master equations and their derivations in different situations has been conducted since 1991, but in effect, most of the results described above stand. A summary can be found in Paz and Zurek (2001) and a discussion of the caveats to the simple conclusions regarding decoherence rates appears in Anglin et al. (1997).

Perhaps the most important development in the study of decoherence is on the experimental front. In the past decade, several experiments probing decoherence in various systems have been carried out. In particular, Michel Brune, Serge Haroche, Jean-Michel Raimond, and their colleagues at *École Normale Supérieure* in Paris (Brune et al. 1996, Haroche 1998) have performed a series of microwave cavity experiments in which they manipulate electromagnetic fields into a Schrödinger-cat-like superposition using rubidium atoms. They probe the ensuing loss of quantum coherence. These experiments have confirmed the basic tenets of decoherence theory. Since then, the French scientists have applied the same techniques to implement various quantum information-processing ventures. They are in the process of upgrading their equipment in order to produce “bigger and better” Schrödinger cats and to study their decoherence.

A little later, Wineland, Monroe, and coworkers (Turchette et al. 2000) used ion traps (set up to implement a fragment of one of the quantum computer designs) to study the decoherence of ions due to radiation. Again, theory was confirmed, further advancing the status of decoherence as both a key ingredient of the explanation of the emergent classicality and a threat to quantum computation. In addition to these developments, which test various aspects of decoherence induced by a real or simulated “large environment,” Pritchard and his coworkers at the Massachusetts Institute of Technology have carried out a beautiful sequence of experiments by using atomic interferometry in order to investigate the role of information transfer between atoms and photons (see Kokorowski et al. 2001 and other references therein). Finally, “analogue experiments” simulating the behavior of the Schrödinger equation in optics (Cheng and Raymer 1999) have explored some of the otherwise difficult-to-access corners of the parameter space.

In addition to these essentially mesoscopic Schrödinger cat decoherence experiments, designs of much more substantial “cats” (for example, mirrors in superpositions of quantum states) are being investigated in several laboratories.

## Classical Limit of Quantum Dynamic

The Schrödinger equation was deduced from classical mechanics in the Hamilton-Jacobi form. Thus, it is no surprise that it yields classical equations of motion when  $\hbar$  can be regarded as small. This fact, along with Ehrenfest’s theorem, Bohr’s correspondence principle, and the kinship of quantum commutators with the classical Poisson brackets, is part of the standard lore found in textbooks. However, establishing the quantum-classical correspondence involves the states as well as the

equations of motion. Quantum mechanics is formulated in Hilbert space, which can accommodate localized wavepackets with sensible classical limits as well as the most bizarre and quantum superpositions. By contrast, classical dynamics happens in phase space. To facilitate the study of the transition from quantum to classical behavior, it is convenient to employ the Wigner transform of a wave function  $\psi(x)$ :

$$W(x, p) = \frac{1}{2\pi\hbar} \int_{-\infty}^{\infty} e^{ipy/\hbar} \psi^* \left( x + \frac{y}{2} \right) \psi \left( x - \frac{y}{2} \right) dy , \quad (20)$$

which expresses quantum states as functions of position and momentum.

The Wigner distribution  $W(x, p)$  is real, but it can be negative. Hence, it cannot be regarded as a probability distribution. Nevertheless, when integrated over one of the two variables, it yields the probability distribution for the other (for example,  $\int W(x, p) dp = |\psi(x)|^2$ ). For a minimum uncertainty wavepacket,  $\psi(x) = \pi^{-\frac{1}{4}} \delta^{-\frac{1}{2}} \exp\{-(x - x_0)^2/2\delta^2 + ip_0x/\hbar\}$ , the Wigner distribution is a Gaussian in both  $x$  and  $p$ :

$$W(x, p) = \frac{1}{\pi\hbar} \exp \left\{ -\frac{(x - x_0)^2}{\delta^2} - \frac{(p - p_0)^2 \delta^2}{\hbar^2} \right\} . \quad (21)$$

It describes a system that is localized in both  $x$  and  $p$ . Nothing else that Hilbert space has to offer is closer to approximating a point in classical phase space. The Wigner distribution is easily generalized to the case of a general density matrix  $\rho(x, x')$ :

$$W(x, p) = \frac{1}{2\pi\hbar} \int_{-\infty}^{\infty} e^{ipy/\hbar} \rho \left( x - \frac{y}{2}, x + \frac{y}{2} \right) dy , \quad (22)$$

where  $\rho(x, x')$  is, for example, the reduced density matrix of the particle discussed before.

The phase-space nature of the Wigner transform suggests a strategy for exhibiting classical behavior: Whenever  $W(x, p)$  represents a mixture of localized wavepackets – as in Equation (21) – it can be regarded as a classical probability distribution in the phase space. However, when the underlying state is truly quantum, as is the superposition in Figure 2, the corresponding Wigner distribution function will have alternating sign – see Figure 4(a). This property alone will make it impossible to regard the function as a probability distribution in phase space. The Wigner function in Figure 4(a) is

$$W(x, p) \sim \frac{(W^+ + W^-)}{2} + \frac{1}{\pi\hbar} \exp \left\{ -\frac{p^2 \delta^2}{\hbar^2} - \frac{x^2}{\delta^2} \right\} \cdot \cos \left( \frac{\Delta x}{\hbar} p \right) , \quad (23)$$

where the Gaussians  $W^+$  and  $W^-$  are Wigner transforms of the Gaussian wavepacket  $\chi^+$  and  $\chi^-$ . If the underlying state had been a mixture of  $\chi^+$  and  $\chi^-$  rather than a superposition, the Wigner function would have been described by the same two Gaussians  $W^+$  and  $W^-$ , but the oscillating term would have been absent.

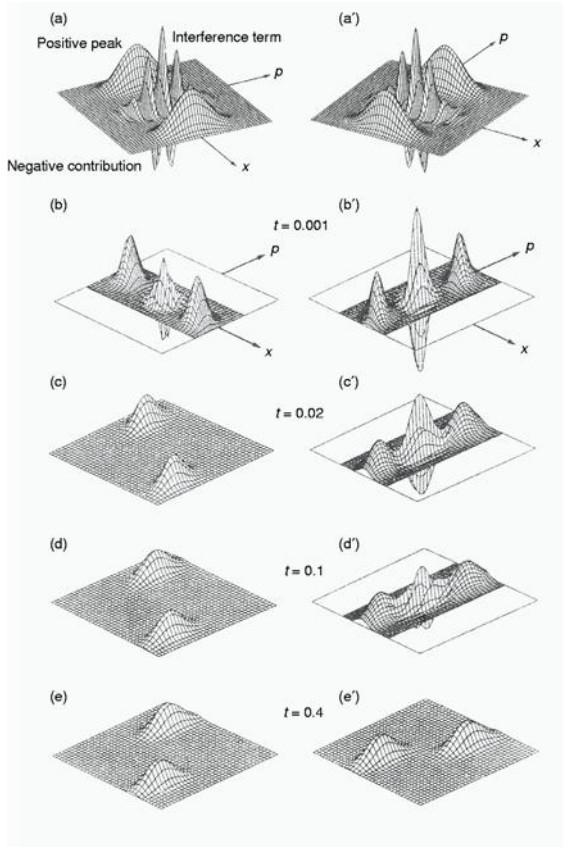


FIGURE 4. Wigner Distributions and Their Decoherence for Coherent Superpositions. (a) The Wigner distribution  $W(x, p)$  is plotted as a function of  $x$  and  $p$  for the cat state of Figure 2. Note the two separate positive peaks as well as the oscillating interference term in between them. This distribution cannot be regarded as a classical probability distribution in phase space because it has negative contributions. (b–e) Decoherence produces diffusion in the direction of the momentum. As a result, the negative and positive ripples of the interference term in  $(x, p)$  diffuse into each other and cancel out. This process is almost instantaneous for open macroscopic systems. In the appropriate limit, the Wigner function has a classical structure in phase space and evolves in accord with the equations of classical dynamics. (a'–e') The analogous initial Wigner distribution and its evolution for a superposition of momenta are shown. The interference terms disappear more slowly on a time scale dictated by the dynamics of the system: Decoherence is caused by the environment coupling to (that is, monitoring) the position of the system – see Equation(16). So, for a superposition of momenta, it will start only after different velocities move the two peaks into different locations.

The equation of motion for  $W(x, p)$  of a particle coupled to an environment can be obtained from Equation (17) for  $\rho(x, x')$ :

$$\frac{\partial W}{\partial t} = \underbrace{-\frac{p}{m} \frac{\partial}{\partial x} W + \frac{\partial V}{\partial x} \frac{\partial}{\partial p} W}_{\text{Liouville Equation}} + \underbrace{2\gamma \frac{\partial}{\partial p} p W}_{\text{Friction}} + \underbrace{D \frac{\partial^2 W}{\partial p^2}}_{\text{Decoherence}}, \quad (24)$$

where  $V$  is the renormalized potential and  $D = 2m\gamma_B T = \eta k_B T$ . The three terms of this equation correspond to the three terms of Equation (17).

The first term is easily identified as a classical Poisson bracket  $\{H, W\}$ . That is, when  $w(x, p)$  is a familiar classical probability density in phase space, then it evolves according to:

$$\frac{\partial w}{\partial t} = -\frac{\partial w}{\partial x} \frac{\partial H}{\partial p} + \frac{\partial w}{\partial p} \frac{\partial H}{\partial x} = \{H, w\} = Lw \quad (25)$$

where  $L$  stands for the Liouville operator. Thus, classical dynamics in its Liouville form follows from quantum dynamics at least for the harmonic oscillator case, which is described rigorously by Equations (17) and (24). (For more general  $V(x)$ , the Poisson bracket would have to be supplemented by quantum corrections of order  $\hbar$ .) The second term of Equation (24) represents friction. The last term results in the diffusion of  $W(x, p)$  in momentum at the rate given by  $D$ .

Classical equations of motion are a necessary but insufficient ingredient of the classical limit: We must also obtain the correct structure of the classical phase space by barring all but the probability distributions of well-localized wavepackets. The last term in Equation (24) has precisely this effect on nonclassical  $W(x, p)$ . For example, the Wigner function for the superposition of spatially localized wave packets – Figure 4(a) – has a sinusoidal modulation in the momentum coordinate produced by the oscillating term  $\cos((\Delta x/\hbar)p)$ . This term, however, is an eigenfunction of the diffusion operator  $\partial^2/\partial p^2$  in the last term of Equation (24). As a result, the modulation is washed out by diffusion at a rate

$$\tau_D^{-1} = -\frac{\dot{W}}{W} = \frac{\left(D \frac{\partial^2}{\partial p^2} W\right)}{W} = \frac{2m\gamma k_B T (\Delta x)^2}{\hbar^2}. \quad (26)$$

Negative valleys of  $W(x, p)$  fill in on a time scale of order  $\tau_D$ , and the distribution retains just two peaks, which now correspond to two classical alternatives—see Figures 4(a) to 4(e). The Wigner function for a superposition of momenta, shown in Figure 4(a'), also decoheres as the dynamics causes the resulting difference in velocities to damp out the oscillations in position and again yield two classical alternatives – see Figures 4(b') to 4(e').

The ratio of the decoherence and relaxation time scales depends on  $\hbar^2/m$  – see Equation (19). Therefore, when  $m$  is large and  $\hbar$  small,  $\tau_D$  can be nearly zero – decoherence can be nearly instantaneous – while, at the same time, the motion of small patches (which correspond to the probability distribution in classical phase space) in the smooth potential becomes reversible. This idealization is responsible

for our confidence in classical mechanics, and, more generally, for many aspects of our belief in classical reality.

The discussion above demonstrates that decoherence and the transition from quantum to classical (usually regarded as esoteric) is an inevitable consequence of the immersion of a system in an environment. True, our considerations were based on a fairly specific model – a particle in a heat bath of harmonic oscillators. However, this is often a reasonable approximate model for many more complicated systems. Moreover, our key conclusions – such as the relation between the decoherence and relaxation time scales in Equation (19) – do not depend on any specific features of the model. Thus, one can hope that the viscosity and the resulting relaxation always imply decoherence and that the transition from quantum to classical can be always expected to take place on a time scale of the order of the above estimates.

## The Predictability Sieve

Since 1991, the understanding of the emergence of the preferred pointer states during the process of decoherence has advanced a great deal. Perhaps the most important advance to date is the predictability sieve (Zurek 1993, Zurek et al. 1993), a more general definition of pointer states that can be used even when the interaction with the environment does not dominate over the self-Hamiltonian of the system. The predictability sieve sifts through the Hilbert space of a system interacting with its environment and selects states that are most predictable. Motivation for the predictability sieve comes from the observation that classical states exist or evolve predictably. Therefore, selecting quantum states that retain predictability in spite of the coupling to the environment is the obvious strategy in search of classicality. To implement the predictability sieve, we imagine a (continuously infinite) list of all the pure states  $\{|\psi\rangle\}$  in the Hilbert space of the system in question. Each of them would evolve, after a time  $t$ , into a density matrix  $\rho_{|\psi\rangle}(t)$ . If the system were isolated, all the density matrices would have the form  $\rho_{|\psi\rangle}(t) = |\psi(t)\rangle\langle\psi(t)|$  of projection operators, where  $|\psi(t)\rangle$  is the appropriate solution of the Schrödinger equation. But when the system is coupled to the environment (that is, the system is “open”),  $\rho_{|\psi\rangle}(t)$  is truly mixed and has a nonzero von Neumann entropy. Thus, one can compute  $\mathcal{H}(\rho_{|\psi\rangle}(t)) = -Tr\rho_{|\psi\rangle} \log \rho_{|\psi\rangle}$ , thereby defining a functional on the Hilbert space  $\mathcal{H}_S$  of the system,  $|\psi\rangle \rightarrow \mathcal{H}(|\psi\rangle, t)$ . An obvious way to look for predictable, effectively classical states is to seek a subset of all  $\{|\psi\rangle\}$  that minimize  $\mathcal{H}(|\psi\rangle, t)$  after a certain, sufficiently long time  $t$ . When such preferred pointer states exist, are well defined (that is, the minimum of the entropy  $\mathcal{H}(|\psi\rangle, t)$  differs significantly for pointer states from the average value), and are reasonably stable (that is, after the initial decoherence time, the set of preferred states is reasonably insensitive to the precise value of  $t$ ), one can consider them as good candidates for the classical domain. Figure A illustrates an implementation of the predictability

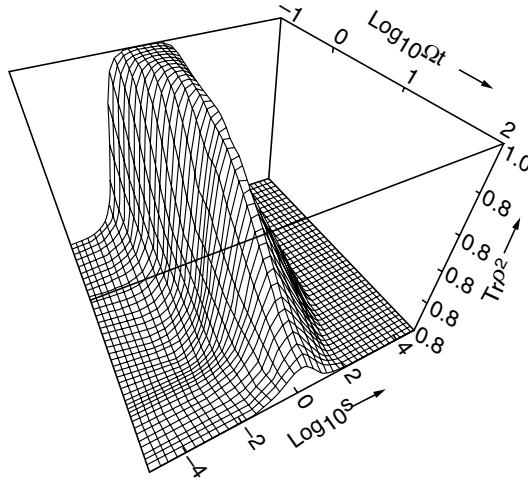


FIGURE A. The Predictability Sieve for the Underdamped Harmonic Oscillator. One measure of predictability is the so-called purity ( $Tr\rho^2$ ), which is plotted as a function of time for mixtures of minimum uncertainty wavepackets in an underdamped harmonic oscillator with  $\gamma/\omega = 10^{-4}$ . The wavepackets start with different squeeze parameters  $s$ . ( $Tr\rho^2$ ) serves as a measure of the purity of the reduced density matrix  $\rho$ . The predictability sieve favors coherent states ( $s = 1$ ), which have the shape of a ground state, that is, the same spread in position and momentum when measured in units natural for the harmonic oscillator. Because they are the most predictable (more than the energy eigenstates), they are expected to play the crucial role of the pointer basis in the transition from quantum to classical.

sieve strategy using a different, simpler measure of predictability – purity ( $Tr\rho^2$ ) – rather than the von Neumann entropy, which is much more difficult to compute.

## Quantum Chaos and Phase Space Aspects of Quantum – Classical Correspondence

Classical mechanics “happens” in phase space. It is therefore critically important to show that quantum theory can – in the presence of decoherence – reproduce the basic structure of classical phase space and that it can emulate classical dynamics. The argument put forward in my original paper (1991) has since been amply supported by several related developments.

The crucial idealization that plays a key role in classical physics is *a point*. Because of the Heisenberg’s indeterminacy principle  $\Delta x \Delta p \geq \hbar/2$ . Hence, quantum

theory does not admit states with simultaneously vanishing  $\Delta x$  and  $\Delta p$ . However, as the study of the predictability sieve has demonstrated, in many situations relevant to the classical limit of quantum dynamics one can expect decoherence to select pointer states that are localized in both  $\Delta x$  and  $\Delta p$ . That is, approximate minimum uncertainty wavepackets are a quantum version of points. They appear naturally in the underdamped harmonic oscillator coupled weakly to the environment (Zurek, 1993, Zurek et al. 1993, Gallis 1996). These results are also relevant to the transition from quantum to classical in the context of field theory with the added twist that the kinds of states selected will typically differ for bosonic and fermionic fields (Anglin and Zurek 1996) because bosons and fermions tend to couple differently to their environments. Finally, under suitable circumstances, einselection can even single out energy eigenstates of the self-Hamiltonian of the system, thus justifying in part the perception of “quantum jumps” (Paz and Zurek 1999).

An intriguing arena for the discussion of quantum - classical correspondence is quantum chaos. To begin with, classical and quantum evolutions from the same initial conditions of a system lead to very different phase space “portraits.” The quantum phase space portrait will depend on the particular representation used, but there are good reasons to favor the Wigner distribution. Studies that use the Wigner distribution indicate that, at the moment when any quantum - classical correspondence is lost in chaotic dynamics, even the averages computed using properties of the classical and quantum states begin to differ (Karkuszewski et al. 2002).

Decoherence appears to be very effective in restoring correspondence. This point, originally demonstrated almost a decade ago (Zurek and Paz 1994, 1995) has since been amply corroborated by numerical evidence (Habib et al. 1998). Basically, decoherence eradicates the small-scale interference accompanying the rapid development of large-scale coherence in quantum versions of classically chaotic systems (refer to Figure B). This outcome was expected. In order for the quantum to classical correspondence to hold, the coherence length  $\ell_C$  of the quantum state must satisfy the following inequality:  $\ell_C = \hbar/(2D\lambda)^{\frac{1}{2}} \ll \chi$ , where  $\lambda$  is the Lyapunov exponent,  $D$  is the usual coefficient describing the rate of decoherence, and  $\chi$  is the scale on which the potential  $V(x)$  is significantly nonlinear:

$$\chi \simeq \sqrt{\frac{V'}{V'''}} .$$

When a quantum state is localized on scales small compared to  $\chi$  (which is the import of the inequality above), its phase space evolution is effectively classical, but because of chaos and decoherence, it becomes irreversible and unpredictable.

A surprising corollary of this line of argument is the realization (Zurek and Paz 1994) that the dynamical second law – entropy production at the scale set by the dynamics of the system and more or less independent of the strength of the coupling to the environment – is a natural and, indeed, an inevitable consequence

of decoherence. This point has been since confirmed in numerical studies (Miller and Sarkar 1999, Pattanayak 1999, Monteoliva and Paz 2000).

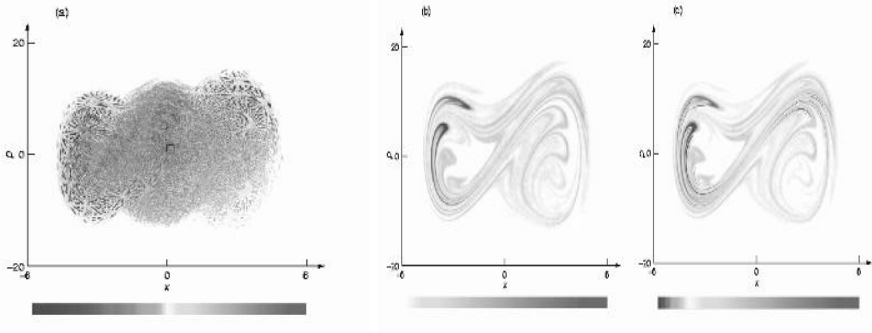


FIGURE B. Decoherence in a Chaotic Driven Double-Well System. This numerical study (Habib et al. 1998) of a chaotic driven double-well system described by the Hamiltonian  $H = p^2/2m - Ax^+ Bx^4 + Fx \cos(\omega t)$  with  $m = 1, A = 10, B = 0.5, F = 10$ , and  $\omega = 6.07$  illustrates the effectiveness of decoherence in the transition from quantum to classical. These parameters result in a chaotic classical system with a Lyapunov exponent  $\lambda \simeq 0.5$ . The three snapshots taken after 8 periods of the driving force illustrate phase space distributions in (a) the quantum case, (b) the classical case, and (c) the quantum case but with decoherence ( $D = 0.025$ ). The initial condition was always the same Gaussian, and in the quantum cases, the state was pure. Interference fringes are clearly visible in (a), which bears only a vague resemblance to the classical distribution in (b). By contrast, (c) shows that even modest decoherence helps restore the quantum-classical correspondence. In this example the coherence length  $\ell_C$  is not much smaller than the typical nonlinearity scale, so the system is on the border between quantum and classical. Indeed, traces of quantum interference are still visible in (c) as blue “troughs,” or regions where the Wigner function is still slightly negative. The change in color from red to blue shown in the legends for (a) and (c) corresponds to a change from positive peaks to negative troughs. In the ab initio classical case (b), there are no negative troughs.

Other surprising consequences of the study of Wigner functions in the quantum-chaotic context is the realization that they develop phase space structure on the scale associated with the sub-Planck action  $\alpha = \hbar^2/A \ll \hbar$ , where  $A$  is the classical action of the system, and that this sub-Planck action is physically significant (Zurek 2001b). This can be seen in Figure B part (a), where a small

black square with the area of  $\hbar$  is clearly larger than the smallest “ripples” in the image. This point was to some extent anticipated by the plots of the Wigner functions of Schrödinger cats (see Figures 4a and 4(a') in this article) a version of which appeared in the 1991 *Physics Today* version of this paper – the interference term of the Wigner function has a sub-Planck structure.

A lot has happened in establishing phase space aspects of quantum - classical correspondence, but a lot more remains to be done. (A more thorough summary of the past accomplishments and remaining goals can be found in Zurek 2001b).

## Quantum Theory of Classical Reality

Classical reality can be defined purely in terms of classical states obeying classical laws. In the past few sections, we have seen how this reality emerges from the substrate of quantum physics: Open quantum systems are forced into states described by localized wavepackets. They obey classical equations of motion, although with damping terms and fluctuations that have a quantum origin. What else is there to explain?

Controversies regarding the interpretation of quantum physics originate in the clash between the predictions of the Schrödinger equation and our perceptions. I will therefore conclude this paper by revisiting the source of the problem – our awareness of definite outcomes. If these mental processes were essentially unphysical, there would be no hope of formulating and addressing the ultimate question – why do we perceive just one of the quantum alternatives? – within the context of physics. Indeed, one might be tempted to follow Eugene Wigner (1961) and give consciousness the last word in collapsing the state vector. I shall assume the opposite. That is, I shall examine the idea that the higher mental processes all correspond to well-defined, but, at present, poorly understood information-processing functions that are being carried out by physical systems, our brains.

Described in this manner, awareness becomes susceptible to physical analysis. In particular, the process of decoherence we have described above is bound to affect the states of the brain: Relevant observables of individual neurons, including chemical concentrations and electrical potentials, are macroscopic. They obey classical, dissipative equations of motion. Thus, any quantum superposition of the states of neurons will be destroyed far too quickly for us to become conscious of the quantum “goings on”. Decoherence, or more to the point, environment-induced superselection, applies to our own “state of mind”.

One might still ask why the preferred basis of neurons becomes correlated with the classical observables in the familiar universe. It would be, after all, so much easier to believe in quantum physics if we could train our senses to perceive nonclassical superpositions. One obvious reason is that the selection of the available interaction Hamiltonians is limited and constrains the choice of detectable observables. There is, however, another reason for this focus on the classical that

must have played a decisive role: Our senses did not evolve for the purpose of verifying quantum mechanics. Rather, they have developed in the process in which survival of the fittest played a central role. There is no evolutionary reason for perception when nothing can be gained from prediction. And, as the predictability sieve illustrates, only quantum states that are robust in spite of decoherence, and hence, effectively classical, have predictable consequences. Indeed, classical reality can be regarded as nearly synonymous with predictability.

There is little doubt that the process of decoherence sketched in this paper is an important element of the big picture central to understanding the transition from quantum to classical. Decoherence destroys superpositions. The environment induces, in effect, a superselection rule that prevents certain superpositions from being observed. Only states that survive this process can become classical.

There is even less doubt that this rough outline will be further extended. Much work needs to be done both on technical issues (such as studying more realistic models that could lead to additional experiments) and on problems that require new conceptual input (such as defining what constitutes a “system” or answering the question of how an observer fits into the big picture).

Decoherence is of use within the framework of either of the two interpretations: It can supply a definition of the branches in Everett’s Many Worlds Interpretation, but it can also delineate the border that is so central to Bohr’s point of view. And if there is one lesson to be learned from what we already know about such matters, it is that information and its transfer play a key role in the quantum universe.

The natural sciences were built on a tacit assumption: Information about the universe can be acquired without changing its state. The ideal of “hard science” was to be objective and provide a description of reality. Information was regarded as unphysical, ethereal, a mere record of the tangible, material universe, an inconsequential reflection, existing beyond and essentially decoupled from the domain governed by the laws of physics. This view is no longer tenable (Wheeler 1991, Landauer 1991). Quantum theory has put an end to this Laplacean dream about a mechanical universe. Observers of quantum phenomena can no longer be just passive spectators. Quantum laws make it impossible to gain information without changing the state of the measured object. The dividing line between what is and what is known to be has been blurred forever. While abolishing this boundary, quantum theory has simultaneously deprived the “conscious observer” of a monopoly on acquiring and storing information: Any correlation is a registration, any quantum state is a record of some other quantum state. When correlations are robust enough, or the record is sufficiently indelible, familiar classical “objective reality” emerges from the quantum substrate. Moreover, even a minute interaction with the environment, practically inevitable for any macroscopic object, will establish such a correlation: The environment will, in effect, measure the state of the object, and this suffices to destroy quantum coherence. The resulting decoherence plays, therefore, a vital role in facilitating the transition from quantum to classical.

## The Existential Interpretation

The quantum theory of classical reality has developed significantly since 1991. These advances are now collectively known as the existential interpretation (Zurek 2001a). The basic difference between quantum and classical states is that the objective existence of the latter can be taken for granted. That is, a system's classical state can be simply "found out" by an observer originally ignorant of any of its characteristics. By contrast, quantum states are hopelessly "malleable" – it is impossible in principle for an observer to find out an unknown quantum state without perturbing it. The only exception to this rule occurs when an observer knows beforehand that the unknown state is one of the eigenstates of some definite observable. Then and only then can a nondemolition measurement (Caves et al. 1980) of that observable be devised so that another observer who knew the original state would not notice any perturbations when making a confirmatory measurement.

If the unknown state cannot be found out – as is indeed the case for isolated quantum systems – then one can make a persuasive case that such states are subjective, and that quantum state vectors are merely records of the observer's knowledge about the state of a fragment of the Universe (Fuchs and Peres 2000). However, einselection is capable of converting such malleable and "unreal" quantum states into solid elements of reality. Several ways to argue this point have been developed since the early discussions (Zurek 1993, 1998, 2001a). In effect, all of them rely on einselection, the emergence of the preferred set of pointer states. Thus, observers aware of the structure of the Hamiltonians (which are "objective," can be found out without "collateral damage", and in the real world, are known well enough in advance) can also divine the sets of preferred pointer states (if they exist) and thus discover the preexisting state of the system.

One way to understand this environment – induced objective existence is to recognize that observers – especially human observers – never measure anything directly. Instead, most of our data about the Universe is acquired when information about the systems of interest is intercepted and spread throughout the environment. The environment preferentially records the information about the pointer states, and hence, only information about the pointer states is readily available. This argument can be made more rigorous in simple models, whose redundancy can be more carefully quantified (Zurek 2000, 2001a).

This is an area of ongoing research. Acquisition of information about the systems from fragments of the environment leads to the so-called conditional quantum dynamics, a subject related to quantum trajectories (Carmichael 1993). In particular one can show that the predictability sieve also works in this setting (Dalvit et al. 2001).

The overarching open question of the interpretation of quantum physics – the "meaning of the wave function" – appears to be in part answered by these recent developments. Two alternatives are usually listed as the only conceivable answers. The possibility that the state vector is purely epistemological (that is, solely a

record of the observer’s knowledge) is often associated with the Copenhagen Interpretation (Bohr 1928). The trouble with this view is that there is no unified description of the Universe as a whole: The classical domain of the Universe is a necessary prerequisite, so both classical and quantum theory are necessary and the border between them is, at best, ill-defined. The alternative is to regard the state vector as an ontological entity – as a solid description of the state of the Universe akin to the classical states. But in this case (favored by the supporters of Everett’s Many Worlds Interpretation), everything consistent with the universal state vector needs to be regarded as equally “real.”

The view that seems to be emerging from the theory of decoherence is in some sense somewhere in between these two extremes. Quantum state vectors can be real, but only when the superposition principle – a cornerstone of quantum behavior – is “turned off” by einselection. Yet einselection is caused by the transfer of information about selected observables. Hence, the ontological features of the state vectors – objective existence of the einselected states – is acquired through the epistemological “information transfer.”

Obviously, more remains to be done. Equally obviously, however, decoherence and einselection are here to stay. They constrain the possible solutions after the quantum – classical transition in a manner suggestive of a still more radical view of the ultimate interpretation of quantum theory in which information seems destined to play a central role. Further speculative discussion of this point is beyond the scope of the present paper, but it will be certainly brought to the fore by (paradoxically) perhaps the most promising applications of quantum physics to information processing. Indeed, quantum computing inevitably poses questions that probe the very core of the distinction between quantum and classical. This development is an example of the unpredictability and serendipity of the process of scientific discovery: Questions originally asked for the most impractical of reasons – questions about the EPR paradox, the quantum-to-classical transition, the role of information, and the interpretation of the quantum state vector – have become relevant to practical applications such as quantum cryptography and quantum computation.

### Acknowledgments

I would like to thank John Archibald Wheeler for many inspiring and enjoyable discussions on “the quantum” and Juan Pablo Paz for the pleasure of a long-standing collaboration on the subject.

### Further Reading

- [1] A. Albrecht, Investigating Decoherence in a Simple System, *Phys. Rev. D* **46** (12), 5504 (1992).
- [2] J. R. Anglin and W. H. Zurek, Decoherence of Quantum Fields: Pointer States and Predictability, *Phys. Rev. D* **53** (12), 7327 (1996).

- [3] J. R. Anglin, J. P. Paz and W. H. Zurek, Deconstructing Decoherence, *Phys. Rev. A* **55** (6), 4041 (1997).
- [4] M. Arndt, O. Nairz, J. VosAndreae, C. Keller, G. van der Zouw, A. Zeilinger, Wave-Particle Duality of C-60 Molecules, *Nature* **401** (6754), 680 (1999).
- [5] A. Aspect, J. Dalibard and G. Roger, Experimental Test of Bell's Inequalities Using Time-Varying Analyzers, *Phys. Rev. Lett.* **49**, 1804 (1982).
- [6] A. Aspect, P. Grangier and G. Rogier, Experimental Tests of Realistic Local Theories via Bell's Theorem, *Phys. Rev. Lett.* **47**, 460 (1981).
- [7] J. S. Bell, On the Einstein Podolsky Rosen Paradox, *Physics* **1**, 195 (1964).
- [8] D. Bohm, In *Quantum Theory*, Chap. 22, p. 611. Englewood Cliffs, NJ: Prentice Hall, 1951.
- [9] N. Bohr, The Quantum Postulate and Recent Development of Atomic Theory, *Nature* **121**, 580 (1928). Reprinted in *Quantum Theory and Measurement*. Edited by Wheeler, J. A., and W. H. Zurek. Princeton, NJ: Princeton University Press.
- [10] V.B. Braginsky, Y. I. Vorontsov and K. S. Thorne, Quantum Nondemolition Measurements, *Science* **209**, 547 (1980).
- [11] M. Brune, E. Hagley, J. Dreyer, X. Maitre, C. Wunderlich, J. M. Raimond and S. Haroche, Observing the Progressive Decoherence of the "Meter" in a Quantum Measurement, *Phys. Rev. Lett.* **77**, 4887 (1996).
- [12] A. O. Caldeira, and A. J. Leggett, Path Integral Approach to Quantum Brownian Motion, *Physica A* **121**, 587 (1983a).
- [13] —, Quantum Tunneling in a Dissipative System, *Ann. Phys* (N. Y.) **149** (2), 374 (1983b).
- [14] —, Influence of Damping on Quantum Interference: An Exactly Soluble Model, *Phys. Rev. A* **31**, 1059 (1985).
- [15] H. J. Carmichael, *An Open Systems Approach to Quantum Optics*, Berlin, Springer Verlag, 1993.
- [16] C. M. Caves, K. S. Thorne, R. W. P. Drever, V. D. Sandberg and M. Zimmerman, On the Measurement of a Weak Classical Force Coupled to a Quantum-Mechanical Oscillator, 1. Issues of Principle. *Rev. Mod. Phys.* **52**, 341 (1980).
- [17] M. S. Chapman, T. D. Hammond, A. Lenef, J. Schmiedmayer, R. A. Rubenstein, E. Smith and D. E. Pritchard, Photon Scattering from Atoms in an Atom Interferometer, *Phys. Rev. Lett.* **75** (21), 3783 (1995).
- [18] C. C. Cheng and M. G. Raymer, Long-Range Saturation of Spatial Decoherence in Wave-Field Transport in Random Multiple-Scattering Media, *Phys. Rev. Lett.* **82** (24), 4807 (1999).
- [19] D. A. R. Dalvit, J. Dziarmaga, W. H. Zurek, Unconditional Pointer States from Conditional Master Equations, *Phys. Rev. Lett.* **86** (3), 373 (2001).
- [20] H. Dekker, Classical and Quantum Mechanics of the Damped Harmonic Oscillator, *Phys. Rep.* **80**, 1 (1981).
- [21] B. S. DeWitt, Quantum Mechanics and Reality, *Phys. Today* **23**, 30 (1970).
- [22] B. S. DeWitt and N. Graham, eds., *The Many-Worlds Interpretation of Quantum Mechanics*. Princeton: Princeton University Press, 1973.

- [23] A. Einstein, B. Podolsky and N. Rosen, Can Quantum-Mechanical Description of Physical Reality Be Considered Complete? *Phys. Rev.* **47**, 777 (1935).
- [24] H. Everett III, “Relative State” Formulation of Quantum Mechanics, *Rev. Mod. Phys.* **29**, 454 (1957).
- [25] R. P. Feynman and F. L. Vernon, The Theory of a General Quantum System Interacting with a Linear Dissipative System, *Ann. Phys.* **24**, 118 (1963).
- [26] J. R. Friedman, V. Patel, W. Chen, S. K. Tolpygo and J. E. Lukens, Quantum Superposition of Distinct Macroscopic States, *Nature* **406** (6791), 43 (2000).
- [27] C. A. Fuchs and A. Peres, Quantum Theory Needs No “Interpretation”, *Phys. Today* **53** (3), 70 (2000).
- [28] M. R. Gallis, Emergence of Classicality via Decoherence Described by Lindblad Operators, *Phys. Rev. A* **53** (2), 655 (1996).
- [29] M. Gell-Mann and J. B. Hartle, Quantum Mechanics in the Light of Quantum Cosmology, In *Complexity, Entropy, and the Physics of Information*. p. 425. Edited by W. H. Zurek. Redwood City: Addison-Wesley, 1990.
- [30] R. B. Griffiths, Consistent Histories and the Interpretation of Quantum Mechanics, *J. Stat. Phys.* **36**, 219 (1984).
- [31] F. Haake and D. F. Walls, In *Quantum Optics IV*. Edited by J. D. Harvey, and D. F. Walls. Berlin: Springer Verlag, 1986.
- [32] S. Habib, K. Shizume and W. H. Zurek, Decoherence, Chaos, and the Correspondence Principle, *Phys. Rev. Lett.* **80** (20), 4361 (1998).
- [33] S. Haroche, Entanglement, Mesoscopic Superpositions and Decoherence Studies with Atoms and Photons in a Cavity, *Physica Scripta* **T76**, 159 (1998).
- [34] J. B. Hartle, The Quantum Mechanics of Cosmology. In *Quantum Cosmology and Baby Universes*, Proceedings of the 1989 Jerusalem Winter School. Edited by S. Coleman, J. B. Hartle, T. Piran, and S. Weinberg. Singapore: World Scientific, 1991.
- [35] B. L. Hu, J. P. Paz and Y. Zhang, Quantum Brownian Motion in a General Environment: Exact Master Equation with Nonlocal Dissipation and Colored Noise, *Phys. Rev. D* **45**, 2843 (1992).
- [36] E. Joos and H. D. Zeh, The Emergence of Classical Properties Through Interaction with the Environment. *Z., Phys. B* **59** 223 (1985).
- [37] Z. P. Karkuszewski, J. Zakrzewski and W. H. Zurek, Breakdown of Correspondence in Chaotic Systems: Ehrenfest Versus Localization Times, *Phys. Rev. A* **65** (4), 042113 (2002).
- [38] D. A. Kokorowski, A. D. Cronin, T. D. Roberts and D. E. Pritchard, From Single-to Multiple-Photon Decoherence in an Atom Interferometer, *Phys. Rev. Lett.* **86** (11), 2191 (2001).
- [39] R. Landauer, Information is Physical, *Phys. Today* **44** (5), 23 (1991).
- [40] A. J. Leggett, S. Chakravarty, A. T. Dorsey, M. P. A. Fisher, A. Garg and W. Zwerger, Dynamics of the Dissipative System, *Rev. Mod. Phys.* **59**, 1 (1987).
- [41] G. J. Milburn and C. A. Holmes, Dissipative Quantum and Classical Liouville Mechanics of the Unharmonic Oscillator, *Phys. Rev. Lett.* **56**, 2237 (1986).
- [42] P. A. Miller and S. Sarkar, Signatures of Chaos in the Entanglement of Two Coupled Quantum Kicked Tops, *Phys. Rev. E* **60**, 1542 (1999).

- [43] C. Monroe, D. M. Meekhof, B. E. King and D. J. Wineland, A “Schrödinger Cat” Superposition State of an Atom, *Science* **272** (5265), 1131 (1996).
- [44] D. Monteoliva and J. P. Paz, Decoherence and the Rate of Entropy Production in Chaotic Quantum Systems, *Phys. Rev. Lett.* **85** (16), 3373 (2000).
- [45] J. E. Mooij, T. P. Orlando, L. Levitov, L. Tian, C. H. van der Wal and S. Lloyd, Josephson Persistent-Current Qubit, *Science* **285** (5430), 1036 (1999).
- [46] C. J. Myatt, B. E. King, Q. A. Turchette, C. A. Sackett, D. Kielpinski, W. M. Itano, et al, Decoherence of Quantum Superpositions Through Coupling to Engineered Reservoirs, *Nature* **403**, 269 (2000).
- [47] H. Ollivier and W. H. Zurek, Quantum Discord: A Measure of the Quantumness of Correlations, *Phys. Rev. Lett.* **88** (1), 017901 (2002).
- [48] R. Omnès, From Hilbert Space to Common Sense, *Ann. Phys.* **201**, 354 (1990).
- [49] —, Consistent Interpretation of Quantum Mechanics, *Rev. Mod. Phys.* **64**, 339 (1992).
- [50] A. K. Pattanayak, Lyapunov Exponents Entropy Production and Decoherence, *Phys. Rev. Lett.* **83** (22), 4526 (1999).
- [51] J. P. Paz and W. H. Zurek, Environment-Induced Decoherence, Classicality, and Consistency of Quantum Histories, *Phys. Rev. D* **48** (6), 2728 (1993).
- [52] —, Quantum Limit of Decoherence: Environment Induced Superselection of Energy Eigenstates, *Phys. Rev. Lett.* **82** (26), 5181 (1999).
- [53] —, In *Coherent Atomic Matter Waves*, Les Houches Lectures, Edited by R. Kaiser, C. Westbrook, and F. Davids. Vol. 72, p. 533. Berlin: Springer, 2001.
- [54] J. P. Paz, S. Habib and W. H. Zurek, Reduction of the Wave Packet: Preferred Observable and Decoherence Time Scale, *Phys. Rev. D* **47**, 488 (1993).
- [55] T. Pfau, S. Splater, Ch. Kurtsiefer, C. R. Ekstrom and J. Mlynek, Loss of Spatial Coherence by a Single Spontaneous Emission, *Phys. Rev. Lett.* **73** (9), 1223 (1994).
- [56] M. O. Scully, B. G. Englert and J. Schwinger, Spin Coherence and Humpty-Dumpty. III. The Effects of Observation, *Phys. Rev. A* **40**, 1775 (1989).
- [57] M. C. Teich and B. E. A. Saleh, Squeezed and Antibunched Light, *Phys. Today* **43** (6), 26 (1990).
- [58] C. D. Tesche, Schrödinger’s Cat: A Realization in Superconducting Devices, *Ann. N. Y. Acad. Sci.* **480**, 36 (1986).
- [59] Q. A. Turchette, C. J. Myatt, B. E. King, C. A. Sackett, D. Kielpinski, W. M. Itano, et al, Decoherence and Decay of Motional Quantum States of a Trapped Atom Coupled to Engineered Reservoirs, *Phys. Rev. A* **62**, 053807 (2000).
- [60] W. G. Unruh and W. H. Zurek, Reduction of a Wave Packet in Quantum Brownian Motion, *Phys. Rev. D.* **40**, 1071 (1989).
- [61] J. Von Neumann, *Mathematische Grundlagen der Quanten Mechanik*. Berlin: Springer-Verlag, English translation by R. T. Beyer. 1955. Mathematical Foundations of Quantum Mechanics. Princeton: Princeton University Press, 1932.
- [62] J. A. Wheeler, Assessment of Everett’s “Relative State” Formulation of Quantum Theory, *Rev. Mod. Phys.* **29**, 463 (1957).
- [63] —, Information, Physics, Quantum: The Search for Links, In *Complexity, Entropy, and the Physics of Information*. p. 3. Edited by W. H. Zurek. Redwood City: Addison-Wesley, 1991.

- [64] J. A. Wheeler and W. H. Zurek, eds., *Quantum Theory and Measurement*, Princeton: Princeton University Press, 1983.
- [65] E. P. Wigner, On the Quantum Correction for Thermodynamic Equilibrium, *Phys. Rev.* **40**, 749 (1932).
- [66] —, Remarks on the Mind-Body Question, In *The Scientist Speculates*, p. 284. Edited by I. J. Good. London: Heineman, 1961.
- [67] —, The Problem of Measurement, *Am. J. Phys.* **3**, 615 (1963).
- [68] —, In *Quantum Optics, Experimental Gravitation, and the Measurement Theory*, Edited by P. Meystre, and M. O. Scully. p. 43. New York: Plenum Press, 1983.
- [69] H. D. Zeh, On the Interpretation of Measurement in Quantum Theory, *Found. Phys.* **1**, 69 (1970).
- [70] W. H. Zurek, Pointer Basis of Quantum Apparatus: Into What Mixture Does the Wave Packet Collapse?, *Phys. Rev. D* **24**, 1516 (1981).
- [71] —, Environment-Induced Superselection Rules, *Phys. Rev. D* **26**, 1862 (1982).
- [72] —, Reduction of the Wave Packet: How Long Does It Take? In *Frontiers of Nonequilibrium Statistical Physics*, Edited by P. Meystre, and M. O. Scully. New York : Plenum, 1984.
- [73] —, Decoherence and the Transition From Quantum to Classical, *Phys. Today* **44** (10), 36 (1991).
- [74] —, Preferred States, Predictability, Classicality, and the Environment-Induced Decoherence, *Prog. Theor. Phys.* **89** (2), 281 (1993).
- [75] —, Decoherence, Chaos, Quantum-Classical Correspondence, and the Algorithmic Arrow of Time, *Physica Scripta* **T76**, 186 (1998).
- [76] —, Einselection and Decoherence from an Information Theory Perspective, *Ann. Phys.* (Leipzig) **9** (11-12), 855 (2000).
- [77] —, Decoherence, Einselection, and the Quantum Origins of the Classical, (2001a), <http://eprints.lanl.gov. quant-ph/0105127> .
- [78] —, Sub-Planck Structure in Phase Space and its Relevance for Quantum Decoherence, *Nature* **412**, 712 (2001b).
- [79] W. H. Zurek and J. P. Paz, Decoherence, Chaos, and the Second Law, *Phys. Rev. Lett.* **72** (16), 2508 (1994).
- [80] —, Quantum Chaos: A Decoherent Definition, *Physica D* **83** (1-3), 300 (1995).
- [81] W. H. Zurek, S. Habib and J. P. Paz, Coherent States via Decoherence, *Phys. Rev. Lett.* **70** (9), 1187 (1993).

Wojciech Hubert Zurek  
 Theory Division,  
 Mail Stop B288, LANL  
 Los Alamos, New Mexico 87545  
 USA  
 e-mail: whzurek@gmail.com

# Monitoring the Decoherence of Mesoscopic Quantum Superpositions in a Cavity

Jean-Michel Raimond and Serge Haroche

**Abstract.** Decoherence is an extremely fast and efficient environment-induced process transforming macroscopic quantum superpositions into statistical mixtures. It is an essential step in quantum measurement and a formidable obstacle for a practical use of quantum superpositions (quantum computing for instance). For large objects, decoherence is so fast that its dynamics is unobservable. Mesoscopic fields stored in a high-quality superconducting millimeter-wave cavity, a modern equivalent to Einstein's 'photon box', are ideal tools to reveal the dynamics of the decoherence process. Their interaction with a single circular Rydberg atom prepares them in a quantum superposition of fields, containing a few photons, with different classical phases. The evolution of this 'Schrödinger cat' state can be later probed with a 'quantum mouse', another atom, assessing its coherence. We describe here the experiments performed along these lines at ENS, and stress the deep links between decoherence and complementarity.

## 1. Introduction

Quantum state superpositions are ubiquitous in the microscopic world. They are at the heart of any interferometry experiment, be them either the fancy quantum interferences of laser cooled atoms or the usual light interferences observed, for instance, in the Young's double slit device.

Quite obviously, these quantum superpositions do not invade our macroscopic world. At our scale, there is not such a thing that an object following two paths at the same time or, to quote once more Schrödinger's provocative wording, a cat that would be suspended in quantum limbs in a quantum superposition of its 'dead' and 'alive' states. In fact, we observe only a tiny fraction of all possible states of an immense Hilbert space.

Decoherence is the extremely efficient mechanism that confines the weirdness of the quantum world at a microscopic scale and that prevents the quantum

monsters from entering our lives [1, 2, 3]. Any quantum system is coupled to an environment. For microscopic systems, made of a single spin, a single atom or a single photon, this coupling results in the usual relaxation mechanism, setting a finite lifetime to the system's energy, for instance.

For a mesoscopic quantum superposition, the environment very rapidly transforms it into a mere statistical mixture, obeying the standard probability laws for exclusive events. The decoherence time scale decreases when a parameter measuring the distance between the states in the superposition increases. For superpositions of very different states, the decoherence time scale is extraordinarily short, making the observation of such quantum superpositions practically impossible (see W. Zurek's and H.D. Zeh's contributions in this Volume).

Observing our classical world is a strong indication of the validity of the decoherence concept. It would, obviously, be much more interesting to study the dynamics of the decoherence, to unveil its inner workings and to put our understanding of this essential phenomenon under close scrutiny.

Testing experimentally decoherence is a challenging task. First, it is so efficient that there is no hope to resolve its dynamics when it comes to macroscopic objects, even much simpler than a cat. One should thus control a single mesoscopic quantum system. Larger than a single atom or a single photon, it should be nevertheless sufficiently isolated from its environment to provide an accessible decoherence time scale. It should first be prepared in a superposition of states at a mesoscopic 'distance' in the system's phase space. Finally, a signal indicating the degree of coherence (of 'quantumness') of the final system's state should be obtained and studied as a function of time, revealing the decoherence dynamics.

Cavity Quantum Electrodynamics [4] and ion trap experiments [5] are ideally suited for these experiments. Both implement a simple quantum system, made up of a single two-level system (a spin-1/2) strongly interacting with a mesoscopic quantum oscillator (a spring). In the cavity QED case, the oscillator is a single mode of a high quality cavity, interacting with a single atom. In the ion trap experiments, the oscillator is the mechanical motion of the ion in the trap, coupled by appropriate laser beams to the ion's internal state. In both cases, the spin/spring interaction can be tailored to cast the oscillator in a mesoscopic quantum state superposition [6, 7]. The decoherence dynamics, unveiled for the first time in a cavity QED experiment [7], has also been studied in the ion trap context [8].

We shall describe here the cavity QED experiments performed at ENS on 'Schrödinger cat states' of the cavity field and their decoherence [4]. These experiments use circular Rydberg atoms interacting, one at a time, with a superconducting cavity. These cavities are a reasonable modern approximation of the 'photon box' that Bohr and Einstein were using in their heated debates about quantum mechanics. They are able to store microwave fields for long times, up to a millisecond, corresponding to quality factors  $Q$  in the  $10^8$  range. Their mode, equivalent to an harmonic oscillator, is thus pretty well isolated from the outside world.

Circular Rydberg states have a high principal quantum number, around 50 in these experiments, and maximum orbital and magnetic quantum numbers. They

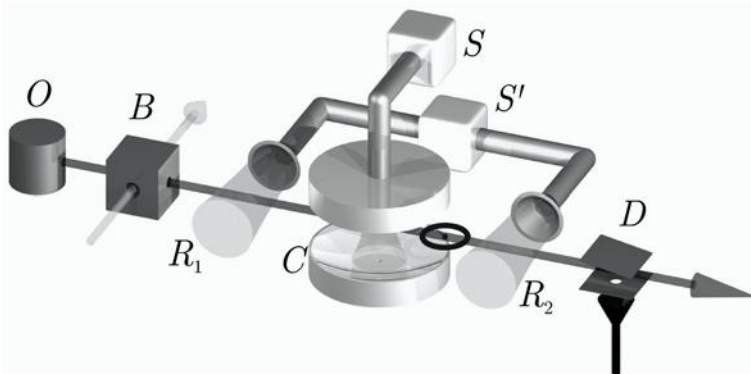


FIGURE 1. Scheme of the ENS cavity QED set-up.

have a nearly macroscopic size: the atomic radius is  $0.1 \mu\text{m}$ , comparable to the size of a living organism, virus or bacteria. They are blessed with remarkable properties [4], being long-lived (radiative lifetime about 30 ms) with a huge dipole strongly coupling the transition between two adjacent states to millimeter-waves. The atomic transition frequency can be tuned by Stark effect in a d.c. electric field. Finally, circular atoms can be detected in a selective and sensitive way using field ionization.

Figure 1 presents the ENS experimental scheme. In box  $B$ , velocity-selected rubidium atoms effusing from oven  $O$  are prepared in the circular states  $|e\rangle$  or  $|g\rangle$ , with principal quantum numbers 51 and 50 respectively. The atomic samples are excited at a given time. Their position is thus known at any time during their 20 cm transit through the apparatus until they are finally detected in the field-ionization counter  $D$ , which discriminates  $|e\rangle$  and  $|g\rangle$ . The atoms are protected from the room-temperature backbody field by a 1K cryogenic environment. The atom number in a sample obeys a Poisson statistics, with much less than one atom on the average. When an event is recorded by  $D$  (detection efficiency  $> 80\%$ ), the probability that it corresponds to more than one atom is negligible. The atomic state can be manipulated before or after the interaction with the cavity  $C$  by resonant classical microwave fields produced in the zones  $R_1$  and  $R_2$  by the additional source  $S'$ .

The  $|e\rangle \rightarrow |g\rangle$  transition, at 51.1 GHz, is resonant or nearly resonant with the superconducting Fabry Perot cavity  $C$ . The photon storage time,  $T_c$ , is of the order of 1 ms. A classical source,  $S$ , injects classical fields in  $C$ , with controlled amplitudes and phases. An electric field applied across the mirrors tunes the atomic transition via the Stark effect in or out of resonance with  $C$ , at well defined times, leading to a precise control of the atom-cavity interaction dynamics.

We shall first, in Section 2, describe the quantum optics theoretical tools necessary to analyze the decoherence experiments. We first briefly recall the field

quantization in a single mode, equivalent to a one-dimensional harmonic oscillator. We then describe two important quantum fields, the coherent states and the Schrödinger cat states. The coherent states are the most classical field states, being produced by classical sources such as  $S$ . They are also the most stable with respect to cavity relaxation, the ‘pointer states’ for the field. The cat states are quantum superpositions of different coherent states and present remarkable quantum features. Finally, we describe cavity mode relaxation, either in the Master equation or in the Monte Carlo trajectories approaches, which shed complementary lights on this important process.

Section 3 is devoted to the production and detection of Schrödinger cat states in the cavity. We describe first the atom-cavity interaction in terms of the ‘dressed states’. We show that the interaction with a single, non-resonant atom transforms a coherent state into a cat, whose decoherence is then theoretically analyzed. We explain how a probe atom, a ‘quantum mouse’ can be used to assess the decoherence of the cavity cat.

Finally, Section 4 is devoted to the perspectives opened for these decoherence studies: creation of very large cats by resonant atom-field interaction, direct measurement of the cat’s Wigner function, providing a detailed insight into the decoherence mechanisms and creation of non-local cat states, merging the Einstein-Podolsky-Rosen [9] non-locality and decoherence.

## 2. A quantum field at the boundary of quantum and classical worlds

### 2.1. A quantum cavity mode

A single field mode is equivalent to a one-dimensional harmonic oscillator. The non-degenerate energy eigenstates are the Fock or ‘photon number states’  $\{|n\rangle\}$   $n > 0$ , whose energy is  $\hbar\omega_c(n + \frac{1}{2})$ , where  $\omega_c$  is the cavity mode angular frequency. The ground state is the vacuum  $|0\rangle$ . The Fock states are an orthogonal set:

$$\langle n|p\rangle = \delta_{np} . \quad (1)$$

The photon annihilation and creation operators  $a$  and  $a^\dagger$  connect the Fock states:

$$a|n\rangle = \sqrt{n}|n-1\rangle ; \quad a^\dagger|n\rangle = \sqrt{n+1}|n+1\rangle . \quad (2)$$

The action of  $a$  on  $|0\rangle$  gives a null vector (it is not possible to annihilate a photon in vacuum). All Fock states can be generated from the vacuum by repeated applications of the photon creation operator:  $|n\rangle = a^{\dagger n}|0\rangle/\sqrt{n!}$ . These operators obey a bosonic commutation rule:  $[a, a^\dagger] = \mathbf{1}$ .

The cavity Hamiltonian is  $H_c = \hbar\omega_c(a^\dagger a + 1/2)$ . Since we are dealing with a single-mode situation, we can redefine the energy origin to get rid of the non-vanishing vacuum state energy. We can thus also use the simpler Hamiltonian:

$$H'_c = \hbar\omega_c a^\dagger a . \quad (3)$$

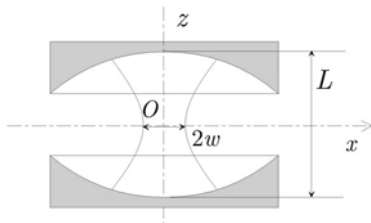


FIGURE 2. Scheme of a microwave Fabry-Perot cavity. The two spherical mirrors separated by  $L$  sustain a Gaussian mode with waist  $w$ . The cavity axis normal to the mirrors is  $Oz$ . The sinusoidal standing wave pattern (with field nodes and antinodes along  $Oz$ ) is not represented. Atoms propagate along  $Ox$  axis.

The cavity mode electric field operator at position  $\mathbf{r}$  writes:

$$\mathbf{E}_c = i\mathcal{E}_0 [\mathbf{f}(\mathbf{r})a - \mathbf{f}^*(\mathbf{r})a^\dagger] , \quad (4)$$

where  $\mathcal{E}_0$  is a normalization factor. The dimensionless vector function  $\mathbf{f}(\mathbf{r}) = \epsilon_c f(\mathbf{r})$  describes the spatial structure of the field mode (relative field amplitude  $f$  and polarization  $\epsilon_c$ ). At the point where the field mode amplitude is maximum, which we also take as the origin,  $f = 1$ .

The normalization factor is obtained by equating the Fock states energies with the integral over space of the expectation value of the electromagnetic energy density  $\epsilon_0 |\mathbf{E}_c|^2$ :

$$\mathcal{E}_0 = \sqrt{\frac{\hbar\omega_c}{2\epsilon_0\mathcal{V}}} . \quad (5)$$

where we define the cavity effective volume  $\mathcal{V}$  by:

$$\mathcal{V} = \int |\mathbf{f}(\mathbf{r})|^2 dV . \quad (6)$$

As a specific example, consider the case of the Fabry-Perot cavity briefly described in Section 1. It is made of two spherical mirrors facing each other (Figure 2). The mode is then a standing wave with a Gaussian transverse profile and a sinusoidal field variation in the longitudinal direction normal to the mirrors, separated by the distance  $L$ . The waist  $w$  characterizes the minimum width of the Gaussian. The mode volume is then  $V = \pi L w^2/4$ . For the specific parameters of the experiment ( $L = 2.7$  cm;  $w = 6$  mm) we have  $V = 0.7$  cm<sup>3</sup>. The field per photon is then:

$$\mathcal{E}_0 = 1.5 \cdot 10^{-3} \text{ V/cm} , \quad (7)$$

a rather large value in S.I. units for a quantum field.

The field quadrature operators correspond to a mechanical oscillator's position and momentum:

$$X = \frac{a + a^\dagger}{2} ; \quad P = \frac{a - a^\dagger}{2i} = \frac{e^{-i\pi/2}a + e^{i\pi/2}a^\dagger}{2} . \quad (8)$$

More generally, phase quadratures are linear combinations of  $a$  and  $a^\dagger$ :

$$X_\varphi = \frac{e^{-i\varphi}a + e^{i\varphi}a^\dagger}{2} ; \quad X_{\varphi+\pi/2} = \frac{e^{-i\varphi}a - e^{i\varphi}a^\dagger}{2i} . \quad (9)$$

They satisfy the commutation rules  $[X_\varphi, X_{\varphi+\pi/2}] = i/2$ , which correspond to the uncertainty relations  $\Delta X_\varphi \Delta X_{\varphi+\pi/2} \geq 1/4$ , where  $\Delta X_\varphi$  and  $\Delta X_{\varphi+\pi/2}$  are conjugate phase quadrature fluctuations.

The eigenstate of the quadrature  $X_\varphi$  corresponding to the real and continuous eigenvalue  $x$  is a non-normalizable state (infinite energy), which obeys the orthogonality and closure relationships:

$$\langle x | x' \rangle_\varphi = \delta(x - x') ; \quad \int |x\rangle_\varphi \langle x| dx = \mathbb{1}, \quad (10)$$

the transformation from the  $|x\rangle_\varphi$  basis to the conjugate basis  $|x\rangle_{\varphi+\pi/2}$  being a Fourier transform:

$$|x\rangle_{\varphi+\pi/2} = \int dy |y\rangle_\varphi \langle y | x \rangle_{\varphi+\pi/2} = \frac{1}{\sqrt{\pi}} \int dy e^{2ixy} |y\rangle_\varphi . \quad (11)$$

Note that two conjugate field quadratures provide coordinates for the quantum field phase space, equivalent to the Fresnel plane for classical fields.

The expectation value  $\langle n | X_\varphi | n \rangle$  of any phase quadrature in a Fock state is zero. There is thus no preferred phase neither in the vacuum nor in any Fock state, a feature which shows that these quantum states are quite different from classical fields. For the vacuum, the quadrature fluctuations are isotropic and correspond to the minimum value compatible with Heisenberg uncertainty relations:  $\Delta X_\varphi^{(0)} = \sqrt{\langle 0 | X_\varphi^2 | 0 \rangle} = 1/2$ . The probability distribution  $P^{(0)}(x)$  of the field quadrature is then a Gaussian:

$$P^{(0)}(x) = |\langle x | 0 \rangle|^2 = \left(\frac{2}{\pi}\right)^{1/2} e^{-2x^2} . \quad (12)$$

In summary, the vacuum field in each mode has isotropic Gaussian fluctuations around zero field.

## 2.2. Coherent states

To describe situations in which the phase of the field is relevant, it is convenient to expand the field on the basis of the coherent states [10, 11], which are more physical than Fock or quadrature states and are experimentally more accessible.

A coherent state of a single field mode is defined as resulting from the translation of the vacuum field in phase space. This translation is represented, in its

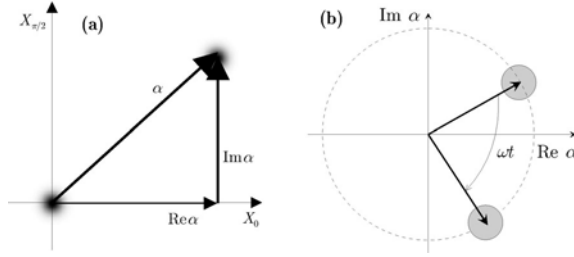


FIGURE 3. Coherent state. (a) Pictorial representation of the action of the displacement operator on the vacuum state. The displacement by a complex amplitude  $\alpha$  amounts to a displacement by  $\text{Re}\alpha$  along the  $X_0$  quadrature axis, followed by a displacement by  $\text{Im}\alpha$  along the  $X_{\pi/2}$  quadrature. (b) Time evolution of a coherent state.

most general form, by the unitary displacement operator:

$$D(\alpha) = e^{\alpha a^\dagger - \alpha^* a} , \quad (13)$$

where  $\alpha = |\alpha| \exp(i\phi)$  is a  $C$ -number whose real and imaginary parts are the projections along the  $X_0$  and  $X_{\pi/2}$  directions respectively of the translation vector. The translated vacuum state is the coherent state  $|\alpha\rangle$ :

$$|\alpha\rangle = D(\alpha)|0\rangle . \quad (14)$$

The translated ‘packet’, whose evolution is determined in the Schrödinger picture by the free field Hamiltonian [Eq. (3)], subsequently rotates at frequency  $\omega_c$  in phase space, without deformation:  $|\alpha(t)\rangle = |\alpha e^{-i\omega_c t}\rangle$ . This corresponds to the best possible approximation of a classical free oscillator motion. Figure 3(a,b) shows how the vacuum state is transformed by translation into a coherent state and how this state freely evolves in phase space. In Figure 3(b), the coherent states are pictorially shown as uncertainty circles of radius unity at the tip of the classical amplitude, a representation that we shall repeatedly use in the following.

In order to make the translation operation more explicit, it is convenient to split the exponential in Eq. (13) in two, separating the contributions of the real and imaginary parts of  $\alpha$ . We make use of the Glauber relation [12]  $e^{A+B} = e^A e^B e^{-[A,B]/2}$  (valid if  $[A, B]$  commutes with  $A$  and  $B$ ) and we get:

$$D(\alpha) = e^{-i\alpha_1 \alpha_2} e^{2i\alpha_2 X_0} e^{-2i\alpha_1 X_{\pi/2}} . \quad (15)$$

Using a mechanical oscillator analogy, the displacement  $D(\alpha)$  can thus be viewed as a translation along space by an amount  $\alpha_1 = \text{Re}(\alpha)$ , followed by a ‘momentum kick’ of magnitude  $\alpha_2 = \text{Im}(\alpha)$ .

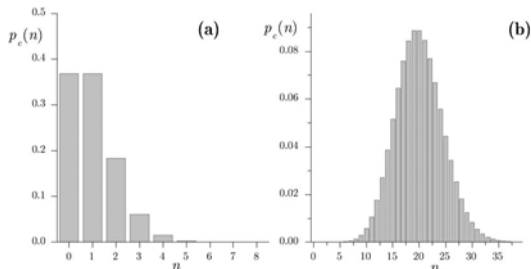


FIGURE 4. Photon number statistical distributions. (a) Coherent field with  $\bar{n} = 1$  photons on the average. (b) Coherent field with  $\bar{n} = 20$ .

Let us compute the probability amplitude for finding the value  $x$  when measuring the quadrature operator  $X_0$  on a field in state  $|\alpha\rangle$ . A straightforward calculation using Eqs. (14) and (15) yields:

$$\langle x | \alpha \rangle = \left( \frac{2}{\pi} \right)^{1/4} e^{-i\alpha_1\alpha_2} e^{2i\alpha_2x} e^{-(x-\alpha_1)^2}, \quad (16)$$

a Gaussian wave packet centered in  $\alpha_1$ , with a phase modulation at frequency  $\alpha_2$  describing the momentum kick. The probability for finding the value  $x$  for the quadrature is thus:

$$P(x) = \left( \frac{2}{\pi} \right)^{1/2} \exp \left[ -2(x - \alpha_1)^2 \right], \quad (17)$$

a translated ground state distribution.

An alternative and useful expression of the displacement operator is obtained by using again the Glauber relation, separating this time the  $a$  and  $a^\dagger$  terms:

$$D(\alpha) = e^{\alpha a^\dagger - \alpha^* a} = \exp \left( -\frac{|\alpha|^2}{2} \right) e^{\alpha a^\dagger} e^{-\alpha^* a}. \quad (18)$$

This form corresponds to the ‘normal ordering’ in quantum optics. If we expand the exponential of operators in series, all the  $a^n$  terms are on the right and the  $a^{\dagger n}$  terms on the left. The action of the  $\exp(-\alpha^* a)$  operator on the right leaves the vacuum unchanged, since only the zero-order term in the expansion yields a non-zero result. Combining Eqs. (14) and (18), we get:

$$|\alpha\rangle = \sum_n c_n(\alpha) |n\rangle \quad \text{with} \quad c_n(\alpha) = \exp \left( -\frac{|\alpha|^2}{2} \right) \frac{\alpha^n}{\sqrt{n!}}. \quad (19)$$

The distribution of photon numbers in a coherent state obeys a Poisson statistics. Figure 4 shows this distribution for  $\alpha = 1$  and  $\alpha = \sqrt{20}$ . The average photon

number  $\bar{n}$  and photon number variances  $\Delta n$  are:

$$\bar{n} = |\alpha|^2 \quad ; \quad \frac{\Delta n}{\bar{n}} = \frac{1}{|\alpha|} = \frac{1}{\sqrt{\bar{n}}} . \quad (20)$$

The relative fluctuation of the photon number is thus inversely proportional to the square root of its average. For large fields, this fluctuation becomes negligible (classical limit).

Coherent states are eigenstates of the photon annihilation operator  $a$ . This essential property is easily derived from Eqs. (2) and (19):

$$a |\alpha\rangle = \alpha |\alpha\rangle \quad \text{and} \quad \langle \alpha | a^\dagger = \langle \alpha | \alpha^* . \quad (21)$$

It is also useful to recall the expression of the scalar product of two coherent states:

$$\langle \alpha | \beta \rangle = e^{-|\alpha|^2/2 - |\beta|^2/2 + \alpha^* \beta} \quad ; \quad |\langle \alpha | \beta \rangle|^2 = e^{-|\alpha - \beta|^2} , \quad (22)$$

which shows that the overlap of two such states decreases exponentially with their ‘distance’ in phase space. Although they are never strictly orthogonal, they become practically so when the distance of their centers is much larger than 1, the radius of the uncertainty circle.

The coherent states constitute a complete set of states in the mode’s Hilbert space:

$$\frac{1}{\pi} \int d\alpha_1 d\alpha_2 |\alpha\rangle \langle \alpha| = \mathbf{1} . \quad (23)$$

Note however that the non-orthogonal coherent state basis is over-complete. The expansion of a state over it is not unique.

Coherent states are easily produced experimentally, by the classical microwave source  $S$  weakly coupled to the cavity mode (see Figure 1). The evolution operator for the mode state under the coupling with a classical current is the displacement operator, transforming the initial vacuum in a coherent state whose amplitude and phase are under experimenter’s control.

As a classical field, a coherent state is defined by a complex amplitude, evolving in the Fresnel plane. The non-vanishing quantum fluctuations of the field quadratures is represented by the uncertainty circle in Figure 3. For very small fields (about one photon on the average) the amplitude is comparable to the uncertainties and quantum fluctuations play an important role. For very large amplitudes, quantum fluctuations are negligible and the coherent state can be viewed as a classical object, with well defined phase and amplitude. Coherent states stored in a cavity thus span the quantum to classical transition, with the mere adjustment of the source controls.

### 2.3. Schrödinger cat states

We give here a special attention to superpositions of two quasi-orthogonal coherent states, represented in the Fresnel plane by two non-overlapping circles. These states are prototypes of Schrödinger cats [13, 14]. We will see later how they can be prepared and used to study the dynamics of decoherence. We enumerate first some of their properties. As a simple example, we consider a linear superposition

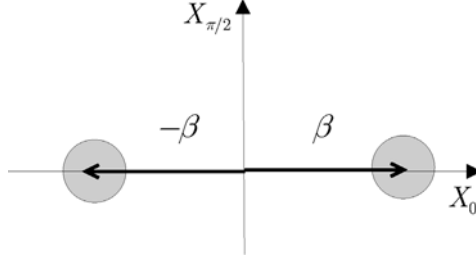


FIGURE 5. Pictorial representation of a  $\pi$ -phase cat in phase space.

with equal weights of two coherent states with opposite phases (see Figure 5). This superposition, called a  $\pi$ -phase cat in the following, writes:

$$|\Psi_{\text{cat}}^{\text{even}}\rangle = \frac{|\beta\rangle + |-\beta\rangle}{\sqrt{2(1 + e^{-2|\beta|^2})}} \approx (1/\sqrt{2})(|\beta\rangle + |-\beta\rangle), \quad (24)$$

where  $\beta$  is the amplitude of the field (taken real). The superscript ‘even’ will be explained below. The denominator in the first r.h.s. term is a normalization factor, taking into account the overlap of  $|\beta\rangle$  and  $|-\beta\rangle$ . If  $|\beta| \gg 1$ , this overlap is negligible and the cat state is expressed by the simpler form given by the second r.h.s. term in Eq. (24).

The coherence between the two states is an essential feature which distinguishes it from a mere statistical mixture. This is made clear by expressing the field density operator:

$$\rho_{\text{cat}} \approx \frac{1}{2} (|\beta\rangle \langle\beta| + |-\beta\rangle \langle-\beta| + |\beta\rangle \langle-\beta| + |-\beta\rangle \langle\beta|). \quad (25)$$

The cat coherence is described by the off-diagonal part of this density operator [last two terms in the r.h.s. of Eq. (25)].

This coherence is displayed by analyzing the field quadrature distribution. Suppose first that we measure  $X_0$ . Its probability distribution is the sum of two Gaussians, centered at  $\pm\beta$ :

$$P_0^{(\text{cat})}(x) \approx \frac{1}{\sqrt{2\pi}} \left( e^{-2(x-\beta)^2} + e^{-2(x+\beta)^2} \right). \quad (26)$$

The probability amplitudes for measuring  $x$  in state  $|+\beta\rangle$  and  $|-\beta\rangle$  do not appreciably overlap and thus cannot interfere: the resulting distribution is simply the sum of those corresponding to the state components. The state coherence is not apparent here. If we measure instead  $X_{\pi/2}$ , the probability distribution is:

$$P_{\pi/2}^{(\text{cat})}(x) \approx \frac{1}{2} \left| \langle x | \beta \rangle + \langle x | -\beta \rangle \right|^2, \quad (27)$$

where the index  $\pi/2$  in  $\langle x |$  indicates an eigenstate of  $X_{\pi/2}$ . The probability  $P_{\pi/2}^{(\text{cat})}(x)$  is the square of the sum of two amplitudes which are both non-zero.

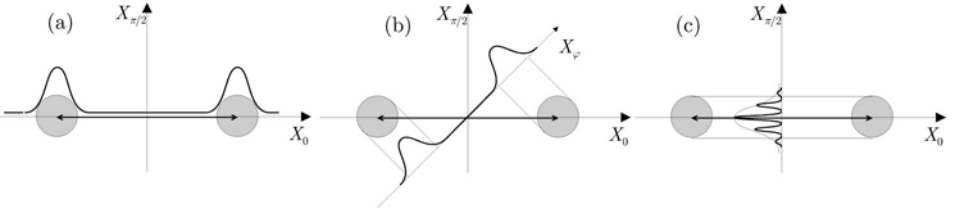


FIGURE 6. Quadratures of an even Schrödinger cat. (a) The  $X_0$  quadrature exhibits well separated Gaussian peaks corresponding to the cat's components. (b) For  $X_{\pi/4}$ , the Gaussian peaks distance is reduced. (c) For  $X_{\pi/2}$  the two peaks merge and fringes show up.

These amplitudes are easy to compute. The scalar product of  $|x\rangle_{\pi/2}$  with  $|\beta\rangle$  is equal to the product of  $|x\rangle_0$  with  $|-i\beta\rangle$ , as a mere rotation in phase space indicates. Using Eq. (16), we get:

$$P_{\pi/2}^{(\text{cat})} \approx \left(\frac{2}{\pi}\right)^{1/2} e^{-2x^2} (1 + \cos 4\beta x) . \quad (28)$$

The probability distribution is a Gaussian centered at  $x = 0$ , modulated by an interference term with fringes having a period  $1/4\beta$ , inversely proportional to the 'cat size'  $\beta$ . This interference is a signature of the coherence of the superposition.

The distribution of any phase quadrature  $X_\varphi$  can be obtained in the same way. The interference term exists only when  $\varphi$  is close to  $\pi/2$ . A graphical representation is very convenient to understand why it is so (Figure 6). For a coherent state, a field quadrature takes non-zero values in an interval corresponding to the projection of the state uncertainty circle on the direction of the quadrature. For a Schrödinger cat state, there are two such intervals, corresponding to the two state components. If  $\beta \gg 1$  and  $\varphi = 0$  [Figure 6(a)], the two intervals are non-overlapping and there is no interference. For a  $\varphi$  value between 0 and  $\pi/2$  [Figure 6(b)], the two intervals are closer than for  $\varphi = 0$ , resulting in two still non-overlapping Gaussians without interference. It is only when  $\varphi$  gets very close to  $\pi/2$  that the two projected intervals overlap along the direction of the quadrature, leading to a large interference term [Figure 6(c)].

Another aspect of the cat states coherence is revealed by considering their photon number distribution. The state given by Eq. (24) develops only along even number states, since the probability for finding  $n$  photons in it is proportional to  $1 + (-1)^n$ , justifying the superscript 'even' in its name. Similarly the cat state:

$$|\psi^{\text{odd}}\rangle = (1/\sqrt{2})[|\beta\rangle - |-\beta\rangle] , \quad (29)$$

develops only along the odd photon numbers. We call it an 'odd phase cat'. The periodicity of the photon number is related to the coherence of the state, since a statistical mixture of  $|\beta\rangle$  and  $|-\beta\rangle$  contains all photon numbers. The modulated

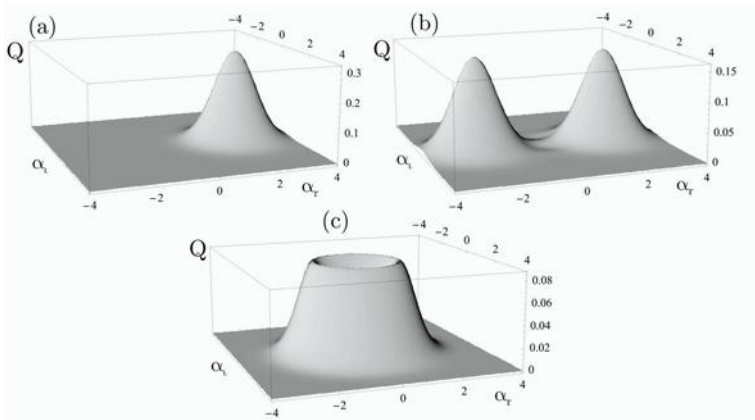


FIGURE 7. Plots of  $Q$  functions. (a) 5 photons coherent state (real amplitude). (b) Schrödinger even cat state, superposition of two 5 photon coherent states with opposite phases. Note the weak interference pattern near the origin. (c) Two-photon Fock state.

photon number distribution is a signature of the even and odd cats coherence, as is the existence of dark fringes in their  $X_{\pi/2}$  quadrature.

It is hence convenient to introduce the photon number parity operator  $\mathcal{P}$  [12] which admits as eigenstates all the superpositions of even photon numbers with the eigenvalue +1 and all the superpositions of odd photon number states with the eigenvalue 1:

$$\mathcal{P} = e^{i\pi a^\dagger a} . \quad (30)$$

The odd and even phase cats  $|\beta\rangle \pm |-\beta\rangle$  are eigenstates of  $\mathcal{P}$  with the +1 and -1 eigenvalues. From Eq. (21), the action of the annihilation operator on an even (odd) phase cat results in the switching of the cat parity:

$$a[|\beta\rangle \pm |-\beta\rangle] = \beta[|\beta\rangle \mp |-\beta\rangle] . \quad (31)$$

Let us remark finally:

$$\mathcal{P}|x\rangle_\varphi = | -x\rangle_\varphi . \quad (32)$$

#### 2.4. A pictorial representation of field states

We used up to now qualitative phase-space representations. These pictures are made fully quantitative by associating unambiguously to the field state, pure or statistical mixture, two functions,  $Q$  and  $W$ , taking real values in phase space [15] and extending in the quantum realm the probability distributions over phase space, which are pivotal in statistical mechanics. They can be plotted and give a vivid description of the state. The knowledge of any one of them is sufficient to reconstruct the field density operator and thus the result probability distribution for any measurement.

**2.4.1. The  $Q$  function.** The field is described by the density operator  $\rho$ . Its  $Q$  function at the point in phase space defined by the complex amplitude  $\alpha$  is:

$$Q(\alpha) = \frac{1}{\pi} \langle \alpha | \rho | \alpha \rangle = \frac{1}{\pi} \text{Tr} [\rho | \alpha \rangle \langle \alpha |] . \quad (33)$$

For a pure state,  $Q$  is the square of the overlap with a coherent state whose amplitude spans the Fresnel plane. It is a real, positive and normalized quantity: the integral of  $Q$  over the whole phase space is equal to 1. An alternative definition of  $Q$  is, using Eq. (14):

$$Q(\alpha) = \frac{1}{\pi} \text{Tr} [|0\rangle \langle 0| D(-\alpha) \rho D(\alpha)] . \quad (34)$$

Thus,  $Q(\alpha)$  is the expectation value of the projector on the vacuum, in the state of the field translated by  $-\alpha$ , leading, as shown below, to a simple experimental determination of  $Q$  [16].

It results directly from Eqs. (33) and (22) that  $Q(\alpha)$  is a Gaussian centered in  $\beta$  for the coherent state  $|\beta\rangle$  [Figure 7(a)]. The  $Q$  function of a Schrödinger cat defined by Eq. (24) is essentially the superposition of two Gaussians, centered at  $\pm\beta$  [Figure 7(b)]. There is a small additional interference term taking non-zero values between these two Gaussians, but it is of the order of the scalar product of the two cat components, vanishingly small as soon as they are separated. The  $Q$  function is thus not appropriate to describe the coherence of a cat. Figure 7(c) shows the  $Q$  function of a  $n = 2$  Fock state, a circular rim around the origin as intuitively expected.

**2.4.2. The Wigner function.** The Wigner distribution  $W(\alpha) = W(x + ip)$  [17] is defined by:

$$W(x, p) = \frac{1}{\pi} \int dx' e^{-2ix'p} \langle x + \frac{x'}{2} | \rho | x - \frac{x'}{2} \rangle . \quad (35)$$

It is the Fourier transform of an off-diagonal matrix element of  $\rho$  in a quadrature representation. The  $W$  function is real and normalized. Contrary to  $Q$ , it can take negative values in domains of phase space, making it clear that it is not a probability distribution. Negative values are, as shown below, a signature of non-classical states.

The  $W$  function of coherent states are again Gaussian functions centered at the amplitude of the state, but their width is  $\sqrt{2}$  times smaller than the one of  $Q$ . The  $W$  function of a  $\pi$ -phase cat is made up of two Gaussian peaks and a large interference pattern between these peaks with an alternance of positive and negative ridges [Figure 8(a)]. This pattern is a signature of the cat's coherence, lacking in the  $W$  function of a statistical mixture. The  $W$  function is thus much better adapted than  $Q$  for the study of a cat's coherence. Figure 8(b) and (c) present the  $W$  function of the  $n = 1$  and  $n = 2$  Fock states which also exhibit negative parts.

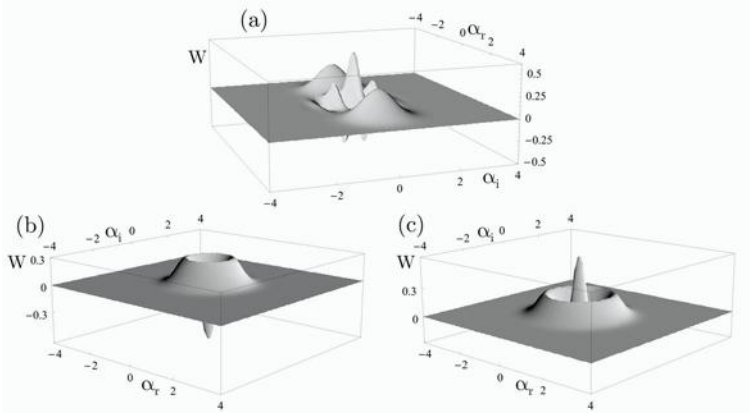


FIGURE 8. Plot of  $W$  functions. (a) Schrödinger cat, superposition of two 5-photon coherent states with opposite phases. (b) One-photon Fock state. (c) Two-photon Fock state.

By inverse Fourier transform of Eq. (35), the matrix elements of the field density operator are:

$$\langle x + \frac{x'}{2} | \rho | x - \frac{x'}{2} \rangle = \int dp e^{2ix'p} W(x, p). \quad (36)$$

The field density operator is thus fully determined by  $W$ . In particular, the probability density of the quadrature  $X_0$ , is:

$$\langle x | \rho | x \rangle = \int dp W(x, p). \quad (37)$$

The probability that  $X_0$  takes a given value  $x$  is obtained by integrating  $W$  for this  $x$  value, along all values of  $p$ . This property holds for any set of orthogonal quadratures. Schrödinger cats, for instance, have quadratures values occurring with 0 probability (see Figure 6), a signature of their non-classical nature. The integral of  $W$  along the orthogonal quadrature vanishes, which is possible only if  $W$  presents alternations of positive and negative values. We thus understand that negativities of  $W$  are related to non-classicality.

We conclude by giving an alternative expression of  $W$  ([18] and L. Davidovich, private communication). Using:

$$|x - \frac{x'}{2}\rangle = e^{-i(x-x')p} D(x + ip) | -\frac{x'}{2} \rangle, \quad (38)$$

and

$$\langle x + \frac{x'}{2} | = \langle \frac{x'}{2} | D(-x - ip) e^{i(x+x')p}, \quad (39)$$

which follow directly from the definition of  $D(\alpha)$  and replacing  $|x \pm x'/2\rangle$  in Eq. (36) by the expressions given by Eqs. (38) and (39), noting finally that  $\mathcal{P}|x'/2\rangle = |-x'/2\rangle$  [see Eq. (32)], we get:

$$W(x, p) = \frac{2}{\pi} \text{Tr}[D(-\alpha)\rho D(\alpha)\mathcal{P}] . \quad (40)$$

The Wigner distribution at  $\alpha$  is the expectation value in the state translated by  $-\alpha$  of the field parity operator. This property leads to a simple experimental determination of  $W$  described in Section 4.2.

## 2.5. Field mode relaxation

**2.5.1. Master equation.** Decoherence is the result of a dissemination of information about a system via its entanglement with an environment  $E$ . For all practical purposes, this information is buried in  $E$  on which no measurement can be performed in practice. The system density operator  $\rho$  is obtained by tracing over  $E$  the system/environment entangled state.

The system relaxation is then described by a master equation, differential equation for  $\rho$  alone. This equation can be derived from a simple environment model [12], a bath of harmonic oscillators, for instance, spanning a wide range of frequencies around the system's eigenfrequencies, in thermal equilibrium at a finite temperature  $T$ . Quite remarkably, the final form of the master equation is model-independent.

For the sake of simplicity, we consider only the zero temperature case. The master equation then writes in the standard Lindblad form:

$$\frac{d\rho}{dt} = -\frac{i}{\hbar} [H'_c, \rho] + \frac{\kappa}{2} [2a\rho a^\dagger - a^\dagger a\rho - \rho a^\dagger a] , \quad (41)$$

where  $\kappa = 1/T_c = \omega_c/Q$  the damping rate of the cavity mode energy. The first term in the r.h.s. describes the Hamiltonian evolution. The second describes the effect of photon escape into  $E$ .

Remarkably, this equation depends only upon the classical energy damping time  $T_c = 1/\kappa$ , which can be measured with macroscopic fields. At finite temperature, additional terms, proportional to  $n_{th}$ , the mean number of thermal photons per mode, describe the creation of thermal excitations in the mode.

It is easy to derive from Eq. (41) the evolution of the photon number distribution  $p(n) = \rho_{nn} = \langle n|\rho|n\rangle$ :

$$\frac{dp(n)}{dt} = \kappa(n+1)p(n+1) - \kappa np(n) . \quad (42)$$

This equation describes a cascade in the Fock states ladder. The lifetime of state  $|n\rangle$  is thus of the order of  $T_c/n$ , decreasing when the number of photon increases. We show below that the lifetime of a coherent state is independent upon its amplitude. That non-classical Fock states are more fragile than semi-classical coherent ones is a first insight into decoherence. We defer to the next section the application of the master equation to a cat state.



FIGURE 9. An environment  $B$  detecting the photon lost by the cavity field.

**2.5.2. Monte Carlo trajectories.** The master equation does not provide a detailed insight into the mechanisms of relaxation. The Monte Carlo wavefunction approach is more convenient for computational purposes and also more insightful. We give here the recipes for the Monte Carlo method in the cavity case and discuss briefly its physical contents. A more detailed account can be found in [19, 20].

The master equation is obtained by tracing over all possible results of a virtual measurement performed over the environment. Let us imagine instead that this measurement is explicitly made and its results recorded. What happens then? For the sake of definiteness, the cavity will be owned by a first operator, called Alice, and Bob has a complete control over the environment.

Bob is to monitor relaxation events, corresponding to the loss of a photon by the mode. He could, for instance (see Figure 9) couple the cavity with a detector, registering a click whenever a photon escapes.

Let us consider a short time interval  $\tau$ . At the beginning, the cavity is in a pure state  $|\phi^{(A)}\rangle$  and Bob's detector in a neutral state  $|0^{(B)}\rangle$ . During the time interval  $\tau$ , the system evolves according to the infinitesimal unitary transformation:

$$|\phi^{(A)}\rangle \otimes |0^{(B)}\rangle \rightarrow \left[ 1 - \frac{1}{2}\kappa\tau(a^\dagger a) \right] |\phi^{(A)}\rangle \otimes |0^{(B)}\rangle + \sqrt{\kappa\tau}a|\phi^{(A)}\rangle \otimes |1^{(B)}\rangle, \quad (43)$$

in which  $|1^{(B)}\rangle$ , orthogonal to  $|0^{(B)}\rangle$ , is the detector's state after photon detection. The time interval  $\tau$  being very short, the probability for losing two photons is negligible. The cavity/environment state is entangled, an essential feature of decoherence.

At the end of this time interval, Bob performs a measurement on its detector, in the  $\{|0^{(B)}\rangle, |1^{(B)}\rangle\}$  basis. The probabilities  $p_1$  and  $p_0$  for finding the environment (equivalent to a single qubit in this simple situation) in  $|1^{(B)}\rangle$  or  $|0^{(B)}\rangle$  are:

$$p_1 = 1 - p_0 = \kappa\tau \langle \phi^{(A)} | a^\dagger a | \phi^{(A)} \rangle. \quad (44)$$

Depending on the outcome of the measurement, the cavity state is projected in one of the states defined as:

$$|\phi_1^{(A)}\rangle = \frac{a|\phi^{(A)}\rangle}{\sqrt{p_1}}, \quad (45)$$

for a photon click and:

$$|\phi_0^{(A)}\rangle = \frac{\left[ 1 - \frac{1}{2}\kappa\tau a^\dagger a \right] |\phi^{(A)}\rangle}{\sqrt{p_0}}. \quad (46)$$

when no click is recorded. Eq. (45) justifies the ‘jump operator’ name coined for  $\sqrt{\kappa}a$ , since it describes the discontinuous change of the mode state when  $B$  is found in  $|1^{(B)}\rangle$ . In the event that  $B$  does not change, Eq. (46) shows that the oscillator state is also modified. It evolves under the effect of an infinitesimal non-unitary transformation produced by the anti-hermitian pseudo-Hamiltonian  $i\hbar\kappa a^\dagger a$ . This non-unitary transformation can be described as a renormalization of the oscillator frequency by the addition of an imaginary term in its frequency ( $\omega \rightarrow \omega - i\kappa/2$ ). It does not conserve the norm of the state, hence the necessity to normalize it by the  $(p_0)^{-1/2}$  factor.

That the cavity state evolves when no photon is recorded by Bob might seem counterintuitive. Recall however that a null measurement provides information on the system and, hence, modifies its state. Recording no photon during  $\tau$  is an indication that the number of photons is more likely to be small. The pseudo-Hamiltonian describes the reduction of the field energy associated to this information. We give below a more detailed insight into this evolution.

At the end of the time interval, the cavity is yet in a pure state, depending upon the measurement result recorded by Bob. A Monte Carlo trajectory is then defined by a series of random measurement results associated to successive time bins of duration  $\tau$ . At each step, the field state undergoes the action of either  $[1 - \kappa\tau a^\dagger a/2]$  or  $a$ , depending upon the measurement result. It is computed by iterating the process, making a random decision according to the probability law (44) to determine whether  $B$  is found in  $|1^{(B)}\rangle$  or  $|0^{(B)}\rangle$  at each stage. The state of  $A$  at the beginning of the  $(n + 1)^{\text{th}}$  step is determined by the outcome of the  $n^{\text{th}}$  measurement and  $B$  is initialized to  $|0^{(B)}\rangle$  at the beginning of each step.

The master equation result is recovered by assuming that Bob’s measurements are left unread. The cavity mode ends up, at the end of the first time interval  $\tau$ , in the density operator averaged over the two possible outcomes:

$$\rho(\tau) = p_0 |\phi_0^{(A)}\rangle\langle\phi_0^{(A)}| + p_1 |\phi_1^{(A)}\rangle\langle\phi_1^{(A)}|. \quad (47)$$

Plugging in this equation the expressions (45) and (46) and keeping the first order terms in  $\tau$ , we get:

$$\rho(\tau) - |\phi^{(A)}\rangle\langle\phi^{(A)}| = -\frac{\kappa\tau}{2} \left[ a^\dagger a, |\phi^{(A)}\rangle\langle\phi^{(A)}| \right]_+ + \kappa\tau a |\phi^{(A)}\rangle\langle\phi^{(A)}| a^\dagger, \quad (48)$$

where  $[\cdot]_+$  is an anti-commutator. Identifying  $(\rho(\tau) - |\phi^{(A)}\rangle\langle\phi^{(A)}|)/\tau$  with  $d\rho/dt$ , we recover the master equation (41).

The Monte-Carlo approach has many advantages. Assuming that Bob is observing the environment and communicating the results of his measurements to Alice means that she can, at all times, describe her system by a wavevector which evolves randomly, according to the unpredictable outcomes of the measurements. Calculating a set of Monte Carlo trajectories can be much more economical, for large photon numbers, or more generally for high-dimensionality systems, than solving the master equation.

Moreover, this approach is adapted to the description of a single realization of an experiment manipulating a unique quantum system. In many modern experiments, an information is continuously extracted from the system's environment and its wave function follows a random trajectory exhibiting explicit quantum jumps [21, 22, 23]. The statistics of these jumps is reproduced by a Monte Carlo simulation involving an environment with as many states as the number of possible exclusive measurements outcomes. In most cases, this number is small and a few quantum states of the environment detectors owned by Bob are enough to simulate the experimental results.

The Monte Carlo procedure is easily applied to the relaxation of a Fock state  $|n\rangle$ . Being an eigenstate of the pseudo-Hamiltonian, a Fock state does not evolve between quantum jumps. Each quantum jump is a transition between two adjacent Fock states. The cavity is always in a Fock state and the photon number undergoes a staircase evolution, with random jumps. The usual exponential decay is recovered by averaging many trajectories. We now turn to the interesting case of an initial coherent state. A Monte Carlo scenario for Schrödinger cat decoherence will be considered in the next section.

**2.5.3. The coherent state paradox.** Let us describe the Monte Carlo trajectories starting from a coherent state  $|\beta\rangle$ . The probability for counting a photon in the first time interval is  $p_1 = \kappa\tau\langle\beta|a^\dagger a|\beta\rangle = \kappa\tau|\beta|^2 = \kappa\tau\bar{n}$ . If a photon is counted, the state is unchanged since  $|\beta\rangle$  is an eigenstate of the jump operator  $\sqrt{\kappa}a$ . An evolution occurs if no photon is recorded. The imaginary frequency contribution to the pseudo Hamiltonian produces a decrease of the state amplitude:

$$|\beta\rangle \rightarrow |\beta e^{-\kappa\tau/2}\rangle. \quad (49)$$

This situation is paradoxical, since the field loses energy only if no photons are counted! How comes that the state does not change when one photon has been lost? We have the combination of two effects, which tend to change the photon number in opposite directions. On the one hand, the loss of a quantum reduces the average energy in the cavity. On the other hand, the photon click provides an information about the state in which the field was just before the photon was emitted, which tends to increase the photon number.

To understand this point, let us ask a simple question: knowing that it has emitted a photon at a given time, what is the probability  $p_c(n)$  that the cavity contained  $n$  photons just before the click? If the photon emission probability were independent on  $n$ ,  $p_c(n)$  would be equal to  $p(n) = e^{-\bar{n}}\bar{n}^n/n!$ , the photon number distribution in the coherent state. In fact, the probability for losing a photon is proportional to  $n$ . It follows that  $p_c(n) = knp(n)$ , where  $k = 1/\bar{n}$  is determined by normalization. Thus:

$$p_c(n) = \frac{np(n)}{\bar{n}} = e^{-\bar{n}}\frac{\bar{n}^{n-1}}{(n-1)!} = p(n-1). \quad (50)$$

For a coherent state,  $p_c(n)$  is equal to  $p(n-1)$ , the unconditional probability that the initial field contains  $n-1$  photons. The maximum of  $p(n-1)$ , hence

of  $p_c(n)$ , occurs for  $n = \bar{n} + 1$ . The knowledge that a click has occurred biases the photon number distribution before this click towards larger  $n$  values, with a photon number expectation exceeding the *a priori* average value by one unit. The loss of the photon signaled by the click brings this number back down to  $\bar{n}$ . The two effects exactly cancel and the state of the field has not changed!

This is a peculiar property of coherent states. For non-poissonian fields with larger fluctuations, the effect could be even more counter-intuitive and result in an overall increase of the photon expectation number, just after the loss of a photon! This situation requires fluctuations in the initial field energy. It does not occur for a Fock state, which loses its energy in an intuitive way.

Why, now, are coherent states losing their energy when no photon clicks are registered? If no photon is detected, it is more likely that the photon distribution has less photons than was *a priori* assumed. To consider an extreme situation, a coherent field has a small probability,  $e^{-\bar{n}}$ , for containing no photon at all. This is the probability that the detector will never click, however long one waits. The longer the period without click, the more likely it becomes that the field is effectively in vacuum. Its wave function evolves continuously, without jump, under the effect of the non-unitary evolution and ends up in  $|0\rangle$ !

The insensitivity of coherent states to jumps make their Monte Carlo trajectories certain. To determine the state at time  $t$ , we have concatenate evolutions during the successive intervals between jumps  $t_1, t_2, \dots, t_i, \dots, t_N$  adding up to  $t$ . Whatever the distribution of these intervals, the final state,  $|\beta e^{-\kappa(t_1+t_2+\dots+t_N)/2}\rangle = |\beta e^{-\kappa t/2}\rangle$  remains pure: coherent states are impervious to entanglement with the environment. They are the ‘pointer states’ of cavity decoherence.

### 3. Cat state generation and decoherence studies

In the last section, we described Schrödinger cat states, quantum superpositions of coherent components with different classical phases. These states are ideal for decoherence studies, since they are pretty well isolated from their environment, being stored in a high- $Q$  cavity. Moreover, their ‘size’, measured by the distance between the two components, can be varied from the microscopic range (single photon fields) to the mesoscopic one. We describe in this section how the interaction between a single Rydberg atom and a coherent state can be harnessed to produce and probe Schrödinger cat states. We first give a brief description of the atom/field interaction.

#### 3.1. The atom/cavity system

We consider a two-level atom whose upper level  $|e\rangle$  is connected to level  $|g\rangle$  by a dipole electric transition at angular frequency  $\omega_{eg}$ . This system is equivalent to a spin-1/2 evolving in an abstract space, with a magnetic field, oriented along the ‘vertical’  $Z$  axis, accounting for the energy difference between  $|e\rangle$  and  $|g\rangle$ . These states correspond to the eigenstates of the spin along  $Z$ , which we denote by  $|+\rangle$  and  $|-\rangle$ .

Any spin or atomic operator can be expanded over the basis made up of the three Pauli matrices  $\sigma_X$ ,  $\sigma_Y$  and  $\sigma_Z$  together with the unity  $\mathbb{1}$ . The atomic Hamiltonian is  $H_a = \hbar\omega_{eg}\sigma_Z/2$ . The atomic raising and lowering operators  $\sigma_{\pm}$  are  $\sigma_{\pm} = (\sigma_X \pm i\sigma_Y)/2$ , with  $\sigma_+|-\rangle = |+\rangle$   $\sigma_-|+\rangle = |-\rangle$   $\sigma_+|+\rangle = 0$   $\sigma_-|-\rangle = 0$ . These atomic excitation creation/annihilation operators have a fermionic commutation  $\{\sigma_-, \sigma_+\} = 1$ , where  $\{, \}$  denotes an anti-commutator. There is a clear analogy between  $\sigma_{\pm}$  and the photon creation and annihilation operators.

The atomic dipole operator is:

$$\mathbf{D} = d(\epsilon_a\sigma_- + \epsilon_a^*\sigma_+) , \quad (51)$$

where  $\epsilon$  is a complex unit vector describing the transition polarization. For the circular states with principal quantum numbers 51 and 50, the transition is  $\sigma$ -polarized and  $d = 1776$  atomic units, a remarkably large value due to the huge size of the Rydberg states.

The complete atom-cavity Hamiltonian writes:

$$H = H_a + H'_c + H_{ac} , \quad (52)$$

where  $H_a$  and  $H'_c$  are the atom and cavity Hamiltonians. The coupling term,  $H_{ac}$ , is  $-\mathbf{D} \cdot \mathbf{E}_c$ , where  $\mathbf{E}_c$  the electric field operator at the atomic location. The Hamiltonian  $H$  has been introduced by Jaynes and Cummings [24] as an approximation to matter-field coupling in free space. It is only in a cavity that it provides a precise description of the atomic dynamics, since the interaction with a single mode dominates the evolution.

We assume first that the atom is sitting at cavity centre [ $f(\mathbf{r}) = 1$ ]. The coupling Hamiltonian is then:

$$H_{ac} = -d[\epsilon_a\sigma_- + \epsilon_a^*\sigma_+] \cdot i\mathcal{E}_0 [\epsilon_c a - \epsilon_c^* a^\dagger] . \quad (53)$$

Its expansion involves four terms. Two are proportional to  $\sigma_- a$  and  $\sigma_+ a^\dagger$ . The first corresponds to a transition from  $|e\rangle$  to  $|g\rangle$ , together with the annihilation of a photon. The second describes the emission of a photon by an atom in a transition from  $|g\rangle$  to  $|e\rangle$ . When the cavity and atomic transition frequencies,  $\omega_c$  and  $\omega_{eg}$ , are comparable, these terms correspond to non-resonant processes. They can be neglected (Rotating Wave Approximation). The two others, proportional to  $\sigma_+ a$  and  $\sigma_- a^\dagger$ , correspond to photon absorption or emission and the atom-cavity coupling reduces to:

$$H_{ac} = -i\hbar\frac{\Omega_0}{2} [a\sigma_+ - a^\dagger\sigma_-] , \quad (54)$$

where we introduce the 'single photon Rabi frequency',  $\Omega_0$ :

$$\Omega_0 = 2\frac{d\mathcal{E}_0\epsilon_a^* \cdot \epsilon_c}{\hbar} . \quad (55)$$

We assumed that  $\epsilon_a^* \cdot \epsilon_c$  is real and positive, hence  $\Omega_0$ . The frequency  $\Omega_0$  measures the strength of the atom-field coupling. It is proportional to the interaction energy of the atomic dipole with a classical field corresponding to a single photon stored in  $C$ . In our experiments  $\Omega_0 = 2\pi \times 50$  kHz, a rather large value. It is much larger

than the cavity relaxation rate, achieving the ‘strong coupling regime’ of cavity QED.

The ‘uncoupled states’, eigenstates of  $H_a + H'_c$ , are the tensor products  $|e, n\rangle$  and  $|g, n\rangle$  of atomic energy eigenstates and cavity Fock states, with the energies  $\hbar(\omega_{eg}/2 + n\omega_c)$  and  $\hbar(-\omega_{eg}/2 + n\omega_c)$ . The ground state of  $H_a + H'_c$  is the non-degenerate  $|g, 0\rangle$  state. When the atom-cavity detuning,  $\Delta_c = \omega_{eg} - \omega_c$ , is much smaller than the atomic frequency, the uncoupled states  $|e, n\rangle$  and  $|g, n+1\rangle$  are degenerate ( $\Delta_c = 0$ ) or nearly degenerate. They form a ladder of equally-spaced two-level manifolds, which are not coupled by  $H_{ac}$ . The diagonalization of the full Hamiltonian amounts to solving separate two-level problems.

**3.1.1. Eigenenergies and eigenvectors.** We consider here the restriction  $H_n$  of the Jaynes and Cummings Hamiltonian to the manifold spanned by  $|e, n\rangle$  and  $|g, n+1\rangle$ . Taking the energy reference at the mid-point between these levels,  $H_n$  writes in matrix form:

$$H_n = \frac{\hbar}{2} \begin{pmatrix} \Delta_c & -i\Omega_n \\ i\Omega_n & -\Delta_c \end{pmatrix}, \quad (56)$$

where

$$\Omega_n = \Omega_0 \sqrt{n+1}. \quad (57)$$

The Rabi frequency  $\Omega_n$  is proportional to  $\sqrt{n+1}$ , relative field amplitude in the  $n$ -photons Fock state.

The eigenvalues of  $H_n$  are :

$$E_n^\pm = \pm \frac{\hbar}{2} \sqrt{\Delta_c^2 + \Omega_n^2}, \quad (58)$$

and the eigenvectors, the ‘dressed states’:

$$|\pm, n\rangle = \cos \theta_n^\pm |e, n\rangle + i \sin \theta_n^\pm |g, n+1\rangle, \quad (59)$$

are generally entangled atom-cavity states. The mixing angles  $\theta_n^\pm$  are given by

$$\tan \theta_n^\pm = \pm \frac{\sqrt{\Delta_c^2 + \Omega_n^2} \mp \Delta_c}{\Omega_n}. \quad (60)$$

The positions of the dressed energies are represented as a function of  $\Delta_c$  on Figure 10. For large detunings, the dressed energies almost coincide with the uncoupled ones  $\pm \hbar \Delta_c / 2$ . At zero detuning, the uncoupled levels cross. The atom-cavity coupling transforms this crossing into an avoided crossing, the minimum distance between the dressed states being  $\hbar \Omega_n$ . We examine now two limiting cases: the resonant case ( $\Delta_c = 0$ ) and the detuned case ( $\Delta_c \gg \Omega$ ).

**3.1.2. Resonant coupling.** In the resonant case, the mixing angles are  $\theta_n^\pm = \pm \pi/4$  and:

$$|\pm, n\rangle = \frac{1}{\sqrt{2}} [|e, n\rangle \pm i |g, n+1\rangle]. \quad (61)$$

The separation of the dressed states at resonance,  $\hbar \Omega_n$ , corresponds to the frequency of the atom-field reversible energy exchange. We consider an atom in

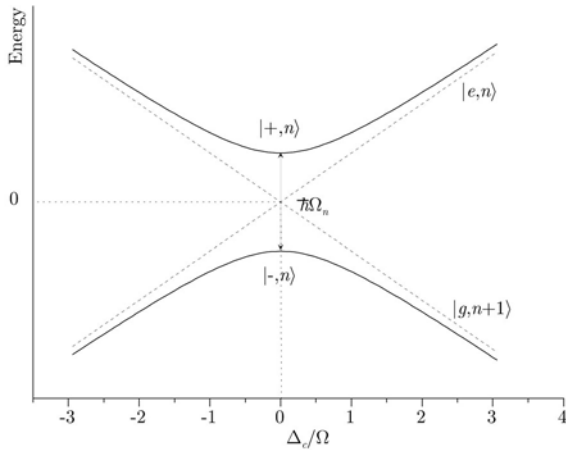


FIGURE 10. Dressed states energies as a function of the atom-cavity detuning  $\Delta_c$ . The uncoupled states energies are represented as dotted lines.

state  $|e\rangle$  at time  $t = 0$  inside the cavity containing  $n$  photons. The initial state,  $|\Psi_e(0)\rangle = |e, n\rangle$ , expands on the dressed states basis as:

$$|\Psi_e(0)\rangle = \frac{1}{\sqrt{2}} [|+, n\rangle + |-, n\rangle] , \quad (62)$$

and becomes at time  $t$ :

$$|\Psi_e(t)\rangle = \frac{1}{\sqrt{2}} \left[ |+, n\rangle e^{-i\Omega_n t/2} + |-, n\rangle e^{i\Omega_n t/2} \right] . \quad (63)$$

The probabilities of finding the atom in  $|e\rangle$  or  $|g\rangle$  are obtained by returning to the uncoupled basis :

$$|\Psi_e(t)\rangle = \cos \frac{\Omega_n t}{2} |e, n\rangle + \sin \frac{\Omega_n t}{2} |g, n+1\rangle . \quad (64)$$

The coupling results in a reversible exchange between  $|e, n\rangle$  and  $|g, n+1\rangle$  at frequency  $\Omega_n$ . This is the Rabi oscillation phenomenon. It can be understood as a ‘quantum beat’ between the two dressed states [see Eq. (63)]. For the initial state  $|e, 0\rangle$  (or  $|g, 1\rangle$ ), this oscillation occurs at the frequency  $\Omega_0$ .

**3.1.3. Non-resonant atom/cavity coupling.** We give here a perturbative treatment valid for large detunings [25, 26]. We assume  $\Delta_c = \omega_{eg} - \omega_c > 0$ , with  $\theta_n \ll 1$ . We develop the eigenstates and eigenenergies in powers of  $\Omega_0 \sqrt{n+1} / \Delta_c$ . To first

order for states and to second order for energies:

$$\begin{aligned}
|+, n\rangle &\approx |e, n\rangle + \frac{\Omega_0\sqrt{n+1}}{2\Delta_c} |g, n+1\rangle \\
|-, n\rangle &\approx -|g, n+1\rangle + \frac{\Omega_0\sqrt{n+1}}{2\Delta_c} |e, n\rangle \\
\frac{1}{\hbar}E_{+,n} &= n\omega_c + \frac{\omega_{eg}}{2} + \frac{\Omega_0^2(n+1)}{4\Delta_c} \\
\frac{1}{\hbar}E_{-,n} &= (n+1)\omega_c - \frac{\omega_{eg}}{2} - \frac{\Omega_0^2(n+1)}{4\Delta_c}.
\end{aligned} \tag{65}$$

The dressed states  $|+, n\rangle$  and  $|-, n\rangle$  are very close to the uncoupled states, which are slightly ‘contaminated’ by the atom-field coupling. The energies of these levels are shifted to second order by an amount proportional to  $n+1$ , combination of a light shift, proportional to  $n$ , and of a Lamb shift effect.

Assume now that we couple an atom in level  $|e\rangle$  with a coherent field  $|\alpha\rangle$  and let the two systems interact for a time  $t$ . Expanding the coherent state on a Fock state basis and taking into account that  $|e, n\rangle$  is very close to the  $|+, n\rangle$  dressed state, we get:

$$\begin{aligned}
|\Psi_{e,\alpha}(0)\rangle &= |e\rangle |\alpha\rangle = \sum_n c_n |e, n\rangle \quad \Rightarrow \\
|\Psi_{e,\alpha}(t)\rangle &\approx \sum_n c_n e^{-in\omega_c t} e^{-i\omega_{eg}t/2} e^{-i\Omega_0^2(n+1)t/4\Delta_c} |e, n\rangle,
\end{aligned} \tag{66}$$

which, in interaction picture yields:

$$\left| \tilde{\Psi}_{e,\alpha}(t) \right\rangle \approx \sum_n c_n e^{-i\Omega_0^2(n+1)t/4\Delta_c} |e, n\rangle = e^{-i\Omega_0^2 t/4\Delta_c} |e\rangle \otimes \left| \alpha e^{-i\Omega_0^2 t/4\Delta_c} \right\rangle. \tag{67}$$

Similarly, for an atom initially in level  $|g\rangle$  we obtain:

$$\left| \tilde{\Psi}_{g,\alpha}(t) \right\rangle \approx \sum_n c_n e^{+i\Omega_0^2 nt/4\Delta_c} |g, n\rangle = |g\rangle \otimes \left| \alpha e^{+i\Omega_0^2 t/4\Delta_c} \right\rangle. \tag{68}$$

The cavity is in a coherent state, phase shifted by an angle  $\pm\Phi_0 = \pm\Omega_0^2 t/4\Delta_c$  depending upon the atomic state. This effect is interpreted by attributing to the atom an index  $N_i = 1 \pm \Omega_0^2/4\Delta_c\omega_c$ , with the + and - signs corresponding respectively to an atom in  $|e\rangle$  or  $|g\rangle$ . With the parameters of our experiment we find, for  $\Delta_c = 3\Omega$ ,  $|N_i - 1| = 10^{-7}$ , a huge value for a single atom effect. Note that this index is linear for extremely low fields only and saturates for average photon numbers of the order of  $(\delta/\Omega_0)^2$ , since the dispersive regime condition is no longer fulfilled. Note also the global quantum phase shift of the system’s state when the atom is in  $|e\rangle$ . This is a cavity Lamb shift effect.

Up to now, we have considered the atom as motionless at cavity center. In the actual experiment, the atom flies across the cavity mode waist  $w$ . The atom-field coupling, proportional to the relative mode amplitude  $f$ , is thus a time-dependent

quantity. In the dispersive regime, the previous results still hold, when the time  $t$  is replaced by an effective interaction time  $t_i^d$  taking into account the integrated atom-field coupling. For a full crossing of the mode:

$$t_i^d = \sqrt{\frac{\pi}{2}} \frac{w}{v}. \quad (69)$$

Note that the same approach can be used in the resonant case, with a different effective interaction time  $t_i^r$ :

$$t_i^r = \sqrt{\pi} \frac{w}{v}. \quad (70)$$

### 3.2. Dispersive cat generation

The phase shift produced by a single atom on a coherent state takes opposite values for levels  $|e\rangle$  and  $|g\rangle$ . Phase shift values as large as a few radians can be reached. The ability of a single atom to shift by a macroscopic angle the phase of a field containing many quanta provides an ideal tool for experiments with cat states. When an atom is sent across the cavity in a superposition of  $|e\rangle$  and  $|g\rangle$ , a mesoscopic cat is produced in the cavity.

**3.2.1. Reading the phase imprint of a single atom.** We first measure these phase shifts. The usual method to measure the phase of a coherent ‘signal’ in quantum optics is homodyning: the signal is mixed with a reference of same frequency and variable phase  $\varphi$ . The phase distribution of the signal is obtained by measuring the intensity of the mixed signal + reference as a function of  $\varphi$ .

We have adapted this general method to our set-up and measured by homodyning the phase shift induced by a single atom on a coherent field [27]. The experimental sequence involves two successive field injections in the cavity, and two atoms. First, a signal field with amplitude  $\beta$  is injected by connecting the cavity to the source  $S$  for  $2 \mu\text{s}$ . The modulus of  $\beta$  is calibrated in an independent experiment, using the light shift on a non-resonant atom [28]. An off-resonant index atom  $A_i$  (atom-cavity detuning  $\Delta_c$ ), prepared with velocity  $v$  in level  $|e\rangle$  or  $|g\rangle$ , is then sent across the cavity and imprints its phase shift  $\pm\Phi_0$  on the field whose amplitude becomes  $\beta \exp(\pm i\Phi_0)$ .

The  $\Phi_0$  value is adjusted by an independent control of the  $\Delta_c$  and  $v$  parameters. The detuning  $\Delta_c$  is tuned from a few tens to a few hundred kHz by Stark-shifting the atomic transition frequency. A second reference field injection follows before the cavity field has had time to appreciably decay. This reference has a complex amplitude  $-\alpha = -\beta \exp(i\varphi)$ . Its modulus is the same as the one of the signal field, but its phase  $\varphi$  can be continuously adjusted.

To probe the final cavity field, we use a second atom,  $A_p$ . This atom is sent in  $|g\rangle$ . It is tuned at resonance with the mode and absorbs the homodyned field. The information provided by the probe atom absorption is used, in a repetitive experiment, to reconstruct the  $Q$  function of the phase-shifted field [16]. Let us recall that  $Q(\alpha)$  is  $1/\pi$  times the probability  $p(0)$  for finding the cavity in the

vacuum, after the field has been translated by the amplitude  $-\alpha$  [see Eq. (34) in Section 2.4]. This translation is realized by reference field injection.

Ideally, we want a dichotomic signal indicating whether the final number of photons is zero or not. Let us call  $P_e(n)$  the probability for finding  $A_p$  in  $|e\rangle$  when there are  $n$  photons in  $C$ . Obviously  $P_e(0) = 0$ . A dichotomic signal would be obtained if  $P_e(n)$  were different from 0 and independent of  $n$  for all  $n \geq 1$ . This is not the case for an arbitrary atom-field effective interaction time  $t_i^r$ , since the atom undergoes a Rabi oscillation whose period is  $n$ -dependent.

It is nevertheless possible to select an optimal effective interaction time  $t_i^r = t_{\text{opt}} = 5\pi/2\Omega_0$ , for which  $P_e(1)$ ,  $P_e(2)$  and  $P_e(3)$  are approximately equal to  $1/2$ . For larger  $n$ 's, this condition is not fulfilled for an ideal quantum Rabi oscillation. However, experimental imperfections wash out the oscillations for large photon numbers. Practically, we also get, to a good approximation,  $P_e(n) = 1/2$  for  $n > 3$ . Hence, the probability  $P_e$  for detecting  $A_p$  in  $|e\rangle$  is  $P_e = [1 - p(0)]/2$  and  $Q(\alpha) = (1 - 2P_e)/\pi$ . The variation of  $P_e$  when  $\varphi$  is swept determines directly  $Q$  along a circle of radius  $|\beta|$ . The experiment is performed with an index atom  $A_i$  either in  $|e\rangle$  or in  $|g\rangle$  or, for reference, without sending  $A_i$ . The experimental signals are shown in Figure 11 ( $\Delta_c/2\pi = 50$  kHz,  $v = 200$  m/s). The coherent field contains 29 photons in average. The open circles represent  $Q$  when  $A_i$  is not sent. This peak serves as a reference for the signals shown as black circles and black squares, which correspond respectively to  $A_i$  in level  $|e\rangle$  or  $|g\rangle$ . The observed phase shift,  $\pm\Phi_0 = \pm 39^\circ$  is in agreement with the theoretical expectations.

**3.2.2. Trapping a cat in an atomic interferometer.** This single-atom index effect can be exploited to generate cat states of the field. We merely have to cast  $A_i$ , prepared initially in  $|e\rangle$ , in a superposition of states  $|e\rangle$  and  $|g\rangle$  by a classical microwave pulse  $R_1$  before  $A_i$  enters the mode. The field then acquires two distinct classical phases at once and gets entangled with the atom. This entanglement can be analyzed by finally detecting the atomic state after the atom exits  $C$ . This analysis is carried out by combining a second microwave pulse  $R_2$  with a state selective detector  $D$ .

Let us follow the successive stages of this experiment. The atom is prepared by  $R_1$  in the superposition  $(|e\rangle + |g\rangle)/\sqrt{2}$ . After it has crossed  $C$ , the atom-field system evolves into the entangled state:

$$|\Psi_1\rangle = \frac{e^{-i\Phi_0}}{\sqrt{2}}|e\rangle \otimes |\beta e^{-i\Phi_0}\rangle + \frac{1}{\sqrt{2}}|g\rangle \otimes |\beta e^{i\Phi_0}\rangle. \quad (71)$$

This is a typical quantum measurement situation, in which a large ‘meter’ (the field) points simultaneously towards different directions corresponding to two orthogonal states of a microscopic system ( $A_i$ ). If  $A_i$  were directly detected at the cavity exit in  $|e\rangle$  or  $|g\rangle$ , the field would be projected in the corresponding coherent state and the quantum ambiguity lost. The atom’s measurement would tell us whether the dispersive index had taken one value or the other.

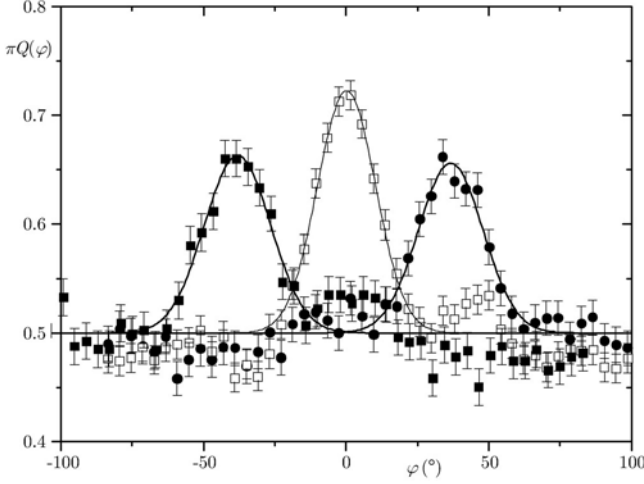


FIGURE 11. Phase-shift of a coherent field. Field phase distribution  $\pi Q(\varphi)$  as a function of the displacement phase  $\varphi$  in degrees. Open squares: reference 29 photons coherent field. Solid circles (squares): phase distribution after interaction with an atom in  $|e\rangle$  ( $|g\rangle$ ). The error bars depict statistical fluctuations. The solid lines are Gaussian fits.

The second microwave pulse  $R_2$  can be used to preserve the blurred state of the meter by erasing the information about the atomic index. Let us apply in  $R_2$  the transformations:

$$|e\rangle \rightarrow \frac{1}{\sqrt{2}} (|e\rangle + e^{i\chi}|g\rangle) \quad ; \quad |g\rangle \rightarrow \frac{1}{\sqrt{2}} (|g\rangle - e^{-i\chi}|e\rangle) \quad , \quad (72)$$

where  $\chi$  can be adjusted freely by setting the relative phase of the  $R_1$  and  $R_2$  pulses. Immediately after  $R_2$ , the combined atom-field state is:

$$|\Psi_2\rangle = \frac{1}{2}|e\rangle \otimes [e^{-i\Phi_0}|\beta e^{-i\Phi_0}\rangle - e^{-i\chi}|\beta e^{i\Phi_0}\rangle] \\ + \frac{1}{2}|g\rangle \otimes [e^{i(\chi-\Phi_0)}|\beta e^{-i\Phi_0}\rangle + |\beta e^{i\Phi_0}\rangle] \quad . \quad (73)$$

The two states  $|e\rangle$  and  $|g\rangle$  are now correlated to two cat states, mutually orthogonal when  $\Phi_0 > 1/\sqrt{n}$ . The phase  $\chi$  of the second Ramsey zone can be adjusted to simplify a little bit the expressions of the cat states. Setting  $\chi = \Phi_0$ , we get:

$$|\Psi_2\rangle = \frac{e^{-i\Phi_0}}{2}|e\rangle \otimes [|\beta e^{-i\Phi_0}\rangle - |\beta e^{i\Phi_0}\rangle] + \frac{1}{2}|g\rangle \otimes [|\beta e^{-i\Phi_0}\rangle + |\beta e^{i\Phi_0}\rangle] \quad . \quad (74)$$

This equation shows that the final detection of the atom projects with equal probabilities the field into one of the two cat states  $[|\beta e^{-i\Phi_0}\rangle \pm |\beta e^{i\Phi_0}\rangle]/\sqrt{2}$ .

When  $\Phi_0 = \pi/2$ , these states become the even and odd  $\pi$ -phase cat states [Eq. (24) and (29)]:

$$|\Psi_2\rangle = -\frac{i}{2}|e\rangle \otimes [|\gamma\rangle - |-\gamma\rangle] + \frac{1}{2}|g\rangle \otimes [|\gamma\rangle + |-\gamma\rangle] , \quad (75)$$

where  $\gamma = -i\beta$ . It is impossible to predict the field state eventually obtained, which is revealed only by the outcome of the atomic measurement.

We shall describe later how this cat can be probed by a ‘quantum mouse’. Before that, the simple detection of the index atom  $A_i$  provides some information about the cat generation and sheds an interesting light onto this experiment. What are then the probabilities for detecting  $A_i$  in either levels?

Let us suppose first that we apply onto  $A_i$  only the  $R_1$  and  $R_2$  pulses. We recognize a Ramsey atomic interferometer [29], widely used in high-precision atomic clocks. The probability,  $P_g$ , for observing finally the atom in level  $|g\rangle$  exhibits modulations (Ramsey fringes) as a function of the relative pulse phase  $\chi$ :  $P_g = (1 + \cos \chi)/2$ . This modulation results from a quantum interference effect. When the atom is finally in  $|g\rangle$ , the transition may occur either during the first pulse,  $R_1$ , or during the second,  $R_2$ . These two quantum paths are indistinguishable and the corresponding probability amplitudes interfere.

When the cavity is inserted between  $R_1$  and  $R_2$ , the interferometric signal provides an information about the atom-cavity interaction. We shall, first, consider the case of an empty cavity. By setting  $\beta = 0$  in Eq. (73), we obtain for the final atom-field system:

$$|\Psi_2^{(\beta=0)}\rangle = \frac{e^{-i\Phi_0}}{2} \left[ 1 - e^{-i(\chi-\Phi_0)} \right] |e, 0\rangle + \frac{1}{2} \left[ 1 + e^{i(\chi-\Phi_0)} \right] |g, 0\rangle , \quad (76)$$

which yields the probabilities  $P_e^0$  and  $P_g^0 = 1 - P_e^0$  for finding the atom in  $|e\rangle$  or  $|g\rangle$ :

$$P_e^0 = 1 - P_g^0 = \frac{1 - \cos(\chi - \Phi_0)}{2} . \quad (77)$$

The fringes are phase shifted by an angle  $\Phi_0$  with respect to their position if there were no cavity between  $R_1$  and  $R_2$ . The phase shift of the atomic superposition between the two pulses reflects the transient Lamb shift of level  $|e\rangle$  in the empty cavity mode (Section 3.1).

When the cavity contains a coherent field with  $\bar{n}$  photons on average, this field undergoes different phase shifts, depending on the state of the atom between  $R_1$  and  $R_2$ . The final cavity field amplitude measures the atomic state between the two pulses. We recognize here the ingredients of a ‘which-path’ experiment.

Such gedanken experiments have been discussed in the early days of quantum theory. A Young interferometer, for instance, produces fringes due to the interference between two quantum paths corresponding to its two slits. Bohr’s complementarity states that these fringes are incompatible with any unambiguous information about the path actually followed by the particle in the interferometer.

We are thus discussing here a complementarity situation. If the two final cavity states are orthogonal, which occurs for  $\Phi_0 > 1/\sqrt{\bar{n}}$ , they could, by the

detection of their phase, tell away the path of the atom. This is enough to destroy the fringes. In more quantitative terms, the contrast of the fringes reveals the amount of entanglement between the atom and the field. When this entanglement is maximum, the fringes are fully suppressed. They have, on the other hand, a maximum contrast when the two systems are separable.

More precisely, the probabilities for finding the atom in  $|e\rangle$  or  $|g\rangle$  when the cavity contains a coherent field with  $\bar{n}$  photons on average are obtained from Eq. (73):

$$\begin{aligned} P_e^{\bar{n}} &= 1 - P_g^{\bar{n}} = \frac{1}{2} \left\{ 1 - \operatorname{Re} \left[ e^{i(\Phi_0 - \chi)} \langle \beta e^{-i\Phi_0} | \beta e^{i\Phi_0} \rangle \right] \right\} \\ &= \frac{1}{2} \left\{ 1 - \cos[\chi - \Phi_0 - \bar{n} \sin(2\Phi_0)] e^{-\bar{n}[1 - \cos(2\Phi_0)]} \right\}. \end{aligned} \quad (78)$$

We recognize in the first line the scalar product of the two final field components, whose analytical expression is given in the last line. The argument  $\bar{n}[1 - \cos(2\Phi_0)]$  of the last exponential in Eq. (78) represents the square of the distance in phase space of the two field components. The Ramsey fringes appear to be phase-shifted by an angle proportional to  $\bar{n}$  and their amplitude is suppressed by a factor decreasing exponentially with the separation of the field components.

We have observed these Ramsey fringes for  $\bar{n} = 9.5$  and  $t_i^d = 19 \mu\text{s}$  [7] for different phase splittings  $\Phi_0$  obtained by varying  $\Delta_c$ . The signals for three different values of  $\Phi_0$  are shown in Figure 12(a) with, in the insets, the final field states phase space representations. The collapse of the fringe amplitude when the field components separate is conspicuous. The fringe contrast is shown versus  $\Phi_0$  in Figure 12(b) and the fringe phase shift in Figure 12(c). In these plots, the points are experimental and the curves given by theory, with an overall contrast adjustment taking into account the imperfections of the Ramsey interferometer. Note that the theoretical formula (78), valid in the dispersive limit, does not apply for the smallest detuning  $\Delta_c = 104 \text{ kHz}$ . An exact expression of the phase shifts based on the exact dressed states is used for the largest values of  $\Phi_0$ .

The experiment is found in excellent agreement with the theory. This is a clear indication that the field components are separated in phase space. The variation of the fringe phase with  $\Phi_0$  reveals the light shift effect experienced by the atom. This variation [Figure 12(c)] yields the calibration of the photon number. Moreover, this experiment presents a direct illustration of the complementarity concept in a simple interferometer arrangement. Note that other complementarity tests have been performed with the same set-up [30].

### 3.3. Decoherence of cavity cats

Before coming to the detection of the cat coherence, we briefly describe its relaxation. We present three different approaches, which shed complementary lights. We give, first, the formal solution of the master equation. We present then an enlightening interpretation of its results, using again the complementarity concept.

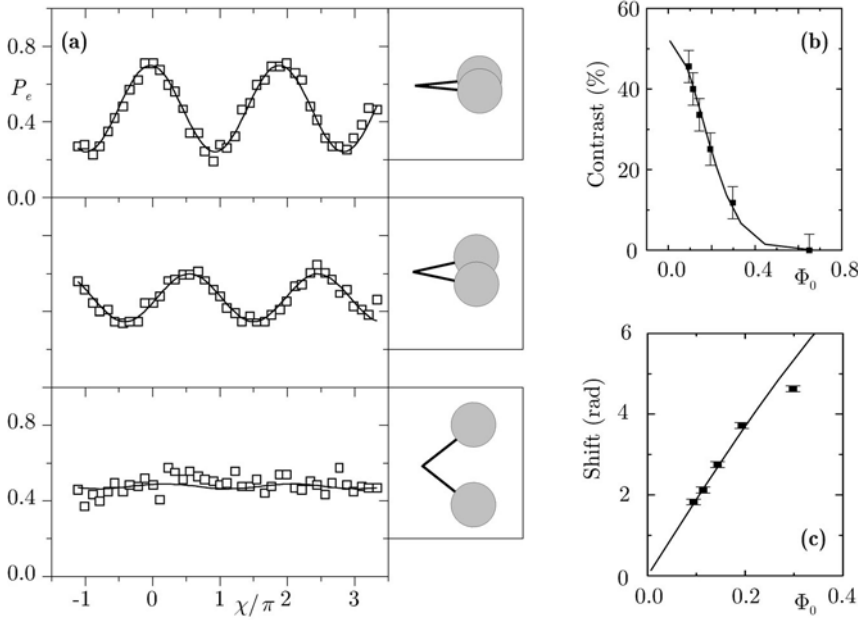


FIGURE 12. Schrödinger cat and complementarity. (a) Ramsey fringes for  $\beta = 3.1$  and three different  $\Phi_0$  values (0.1, 0.2 and 0.69 radians, corresponding to  $\Delta_c/2\pi = 712$ , 347 and 104 kHz respectively from top to bottom). The insets give a pictorial representation of the two field phase components. (b) Ramsey fringes contrast versus  $\Phi_0$ . The solid line corresponds to the theoretical predictions, scaled by the finite Ramsey interferometer contrast. (c) Fringes shift (in radians) versus  $\Phi_0$ . The slope of the fitted line provides a calibration of the photon number.

Finally, we discuss Monte Carlo trajectories for the field parity. For the sake of simplicity, we consider only the zero temperature case.

**3.3.1. Solution of the master equation.** Under relaxation, a coherent state remains coherent, with an amplitude  $\beta(t) = \beta e^{-\kappa t/2}$  decaying exponentially with time. Its density operator reduces to a projector  $\rho(t) = |\beta(t)\rangle\langle\beta(t)|$ . Coherent states are ‘pointer states’ of the field, impervious to entanglement with the environment. It is convenient to study the evolution of an arbitrary state by expanding it on a coherent state basis. We do not recall here the derivation of the cat density

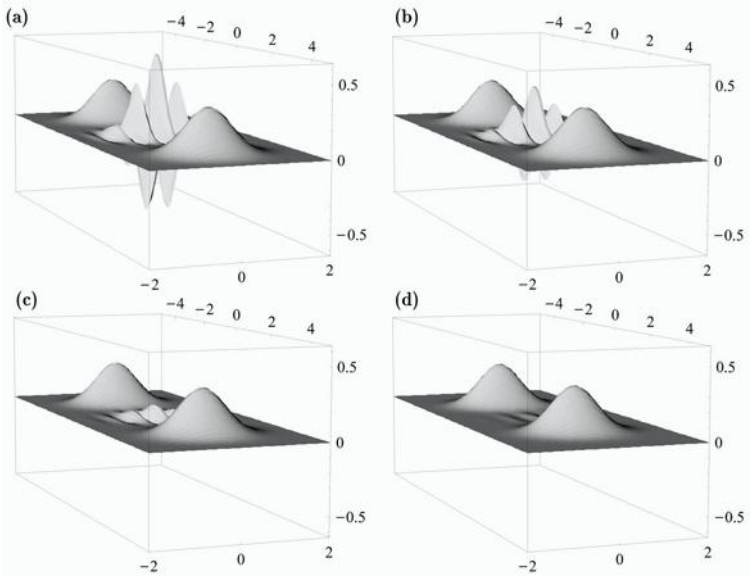


FIGURE 13. Evolution of the Wigner function of a cat state (10 photons on the average). (a) to (d):  $t = 0$ ,  $t = T_c/20$ ,  $t = T_c/5$  and  $t = T_c/2$  respectively.

operator versus time [31], leading to:

$$\rho^\pm(t) = \frac{1}{2} \left[ |\beta(t)\rangle\langle\beta(t)| + |-\beta(t)\rangle\langle-\beta(t)| \pm e^{-2\bar{n}(1-e^{-\kappa t})} (|\beta(t)\rangle\langle-\beta(t)| + |-\beta(t)\rangle\langle\beta(t)|) \right]. \quad (79)$$

The fast decay of the coherence terms is described by the exponential coefficient of the off-diagonal terms in Eq. (79). It decays at short times as  $\exp(-2\bar{n}\kappa t)$  and the coherent cat turns, for  $t > 1/\bar{n}\kappa$ , into a mixture of states. This relaxation process exhibits the essential features of the decoherence of a mesoscopic state superposition. It is much faster than the cavity energy relaxation and gets faster and faster when the ‘size’ of the cat, measured by the average photon number in the coherent components, increases.

This fast decoherence is pictorially exhibited by the Wigner functions, represented at four different times in Figure 13 for an even cat state containing  $\bar{n} = 10$  photons on average. The decoherence process appears clearly on these plots, which exhibit two very different time constants. After a very short time, the interference pattern near the origin, the ‘cat whiskers’, which are a signature of its coherence, have been washed out, leaving only the two Gaussian peaks, which slowly relax down to vacuum.

**3.3.2. Decoherence and complementarity.** The master equation approach does not provide a deep insight into decoherence mechanisms. We give now a heuristic derivation of Eq. (79), directly describing the environment evolution. This intuitive approach emphasizes the deep link between decoherence and complementarity [32].

A standard model for the environment  $E$  is a bath of harmonic oscillators labeled by the index  $i$ , linearly coupled to  $C$ . Their frequencies span a wide range around  $\omega_c$ . Starting from a coherent state  $|\beta\rangle$  at time  $t = 0$  and an empty environment, the global cavity-environment system evolves at time  $t$  into a non-entangled state:

$$|\Psi^{CE}(t)\rangle = |\beta(t)\rangle \otimes \prod_i |\epsilon_i(t)\rangle, \quad (80)$$

where  $\beta(t) = \beta e^{-\kappa t/2}$  and  $\epsilon_i(t)$  is the very small complex amplitude at time  $t$  of the  $i^{\text{th}}$  oscillator in  $E$ . Due to the linear coupling between  $C$  and the environment oscillators, the phase of  $\epsilon_i(t)$  is linearly related to the phase of  $\beta$ . Energy conservation requires moreover that the total number of quanta in  $E$  equals the number of photons lost by  $C$ :

$$\sum_i |\epsilon_i(t)|^2 = \bar{n} (1 - e^{-\kappa t}). \quad (81)$$

Suppose now that we prepare at  $t = 0$  the field in a cat state:

$$|\Psi_{\text{cat}}(0)\rangle = \frac{e^{i\psi_1}}{\sqrt{2}} |\beta e^{i\Phi}\rangle + \frac{e^{i\psi_2}}{\sqrt{2}} |\beta e^{-i\Phi}\rangle. \quad (82)$$

The state of the  $C+E$  system at time  $t$  is obtained by superposing the contributions of the two parts of the cat, each being given by an expression of the form (80). Noting that, when  $\beta$  is phase shifted by  $\pm\Phi$ , the same shift is experienced by the  $\epsilon_i(t)$  amplitudes, we have:

$$\begin{aligned} |\Psi_{\text{cat}}^{CE}(t)\rangle &= \frac{e^{i\psi_1}}{\sqrt{2}} |\beta(t)e^{i\Phi}\rangle \otimes \prod_i |\epsilon_i(t)e^{i\Phi}\rangle \\ &\quad + \frac{e^{i\psi_2}}{\sqrt{2}} |\beta(t)e^{-i\Phi}\rangle \otimes \prod_i |\epsilon_i(t)e^{-i\Phi}\rangle. \end{aligned} \quad (83)$$

The two parts of the cat are correlated to two states of  $E$ :

$$|E^+(t)\rangle = \prod_i |\epsilon_i(t)e^{i\Phi}\rangle, \quad (84)$$

and

$$|E^-(t)\rangle = \prod_i |\epsilon_i(t)e^{-i\Phi}\rangle, \quad (85)$$

each of which is the product of minute copies of the cavity cat components disseminated in the environment. Each oscillator in  $E$  is involved in a superposition of two states with a very small amplitude  $\epsilon_i$  and a large phase splitting  $2\Phi$ , a

‘Schrödinger kitten’ so to speak. The states  $|E^+(t)\rangle$  and  $|E^-(t)\rangle$  get quickly mutually orthogonal. Using Eqs. (22) and (81), we find:

$$\begin{aligned} \langle E^-(t)|E^+(t)\rangle &= \exp \left[ - \sum_i |\epsilon_i(t)|^2 (1 - e^{2i\Phi}) \right] \\ &= \exp \left[ -\bar{n}(1 - e^{-\kappa t})(1 - e^{2i\Phi}) \right], \end{aligned} \quad (86)$$

an expression which goes very rapidly to zero as  $t$  increases. The fast loss of coherence is a complementarity effect. It is a matter of information about the cat state leaking into  $E$ . The final states of each oscillator in  $E$  have a near unity overlap (since  $|\epsilon_i|^2 \ll 1$ ), but there are very many of them and the product of their scalar products quickly vanishes.

In other words, an information about the phase  $\pm\Phi$  of the cat state components could not be obtained from a single environment oscillator whose amplitude is very small and hence phase fluctuations very large. It could however be recovered, at least in principle, from a measurement of the environment as a whole, combining small amounts of information disseminated among the elementary oscillators. This is enough to kill the cat coherence and the interference effects associated to it. When tracing over  $E$ , the cat coherence is multiplied by  $\langle E^-(t)|E^+(t)\rangle$  and  $\rho(t)$  finally writes:

$$\begin{aligned} \rho(t) &= \frac{1}{2} \left\{ |\beta(t)e^{i\Phi}\rangle\langle\beta(t)e^{i\Phi}| + |\beta(t)e^{-i\Phi}\rangle\langle\beta(t)e^{-i\Phi}| \right. \\ &\quad \left. + \langle E^-(t)|E^+(t)\rangle e^{i(\psi_1 - \psi_2)} |\beta(t)e^{i\Phi}\rangle\langle\beta(t)e^{-i\Phi}| + \text{h.c.} \right\}. \end{aligned} \quad (87)$$

Setting  $\Phi = \pi/2$  and  $\psi_1 - \psi_2 = 0$  or  $\pi$ , we recover, as expected, Eq. (79) giving the evolution of an even or odd  $\pi$ -phase cat.

**3.3.3. Parity jumps of a  $\pi$ -phase cat.** We now turn to the Monte Carlo picture. Let us imagine that we use the set-up of Figure 9 to follow the evolution of a field initially prepared in the even cat state  $|\Psi_{\text{cat}}^+(0)\rangle = [|\beta\rangle + |-\beta\rangle]/\sqrt{2}$ . The photon clicks are counted in successive time bins of duration  $\tau$ . Until the first click at time  $t_1$ , the non-unitary evolution simply shrinks the amplitude of the cat components, turning  $\beta$  into  $\beta(t_1) = \beta e^{-\kappa t_1/2}$ . The cat state is continuously changed into  $|\Psi_{\text{cat}}^+(t_1)\rangle = [|\beta(t_1)\rangle + |-\beta(t_1)\rangle]/\sqrt{2}$ .

The first click corresponds to a cavity state quantum jump, described by the annihilation operator  $a$ . According to Eq. (31), the cat parity suddenly switches, the field state jumping from  $|\Psi_{\text{cat}}^+(t_1)\rangle$  to  $|\Psi_{\text{cat}}^-(t_1)\rangle = [|\beta(t_1)\rangle - |-\beta(t_1)\rangle]/\sqrt{2}$ . The shrinking of the cat components then resumes until a second jump restores the initial parity and so on. As long as the field energy has not appreciably decayed, the probability of occurrence of a click in a time bin is  $p_1 = \kappa\bar{n}\tau$  and the average duration between clicks is  $\tau_D = 1/(\kappa\bar{n})$ . On each Monte Carlo trajectory, a fast random parity jumping is combined with a slow deterministic shrinking of the amplitude. The characteristic rates of these evolutions are in the ratio  $\bar{n}$ .

The information provided by a click has an immediate effect on a field in a superposition of two coherent states, even if each of them, prepared separately in  $C$ , would remain unchanged. This is a genuine quantum effect. The information provided by the click changes the relative quantum phase between the two parts of the field wave-function and, hence, its parity.

Assuming that the photon counter is perfect, the parity of the number of clicks recorded until time  $t$  would tell us without ambiguity whether the field is in the state  $|\Psi_{\text{cat}}^+(t)\rangle$  or  $|\Psi_{\text{cat}}^-(t)\rangle$ . We could thus follow a Monte Carlo trajectory in which the field would be a perfect, albeit random cat state. Observing the environment makes it thus possible, at least in principle, to keep the cat coherence alive for a time of the order of  $T_c = 1/\kappa$ . This continuous observation does not give us the power, though, to choose at a given time the parity of the cat. We can merely record it.

Monitoring the environment is of course but a gedanken experiment. It is more realistic, if extremely difficult, to keep the cat's coherence by monitoring the cavity itself. As we shall see in the next section, the cavity photon number parity can be measured non-destructively [33]. A stream of probe atoms could then record in real time the decaying cat's parity jumps.

In this ideal situation, the action of these jumps may be, to some extent, canceled. Whenever the cat parity changes, an atom is sent into the cavity, interacts resonantly with it and emits a photon in the mode, restoring the parity. Numerical simulations show that a cat state's coherence could be preserved, by this quantum feedback procedure, over times of the order of  $T_c$  [34, 35]

As soon as we give up to monitor parity jumps, the field is described by a density operator  $\rho$ , obtained by averaging Monte Carlo trajectories. After a time of the order of  $\tau_D = 1/\bar{n}\kappa$  there are statistically as many trajectories with even or odd click numbers. The density operator is then the sum with equal weights of projectors on even and odd cats:

$$\rho_A(t > \tau_D) \sim \frac{1}{2}|\Psi_{\text{cat}}^+(t)\rangle\langle\Psi_{\text{cat}}^+(t)| + \frac{1}{2}|\Psi_{\text{cat}}^-(t)\rangle\langle\Psi_{\text{cat}}^-(t)|. \quad (88)$$

It can be equivalently expressed as an incoherent sum with equal weights of projectors on the  $|\beta(t)\rangle$  and  $|\!-\beta(t)\rangle$  states. We thus retrieve the result predicted by an exact solution of the master equation.

### 3.4. Probing the cat with a quantum mouse

The detection of the index atom  $A_i$  leaves in  $C$  a Schrödinger cat. How can we probe its fast relaxation towards a statistical mixture of coherent components? We must rely on an atomic signal to get an indirect information about the field. After some free evolution time, we probe  $C$  with a second atom,  $A_p$ . Elaborating on Schrödinger's metaphor,  $A_p$  is a 'quantum mouse' sent in  $C$  to probe the coherence of the relaxing cat state left by  $A_i$ .

Let us first discuss this experiment in simple qualitative terms. Atom  $A_i$ , interacting with the initial coherent state  $|\beta\rangle$ , leaves in  $C$  a quantum superposition of  $|\beta \exp i\Phi_0\rangle$  and  $|\beta \exp -i\Phi_0\rangle$ . The mouse  $A_p$  undergoes the same transformations

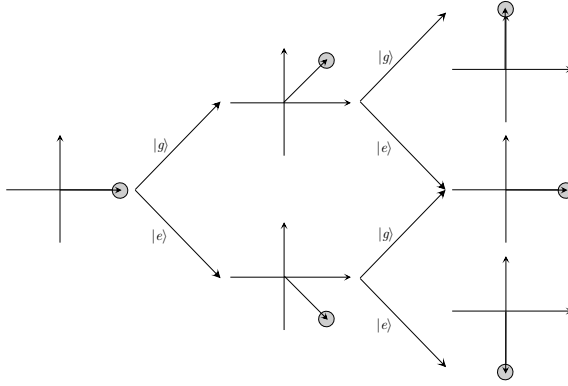


FIGURE 14. The interfering paths in the two atom experiment.

as  $A_i$  in  $R_1$  and  $R_2$  and produces the same quantum superposition of phase shifts on the cavity field. Each of the phase components left by  $A_i$  is thus again split in two parts dephased by  $\pm\Phi_0$ . This process is pictorially represented in Figure 14.

The cavity finally contains a three-components cat. The phases  $\pm 2\Phi_0$  correspond to the situations in which  $A_i$  and  $A_p$  crossed  $C$  in the same state  $[(|e\rangle, |e\rangle)$  or  $(|g\rangle, |g\rangle)]$ . Two different paths,  $(|e\rangle, |g\rangle)$  or  $(|g\rangle, |e\rangle)$ , lead to a component with zero phase. The atomic states, here, correspond to the cavity crossing. The Ramsey pulse  $R_2$  mixes the states at the exit of  $C$ . The atomic detection in  $D$  thus does not provide any information about the states in  $C$  (a ‘quantum eraser’ situation). The two paths leading to the zero-phase component are indistinguishable, resulting in a quantum interference. This interference vanishes when decoherence has turned the cat superposition into a statistical mixture before  $A_p$  enters  $C$ . Let us show now that this interference process reflects on an atomic signal  $\eta$ :

$$\eta = P_{g|g} - P_{e|g} , \quad (89)$$

where  $P_{g|g}$  and  $P_{e|g}$  are the conditional probabilities for detecting the mouse atom  $A_p$  in  $|g\rangle$  or  $|e\rangle$ , provided  $A_i$  has been detected in  $|g\rangle$ .

Let us thus follow the successive state transformations, taking relaxation into account with the simple kitten model presented in the previous section. When  $A_i$  has been detected in  $|g\rangle$ , according to Eq. (74), the field has been prepared at  $t = 0$  in:

$$|\Psi_{\Phi_0}^+\rangle = \frac{1}{\sqrt{2}} [|\beta e^{-i\Phi_0}\rangle + |\beta e^{i\Phi_0}\rangle] . \quad (90)$$

We assume here that the decoherence time scale is much longer than the atom-field interaction time  $t_i^d$ . Decoherence is then negligible during  $t_i^d$  and only takes place during the time interval  $t$  between the  $A_i$  and  $A_p$ . When  $A_p$  enters the apparatus, the field state has been partially entangled with  $E$ , the cavity+environment state

being:

$$|\Psi^{CE}(t)\rangle = \frac{1}{\sqrt{2}} \left[ |\beta e^{-i\Phi_0}\rangle \otimes |E^-(t)\rangle + |\beta e^{i\Phi_0}\rangle \otimes |E^+(t)\rangle \right], \quad (91)$$

where  $|E^-(t)\rangle$  and  $|E^+(t)\rangle$  are the environment states defined by Eqs. (84) and (85). The probe atom  $A_p$  then interacts with  $C$ . As  $A_i$ , it crosses  $C$  in a time short compared to the decoherence time. The environment remains spectator during this interaction. Using the superposition principle, we can compute separately the effect of the  $A_p - C$  interaction on the two parts of the cat state and add the resulting contributions:

$$\begin{aligned} |\Psi^{A_i EA_p}(t)\rangle &= \frac{1}{2\sqrt{2}} \left[ e^{-i\Phi_0} |e_2\rangle \otimes (|\beta e^{-2i\Phi_0}\rangle - |\beta\rangle) \right. \\ &\quad \left. + |g_2\rangle \otimes (|\beta e^{-2i\Phi_0}\rangle + |\beta\rangle) \right] \otimes |E^-(t)\rangle \\ &+ \frac{1}{2\sqrt{2}} \left[ e^{-i\Phi_0} |e_2\rangle \otimes (|\beta\rangle - |\beta e^{2i\Phi_0}\rangle) \right. \\ &\quad \left. + |g_2\rangle \otimes (|\beta\rangle + |\beta e^{2i\Phi_0}\rangle) \right] \otimes |E^+(t)\rangle. \end{aligned} \quad (92)$$

We get the three phase components represented in Figure 14. The first two and last two lines in the r.h.s. describe the ‘offsprings’ of the  $|\beta e^{-i\Phi_0}\rangle$  and  $|\beta e^{i\Phi_0}\rangle$  components of the cat left by  $A_i$  in  $C$ . Each one is tagged by a different environment state, carrying some information about its the phase. We get thus the probabilities  $P_{g|g}$  and  $P_{e|g}$  for detecting the second atom in  $|g\rangle$  or  $|e\rangle$  (after having found  $A_i$  in  $|g\rangle$ ):

$$\begin{aligned} P_{g|g} &= \frac{1}{2} + \frac{1}{4} \text{Re} \langle E^-(t) | E^+(t) \rangle; \\ P_{e|g} &= \frac{1}{2} - \frac{1}{4} \text{Re} \langle E^-(t) | E^+(t) \rangle. \end{aligned} \quad (93)$$

Replacing  $\langle E^-(t) | E^+(t) \rangle$  by its expression (86), we obtain in the case  $2\Phi_0 \neq \pi$ :

$$\begin{aligned} \eta(t) &= P_{g|g} - P_{e|g} = \frac{1}{2} \text{Re} \exp \left[ -\bar{n}(1 - e^{-\kappa t})(1 - e^{2i\Phi}) \right] \\ &= \frac{1}{2} e^{-2\bar{n}(1 - e^{-\kappa t}) \sin^2 \Phi_0} \cos \left[ \bar{n}(1 - e^{-\kappa t}) \sin(2\Phi_0) \right]. \end{aligned} \quad (94)$$

For  $\kappa t \ll 1$  this expression can be approximated by:

$$\eta(t) \approx \frac{1}{2} e^{-2\bar{n}\kappa t \sin^2 \Phi_0} \cos[\bar{n}\kappa t \sin(2\Phi_0)]. \quad (95)$$

The two-atom correlation signal varies from 1/2 to 0 as decoherence proceeds. Its evolution is described by the product of a decaying exponential by a cosine function of time. The decay rate of the exponential,  $1/T_D = 2\kappa\bar{n} \sin^2 \Phi_0$ , is the cavity damping rate  $\kappa$  multiplied by the square of the distance in phase space  $D^2 = 2\bar{n} \sin^2 \Phi_0$  of the initial cat components. This is, once again, a characteristic feature of decoherence. The cosine factor is very close to 1 at the beginning of the evolution. When  $\eta(t)$  is already strongly reduced, this factor can change

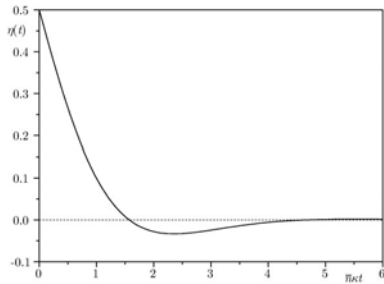


FIGURE 15. Theoretical value of the correlation signal  $\eta(t)$  for  $2\Phi_0 = \pi/2$ , as a function of  $\kappa\bar{n}t$ .

sign, adding a modulation in the tail of the  $\eta(t)$  function. Figure 15 represents the theoretical variation of  $\eta(t)$  for  $2\Phi_0 \sim \pi/2$ . Note that the maximum  $\eta$  value is twice larger (1) when  $\Phi_0 = \pi/2$ , because then the two states  $|\beta e^{-2i\Phi_0}\rangle$  and  $|\beta e^{+2i\Phi_0}\rangle$  coincide. This gives rise to another interference effect in the  $P_{g|g}$  and  $P_{e|g}$  probabilities.

Sending pairs of atoms across the Ramsey interferometer, we have observed the evolution of  $\eta$  [7]. The cavity damping time in this early experiment was  $160 \mu\text{s}$ , making the decoherence fast and limiting the experiment to small values of  $\bar{n}$ . The cat state prepared by the first atom contained  $\bar{n} = 3.3$  or  $5.1$  photon on average. The phase splitting  $2\Phi_0$  was set at two values (100 and 50 degrees) by choosing the detuning  $\Delta_c$  (70 kHz and 170 kHz respectively). The separation  $t$  between the two atoms was varied between  $30 \mu\text{s}$  and  $250 \mu\text{s}$ .

Figure 16 shows  $\eta(t)$  for  $\bar{n} = 3.3$  and two splitting angles. The points are experimental and the lines theoretical. Note that the theory is not restricted to the simple perturbative analysis developed above. It includes higher order terms in  $\Omega_0/\Delta_c$  correcting the expression of the cat states at  $\Delta_c = 70$  kHz. We have also incorporated the finite Ramsey fringes contrast, which explains why the maximum correlation is only 0.18.

The correlation signals decrease with  $t$ , revealing directly the dynamics of decoherence. The agreement with the theoretical model is excellent. Most strikingly, decoherence proceeds at a faster rate when the distance between cat state components increases. A decoherence time  $\approx 0.24/\kappa$ , much shorter than the photon decay time, is found for the larger cat ( $\Delta_c = 70$  kHz). A similar agreement with theory is obtained when comparing, for the same  $\Delta_c = 70$  kHz,  $\eta(t)$  for different  $\bar{n}$  values (5.1 and 3.3).

The CQED cat experiments are, as discussed above, models of an ideal quantum measurement. The coherent field is a meter measuring the state of the first atom crossing the cavity and evolving under the effect of their interaction into a mesoscopic superposition. This decoherence experiment illustrates vividly the

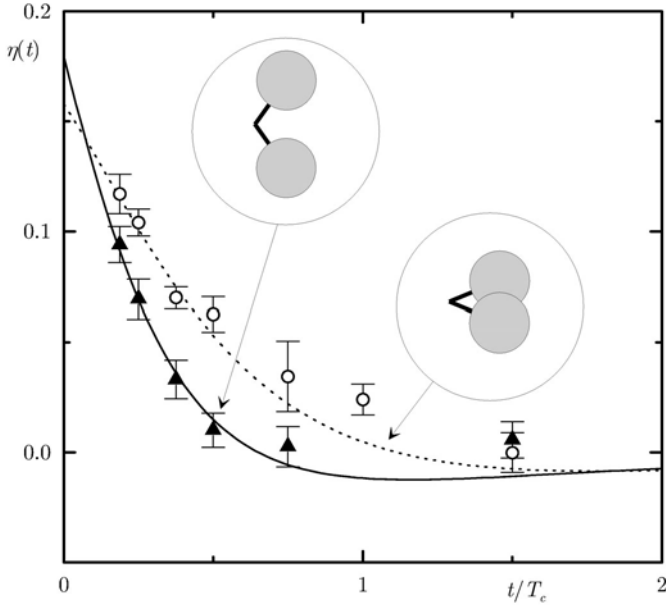


FIGURE 16. Two-atom correlation signal  $\eta$  as a function of  $t/T_c$  for an atom-cavity detuning  $\Delta_c/2\pi = 170$  kHz (open circles) and  $\Delta_c/2\pi = 70$  kHz (solid triangles). The points are experimental, with statistical error bars. The curves present the theoretical signal, scaled by a factor taking into account experimental imperfections. The cat phase components are pictorially depicted in the insets.

fast evolution of the atom+meter state towards a statistical mixture and the increasing difficulty to maintain quantum coherence when the distance between the components of the mesoscopic superposition is increased.

#### 4. The future of cavity cats

We have presented above a first experiment on decoherence dynamics. It would be quite interesting to dive deeper into the quantum/classical transition and to test our understanding of decoherence in this textbook situation. It is thus essential to get more information on the relaxing cat state than provided by the correlation  $\eta$ . Finally, it would be interesting to merge two of the most intriguing features of the quantum world: decoherence and non-locality. We address these issues here. We show first that the resonant atom-field interaction can produce efficiently very large cat states. We present a direct measurement of the cavity field Wigner function.

Finally, we discuss an experiment under construction aiming at the preparation of non-local Schrödinger cat states.

#### 4.1. Generation of large cats by resonant atom-field interaction

In the preceding section, we learned how to generate Schrödinger cats via the dispersive atom-cavity interaction, valid when the atom-cavity detuning is large and the photon number small. It is tempting to increase the photon number and to decrease  $\Delta_c$  in order to generate ‘larger’ cats. What happens then when  $\Delta_c$  goes all the way to zero? What is the index of refraction of a single resonant atom? In the classical Lorentz model of harmonically bound electrons [36], the answer is simple: the index is one. When it comes to a mesoscopic field, the situation is more interesting. The atom is indeed in a quantum superposition of two very large indices, resulting in the efficient generation of a Schrödinger cat state.

**4.1.1. Quantum Rabi oscillations in a mesoscopic field.** We thus return to the interaction of a single atom, initially in  $|e\rangle$ , with a coherent state  $|\alpha\rangle = \sum_n c_n |n\rangle$  containing  $\bar{n} = |\alpha|^2$  photons on the average. The initial atom-cavity state,  $|e\rangle \otimes |\alpha\rangle$ , can be expanded on the dressed atom state basis  $|\pm, n\rangle$  and the evolution easily computed. The state at the effective interaction time  $t_i$  is:

$$|\Psi\rangle = \frac{1}{\sqrt{2}} [|\Psi_1\rangle + |\Psi_2\rangle], \quad (96)$$

where

$$|\Psi_1\rangle = \frac{1}{\sqrt{2}} \left[ \sum_n c_n e^{i\Omega_0 \sqrt{n+1} t_i / 2} (|e, n\rangle - i|g, n+1\rangle) \right], \quad (97)$$

and

$$|\Psi_2\rangle = \frac{1}{\sqrt{2}} \left[ \sum_n c_n e^{-i\Omega_0 \sqrt{n+1} t_i / 2} (|e, n\rangle + i|g, n+1\rangle) \right]. \quad (98)$$

This is an exact expression. The probability  $P_e(t)$  for finding the atom in  $|e\rangle$  is simply:

$$P_e(t) = \sum_n |c_n|^2 \frac{1 + \cos \Omega_0 \sqrt{n+1} t_i}{2}, \quad (99)$$

a sum of terms oscillating at the frequencies  $\Omega_0 \sqrt{n+1}$ , weighted by the probability for getting the corresponding photon number  $n$  in the initial coherent cavity state.

Figure 17 shows  $P_e(t)$  for  $\bar{n} = 15$ . This Rabi oscillation signal presents remarkable features, which attracted a lot of interest in the early days of quantum optics [37, 38]. At short times, when  $\bar{n} \gg 1$ , an oscillation is observed at a frequency  $\Omega_0 \sqrt{\bar{n}+1}$ , proportional to the classical field amplitude. This oscillation is quite rapidly damped away and  $P_e$  reaches a stationary 1/2 value. This ‘collapse’ is due to the dispersion of Rabi frequencies in Eq. (99). At much longer times, however, the oscillations ‘revive’, due to the rephasing of the finite set of oscillating terms in Eq. (99). This revival is directly linked to the quantization of the Rabi oscillation spectrum and, hence, to the field energy quantization itself.

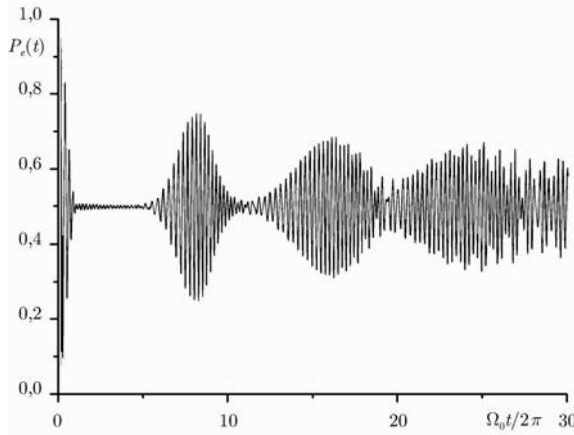


FIGURE 17. Quantum revivals: computed probability  $P_e(t)$  for finding the atom in state  $|e\rangle$  versus the interaction time  $t$  in units of  $2\pi/\Omega_0$ . The cavity contains initially an  $\bar{n} = 15$  photons coherent field.

This explains the theoretical interest devoted to this phenomenon [39, 40, 41, 42]. We give below an enlightening interpretation of the collapse and revival in terms of complementarity.

The expression (96) is explicit, but does not provide a physical insight into the field evolution. We proceed thus to obtain a more explicit, if approximate, expression of the atom-cavity state, following [40]. We separate the kets  $|\Psi_1\rangle$  and  $|\Psi_2\rangle$  into an atom and a field part. With a mere redefinition of the running index  $n$ :

$$|\Psi_1\rangle = \frac{1}{\sqrt{2}} \left[ \sum_n c_n e^{i\Omega_0 \sqrt{n+1} t_i/2} |e, n\rangle - i \sum_n c_{n-1} e^{i\Omega_0 \sqrt{n} t_i/2} |g, n\rangle \right], \quad (100)$$

still an exact expression. We now assume that  $\bar{n}$  and the photon number variance  $\Delta N = \sqrt{\bar{n}}$  are much larger than 1. The  $c_n$  amplitudes are slowly varying functions of  $n$  and we can set  $c_n \approx c_{n-1}$ . We use, in the exponentials, a first order expansion of  $\sqrt{n+1}$ :

$$\frac{\Omega_0 \sqrt{n+1} t_i}{2} \approx \frac{\Omega_0 \sqrt{n} t_i}{2} + \frac{\Omega_0 t_i}{4\sqrt{n}}, \quad (101)$$

which leads to:

$$|\Psi_1\rangle = \frac{1}{\sqrt{2}} \left[ \sum_n c_n e^{i\Omega_0 \sqrt{n} t_i/2} |n\rangle \right] \left[ e^{i\Omega_0 t_i/4\sqrt{\bar{n}}} |e\rangle - i |g\rangle \right], \quad (102)$$

a product of independent atom and field states.

We then expand the  $\sqrt{n}$  term around  $n = \bar{n}$ , up to the first order:

$$\sqrt{n} = \frac{\sqrt{\bar{n}}}{2} + \frac{n}{2\sqrt{\bar{n}}} . \quad (103)$$

This is legitimate since  $\Delta N \ll \bar{n}$ . We get:

$$\begin{aligned} |\Psi_1\rangle &= \frac{1}{\sqrt{2}} e^{i\Omega_0\sqrt{\bar{n}}t_i/4} \left[ \sum_n c_n e^{in\Omega_0 t_i/4\sqrt{\bar{n}}} |n\rangle \right] \\ &\otimes \left[ e^{i\Omega_0 t_i/4\sqrt{\bar{n}}} |e\rangle - i|g\rangle \right] . \end{aligned} \quad (104)$$

The field state reduces thus to:

$$\sum_n c_n e^{in\Omega_0 t_i/4\sqrt{\bar{n}}} |n\rangle = |\beta e^{i\Omega_0 t_i/4\sqrt{\bar{n}}}\rangle , \quad (105)$$

a coherent state obtained from the initial one by a phase shift  $\Omega_0 t_i/4\sqrt{\bar{n}}$ .

A similar calculation is performed for  $|\Psi_2\rangle$ . Grouping all the terms, we finally obtain the atom-field wavefunction as:

$$|\Psi(t_i)\rangle \approx \frac{1}{\sqrt{2}} \left[ |\Psi_a^+(t_i)\rangle \otimes |\Psi_f^+(t_i)\rangle + |\Psi_a^-(t_i)\rangle \otimes |\Psi_f^-(t_i)\rangle \right] , \quad (106)$$

where the atom wavefunctions write:

$$|\Psi_a^\pm\rangle = \frac{1}{\sqrt{2}} e^{\pm i\Omega_0\sqrt{\bar{n}}t_i/2} \left[ e^{\pm i\Omega_0 t_i/4\sqrt{\bar{n}}} |e\rangle \mp i|g\rangle \right] , \quad (107)$$

and the field ones:

$$|\Psi_f^\pm\rangle = e^{\mp i\Omega_0\sqrt{\bar{n}}t_i/4} |\beta e^{\pm i\Omega_0 t_i/4\sqrt{\bar{n}}}\rangle . \quad (108)$$

Equation (106) describes a quantum superposition involving two coherent states rotating slowly, at an angular frequency  $\Omega_0/4\sqrt{\bar{n}}$ , in opposite directions in phase space, away from the initial state  $|\alpha\rangle$ . These components are correlated to atomic states, superpositions of  $|e\rangle$  and  $|g\rangle$  with equal weights, also rotating slowly in opposite directions in the equatorial plane of the Bloch sphere, so that the phase relationship between the atomic dipole and the associated field components are kept throughout the evolution.

In other words, a resonant atom, initially in state  $|e\rangle$ , is in a quantum superposition of two opposite indices of refraction and leads to a cat state preparation. The components angular frequencies,  $\pm\Omega_0/4\sqrt{\bar{n}}$ , go to zero in the classical limit of a very large field (obtained by letting  $\bar{n} \rightarrow \infty$  and  $\Omega_0 \rightarrow 0$  so that the Rabi frequency  $\Omega_0\sqrt{\bar{n}}$  remains constant). This phase separation is thus a mesoscopic feature, directly related to the photon graininess. Its velocity is larger than for any finite atom-cavity detuning, much faster than in the dispersive regime. The resonant method is thus optimal for the preparation of photonic cats with many photons.

We have so far overlooked the global phase factors multiplying the expressions of the  $|\Psi_a^\pm\rangle$  and  $|\Psi_f^\pm\rangle$  states. They evolve at frequencies about  $\bar{n}$  times larger than the phase drift frequency. In the  $(|\Psi_1\rangle + |\Psi_2\rangle)/\sqrt{2}$  superposition, though, their

role is essential. They give rise to the interference effect responsible for the Rabi oscillation. The study of the photonic cat evolution is thus intimately related to the dynamics of the precession between  $|e\rangle$  and  $|g\rangle$ .

This leads to a simple interpretation of the quantum Rabi collapse and revivals, again in terms of complementarity. At short times, the two coherent components overlap and the quantum interference and hence the Rabi oscillations show up. Soon, the two coherent components separate. The cavity field acts then as a which-path detector for the interfering atomic states, and the Rabi oscillations disappear. The evolution does not stop, though, since the slow rotation of the coherent states in phase space goes on. After a time  $t_r$  such that  $t_r\Omega_0/4\sqrt{\bar{n}} = \pi$ , the coherent states have undergone a  $\pi$  rotation in opposite directions. They again overlap. The which-path information is erased and the atom-field entanglement is broken. The Rabi oscillations revive. A series of revivals is thus expected, corresponding to the periodic overlaps of the counter-rotating fields. That these revivals get progressively broadened, with a lower than unity contrast, as conspicuous on Figure 17, is due to higher order terms neglected in our approximations.

**4.1.2. Observing the field phase separation.** We have evidenced the resonant phase separation via a measurement of the final field phase distribution [43]. The experiment is similar to the measurement of the dispersive phase shifts described above. It involves two successive field injections and two atoms. A first coherent state  $|\alpha\rangle$  is prepared, with  $\bar{n}$  between 10 and 40. A resonant atom  $A_r$  is sent across the cavity at a fixed velocity  $v_1 = 335$  m/s or  $v_2 = 200$  m/s (corresponding to a total effective interaction time  $t_i = 32$   $\mu$ s or  $52$   $\mu$ s).

A second coherent field  $|\beta\rangle = |-\alpha e^{i\varphi}\rangle$ , with the same amplitude as the first, but a variable phase  $\varphi$ , is then added in  $C$ . A probe atom,  $A_p$ , also resonant with  $C$ , follows. Its absorption yields as above the  $Q$  function of the field left in the cavity by  $A_r$ .

Figure 18 presents  $Q(\alpha e^{i\varphi})$  versus  $\varphi$  for  $\bar{n} = 29$  and  $t_i = 52$   $\mu$ s. As expected, a double peak distribution is obtained, with a phase splitting of 1.3 radians, in good agreement with the theoretical value  $\Omega_0 t_i / 2\sqrt{\bar{n}} = 1.5$  radians. We have checked that the splitting is proportional to  $t_i$  and inversely proportional to  $\alpha$ . The observed phase shifts are in good agreement with the simple first order calculation presented above and in excellent agreement with a numerical simulation of the exact atom-cavity interaction [43]. The maximum phase splitting, for  $\bar{n} = 15$  and  $t_i = 52$   $\mu$ s, was  $90^\circ$ , a phase space separation much larger than what can be obtained in the dispersive regime.

**4.1.3. Checking the cat coherence.** The  $Q$  function measurement does not provide any hint about the coherent nature of the superposition. The simplest coherence assessment would be the spontaneous Rabi revival observation. Unfortunately, even for a relatively small cat with  $\bar{n} = 13$ , the revival time  $t_r = 4\pi\sqrt{\bar{n}}/\Omega_0 = 260$   $\mu$ s is prohibitively long.

It is possible to bypass this difficulty and to force the system to undergo an early revival. The trick is to let the field components separate in phase space

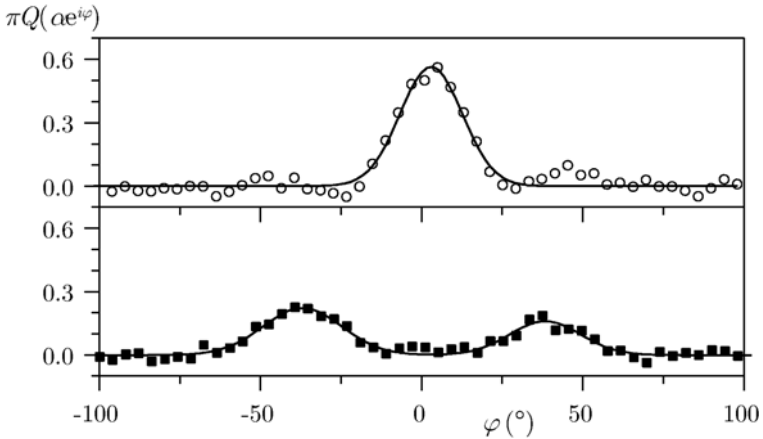


FIGURE 18. Phase distribution  $Q(\alpha e^{i\varphi})$  (in units of  $1/\pi$ ) for the resonant cat state. Top curve: initial coherent field, with 29 photons on the average. Bottom: phase distribution at  $t_i = 52 \mu\text{s}$ . The points are experimental and the solid curves are Gaussian fits.

until a time  $T$ , shorter than  $t_r/2$ , then to force them to come back on their tracks and to recombine at the initial phase. The recombination time,  $2T$ , can then be shorter than  $t_r$ . This method, reminiscent of the spin echoes used in NMR, has been proposed by Morigi *et al.* [44].

The system's evolution is ruled by the Jaynes Cummings Hamiltonian, given at resonance and cavity center by  $H_{ac}$  [see Eq. (54)]. We time the evolution with a 'clock' synchronized on the effective interaction time  $t_i$ . The experiment can be described as if the atom was sitting at cavity center. In an echo sequence, the system evolution from time 0 to  $T$  is described by the evolution operator  $U_1 = \exp(-iH_{ac}T/\hbar)$ . The atom undergoes, at time  $T$ , a percussional phase kick corresponding to the unitary operation  $\sigma_Z$ . This kick can be produced by an electric field pulse, transiently shifting the atomic levels via Stark effect. This pulse phase shifts by  $\pi$  the atomic dipole states, reversing their phase relationship with the associated coherent component. The evolution of the coupled atom-field states is then reversed, both in the Fresnel plane and in the equatorial plane of the Bloch sphere.

More quantitatively, after the phase shifting pulse, the Jaynes-Cummings evolution resumes for the remaining time  $t_i - T$ , with the evolution operator  $U_2 = \exp[-iH_{ac}(t_i - T)/\hbar]$ . The overall evolution operator is:

$$U = U_2 \sigma_Z U_1 = \sigma_Z^2 U_2 \sigma_Z U_1 = \sigma_Z e^{-iH_{ac}(2T - t_i)/\hbar}, \quad (109)$$

where we have used the identity  $\sigma_Z^2 = 1$  and:

$$\sigma_Z H_{ac} \sigma_Z = -H_{ac} . \quad (110)$$

Eq. (110) means that the evolution after the phase kick is the time-mirror image of the evolution between 0 and  $T$ . At time  $t_i = 2T$ , the evolution brings the system back to its initial state, up to a global  $\pi$ -phase shift between the amplitudes associated to levels  $|e\rangle$  and  $|g\rangle$ . Provided the whole evolution has been coherent, Rabi oscillations, exactly identical to the initial ones, show up around  $2T$ .

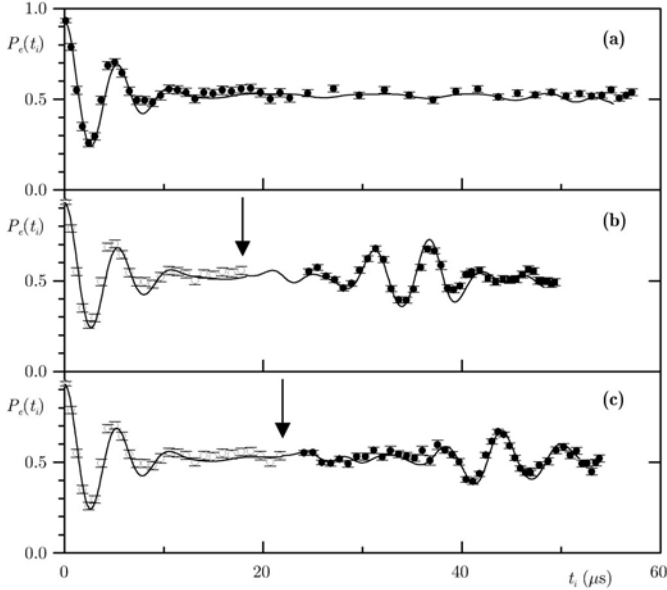


FIGURE 19. Experimental echo signals. Probability  $P_e$  for detecting the atom in  $|e\rangle$  as a function of the atom-cavity effective interaction time  $t_i$ . The points are experimental with statistical error bars and the solid lines are a theoretical fit. (a) Rabi collapse without Stark pulse. (b) and (c) Stark pulse applied at 18 and 22  $\mu\text{s}$  respectively (vertical arrows). The first part of the signal (open circles) is reproduced from (a) for visual convenience.

We have applied this time reversal method to the study of the Rabi oscillation in our CQED set-up [45]. The atomic velocity is set at  $v = 156$  m/s and  $\bar{n} = 13.6$ . The atom is tuned into resonance with  $C$  at  $t_i = 0$ . The Rabi oscillation starts and collapses while the atom is still near cavity entrance. In a preliminary experiment, this signal is recorded by freezing the evolution at increasing times. The final atomic state is recorded and we reconstruct the probability  $P_e(t_i)$  for finding the atom in level  $|e\rangle$ . The Rabi collapse signal is shown in Figure 19(a).

We then perform the echo experiment. The Stark phase kicking pulse is applied to the atom when it reaches cavity center, long after the Rabi collapse is complete. The atomic frequency then resumes its resonant value and the atomic evolution proceeds until a final time  $t_i = t_f$ , at which the atom is suddenly detuned. The frozen atomic state is analyzed by the atomic detector. Traces 19(b) and (c) show the signals obtained when the kicking pulse occurs at the effective time  $t_i = T = 18 \mu\text{s}$  and  $22 \mu\text{s}$  respectively. The echo signals around time  $2T$  are clearly observed, with a contrast about 50% of the ideal value. The kicking time  $T = 22 \mu\text{s}$  corresponds to 2.5 damping times of the initial Rabi signal. The maximum separation of the field components reaches 0.90 radians, about three times the phase fluctuation of the initial coherent field ( $1/\sqrt{\bar{n}} = 0.27$  radian). The components of the field are thus well separated, before being recombined by the time reversal operation. This echo signal reveals the existence of a mesoscopic coherence in the atom-field system between the collapse and the induced revival time.

The induced revival signal could, in principle, be used to assess the decoherence process. The observed echo contrast should be directly related to the decoherence integrated from  $t_i = 0$  to  $t_i = 2T$ . In practice, this analysis cannot be carried out because the echo is affected by experimental imperfections. A numerical simulation of the system's evolution (including the effect of decoherence due field damping in the cavity and all known causes of imperfections), shown as solid lines in Figure 19, indicates that the contrast reduction is dominated by mundane imperfections. Decoherence would take over for longer echo times, whose observation requires the use of slower atoms, not readily available.

**4.1.4. How big a cat?** What is the maximal practical size of a cat in these cavity QED experiments? The longest cavity damping time obtained in 2005, is  $T_c = 14$  ms, a two-order of magnitude increase with respect to the 1996 experiment [7], opening the way to much fatter photonic cats. The limit to the cat size can be evaluated by comparing the time required to prepare and probe it to its decoherence time. With the optimal resonant coupling, the effective interaction time  $t_i$  needs to be such that  $\Omega_0 t_i / 2\sqrt{\bar{n}} \sim \pi$ , i.e.  $t_i \sim (2\pi/\Omega_0)\sqrt{\bar{n}}$ . It should be shorter than the decoherence time  $1/2\kappa\bar{n} = T_c/2\bar{n}$ , thus:

$$\bar{n} < \left(\frac{\Omega_0 T_c}{2\pi}\right)^{2/3} = \left(\frac{\Omega_0 Q}{2\pi\omega}\right)^{2/3}. \quad (111)$$

An increase in  $T_c$  and  $Q$  by two orders of magnitude corresponds to a  $10^{2/3} \approx 20$ -fold improvement over the limit ( $\bar{n} \approx 5$ ) of the early cat experiments. Cat states with  $\bar{n}$  as large as 100 are thus in view.

The  $Q$  factor is still limited by mirror imperfections. With ideally smooth mirrors, and low enough temperature we could reach the diffraction limit, when the losses occur by photon scattering at the edge of the mirrors. With the current Fabry-Perot geometry, this would correspond to  $Q \approx 4 \cdot 10^{11}$ , or  $T_c = 1.4$  s, again a two orders of magnitude improvement. We can dream of another 20-fold increase

in the cat size up to 2000 photons. This limit would be difficult to break, but it leaves a lot of room for decoherence experiments.

#### 4.2. Imaging Schrödinger cats: a direct determination of the cavity field Wigner function

The smoking guns of cat coherence obtained so far do not provide a full insight into the cavity state. It would be much more interesting to reconstruct the field's Wigner function  $W$ , which provides a full information about the cat and its coherence. We made a first step in this direction by measuring the Wigner distribution of a non-classical cavity field, here an approximate single-photon state [33].

The method was proposed by Lutterbach and Davidovich [46]. Let us recall Eq. (40):  $W(\alpha)$  is the average of the parity operator  $\mathcal{P}$  in the field translated by  $-\alpha$ . This translation, action on  $C$  of a displacement operator  $D_1$ , is easily produced by the source  $S$ . To measure  $\langle P \rangle$  [33], we send across  $C$  a probe atom  $A_p$ , initially in  $|g\rangle$ , tuned off-resonance from  $C$ . The  $|e\rangle \rightarrow |g\rangle$  transition is transiently light-shifted by the cavity field, resulting in a phase shift of the atomic coherence. We adjust the atom-cavity detuning,  $\delta = 2\pi \times 105$  kHz, and the atomic velocity,  $v = 154$  m/s, so that a single photon produces a  $\pi$ -phase shift on the  $|e\rangle/|g\rangle$  coherence.

This phase shift is revealed by the Ramsey interferometer sandwiching  $C$ . The probability  $P_e$  for detecting  $A_p$  in  $|e\rangle$  is modulated versus the relative phase  $\phi$  of the  $R_1$  and  $R_2$  Ramsey pulses resonant with the  $|e\rangle \rightarrow |g\rangle$  transition:  $P_e = (1 + \cos \phi)/2$ . An  $n$ -photon field in  $C$  shifts the interference pattern by  $n\pi$ . When the photon distribution is  $p_n$  after  $D_1$ ,  $P_e$  becomes  $P_e(\phi) = [1 + \sum_n (-1)^n p_n \cos \phi]/2 = [1 + \langle P \rangle \cos \phi]/2$ . Hence,  $W$  is directly related to the Ramsey fringes contrast  $c(\alpha)$ :

$$W = \frac{2}{\pi} \langle P \rangle = \frac{2}{\pi} c(\alpha) = \frac{2}{\pi} [P_e(0, \alpha) - P_e(\pi, \alpha)] . \quad (112)$$

We have applied this procedure to the residual thermal field in the cavity and to an approximate single-photon Fock state, prepared through an atomic emission in  $C$ . The latter results are shown in Figure 20. Panels (a) and (b) present the Ramsey fringes for two displacement amplitudes  $\alpha = 0$  and  $\alpha = 0.81$  ( $W$  being phase-independent, we need not tune the phase of  $D_1$  and can assume that  $\alpha$  is real). The fringe phase is shifted by  $\pi$  between these two values, indicating a sign change for  $W$ , from negative (small  $\alpha$ ) to positive (large  $\alpha$ )

The fringes are fitted with sine curves [solid lines in Figure 20(a)-(b)], providing the contrast  $c(\alpha)$  ( $\pm 0.02$  uncertainty). Figure 20(c) presents the Wigner distribution values deduced from these fits (dots). The measurements are affected by the finite intrinsic contrast of the Ramsey interferometer. We thus multiply the raw data by a 4.16 factor, in order to obtain a normalized Wigner function. The measured  $W$  function is negative around the origin, revealing the non-classical nature of the cavity state. The solid line in Figure 20(c) is a fit on a mixture of Fock states with an adjustable photon distribution,  $p_n$ . The inferred  $p_n$  is shown in Figure 20(d). It exhibits a 71% probability for the one-photon state. This value is in agreement with a model of experimental imperfections taking cavity relaxation into account.

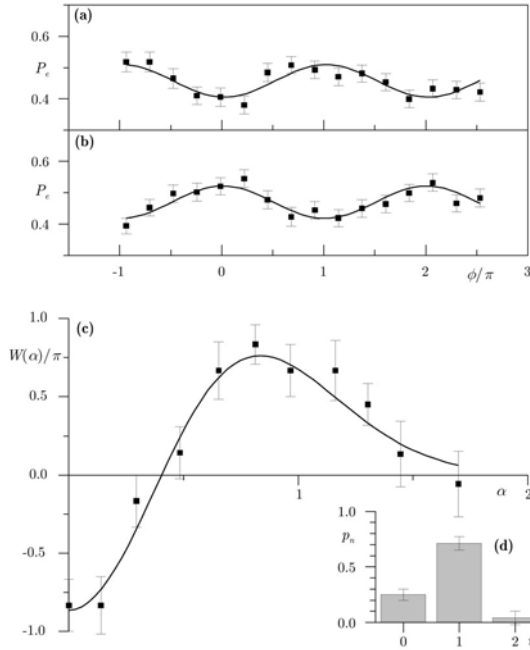


FIGURE 20. Determination of the ‘one-photon’ Wigner function. (a) Ramsey fringes for  $\alpha = 0$ . Probability  $P_e$  for detecting the atom in state  $|e\rangle$  as a function of the Ramsey interferometer phase  $\phi/\pi$ . Dots are experimental with statistical error bars. The solid curve is a sine fit. (b) Ramsey fringes for  $\alpha = 0.81$ . (c) Dots:  $W(\alpha)$  with error bars reflecting the uncertainty on the Ramsey fringes fit. The solid line is a theoretical fit. (d) Corresponding photon number distribution  $p_n$ .

This measurement opens interesting perspectives for the monitoring of the cat relaxation. It should be possible, in the near future, to reconstruct experimentally the evolution of the cat’s Wigner function shown in Figure 13.

### 4.3. Towards non-local cats

The Wigner function measurement can be used for the investigation of a new type of quantum field, merging two intriguing aspects of quantum mechanics: a non-local Schrödinger cat state. This state is a mesoscopic quantum superposition, exhibiting a fast decoherence as the cats encountered so far. At the same time, it exhibits the non-local properties of an EPR pair of particles and could lead to the observation of a violation of Bell inequalities [47]. This violation should be rapidly washed out by decoherence process.

We have in mind an experiment with two cavities,  $C_1$  and  $C_2$ , tuned slightly off-resonance with the  $|g\rangle \rightarrow |e\rangle$  transition, initially prepared in the same coherent state  $|\gamma\rangle$  by two classical sources  $S_1$  and  $S_2$ . An atom is prepared, in a first Ramsey zone  $R_1$  before  $C_1$ , in a coherent superposition  $(|g\rangle + |i\rangle)/\sqrt{2}$ , where  $|i\rangle$  is the circular state with principal quantum number 49. When in  $|i\rangle$ , the atom is far off-resonance and leaves the cavity fields unchanged. When in  $|g\rangle$ , the atom produces instead a  $\pi$ -phase shift of both fields. A second Ramsey zone,  $R_2$ , after  $C_2$  mixes again  $|g\rangle$  and  $|i\rangle$ , erasing any information about the atomic state in the cavities. The atomic detection in  $|g\rangle$  then projects the two cavities into:

$$|\Psi\rangle = \frac{1}{\sqrt{N}} (|\gamma, \gamma\rangle + |-\gamma, -\gamma\rangle) , \quad (113)$$

where  $N$  is a normalization factor, close to 2 for large  $\alpha$  values. This is a mesoscopic quantum superposition and also a non-local pair, since the two cavity field amplitudes exhibit quantum correlations.

In EPR experiments with spin pairs [48, 49], the Bell inequalities involve averages of products of binary spin observables ( $-1$  or  $+1$ ) for four settings of the detection axes. In the two-field mode case, the spin observables are replaced by the photon number parity  $\mathcal{P}$ , another binary observable. Independently adjustable displacements in both cavities play the role of the detection axes settings. The Bell signal,  $S_b$ , involves then four values of the joint cavities four-dimensional Wigner function  $W(\alpha_1, \alpha_2)$  [47]:

$$S_b = \frac{\pi^2}{4} |W(\alpha', \beta') + W(\alpha, \beta') + W(\alpha', \beta) - W(\alpha, \beta)| . \quad (114)$$

It should be lower than 2 for any local realistic description. It can reach  $2\sqrt{2}$  for large  $\alpha$  values. It is already 2.6 for a two-photon cat ( $\gamma = \sqrt{2}$ ).

The joint Wigner function can be determined as for a single cavity, with independent displacements of the cavity fields performed by  $S_1$  and  $S_2$  followed by a probe atom prepared in  $R_1$  in a superposition of  $|e\rangle$  and  $|g\rangle$ , whose coherence undergoes two  $\pi$ -phase shifts per photon in both cavities. The accumulated phase shift is probed in  $R_2$ . The contrast of the Ramsey fringes is then directly proportional to  $W$ . We have numerically simulated this experiment for two cavity damping times,  $T_c = 30$  ms and 300 ms, taking into account the exact atom-field interaction [50]. The results are presented in Figure 21 as a function of the delay  $T$  between state preparation and measurement. The Bell signal is above the classical limit for a short time interval and undergoes a fast decoherence.

This experiment puts severe requirement on the cavity quality, since the decoherence of the Bell signal is pretty fast. However, as mentioned above, we have recently obtained  $T_c = 14$  ms, already such that a violation of a Bell inequality could be observed in a short time interval for small photon numbers. This is certainly a strong incentive to build a two-cavity experiment.

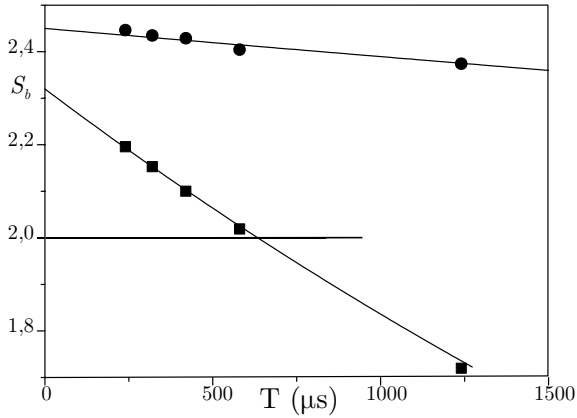


FIGURE 21. Bell signal  $S_b$  as a function of the time delay  $T$  between state preparation and analysis. The dots correspond to experimental simulations with  $T_c = 30$  ms (squares) and 300 ms (circles). The lines are linear fits.

## 5. Conclusion

Cavity QED experiments with circular Rydberg atoms and superconducting cavities are well adapted to the experimental study of the decoherence dynamics. The interaction of a single atom with a mesoscopic field, either in the resonant or dispersive regimes, produces quantum superpositions of coherent components with different classical phases, mesoscopic versions of the famous Schrödinger cat state. The decoherence transforms these superpositions into statistical mixtures in a time much shorter than the cavity energy lifetime. Probing the field quantum state with another atom makes it possible to unveil directly the decoherence process.

There is clearly much to do after the first qualitative measurements presented here. The development of new techniques to image the cavity state, such as the direct determination of the cavity field Wigner function, the realization of cavities with a much higher quality factors, open the way to detailed, ‘metrologic’ studies of the decoherence of pretty large Schrödinger cats.

A new experimental set-up is presently in construction in our laboratory. It should circumvent many of the limitations of the present apparatus. It will incorporate two separate cavities, making it possible to prepare and probe the non-local cats described above. Besides these fundamental aspects, it will also be well suited for the realization of complex quantum information manipulations [4].

## References

- [1] H. D. Zeh, *Found. Phys.* **1**, 69 (1970).
- [2] W. H. Zurek, Decoherence and the transition from quantum to classical, *Phys. Today* **44**, 36 (octobre 1991).
- [3] W. H. Zurek, Decoherence, einselection, and the quantum origins of the classical, *Rev. Mod. Phys.* **75**, 715 (2003).
- [4] J.-M. Raimond, M. Brune, and S. Haroche, Manipulating quantum entanglement with atoms and photons in a cavity, *Rev. Mod. Phys.* **73**, 565 (2001).
- [5] D. Leibfried, R. Blatt, C. Monroe, and D. J. Wineland, Quantum dynamics of single trapped ions, *Rev. Mod. Phys.* **75**, 281 (2003).
- [6] C. Monroe, D. M. Meekhof, B. E. King, and D. J. Wineland, A “Schrödinger cat” superposition state of an atom, *Science* **272**, 1131 (1996).
- [7] M. Brune, E. Hagley, J. Dreyer, X. Maître, A. Maali, C. Wunderlich, J.-M. Raimond, and S. Haroche, Observing the progressive decoherence of the meter in a quantum measurement, *Phys. Rev. Lett.* **77**, 4887 (1996).
- [8] Q. J. Myatt, B. E. King, Q. A. Turchette, C. A. Sackett, D. Kielpinski, W. M. Itano, C. Monroe, and D. J. Wineland, Decoherence of quantum superpositions through coupling to engineered reservoirs, *Nature (London)* **403**, 269 (2000).
- [9] A. Einstein, B. Podolsky, and N. Rosen, Can quantum mechanical description of physical reality be considered complete? *Phys. Rev.* **47**, 777 (1935).
- [10] R. J. Glauber, Coherent and incoherent states of the radiation field, *Phys. Rev.* **131**, 2766 (1963).
- [11] U. M. Titulaer and R. J. Glauber, Density operators for coherent fields, *Phys. Rev.* **145**, 1041 (1966).
- [12] S. M. Barnett and P. M. Radmore, *Methods in Theoretical Quantum Optics*, Oxford University Press, Oxford, 1997.
- [13] V. Buzek, H. Moya-Cessa, P. L. Knight, and S. D. L. Phoenix, Schrödinger-cat states in the resonant Jaynes-Cummings model: Collapse and revival of oscillations of the photon-number distribution, *Phys. Rev. A* **45**, 8190 (1992).
- [14] M. Brune, S. Haroche, J.-M. Raimond, L. Davidovich, and N. Zagury, Manipulation of photons in a cavity by dispersive atom-field coupling: Quantum non demolition measurements and generation of Schrödinger cat states, *Phys. Rev. A* **45**, 5193 (1992).
- [15] W. P. Schleich, *Quantum Optics in Phase Space*, Wiley, Berlin, 2001.
- [16] J.-M. Raimond, T. Meunier, P. Bertet, S. Gleyzes, P. Maioli, A. Auffeves, G. Nogues, M. Brune, and S. Haroche, Probing a quantum field in a photon box, *J. Phys. B* **38**, S535 (2005).
- [17] E. P. Wigner, On the quantum correction for thermodynamic equilibrium, *Phys. Rev.* **40**, 749 (1932).
- [18] K. E. Cahill and R. J. Glauber, Ordered expansions in boson amplitude operators, *Phys. Rev.* **177**, 1857 (1969).
- [19] J. Dalibard, Y. Castin, and K. Mølmer, Wave-function approach to dissipative processes in quantum optics, *Phys. Rev. Lett.* **68**, 580 (1992).
- [20] M. B. Plenio and P. L. Knight, The quantum-jump approach to dissipative dynamics in quantum optics, *Rev. Mod. Phys.* **70**, 101 (1998).

- [21] T. Sauter, W. Neuhauser, R. Blatt, and P. Toschek, Observation of quantum jumps, *Phys. Rev. Lett.* **57**, 1696 (1986).
- [22] J. C. Bergquist, R. G. Hulet, W. M. Itano, and D. J. Wineland, Observation of quantum jumps in a single atom, *Phys. Rev. Lett.* **57**, 1699 (1986).
- [23] C. Cohen-Tannoudji and J. Dalibard, Single-atom laser spectroscopy - looking for dark periods in fluorescence, *EuroPhys. Lett.* **1**, 441 (1986).
- [24] E. T. Jaynes and F. W. Cummings, Comparison of quantum and semiclassical radiation theories with application to the beam maser, *Proc. IEEE* **51**, 89 (1963).
- [25] S. Haroche and J.-M. Raimond, Manipulation of non-classical field states in a cavity by atom interferometry, In P. Berman, editor, *Advances in Atomic and Molecular Physics, supplement 2*, page 123. Academic Press, New York, 1994.
- [26] S. Haroche. Cavity quantum electrodynamics, In J. Dalibard, J.-M. Raimond, and J. Zinn-Justin, editors, *Fundamental Systems in Quantum Optics, Les Houches Summer School, Session LIII*, page 767. North Holland, Amsterdam, 1992.
- [27] P. Maioli, T. Meunier, S. Gleyzes, A. Auffeves, G. Nogues, M. Brune, J.-M. Raimond, and S. Haroche, Non-destructive Rydberg atom counting with mesoscopic fields in a cavity, *Phys. Rev. Lett.* **94**, 113601 (2005).
- [28] M. Brune, P. Nussenzveig, F. Schmidt-Kaler, F. Bernardot, A. Maali, J.-M. Raimond, and S. Haroche, From Lamb shifts to light shifts: Vacuum and subphoton cavity fields measured by atomic phase sensitive detection, *Phys. Rev. Lett.* **72**, 3339 (1994).
- [29] N. F. Ramsey. *Molecular Beams*, International series of monographs on physics, Oxford University Press, Oxford, 1985.
- [30] P. Bertet, S. Osnaghi, A. Rauschenbeutel, G. Nogues, A. Auffeves, M. Brune, J.-M. Raimond, and S. Haroche, A complementarity experiment with an interferometer at the quantum-classical boundary, *Nature (London)* **411**, 166 (2001).
- [31] L. Davidovich, M. Brune, J.-M. Raimond, and S. Haroche, Mesoscopic quantum coherences in cavity QED: Preparation and decoherence monitoring schemes, *Phys. Rev. A* **53**, 1295 (1996).
- [32] J.-M. Raimond, M. Brune, and S. Haroche, Reversible decoherence of a mesoscopic superposition of field states, *Phys. Rev. Lett.* **79**, 1964 (1997).
- [33] P. Bertet, A. Auffeves, P. Maioli, S. Osnaghi, T. Meunier, M. Brune, J.-M. Raimond, and S. Haroche, Direct measurement of the Wigner function of a one-photon Fock state in a cavity, *Phys. Rev. Lett.* **89**, 200402 (2002).
- [34] M. Fortunato, J.-M. Raimond, P. Tombesi, and D. Vitali, Autofeedback scheme for schrödinger cat preservation in microwave cavities, *Phys. Rev. A* **60**, 1687 (1999).
- [35] S. Zippilli, D. Vitali, P. Tombesi, and J.-M. Raimond, Scheme for decoherence control in microwave cavities, *Phys. Rev. A* **67**, 052101 (2003).
- [36] J. D. Jackson, *Classical Electrodynamics*, Wiley, New York, second edition, 1975.
- [37] A. Faist, E. Geneux, P. Meystre, and A. Quattropani, Coherent radiation in interaction with two-level system, *Helv. Phys. Acta* **45**, 956 (1972).
- [38] J. H. Eberly, N. B. Narozhny, and J. J. Sanchez-Mondragon, Periodic spontaneous collapse and revival in a simple quantum model, *Phys. Rev. Lett.* **44**, 1323 (1980).
- [39] P. L. Knight and P. M. Radmore, Quantum origin of dephasing and revivals in the coherent-state Jaynes-Cummings model, *Phys. Rev. A* **26**, 676 (1982).

- [40] J. Gea-Banacloche, Atom and field evolution in the Jaynes and Cummings model for large initial fields, *Phys. Rev. A* **44**, 5913 (1991).
- [41] M. Fleischhauer and W. P. Schleich, Revivals made simple: Poisson summation formula as a key to the revivals in the Jaynes–Cummings model, *Phys. Rev. A* **47**, 4258 (1993).
- [42] V. Buzek and P. L. Knight, Quantum interference, superposition states of light and non-classical effects, In *Progress in Optics XXXIV*, volume 34, page 1. Elsevier, 1995.
- [43] A. Auffeves, P. Maioli, T. Meunier, S. Gleyzes, G. Nogues, M. Brune, J.-M. Raimond, and S. Haroche, Entanglement of a mesoscopic field with an atom induced by photon graininess in a cavity, *Phys. Rev. Lett.* **91**, 230405 (2003).
- [44] G. Morigi, E. Solano, B.-G. Englert, and H. Walther, Measuring irreversible dynamics of a quantum harmonic oscillator, *Phys. Rev. A* **65**, 040102 (2002).
- [45] T. Meunier, S. Gleyzes, P. Maioli, A. Auffeves, G. Nogues, M. Brune, J.M. Raimond, and S. Haroche, Rabi oscillations revival induced by time reversal: a test of mesoscopic quantum coherence, *Phys. Rev. Lett.* **94**, 010401 (2005).
- [46] L. G. Lutterbach and L. Davidovich, Method for direct measurement of the Wigner function in cavity QED and ion traps, *Phys. Rev. Lett.* **78**, 2547 (1997).
- [47] K. Banaszek and K. Wodkiewicz, Testing quantum nonlocality in phase space, *Phys. Rev. Lett.* **82**, 2009 (1999).
- [48] A. Aspect, J. Dalibard, and G. Roger, Experimental test of Bell’s inequalities using time-varying analysers, *Phys. Rev. Lett.* **49**, 1804 (1982).
- [49] A. Zeilinger, Experiment and the foundations of quantum physics, *Rev. Mod. Phys.* **71**, S288 (1999).
- [50] P. Milman, A. Auffeves, F. Yamaguchi, M. Brune, J.M. Raimond, and S. Haroche, A proposal to test Bell’s inequalities with mesoscopic non-local states in cavity qed, *Eur. Phys. J. D* **32**, 233 (2005).

Jean-Michel Raimond  
Laboratoire Kastler Brossel  
Département de Physique de l’Ecole Normale Supérieure  
24, rue Lhomond  
F-75231 Paris Cedex 05  
France  
e-mail: [jmr@lkb.ens.fr](mailto:jmr@lkb.ens.fr)

Serge Haroche  
Collège de France  
11, place Marcelin Berthelot  
F-75231 Paris Cedex 05  
France  
e-mail: [haroche@physique.ens.fr](mailto:haroche@physique.ens.fr)

# Approaches to Quantum Error Correction

Julia Kempe

**Abstract.** In a ground breaking discovery in 1994, Shor has shown that quantum computers, if built, can factor numbers efficiently. Since then quantum computing has become a burgeoning field of research, attracting theoreticians and experimentalists alike, and regrouping researchers from fields like computer science, physics, mathematics and engineering. Quantum information is very fragile and prone to decoherence. Yet by the middle of 1996 it has been shown that fault-tolerant quantum computation is possible. We give a simple description of the elements of quantum error-correction and quantum fault-tolerance. After characterizing quantum errors we present several error correction schemes and outline the elements of a full fledged fault-tolerant computation, which works error-free even though all of its components can be faulty. We also mention alternative approaches to error-correction, so called error-avoiding or decoherence-free schemes.

We have persuasive evidence that a quantum computer would have extraordinary power. But will we ever be able to build and operate them?

A quantum computer will inevitably interact with its environment, resulting in decoherence and the decay of the quantum information stored in the device. It is the great technological (and theoretical) challenge to combat decoherence. And even if we can suitably isolate our quantum computer from its surroundings, errors in the quantum gates themselves will pose grave difficulties. Quantum gates (as opposed to classical gates) are unitary transformations chosen from a *continuous* set; they cannot be implemented with perfect accuracy and the effects of small imperfections in the gates will accumulate, leading to an eventual failure of the computation. Any reasonable correction-scheme must thus protect against small unitary errors in the quantum gates as well as against decoherence. Furthermore we must not ignore that the correction and recovery procedure itself can introduce new errors; successful fault-tolerant quantum computation must also deal with this issue.

The purpose of this account is to give an overview of the main approaches to quantum error correction. There exist several excellent reviews of the subject,

which the interested reader may consult (see [Pre98b],[Pre99], [NC00], [KSV02], [Ste99, Ste01] and more recently [Got05]).

## 1. Introduction

*“We have learned that it is possible to fight entanglement with entanglement.”*  
*John Preskill, 1996*

In a ground breaking discovery in 1994, Shor [Sho94] has shown that quantum computers, if built, can factor numbers efficiently. Since then quantum computing has become a burgeoning field of research, attracting theoreticians and experimentalists alike, and regrouping researchers from fields like computer science, physics, mathematics and engineering. One more reason for the enormous impetus of this field is the fact that by the middle of 1996 it has been shown how to realize *fault-tolerant* quantum computation. This was not at all obvious; in fact it was not even clear how any form of quantum error-correction could work. Since then many new results about the power of quantum computing have been found, and the theory of quantum fault-tolerance has been developed and is still developing now.

In what follows we will give a simple description of the elements of quantum error-correction and quantum fault-tolerance. Our goal is to convey the necessary intuitions both for the problems and their solutions. In no way will we attempt to give the full and formal picture. This account is necessarily restricted with subjectively chosen examples and approaches and does not attempt to describe the whole field of quantum fault-tolerance, which has become a large subfield of quantum information theory of its own.

The structure of this account is the following. First we will describe why quantum error correction is a non-trivial achievement, given the nature of quantum information and quantum errors. Then we will briefly review the main features of a quantum computer, since, after all, this is the object we want to protect from errors, and it is also the object which will allow us to implement error-correction. Then we will give the first example of a quantum error-correcting code (the Shor-code), followed by other error correction mechanisms. We proceed to outline the elements of a full fledged fault-tolerant computation, which works error-free even though all of its components can be faulty. We mention alternative approaches to error-correction, so called error-avoiding or decoherence-free schemes. We finish with an outlook on the future. We will try to keep technical details and generalizations to a minimum; the interested reader will find more details, as well as suggestions for further reading, in the appendix.

## 2. The subtleties of quantum errors

*“Small errors will accumulate and cause the computation to go off track.”*  
*Rolf Landauer, 1995, in “Is quantum mechanics useful?”*

A quantum machine is far more susceptible to making errors than classical digital machines.

Not only is a quantum system more prone to decoherence resulting from unwanted interaction between the quantum system and its environment, but also, when manipulating quantum information we can only implement the desired transformation up to a certain precision. Until 1995 it was not clear at all if and how quantum error correction could work.

The second big breakthrough towards quantum computing (after Shor's algorithm) was the insight that quantum noise can be combatted or that quantum error protection and correction is possible. The first big step in this direction was again made by Peter Shor in his "*Scheme for reducing decoherence in a quantum memory*" in 1995 [Sho95].

This was indeed an amazing piece of work: the difficulties facing the introduction of classical error-correction ideas into the quantum realm seemed formidable. In fact there was a large number of reasons for pessimism. Let us cite but a few of the apparent obstacles:

(1) There is a hugely successful theory of classical error correction which allows to protect against classical errors. However, classical errors are *discrete* by their nature. In the most common case where the information is encoded into a string of bits, the possible errors are bit-flips or erasures. A quantum state is a priori continuous, and hence also the error is continuous. Similarly, quantum *operations* are continuous by their nature, and will necessarily only be implemented with a certain precision, but never exactly. As noted by Landauer [Lan95], small errors can accumulate over time and add up to large, uncorrectable errors. Moreover it is not clear how to adapt the discrete theory of error correcting codes to the quantum case.

(2) A second objection is that to protect against errors, the information must be encoded in a redundant way. However, the quantum no-cloning theorem [Die82, WZ82], which follows directly from the linearity of quantum mechanics, shows that it is impossible to copy an unknown quantum state. How then can the information be stored in a redundant way?

(3) Another point is the following: in order to correct an error, we need to first acquire some information about the nature and type of error. In other words we need to observe the quantum system, to perform a measurement. But any measurement collapses the quantum system and might destroy the information we have encoded in the quantum state. How then shall we extract information about the error without destroying the precious quantum superposition that contains the information?

Many researchers in the field were pessimistic about the prospects of error-correction and Shor's result came as a great surprise to many. All the initial objections let us appreciate the elegance of the solution even more. But before giving the key ingredients, we need to briefly review the object we want to protect from errors, the actual quantum machine.

### 3. What is a quantum computer?

*“The more success the quantum theory has, the sillier it looks.”*

*Albert Einstein, 1912*

There are nearly as many proposals for the hardware of a quantum computer today, as there are experimental quantum physicists. The ultimate shape and function of a quantum computer will depend on the physical system used, be it optical lattices, large molecules, crystals or silicon based architectures. Nonetheless, each of these implementations have some key elements in common, since they all implement the quantum computing model.

What are the key ingredients of a quantum computer? A quantum computer is a machine that processes basic computational units, so called *qubits*, quantum two-level systems. (Although there might be quantum machines which process higher-dimensional quantum systems, we will restrict ourselves for simplicity to the case of two-level systems.) Qubits are two-dimensional quantum states spanned by two basis-states, which we conventionally call  $|0\rangle$  and  $|1\rangle$ , alluding to the classical bits of a standard computer. Hence the general state of a qubit is

$$|\psi\rangle = \alpha|0\rangle + \beta|1\rangle \quad |\alpha|^2 + |\beta|^2 = 1 ,$$

where  $\alpha$  and  $\beta$  are complex numbers. In each implementation of a quantum computer these basis states  $|0\rangle$  and  $|1\rangle$  need to be identified; they usually correspond to two chosen states of a larger system. For any quantum computation, *fresh* qubits have to be supplied in a known state, which is usually taken to be the  $|0\rangle$  state.

A quantum computer implements a *unitary* transformation on the space of several qubits, as consistent with the laws of quantum mechanics. However, in the context of computation, each unitary is decomposed into *elementary* gates, where each gate acts on a small number of qubits only. These elementary gates constitute a universal gate set, which allows to implement any unitary operation on the set of qubits. There are several universal gate sets, but we will mention only two, which are relevant for what follows. The first such set is continuous, and consists of all one-qubit unitaries, together with the controlled NOT or CNOT. The action of the CNOT on the basis states  $|00\rangle, |01\rangle, |10\rangle, |11\rangle$  is as follows

$$CNOT = \begin{pmatrix} 1 & 0 & 0 & 0 \\ 0 & 1 & 0 & 0 \\ 0 & 0 & 0 & 1 \\ 0 & 0 & 1 & 0 \end{pmatrix} .$$

In quantum circuit design it is often depicted as in Fig. 1.

It is possible to implement any unitary operation by a sequence of CNOT and single qubit unitary operations on the qubits.

The second set of universal gates is *discrete*. It contains the gates  $H$ ,  $\pi/8$ ,  $Z$  and  $CNOT$ . The first three gates are single qubit gates.  $H$  is called the *Hadamard* transform,  $\pi/8$  is a phase gate and  $Z$  is known to physicists as one of the Pauli

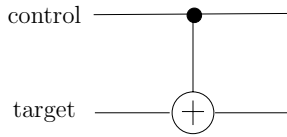


FIGURE 1. The top qubit is the *control* qubit. If it is in the state  $|0\rangle$ , then the *target* qubit stays unchanged, if it is in the state  $|1\rangle$ , the target qubit is flipped from  $|0\rangle$  to  $|1\rangle$  and vice versa.

matrices  $\sigma_z$ .<sup>1</sup> On the basis  $|0\rangle, |1\rangle$ , they act as

$$H = \frac{1}{\sqrt{2}} \begin{pmatrix} 1 & 1 \\ 1 & -1 \end{pmatrix} \quad \pi/8 = \begin{pmatrix} e^{i\frac{\pi}{8}} & 0 \\ 0 & e^{-i\frac{\pi}{8}} \end{pmatrix} \quad Z = \begin{pmatrix} 1 & 0 \\ 0 & -1 \end{pmatrix}.$$

All experimental proposals, in one way or another, demonstrate the ability to induce the transformations corresponding to this (or some other universal) gate set. Note that it is absolutely crucial to implement the two-qubit gate CNOT (or some other suitable two-qubit gate), as single qubit operations alone are clearly not universal.

This gate set is discrete, it contains only four gates. However, this comes at a price. It is not in general possible to implement any unitary transformation with a sequence drawn from this gate set. But it is possible to *approximate* any unitary to arbitrary accuracy using gates from this set. (Here accuracy is measured as the spectral norm of the difference between the desired unitary matrix and the actually implemented unitary matrix.) This is good enough for our purposes.

The last ingredient of a quantum computer is the *read-out*, or measurement. At the end of the day, when we want to extract the result of the quantum computation, we need to observe the quantum system, to gain information about the result.

In general one assumes that each qubit (or the qubit carrying the result of the computation) is measured in some basis. The classical result represents the outcome of the computation.

Schematically, then, a quantum computer looks like in Fig. 2.

#### 4. What is a quantum error?

*“Had I known that we were not going to get rid of this damned quantum jumping, I never would have involved myself in this business!”*

*Erwin Schrödinger*

Quantum computers are notoriously susceptible to quantum errors, and this is certainly the reason we did not yet succeed in building a scalable model. The

<sup>1</sup>Note that the  $Z$  gate is not necessary for universality, as it can be generated from the other gates in the set. However, it is often included for convenience, as it becomes necessary in many fault-tolerant gate sets.

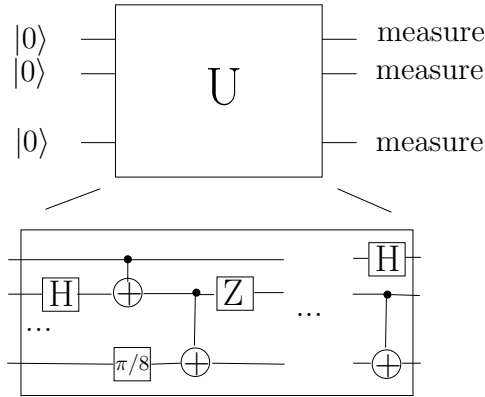


FIGURE 2. A quantum computer, schematically. Fresh qubits, initialized in the state  $|0\rangle$ , are supplied as the input to the unitary transform  $U$ .  $U$  is composed of elementary gates affecting at most 2 qubits. At the end of the computation the qubits are measured.

problem is that our quantum system is inevitably in contact with a larger system, its *environment*. Even if we make heroic efforts to isolate a quantum system from its environment, we still have to manipulate the information inside it in order to compute, which again will introduce errors. Were it not for the development of methods of quantum error correction, the prospects for quantum computing technology would not be bright. In order to describe quantum error correction we need to get a clear picture of what the noise processes affecting our machine are.

But how do we describe a quantum error?

Let us study the example of a single qubit. This qubit might undergo some random unitary transformation, or it might decohere by becoming entangled with the environment. In general it will undergo some unitary transformation in the *combined* system of qubit and environment. Let us call  $|E\rangle$  the state of the environment before the interaction with the qubit. Then the most general unitary transformation on system and environment can be described as

$$\begin{aligned}
 U : \quad |0\rangle \otimes |E\rangle &\longrightarrow |0\rangle \otimes |E_{00}\rangle + |1\rangle \otimes |E_{01}\rangle \\
 |1\rangle \otimes |E\rangle &\longrightarrow |0\rangle \otimes |E_{10}\rangle + |1\rangle \otimes |E_{11}\rangle.
 \end{aligned}$$

Here  $|E_{ij}\rangle$  represent not necessarily orthogonal or normalized states of the environment, with the only constraint that the total evolution be unitary. The unitary  $U$  *entangles* our qubit with the environment. Potentially, this entanglement will lead to decoherence of the information stored in the qubit.

Suppose now the qubit is in the state  $\alpha|0\rangle + \beta|1\rangle^2$ . Now if the qubit is afflicted by an error, it evolves as

$$\begin{aligned}
 (\alpha|0\rangle + \beta|1\rangle) \otimes |E\rangle &\longrightarrow \alpha(|0\rangle \otimes |E_{00}\rangle + |1\rangle \otimes |E_{01}\rangle) + \beta(|0\rangle \otimes |E_{10}\rangle + |1\rangle \otimes |E_{11}\rangle) \\
 &= (\alpha|0\rangle + \beta|1\rangle) \otimes \frac{1}{2}(|E_{00}\rangle + |E_{11}\rangle) && \text{identity} \\
 &+ (\alpha|0\rangle - \beta|1\rangle) \otimes \frac{1}{2}(|E_{00}\rangle - |E_{11}\rangle) && \text{phase flip} \\
 &+ (\alpha|1\rangle + \beta|0\rangle) \otimes \frac{1}{2}(|E_{01}\rangle + |E_{10}\rangle) && \text{bit flip} \\
 &+ (\alpha|1\rangle - \beta|0\rangle) \otimes \frac{1}{2}(|E_{01}\rangle - |E_{10}\rangle) && \text{bit \& phase flip.}
 \end{aligned} \tag{1}$$

Intuitively, we may interpret this expansion by saying that one of four things happens to the qubit: nothing, a bit flip, a phase flip or a combination of bit flip and phase flip. This will be made more precise in the next section, where we see that quantum error correction will include a *measurement* of the error, collapsing the state into one of the four possibilities above. This way, even though the quantum error is continuous, it will become *discrete* in the process of quantum error correction. We will denote the four errors acting on a qubit as

$$\begin{aligned}
 \underbrace{I = \begin{pmatrix} 1 & 0 \\ 0 & 1 \end{pmatrix}}_{\text{identity}} & \quad \underbrace{X = \begin{pmatrix} 1 & 0 \\ 0 & -1 \end{pmatrix}}_{\text{phase flip}} & \quad \underbrace{Z = \begin{pmatrix} 0 & 1 \\ 1 & 0 \end{pmatrix}}_{\text{bit flip}} \\
 & & \underbrace{Y = XZ = \begin{pmatrix} 0 & -1 \\ 1 & 0 \end{pmatrix}}_{\text{bit \& phase flip}}. \tag{2}
 \end{aligned}$$

These four matrices form the so called *Pauli group*. Another way of saying the above is to realize that these four errors span the space of unitary matrices on one qubit, i.e. any matrix can be expressed as a linear combination of these four matrices (with complex coefficients). If we trace out the environment (average over its degrees of freedom, see App. B.2), the resulting operator can be expanded in terms of the Pauli group, we can attach a probability to each Pauli group element. Often the analysis of fault-tolerant architectures is simplified by assuming that the error is a random non-identity Pauli matrix with equal probability  $\varepsilon/3$ , where  $\varepsilon$  is the *error rate*.

We now make a crucial assumption: that the error processes affecting different qubits are *independent* from each other. A quantum error correcting code, then, will be such that it can protect against these four possible errors. Once the error

---

<sup>2</sup>Of course our qubit could be part of a larger quantum state of several qubits. It might be entangled with other qubits which are unaffected by errors. So the coefficients  $\alpha$  and  $\beta$  need not be numbers, they can be states that are orthogonal to both  $|0\rangle$  and  $|1\rangle$ .

has become discrete it is much more obvious how to apply and extend classical error correction codes, which are able to protect information against a bit flip.

We have so far only analyzed errors due to decoherence, but have neglected errors due to imperfections in the gates, in the measurement process and in preparation of the initial states. All these operations can be faulty. A natural assumption is again that these imperfections are independent of each other. In a similar fashion as before we can discretize the errors in a quantum gate. We can model a faulty gate by assuming that it is a perfect gate, followed by an error. For a one-qubit gate this error is the same as given in Eq. (1). For a two-qubit gate we assume that both qubits undergo possibly correlated decoherence. Similar reasoning as in Eq. (1) shows, that in that case the error is a linear combination of 16 possible errors, resulting from all combinations of the errors in Eq. (2) on both qubits. Again, often the additional assumption is made that all 15 non-identity errors appear with equal probability  $\varepsilon_2/15$ , where  $\varepsilon_2$  is the two-qubit gate error rate. In a similar fashion we will deal with measurement and state preparation errors.

Note that our analysis of the error is somewhat simplified. Several tools have been developed to study quantum decoherence and quantum noise. Some of these formalisms are described in more detail in App. B. As already mentioned, in order to give methods for quantum error correction, some assumptions about the nature of the noise have to be made. In one of the common models of noise in a quantum register it is assumed that each qubit interacts *independently* with the environment in a Markovian fashion<sup>3</sup>; the resulting errors are single qubit errors affecting each qubit independently at random. More details on models of quantum noise are given in App. C.

## 5. The first error correction mechanisms

*“Correct a flip and phase – that will suffice.  
If in our code another error’s bred,  
We simply measure it, then God plays dice,  
Collapsing it to X or Y or Zed.”  
Daniel Gottesman, in “Error Correction Sonnet”*

We have seen how entanglement with the environment can cause errors that result in a complete loss of the quantum information. However, entanglement will also allow us to *protect* the information in a non-local way. If we distribute the information over several qubits in a way that it cannot be accessed by measuring just a few of the qubits, then by the same token it cannot be damaged if the environment interacts with just a few of the qubits.

A marvelous machinery has been developed in the classical world to protect classical information, the theory of error correcting codes. The simplest possible

---

<sup>3</sup>This means that the environment maintains no memory of the errors, which are thus *uncorrelated* in *time* and qubit *location*.

such code is the *repetition* code: each bit is replaced by three of its copies:

$$\mathcal{C} : \quad 0 \longrightarrow 000 \quad 1 \longrightarrow 111.$$

This code clearly protects against one bit flip error. If a bit is flipped, we can still decode the information by majority voting. Only if two bit flips happen we will be unable to correctly decode the information. But if we assume that the probability of a bit flip is  $\varepsilon$  and independent on each bit, then the probability that we cannot correct a bit flip is  $3\varepsilon^2(1 - \varepsilon) + \varepsilon^3$  (there are three possible ways to have two bit flips and one way to have three bit flips). If we would not encode the information at all the error probability is  $\varepsilon$ , so as long as  $\varepsilon < 1/2$  we gain by encoding.

But how can we extend this idea to the quantum setting? There is no way to copy quantum information. There are not only bit flip, but also phase flip errors (and combinations of both). And moreover a measurement for majority vote will cause disturbance.

Shor was the first to overcome all these obstacles [Sho95]. He gave the most straightforward quantum generalization of the repetition code. Suppose we want to just deal with bit flip errors. We encode a single qubit with the repetition code on the basis states, i.e.

$$|0\rangle \longrightarrow |000\rangle \quad |1\rangle \longrightarrow |111\rangle,$$

such that

$$\alpha|0\rangle + \beta|1\rangle \longrightarrow \alpha|000\rangle + \beta|111\rangle. \quad (3)$$

This encoding can be realized with the circuit in Fig. 3.

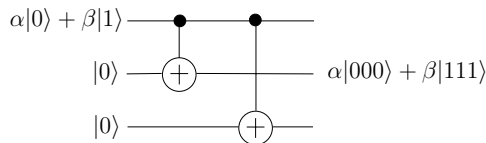


FIGURE 3. The CNOTs flip the target qubit if the first qubit is in the state  $|1\rangle$ . Note that the transformation does not *copy* the state of the first qubit to the other two qubits, but rather implements the transformation of Eq. (3).

Now suppose a bit flip happens, say on the first qubit. The state becomes  $\alpha|100\rangle + \beta|011\rangle$ . If we measured the qubits in the computational basis, we would obtain one of the states  $|100\rangle$  or  $|011\rangle$ , but we would destroy the quantum superposition. But what if instead we measured the *parity* of all pairs of qubits, without acquiring any additional information? For instance we can measure the parity of the first two qubits with the circuit in Fig. 4.

In our example, a parity measurement does not destroy the superposition. If the first qubit is flipped, then both  $|100\rangle$  and  $|011\rangle$  have the same parity 1 on the first two qubits. If no qubit is flipped and the code word is still in the state of Eq. (3) this parity will be 0 for both  $|000\rangle$  and  $|111\rangle$ . If the error is a *linear*

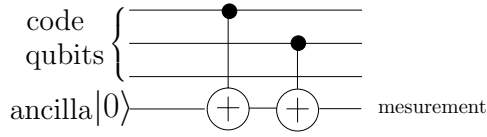


FIGURE 4. Circuit to measure the parity of the first two qubits of the quantum code word. Each CNOT flips the ancilla qubit if the source qubit is in the state  $|1\rangle$ . If the first two qubits are in the state  $|00\rangle$ , the ancilla is left in the state  $|0\rangle$ . If these qubits are in the state  $|11\rangle$  the ancilla is flipped twice and its state is also  $|0\rangle$ . Otherwise it is flipped once by one of the CNOTs.

combination of identity and bit flip, similar to Eq. (1), then the measurement will collapse the state into one of the two cases. Let us adapt Eq. (1) to the case of only a bit flip error on one qubit ( $|E_{00}\rangle = |E_{11}\rangle$ ,  $|E_{01}\rangle = |E_{10}\rangle$  and  $|E_{01}\rangle$  and  $|E_{00}\rangle$  are orthogonal) and write

$$(\alpha|0\rangle + \beta|1\rangle) \otimes |E\rangle \longrightarrow \underbrace{\sqrt{1-\varepsilon}(\alpha|0\rangle + \beta|1\rangle)}_{\text{identity}} \otimes |\tilde{E}_{00}\rangle + \underbrace{\sqrt{\varepsilon}(\alpha|1\rangle + \beta|0\rangle)}_{\text{bit flip}} \otimes |\tilde{E}_{01}\rangle, \quad (4)$$

where we have normalized the state of the environment ( $|\tilde{E}_{00}\rangle$  and  $|\tilde{E}_{01}\rangle$  have norm 1)<sup>4</sup>. The probability that the parity measurement collapses to the bit flip case is  $\varepsilon$ , the probability to project onto a state where no error has happened is  $1 - \varepsilon$ . Imagine now that each of the three qubits of the code undergoes the same error process of Eq. (4). This gives a threefold tensor product of Eq. (4) (each qubit has its own environment state), which shows that the probability of no error becomes  $(1 - \varepsilon)^3 \geq 1 - 3\varepsilon$ , and the probability of each of the single qubit errors is  $\varepsilon(1 - \varepsilon) < \varepsilon$ . Of course there is now a nonzero probability that the state will be collapsed to a state where two or even three single qubit errors occurred; however, the total probability of this happening is given by  $3\varepsilon^2(1 - \varepsilon) + \varepsilon^3 \leq 3\varepsilon^2$ .

This mechanism illustrates how a measurement that detects the error, also discretizes it. The parity measurement *disentangles* the code qubits from the environment and acquires information about the error. The three parities (for each qubit pair of the code word) give complete information about the location of the bit flip error. They constitute what is called the error *syndrome* measurement. The syndrome measurement does not acquire any information about the encoded superposition, and hence it does not destroy it. Depending on the outcome of the syndrome measurement, we can correct the error by applying a bit flip to the appropriate qubit.

<sup>4</sup>Note, that if we trace out the environment (see App. B.2), we obtain a process where with probability  $1 - \varepsilon$  nothing happens, and with probability  $\varepsilon$  the bit is flipped.  $\varepsilon$  defines the *rate* of error.

We have successfully resolved the introduction of redundancy, the discretization of errors and a way to measure the syndrome without destroying the information. We still need to take care of phase flip errors. We have been able to protect against bit flip errors by encoding the bits redundantly. The idea is to also encode the phase of the state in a redundant fashion. Shor's idea was to encode a qubit using *nine* qubits in the following way:

$$\begin{aligned} |0\rangle_{enc} &= \frac{1}{\sqrt{2^3}} (|000\rangle + |111\rangle) (|000\rangle + |111\rangle) (|000\rangle + |111\rangle) \\ |1\rangle_{enc} &= \frac{1}{\sqrt{2^3}} (|000\rangle - |111\rangle) (|000\rangle - |111\rangle) (|000\rangle - |111\rangle). \end{aligned} \quad (5)$$

Note that with this encoding, each of the blocks of three qubits is still encoded with a repetition code, so we can still correct bit flip errors in a fashion very similar to above. But what about phase errors? A phase flip error, say on one of the first three qubits, acts as:

$$\begin{aligned} |0\rangle_{enc} &\xrightarrow{\text{phase flip}} \frac{1}{\sqrt{2^3}} (|000\rangle - |111\rangle) (|000\rangle + |111\rangle) (|000\rangle + |111\rangle) \\ |1\rangle_{enc} &\xrightarrow{\text{phase flip}} \frac{1}{\sqrt{2^3}} (|000\rangle + |111\rangle) (|000\rangle - |111\rangle) (|000\rangle - |111\rangle). \end{aligned}$$

We need to detect this phase flip *without* measuring the information in the state. To achieve this we will follow the ideas developed for the bit flip and measure the parity of the phases on each pair of two of the three blocks. There is an interesting and useful duality between bit flip and phase flip errors. Let us look at a different basis for qubits, given by the states

$$|+\rangle = \frac{1}{\sqrt{2}} (|0\rangle + |1\rangle) \quad |-\rangle = \frac{1}{\sqrt{2}} (|0\rangle - |1\rangle).$$

The change from the standard basis to the  $|\pm\rangle$ -basis we apply the Hadamard transform  $H$ . Now note that a phase flip error acts as

$$|+\rangle \xrightarrow{\text{phase flip}} |-\rangle \quad |-\rangle \xrightarrow{\text{phase flip}} |+\rangle. \quad (6)$$

In other words a phase flip in the standard basis becomes a *bit flip* in the  $|\pm\rangle$ -basis. If we apply a Hadamard transform to each of the three qubits of a block of the Shor code, we obtain

$$\begin{aligned} H^{\otimes 3} \frac{1}{\sqrt{2}} (|000\rangle + |111\rangle) &= \frac{1}{2} (|000\rangle + |110\rangle + |101\rangle + |011\rangle) \\ H^{\otimes 3} \frac{1}{\sqrt{2}} (|000\rangle - |111\rangle) &= \frac{1}{2} (|111\rangle + |001\rangle + |010\rangle + |100\rangle). \end{aligned}$$

Note that the parity of each of the bitstrings for positive phase is *even* and for negative phase it is *odd*. We can see that if two blocks have different phase, then the parity of its constituent 6 qubits is odd, otherwise it is even. Hence, in order to detect a phase error, we just need to measure the parity of all qubits in the three possible pairs of blocks in the  $|\pm\rangle$  basis. The circuit in Fig. 5 does exactly that.

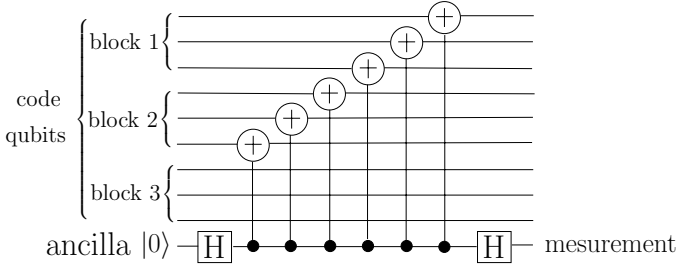


FIGURE 5. Circuit to measure the parity of the *phase* of the first and the second block of three qubits. In the  $|\pm\rangle$ -basis a CNOT acts on target (t) and control (c) bit as  $|+\rangle_t|\pm\rangle_c \rightarrow |+\rangle_t|\pm\rangle_c$  and  $|-\rangle_t|\pm\rangle_c \rightarrow |-\rangle_t|\mp\rangle_c$ , i.e. it flips the *control* bit in the  $|\pm\rangle$  basis if the *target* bit is  $|-\rangle_c$ . This way the ancilla bit is flipped an even number of times from  $|+\rangle$  to  $|-\rangle$  if blocks 1 and 2 have the same phase, and an odd number of times if they have different phase.

The nine-bit Shor code above protects against bit and phase flip, and also against a combination of both (when *both* bit and phase flip are detected, the error is  $XZ$ ). Note again, that we assume that *each* of the qubits undergoes some error at rate  $\varepsilon$ . Hence, by the discretization resulting from the error-recovery measurement, the state will be projected onto either a state where no error has occurred (with probability  $\geq 1-9\varepsilon$ ) or a state with a large error (single qubit, two qubit etc.). This code protects against all single qubit errors. Only when two or more errors occur (which happens with probability  $\leq 36\varepsilon^2$ ) the error is irrecoverable. Comparing this with the error rate of an unencoded qubit,  $\varepsilon$ , we see that this code is advantageous whenever  $\varepsilon \leq 1/36$ .

## 6. Quantum Error Correcting Codes

*“If people do not believe that mathematics is simple, it is only because they do not realize how complicated life is.”*

*John von Neumann*

Let us internalize the crucial properties of Shor’s code: A small part of the Hilbert space of the system is designated as the *code subspace*  $\mathcal{C}$ . In the Shor code  $\mathcal{C}$  is spanned by the two states in Eq. (5). We have a discrete set of correctable errors  $\{\mathbf{E}_\alpha\}$ . Each of the correctable errors  $\mathbf{E}_\alpha$  maps the code space  $\mathcal{C}$  to a mutually *orthogonal* error space. We can make a measurement that tells us in which of the mutually orthogonal spaces the system resides, and hence exactly infer the error. The error can be repaired by applying an appropriate unitary transformation ( $\mathbf{E}_\alpha^\dagger$ ).

These ideas have been formalized to define *quantum error correcting codes* (QECCs). An  $(N, K)$  quantum error correcting code  $\mathcal{C}$  is a  $K$  dimensional subspace of an  $N$  dimensional Hilbert space (coding space  $\mathcal{H}$ ) together with a recovery

(super)operator  $\mathcal{R}$ . The recovery operator usually consists of some sort of measurement (to detect the error) followed by a conditional unitary to correct it, but we do not necessarily have to think about it in this way. The code  $\mathcal{C}$  is  $\mathcal{E}$ -correcting if on the code-space an error followed by recovery restores the codeword, i.e.

$$\mathcal{R} \circ \mathcal{E} = \mathcal{I} \quad \text{on } \mathcal{C}$$

It has been shown [BDSW96, KL97] that QECC's exist for the set of errors if the following conditions (*QECC-conditions*) are satisfied:

**QECC-conditions:** Let  $\mathbf{E}$  be a discrete linear base set for  $\mathcal{E}$  and let the code  $\mathcal{C}$  be spanned by the basis  $\{|\Psi_i\rangle : i = 1 \dots K\}$ . Then  $\mathcal{C}$  is an  $\mathcal{E}$ -correcting QECC if and only if  $\forall |\Psi_i\rangle, |\Psi_j\rangle \in \mathcal{C}$

$$\langle \Psi_j | \mathbf{E}_\beta^\dagger \mathbf{E}_\alpha | \Psi_i \rangle = c_{\alpha\beta} \delta_{ij} \quad \forall \mathbf{E}_\alpha, \mathbf{E}_\beta \in \mathbf{E}. \quad (7)$$

What this means is the following: Errors  $\mathbf{E}_\alpha, \mathbf{E}_\beta \in \mathbf{E}$  acting on *different* orthogonal codewords  $|\Psi_i\rangle$  take these codewords to *orthogonal* states ( $\langle \Psi_i | \mathbf{E}_\beta^\dagger \mathbf{E}_\alpha | \Psi_j \rangle = 0$ ). Otherwise errors would destroy the perfect distinguishability of orthogonal codewords and no recovery would be possible. On the other hand for different errors acting on the *same* codeword  $|\Psi_i\rangle$  we only require that  $\langle \Psi_i | \mathbf{E}_\beta^\dagger \mathbf{E}_\alpha | \Psi_i \rangle$  does not depend on  $i$ . Otherwise we would – in identifying the error – acquire some information about the encoded state  $|\Psi_i\rangle$  and thus inevitably disturb it.

We usually think of the errors  $\mathbf{E}_\alpha$  to be a subset of the Pauli group with up to  $t$  non-identity Pauli matrices (for a  $t$ -error correcting QECC).

It is now possible to make the connection to the theory of classical error correcting codes. It turns out that there are families of classical codes with certain properties (concerning their dual) which make good quantum error correcting codes [Ste96b, CS96]. The codes have become known as Calderbank-Shor-Steane codes (CSS codes). It has been shown that for any number  $t$  of correctable errors, there is a QECC which can correct up to  $t$  errors (bit flip, phase flip and combination). As a result this code reduces the error for an unencoded qubit,  $\varepsilon$ , to  $c\varepsilon^{t+1}$ , where  $c$  is a constant depending on the code.

To illustrate this connection to classical codes we will briefly describe the smallest code in that family, which was first given by Steane [Ste96b]. This is the so called 7 qubit *Steane code*, based on the classical 7-bit Hamming code. The classical Hamming code encodes one bit into 7 bits. The codewords can be characterized by the *parity check* matrix

$$H = \begin{pmatrix} 0 & 0 & 0 & 1 & 1 & 1 & 1 \\ 0 & 1 & 1 & 0 & 0 & 1 & 1 \\ 1 & 0 & 1 & 0 & 1 & 0 & 1 \end{pmatrix}. \quad (8)$$

The code is the kernel of  $H$ , i.e. each code word is a 7-bit vector  $v_{\text{code}}$  such that  $H \cdot v_{\text{code}} = (0, 0, 0)^T$  in  $GF(2)$  arithmetic.  $H$  has three linearly independent rows (over  $GF(2)$ ), so the kernel is spanned by four linearly independent code words, and hence there are 16 different code words. If an error affects the  $i$ th bit of the codeword, this codeword is changed to  $v_{\text{code}} + e_i$ . The parity check matrix of the

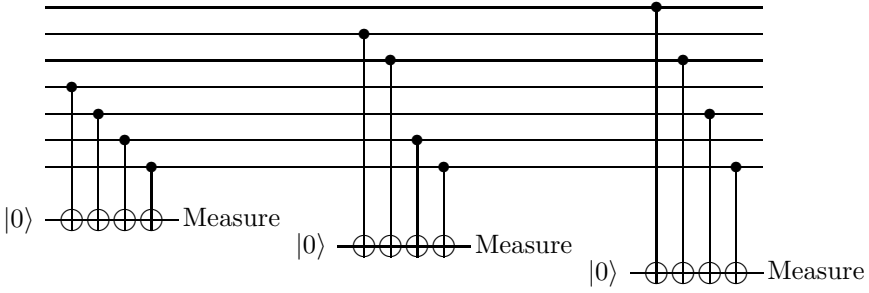


FIGURE 6. Computation of the bit-flip syndrome for Steane’s 7-qubit code. The three ancilla qubits carry the error syndrome.

resulting word is  $H(v_{\text{code}} + e_i) = He_i \neq 0$ , which is just the  $i$ th column of  $H$ . Since all columns of  $H$  are distinct, each  $e_i$  has a different *error syndrome* and we can infer  $e_i$  from it.

Steane’s code, derived from the Hamming code, is the following:

$$\begin{aligned}
 |0\rangle_{\text{code}} &= \frac{1}{\sqrt{8}} \left( \sum_{\substack{\text{even } v \\ \in \text{Hamming}}} |v\rangle \right) \\
 &= \frac{1}{\sqrt{8}} \left( |0000000\rangle + |0001111\rangle + |0110011\rangle + |0111100\rangle \right. \\
 &\quad \left. + |1010101\rangle + |1011010\rangle + |1100110\rangle + |1101001\rangle \right), \\
 |1\rangle_{\text{code}} &= \frac{1}{\sqrt{8}} \left( \sum_{\substack{\text{odd } v \\ \in \text{Hamming}}} |v\rangle \right) \\
 &= \frac{1}{\sqrt{8}} \left( |1111111\rangle + |1110000\rangle + |1001100\rangle + |1000011\rangle \right. \\
 &\quad \left. + |0101010\rangle + |0100101\rangle + |0011001\rangle + |0010110\rangle \right),
 \end{aligned} \tag{9}$$

i.e.  $|0\rangle_{\text{code}}$  is the superposition of all even and  $|1\rangle_{\text{code}}$  the superposition of all odd codewords. Note that all states appearing in the code words are Hamming code words, and hence a single bit flip can be detected by a simple parity measurement, as in Fig. 6.

To deal with phase flip errors we use the observation of Eq. (6), that phase flip errors correspond to bit flip errors in the  $|\pm\rangle$  basis. But if we change to this

basis by applying the Hadamard transform to each bit, we obtain

$$\begin{aligned}
 H^{\otimes 7}|0\rangle_{\text{code}} &= \frac{1}{4} \left( \sum_{\substack{v \in \\ \text{Hamming}}} |v\rangle \right) = \frac{1}{\sqrt{2}} (|0\rangle_{\text{code}} + |1\rangle_{\text{code}}) , \\
 H^{\otimes 7}|1\rangle_{\text{code}} &= \frac{1}{4} \left( \sum_{\substack{v \in \\ \text{Hamming}}} (-1)^{wt(v)} |v\rangle \right) = \frac{1}{\sqrt{2}} (|0\rangle_{\text{code}} - |1\rangle_{\text{code}}) \quad (10)
 \end{aligned}$$

(where  $wt(v)$  denotes the weight of  $v$ ). The key point is that in the  $|\pm\rangle$  basis, like in the  $|0\rangle, |1\rangle$  basis,  $|0\rangle_{\text{code}}$  and  $|1\rangle_{\text{code}}$ , are superpositions of Hamming codewords. Hence, in the rotated basis, as in the original basis, we can perform the Hamming parity check to diagnose bit flips, which are phase flips in the original basis. Assuming that only one qubit is in error, performing the parity check in both bases completely diagnoses the error, and enables us to correct it.

The core observation that allows to generalize Steane's construction to codes that encode more bits and can correct more errors is the following: If a quantum code word is a linear superposition over classical code words that form a code  $\mathcal{C}$ , then in the  $|\pm\rangle$  basis this code word is a linear superposition over the code words of the *dual* code  $\mathcal{C}^\perp$ , where  $\mathcal{C}^\perp = \{u : u \cdot v = 0 \ \forall v \in \mathcal{C}\}$ . This can be derived when looking at the action of the Hadamard transform on  $n$ -bit strings  $|x\rangle$ :

$$H^{\otimes n}|x\rangle = \frac{1}{\sqrt{2^n}} \sum_{y \in \{0,1\}^n} (-1)^{x \cdot y} |y\rangle.$$

As it is easy to see from Eq. (8), the Hamming code is its own dual, and hence we can use its properties to correct phase errors. In general, the CSS constructions find a code  $\mathcal{C}_1$  (for the bit flip errors) such that its dual,  $\mathcal{C}_1^\perp$ , contains a sufficiently good code  $\mathcal{C}_2$  (for the phase flip errors).

Having seen the nine qubit Shor code and the seven qubit Steane code, one can ask what the minimal overhead for a quantum code that corrects a single error is. It turns out that the smallest quantum code that achieves this has five qubits, and that this is optimal [LMPZ96].

Gottesman developed a very powerful formalism, so called *stabilizer codes*, that generalizes both the Shor code and CSS codes and gave fault tolerant constructions for them (for more details see App. D).

## 7. Fault-tolerant computation

*“When you have faults, do not fear to abandon them.”*

*Confucius*

We have seen that good quantum error correction codes exist. But so far we have worked under the assumption, that the error recovery procedure is *perfect*. Of course, error recovery will never be flawless. Recovery is itself a quantum

computation that will be prone to decoherence. We must ensure that errors do not *propagate* during recovery. For instance, if an error occurs in the ancilla bit in the parity measurement of Fig. 5, *all* six qubits interacting with it might be corrupted; the error propagates catastrophically. In fault-tolerant computing design, care is taken to avoid this type of error spreading, and other possible introduction and propagation of error. But even if we manage to avoid error spreading during recovery, that is not enough. A quantum computer does more than just *store* information, it also *processes* it. Of course we could decode, perform a gate and encode, but this procedure would temporarily expose quantum information to decoherence. Instead, we must apply our quantum gates directly to the encoded data.

### 7.1. Guidelines of fault-tolerance

The quantum circuit model gives us a good intuition about the points in a computation that potentially can introduce errors and corrupt the computation. We need to be able to faultlessly *prepare* the initial state, *compute* with a sequence of quantum gates and *measure* the output. Using a code to protect our computation against noise, we also need to assure faultless *encoding*, *decoding* and *correction*. Each qubit will be encoded into a separate block and quantum logic has to be applied directly *on the encoded states* so that the information is never exposed to noise without protection. This gives us the following guidelines of fault-tolerance: **Encoding/Decoding/State Preparation.** The procedure to encode/decode the information into a code should not introduce more errors than the code can correct. In the case of a 1-error correcting QECC encoding should not introduce more than one error per encoded block. Often the only states that need to be encoded are some  $|00\dots 0\rangle$  states at the beginning of the computation, it is then sufficient to ensure fault-tolerant *state-preparation*.

**Error-detection and Recovery.** These procedures (for a QECC), usually realized by a set of quantum gates together with auxiliary qubits, should again not introduce more than one error per block.

**Quantum gates.** should not introduce more than one error per encoded block. Furthermore they should not *propagate* already existing errors from one qubit to several others in the same block.

**Measurement.** should not introduce more than one error per block. Furthermore the measurement result must have probability of error of order  $\varepsilon^2$ , where  $\varepsilon$  is the probability of failure of any of the components in the measurement procedure. This is because the measurement result may be used to control other operations in a quantum computer.

### 7.2. Fault-tolerant error correction

With these guidelines in place, we will now illustrate how fault-tolerant recovery can be achieved, using the Steane code in Eq. (9) as our example. The error-measurement circuit in Fig. 6 is not fault-tolerant, as each of the CNOT gates can propagate a single phase error on the ancilla qubit to all four of the code qubits. To

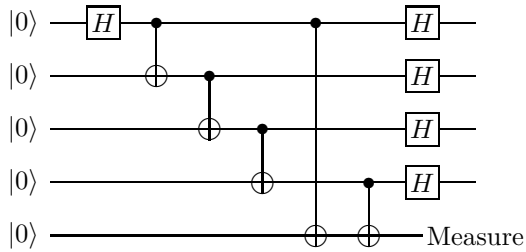


FIGURE 7. Construction and verification of the  $|\text{ancilla}\rangle$  state. If the measurement outcome is 1, then the state is discarded and a new  $|\text{ancilla}\rangle$  state is prepared.

prevent this propagation, we need to expand the ancilla into four qubits, each one the target of only one CNOT gate. But now we are again faced with the problem that our measurement should only reveal information about the *error* (the parity) but not about the encoded state. We circumvent this problem by preparing the ancilla in the following state:

$$|\text{ancilla}\rangle = \frac{1}{\sqrt{8}} (|0000\rangle + |1100\rangle + |1010\rangle + |1001\rangle + |0110\rangle + |0101\rangle + |0011\rangle + |1111\rangle),$$

i.e. in a superposition of all even bit strings. The crucial observation is that on this state one bit flip or three bit flips on any qubits all have the same effect, they transform it to the superposition of odd bit strings. Similarly, this state is invariant under any even number of bit flips. This means that we can infer the syndrome bit from the parity of the ancilla bits, it suffices to measure the ancilla in the end. Hence our syndrome measurement obeys the guidelines of fault-tolerance. To prepare the ancilla, we can use the circuit in Fig. 7, which at the same time allows *verification* of correct ancilla preparation.

The ancilla state must be verified before it is used, because a single error in the preparation of the ancilla state can propagate and cause two phase errors in the  $|\text{ancilla}\rangle$  state. Hence the circuit in Fig. 7 also verifies that multiple phase errors do not occur. If it fails the test it should be discarded, and the preparation procedure repeated.

Moreover, a single syndrome measurement might be faulty. Thus, the syndrome measurement should be repeated for accuracy; only if the same result is measured twice in a row should it be accepted.

With all the precautions above, recovery will only fail if two independent errors occur in this entire procedure. The probability that this happens is still

$c\epsilon^2$  for some constant  $c$ , but because there are now many more gates and steps involved the constant  $c$  can be quite large.

In a conceptually similar fashion it is possible to *encode* a qubit and to measure it in a basis spanned by  $|0\rangle_{\text{code}}$  and  $|1\rangle_{\text{code}}$  while following the guideline of fault-tolerance. For details the reader should consult e.g. [Sho96, Ste97, Pre98b, Pre99, Pre98a] or the work of Gottesman (e.g. [Got97c]) for fault-tolerant construction for CSS and other codes in the stabilizer formalism (see App. D).

### 7.3. Fault-tolerant computation

We have seen how to recover *stored* quantum information, even when recovery is faulty. But we also want to *compute*, and the gates we use will be faulty as well. This means that we must be able to apply the gates directly to the encoded data, without introducing errors uncontrollably and following the guidelines of fault-tolerance.

In fact, staying with the 7-qubit Steane code, it is easy to implement some single qubit gates directly on the encoded data. We have seen that the bitwise Hadamard transform implements an *encoded* Hadamard transform on the code-words (see Eq. (10)). This means we can apply it without propagating errors and such that each gate introduces at most one new error. Similarly, it is easy to see that the bitwise  $X$  gate induces an encoded  $X_{\text{enc}}$  because even code words get mapped to odd ones and vice versa. Moreover the bitwise  $Z$  gate (which is just  $HXH$ ) implements the encoded  $Z$ . In the same way the  $\frac{\pi}{4}$  gate (a diagonal single qubit unitary with diagonal  $(1, i)$ ) can be implemented by applying it bitwise to the encoded data.

Also, it is not hard to see that the bitwise CNOT between two quantum code words, i.e. a CNOT from the first qubit of the first code word to the first qubit of the second code word, a CNOT from the second qubit of the first code word, to the second qubit of the second and so on, implements a global CNOT between two code words. We call such an implementation of an encoded two qubit gate *transversal*. This is very promising, but the set of operation we can implement fault-tolerantly is not yet universal. We also need to implement the  $\pi/8$  gate for a universal set of gates. Unfortunately it seems to be impossible to implement the  $\pi/8$  gate in a fault-tolerant way. There are several ways to circumvent this problem. Shor, for instance, gave a way to complete the universal set by giving a transversal implementation of a three qubit gate, the Toffoli gate [Sho96]. However, we will follow a slightly different route here. It turns out that the gates  $\{X, \frac{\pi}{4}, CNOT\}$  are universal, provided we can measure a code word in the  $|0\rangle_{\text{code}}, |1\rangle_{\text{code}}$  basis and we have access to the state

$$|\pi/8_+\rangle_{\text{code}} = |0\rangle_{\text{code}} + \exp(i\frac{\pi}{4})|1\rangle_{\text{code}}.$$

It has been shown that there is a fault-tolerant preparation and verification procedure for the state  $|\pi/8_+\rangle_{\text{code}}$ , which is similar in spirit to the one in Fig. 7.

Several variants of fault-tolerant universal quantum computation have been developed for this and other codes, like CSS codes and stabilizer codes. They differ

in the details of ancilla preparation and number of interactions with the code word. As a result it is possible to implement computation and error correction following the guidelines of fault-tolerance.

## 8. Concatenated coding and the threshold

*“Much of modern art is devoted to lowering the threshold of what is terrible.”*  
Susan Sontag

We have seen how to encode quantum data, how to perform fault-tolerant recovery and how to compute fault tolerantly on encoded states. However, this is still not sufficient to implement quantum algorithms. Quantum codes exist that can correct up to  $t$  errors, where  $t$  can be as large as we wish, and on which we can compute fault-tolerantly. This means that if our error rate and gate and measurement failure rate is  $\varepsilon$ , then computation will only fail with probability of order  $\varepsilon^{t+1}$  for a  $t$  of our choice. So what is the problem?

The crux is the complexity of the recovery procedure. With large  $t$  we reach a point where the recovery procedure takes so much time that it becomes likely that  $t + 1$  errors occur in a block. The number of steps required for recovery scales as a power of  $t$ ,  $t^a$  with exponent  $a > 1$ . That means that the probability to have  $t + 1$  errors before a recovery step is completed, scales as  $(t^a \varepsilon)^{t+1}$ . This expression is minimized when  $t = c\varepsilon^{-\frac{1}{a}}$  for some constant  $c$  and its value is at least  $p_{\text{fail}} = \exp(-ca\varepsilon^{-\frac{1}{a}})$ . This means that per error correction cycle our probability to fail is at least  $p_{\text{fail}}$ . If we have  $N$  such cycles, our failure probability is  $Np_{\text{fail}} = \exp(-ca \log N \varepsilon^{-\frac{1}{a}})$ . If we want to keep this (much) smaller than 1, our error rate  $\varepsilon$  has to scale as  $\frac{1}{(\log N)^a}$ , i.e. the longer the computation, the more accuracy we need; an unrealistic assumption.

To overcome this problem, a special kind of hierarchical approach is used [KLZ98] (see also [Kit97, AB97]). Ideas related to this approach go back to pioneering works of John von Neumann, who established a theory of fault-tolerant computation for noisy classical computers [Neu56].

Suppose that we encode our information into a code, like Steane’s code. Then, in turn, we encode each qubit of this encoded qubit using again Steane’s code, and so on. We obtain several layers of encoded qubits, say  $k$  layers, and the total number of qubits is  $7^k$ . This type of code is called *concatenated* code.

The exact calculations behind the threshold theorem are rather intricate. Let us only give a rough intuition. The idea is to perform error recovery most often at the lowest level, and less and less often at higher levels of the hierarchy, which have more qubits. We recursively apply the idea of simulating a circuit using an encoded circuit, constructing a hierarchy of quantum circuits. Suppose in the first stage the original qubit is encoded in a quantum code whose encoded qubits are again encoded in a quantum code and so on. Each level has some error recovery cycles. If the failure probability at the lowest level of this code is  $\varepsilon$  then the failure probability at the next level of encoding is  $c\varepsilon^2$  (remember that the Steane code

reduces the error rate from first to second order), where  $c$  counts all possibilities that two errors can occur, given the number of gates in the recovery procedure and the fault-tolerant application of gates. Continuing with this reasoning, the *effective* error rate at the next level is  $c\varepsilon^2$ , and error recovery reduces the error to  $c(c\varepsilon^2)^2$ . Proceeding level by level, we see that at the  $k$ th level of the hierarchy an error on one of the sub-blocks only has probability  $(c\varepsilon)^{2^k}/c$ . We see that if our noise rate is below a certain threshold,  $\varepsilon < \varepsilon_{th} \equiv 1/c$ , then the error is reduced in each level of concatenation. This gives the *error threshold* for fault-tolerant quantum computation.

How does the total size of the circuit grow? Let's assume that one level of encoding requires an overhead of  $G$  gates to fault-tolerantly perform a gate and error-correct. Then the size of the simulating circuit grows as  $G^k$ . Let us see when this concatenation procedure gives a small enough failure probability:

Assume the initial quantum circuit we want to emulate has  $N$  gates and we wish to achieve a final accuracy  $p_{\text{success}}$ . In such a circuit each gate has to be accurate to  $p_{\text{success}}/N$  (gate errors add linearly). To achieve this we concatenate  $k$  times so that

$$\frac{(c\varepsilon)^{2^k}}{c} = \varepsilon_{th} \left(\frac{\varepsilon}{\varepsilon_{th}}\right)^{2^k} \leq \frac{p_{\text{success}}}{N}$$

or

$$2^k \leq \frac{\log(N\varepsilon_{th}/p_{\text{success}})}{\log(\varepsilon_{th}/\varepsilon)}$$

If  $\varepsilon$  is smaller than the threshold value, such a  $k$  can be found. For error rates below the threshold we can achieve arbitrary accuracy by concatenation. Per initial gate the final circuit will have

$$G^k = 2^{k \log G} \leq \left( \frac{\log(N\varepsilon_{th}/p_{\text{success}})}{\log(\varepsilon_{th}/\varepsilon)} \right)^{\log G} = \text{poly}(\log N)$$

gates and so its final size will be  $N \text{poly}(\log N)$  which is only polylogarithmically larger than the original  $N$ .

Note that we have crudely simplified our calculations. Estimating the threshold is an extremely intricate task. Its value depends on the details of the code and fault-tolerance constructions used. It also depends on whether we assume the classical syndrome processing to be perfect or not. In all cases it seems that we need high parallelization and a supply of fresh ancilla qubits during the computation. For a long time the actual value of the threshold has been estimated by optimists and pessimists to lie somewhere between  $10^{-4}$  and  $10^{-7}$ . Recent work seems to indicate that it can be even as high as 3% [Kni05] (see also [AGP05, Rei05]) and optimized numerical simulations of fault-tolerant protocols suggest a threshold as high as 5% (however, to tolerate this much error existing protocols require enormous overhead).

## 9. Error avoidance and Decoherence Free Subsystems

*“It is well known that “problem avoidance” is an important part of problem solving.”*

*Edward de Bono*

In all our previous analysis we have assumed that the errors behave independently and affect few qubits at a time. What, if this is not the case? There are situations, where groups of qubits interact with the environment in a *collective* fashion, possibly undergoing a correlated error. For these cases the theory of decoherence-free subspaces and subsystems has been developed, sometimes also called *error-avoiding* codes. These codes come into play when the decoherence process is in some sense not local, but collective, involving groups of qubits.

Let us give a classical example. Assume we have an error process that with some probability flips all bits in a group, and otherwise does nothing. In this case we can encode a classical bit as

$$0 \longrightarrow 00 \qquad 1 \longrightarrow 01.$$

The error process will change the encoded states to

$$00 \longrightarrow 11 \qquad 01 \longrightarrow 10.$$

But no matter if the error has acted or not, the *parity* of the bit string is unchanged. So when we decode, we will associate 00 and 11 with the encoded 0 bit and 01 and 10 with the encoded 1. Note that we will be able to decode correctly *no matter* how high the rate of error is! The error does not touch the invariant, parity, into which we encode. That means that our encoded information has managed to completely *avoid* the error, we have given the simplest error-avoiding code.

A lot of research has been done to generalize this to the quantum case (see e.g. [Kem01, Bac01, LW03] for surveys). The noise model is in general derived from the Hamiltonian picture (see App. B.1) or from the Markovian picture (see App. B.3), a brief derivation is given in App. E. In general the underlying assumption is that several qubits couple collectively to the environment and are affected by a symmetric decoherence process. In systems where this form of decoherence is dominant at the qubit level, error-avoiding codes as part of the error-correction scheme are advantageous.

We will content ourselves with briefly describing one example. For one of the most common collective decoherence processes the noise operators on  $n$  qubits (see App. E) in the Hamiltonian picture (App. B.1) are given by  $S_\alpha = \sum_{i=1}^n \sigma_\alpha^i$ , where  $\sigma_\alpha^i$  is a Pauli matrix ( $\alpha = \{x, y, z\}$ ) on the  $i$ th qubit. Intuitively this means that the possible unitary errors are  $\exp(itS_\alpha)$ . The condition for decoherence-free subspaces is that

$$S_\alpha |\text{codeword}\rangle = c_\alpha |\text{codeword}\rangle,$$

or in other words that the code space is a simultaneous eigenspace of each  $S_\alpha$  with eigenvalue  $c_\alpha$ . If this is the case, each unitary noise operator only introduces an unobservable phase  $\exp(itc_\alpha)$  on the code space.

Let us look at an encoding of 4 qubits:

$$\begin{aligned} |0\rangle_{\text{code}} &= |s\rangle \otimes |s\rangle \\ |1\rangle_{\text{code}} &= \frac{1}{\sqrt{3}} (|t_+\rangle \otimes |t_-\rangle - |t_0\rangle \otimes |t_0\rangle + |t_-\rangle \otimes |t_+\rangle), \end{aligned}$$

where  $|s\rangle = \frac{|01\rangle - |10\rangle}{\sqrt{2}}$  and  $|t_{-,0,+}\rangle = \{|00\rangle, \frac{|01\rangle + |10\rangle}{\sqrt{2}}, |11\rangle\}$ . It is easy to see that  $S_\alpha |0\rangle_{\text{code}} = S_\alpha |1\rangle_{\text{code}} = 0$  for  $\alpha = \{x, y, z\}$  (i.e. that the coefficients  $c_\alpha = 0$ ). This means that both code states are invariant under collective noise. If we encode our information into the subspace spanned by  $|0\rangle_{\text{code}}$  and  $|1\rangle_{\text{code}}$ , it will completely avoid the errors; it resides in a “quiet” part of the space, a *decoherence-free* subspace.

This idea has been generalized to a wide variety of encodings (in particular to decoherence-free *subsystems*, see App. E for a little more detail) and against several kinds of collective noise. It has been shown how to *compute* on these codes (e.g. [KBLW01]) and how to use them in a fault-tolerant framework.

Of course the noise in a real implementation of a quantum computer will be a mixture of independent statistical noise, and coupled collective noise, depending on the specific quantum hardware used. The idea is to use a hierarchical construction of concatenated quantum codes, as in the threshold construction of Sec. 8, where the lower levels of the hierarchy use error correction (or avoidance) schemes that are highly specialized to the anticipated noise process, whereas higher levels are similar to the known fault-tolerant constructions for QECCs (see e.g. [LBW99] for a DFS-QECC concatenation scheme).

## 10. Conclusion and Epilogue

*“The best thing about the future is that it only comes one day at a time.”*  
Abraham Lincoln

Without doubt work on quantum fault-tolerance is of prime importance if we want to build quantum machines. In the late 1990’s pioneering work has established that fault-tolerant quantum computation is *possible*, and we have estimates for the *error threshold*, the maximum error a component can undergo such that the computation still proceeds without catastrophic error. On the way we have gained new insights into the nature of decoherence and about the methods and tools used to model and describe it.

At this point we need to optimize the details of fault-tolerant schemes and to generate new ideas to improve the threshold. Current experimental results show that the accuracy in implementations of the quantum circuit model is on the order of several percent in the best case, whereas most estimates of the threshold give numbers of the order of  $10^{-4}$  or less.

The task for current research is to analyze the threshold for particular codes and to develop new elements of fault-tolerance that improve the threshold. For instance only recently the existence of a threshold for the Steane code has been

shown [AGP05, Rei05]. New elements have been developed to improve the threshold, like for instance schemes based on postselection [Kni04]. Using new ingredients, the threshold has now been estimated to be on the order of 3%, albeit with an enormous overhead in the circuit architecture [Kni05].

Another avenue of research is to explore other models of quantum computing, different from the quantum circuit model, which can be inherently more robust against noise. One idea, initiated by Kitaev [Kit03], is a scheme for intrinsically fault-tolerant quantum hardware, designed to be robust against localized inaccuracies. In this scheme (quantum computing by anyons) gates exploit non-Abelian Aharonov-Bohm interactions among separated quasiparticles on a 2D lattice (see also e.g. [SBFH05]).

Another potentially more robust model is the model of adiabatic quantum computation, where computation is achieved by adiabatically tuning a set of Hamiltonians, and where the system is always in the instantaneous groundstate. In this system there is a gap between the groundstate and the first excited state at all times, which might make the state more robust to noise (see [FGG<sup>+</sup>01, AvDK<sup>+</sup>04, CFP02]). Yet another model is the measurement based *one-way* quantum computer [BR01]. Here quantum computation is achieved by measuring single qubits of a suitably prepared initial state. The fault-tolerance properties of this system have recently been explored in [ND05].

All these developments allow us to be optimistic about the future of a quantum computing machine. One day we might be able to combat decoherence and have large scale entangled states operate for us. The consequences not only for computation, but also for our understanding of the fundamental processes behind decoherence will be formidable.

## Appendix A. Further Reading

An ever growing community of researchers has been and is working an error correction and fault-tolerance in the quantum setting, and it is impossible to mention all of them in this framework. What follows is a selection of some of the milestones and recent developments, where the interested reader can find more information.

That quantum error correcting codes exist was first pointed out by Shor [Sho95] and Steane [Ste96b] in the end of 1995. By early 1996 it was shown by Steane [Ste96a] and Calderbank and Shor [CS96] that *good* codes exist, i.e. codes that are capable to correct many errors. The quantum error correction conditions where formalized by Knill and Laflamme [KL97] and Bennett et al. [BDSW96]<sup>5</sup>.

The first fully *fault-tolerant recovery* scheme, which takes into account that encoding, error-correction and decoding are themselves noisy operations, was developed by Shor in 1996 [Sho96]. Methods for fault-tolerant recovery where independently developed by Kitaev.

---

<sup>5</sup>These authors also analyzed schemes based on random codes.

The first to show that there is an *accuracy threshold* for *storage* of quantum information were Knill and Laflamme [KL96] and for *quantum computation* Knill, Laflamme and Zurek [KLZ96] in 1996 (see also [KLZ98]). Similar results were reported by Kitaev [Kit97] and Aharonov and Ben-Or [AB97].

The theory of *stabilizer codes* and of fault-tolerance in the powerful stabilizer formalism was developed by Gottesman (see e.g. [Got97c])<sup>6</sup>.

Since then several researchers have sharpened the threshold and developed new techniques to analyze and improve it. See for instance the recent work of Steane [Ste99, Ste03], Knill [Kni04, Kni05], Aliferis, Gottesman and Preskill [AGP05] and Reichardt [Rei05] and [FKSS04] for a dynamical systems approach.

In the literature the terms "sub-" and "superradiance" are often encountered in connection with *collective decoherence* processes. Decoherence-free subspaces have been studied by several researchers (see for example [DG98, ZR97, Zan97, Zan98] in the context of storage, and [LCW98, BLW99, BKLW00, KBLW01, DBK<sup>+</sup>00] in the context of fault-tolerant computation and [LBW99] in combination with QECCs). Decoherence-free subsystems have been introduced by [VKL99, KLV00], also in the connection with dynamic decoupling techniques. Since then there has been a lot of active effort to adapt codes to various collective noise processes.

The threshold has also been inspected in the light of various (local) error models. For instance [TB05] discuss the fault-tolerant threshold for local *non-Markovian* noise (see also [ALZ05] and references therein for a recent controversy about the nature of errors and an analysis of error models that seem to not allow fault-tolerant computation in [Kal05]).

Apart from the quantum circuit model alternative proposals for quantum architectures have been developed, which could be potentially more robust than the quantum circuit model. One example, developed by Kitaev, is the model of computation via *anyons* (see [Kit03] for an analysis of its fault-tolerance properties, or e.g. Freedman et al. [FKLW01]). Another recent example is the measurement based *quantum cluster* model [BR01] introduced by Briegel and Raussendorf. Recently, fault-tolerance has been analyzed in this model by Nielsen and Dawson [ND05]. The *adiabatic model* of quantum computation has been introduced by Farhi et al. [FGG<sup>+</sup>01] and shown to be equivalent to the quantum circuit model in [AvDK<sup>+</sup>04]. Childs et al. have discussed its robustness in [CFP02].

## Appendix B. How to model decoherence

No quantum system can be perfectly isolated from its surroundings and be viewed as perfectly closed. In the physical world, degrees of freedom are usually interacting with many other degrees of freedom. In fact, the understanding of this point is crucial for the explanation of why classical mechanics in the macroscopic world

---

<sup>6</sup>See also work by Calderbank, Rains, Shor and Sloane, which develop stabilizer codes as codes over GF(4) [CRSS98]

emerges out of the microscopic operation of quantum mechanics. Even if we find quantum computer elements that interact only weakly with the rest of the world (achievable most likely if they are themselves of atomic or near-atomic dimensions), for short times the evolution will be unitary, but eventually even weak interactions will cause significant departure from unitarity. Physical systems have a characteristic time for loss of unitarity, which is known in the field of mesoscopic physics as the “dephasing time”. It is often extremely short (for a table of dephasing times for various systems see [DiV95]), for example for the state of an electron traversing a gold wire at temperature less than 1K it is of order  $10^{-13}$  seconds.

We refer to the effects of noise due to unwanted coupling with the environment as decoherence<sup>7</sup>. An early treatise on quantum noise from a rather mathematical point of view is due to Davies [Dav76]. Caldeira and Leggett [CL83] in 1983 undertook one of the first and most complete studies of an important model, the *spin-boson model*.

Within the context of quantum computers these studies were taken up by Unruh [Unr95] in 1995 and developed by many others (e.g. Palma et al. [PSE96], Zanardi [Zan97, Zan98]). Over the past few years work on quantum computation has generated profound insights into the nature of decoherence.

### B.1. Hamiltonian Picture

To model the dynamics of a register of qubits (quantum computer) with its surroundings we imagine the system immersed into its environment (often called bath) and the whole (quantum register plus environment) as a closed system described in a general way by the following Hamiltonian:

$$\mathbf{H} = \mathbf{H}_S \otimes \mathbf{I}_B + \mathbf{I}_S \otimes \mathbf{H}_B + \mathbf{H}_I, \quad (11)$$

where  $\mathbf{H}_S$  ( $\mathbf{H}_B$ ) [the system (bath) Hamiltonian] acts on the system (bath) Hilbert space  $\mathcal{H}_S$  ( $\mathcal{H}_B$ ),  $\mathbf{I}_S$  ( $\mathbf{I}_B$ ) is the identity operator on the system (bath) Hilbert space, and  $\mathbf{H}_I$ , which acts on both the system and bath Hilbert spaces  $\mathcal{H}_S \otimes \mathcal{H}_B$ , is the interaction Hamiltonian containing all the nontrivial couplings between system and bath. In general  $\mathbf{H}_I$  can be written as a sum of operators which act separately on the system ( $\mathbf{S}_\alpha$ 's) and on the bath ( $\mathbf{B}_\alpha$ 's):

$$\mathbf{H}_I = \sum_{\alpha} \mathbf{S}_{\alpha} \otimes \mathbf{B}_{\alpha}. \quad (12)$$

(Note that this decomposition is not necessarily unique.)

In the absence of an interaction Hamiltonian ( $\mathbf{H}_I = 0$ ), the evolution of the system and the bath are separately unitary:  $\mathbf{U}(t) = \exp[-i\mathbf{H}t] = \exp[-i\mathbf{H}_S t] \otimes \exp[-i\mathbf{H}_B t]$  (we set  $\hbar = 1$  throughout). Information that has been encoded (mapped) into states of the system Hilbert space remains encoded in the system

---

<sup>7</sup>An unfortunate confusion in terms has arisen with the word “decoherence”. Historically it has been used to refer just to a phase damping process – a specific type of noise – cf. e.g. Zurek [Zur91]. Zurek and others realized the unique role played by phase damping in the transition from a quantum to a classical world. However, in the quantum computing community by and large the term “decoherence” is now used to refer to *any noise process* in quantum processing.

Hilbert space if  $\mathbf{H}_I = 0$ . However in the case when the interaction Hamiltonian contains nontrivial couplings between the system and the bath, information that has been encoded over the system Hilbert space does not remain encoded over solely the system Hilbert space but spreads out instead into the combined system and bath Hilbert space as the time evolution proceeds.

Very often to describe decoherence in more specific contexts [Unr95, PSE96] it is convenient to model the environment (the bath) as a mass-less scalar field, usually assumed to be in a thermal state (described by a density matrix in Fock-space, the state space used to model *fields*). Its (infinite dimensional) Hilbert space is spanned by

$$\bigotimes_{\mathbf{k}} |i\rangle_{\mathbf{k}} \quad i \in \{0, 1, 2, \dots\}$$

where  $\mathbf{k}$  labels the *modes*. On each mode (factor in the tensor product) we have two operators, the *lowering operator*  $\mathbf{b}_{\mathbf{k}}$  given by  $\mathbf{b}_{\mathbf{k}}|i\rangle_{\mathbf{k}} = \sqrt{i}|i-1\rangle_{\mathbf{k}}$  and the *raising operator*  $\mathbf{b}_{\mathbf{k}}^\dagger$  given by  $\mathbf{b}_{\mathbf{k}}^\dagger|i\rangle_{\mathbf{k}} = \sqrt{i+1}|i+1\rangle_{\mathbf{k}}$ . Note that  $\mathbf{b}_{\mathbf{k}}^\dagger\mathbf{b}_{\mathbf{k}}|i\rangle_{\mathbf{k}} = i|i\rangle_{\mathbf{k}}$ , i.e.  $|i\rangle_{\mathbf{k}}$  is an *eigenstate* of the *number operator*  $\mathbf{b}_{\mathbf{k}}^\dagger\mathbf{b}_{\mathbf{k}}$ .

The quantum register is described by an arrangement of  $n$  two-level systems (spins). This results in the *spin-boson model*, where the bath Hamiltonian can be written as

$$\mathbf{H}_B = \sum_k \omega_k \mathbf{B}_k$$

and, e.g., for the spin-boson Hamiltonian,  $\mathbf{B}_k = \mathbf{b}_k^\dagger \mathbf{b}_k$  [LCD<sup>+</sup>87], and  $\mathbf{b}_k^\dagger$ ,  $\mathbf{b}_k$  are respectively creation and annihilation operators of bath mode  $k$ . The interaction Hamiltonian is given by

$$\mathbf{H}_I = \sum_{i=1}^n \sum_{\alpha=+,-,z} \sum_k g_{ik}^\alpha \sigma_\alpha^i \otimes \tilde{\mathbf{B}}_k^\alpha + h.c., \quad (13)$$

where  $g_{ik}^\alpha$  is a coupling coefficient and  $h.c.$  denotes the hermitian conjugate. In the spin-boson model one would have  $\tilde{\mathbf{B}}_k^+ = \mathbf{b}_k$ ,  $\tilde{\mathbf{B}}_k^- = \mathbf{b}_k^\dagger$  and  $\tilde{\mathbf{B}}_k^z = \mathbf{b}_k^\dagger + \mathbf{b}_k$ . Thus  $\sigma_\pm^i \otimes \tilde{\mathbf{B}}_k^\pm$  expresses a dissipative coupling (in which energy is exchanged between system and environment), and  $\sigma_z^i \otimes \tilde{\mathbf{B}}_k^z$  corresponds to a phase damping process (in which the environment randomizes the system phases, e.g., through elastic collisions).

## B.2. Operator Sum Picture

The evolution of a quantum state in the entire space is unitary in a closed system of which we can observe and control all parts. Very often, however, this is not the case: imagine for example that we perform a certain measurement and then “forget” or lose the measurement outcome. As a result we know that the state has collapsed into some eigenstate of the measurement operator, but not into which one, and we will have to assign probabilities to each of them to model the current state of the system. Take the example of a qubit  $|\psi\rangle = \alpha|0\rangle + \beta|1\rangle$  and

the measurement in the computational basis. Performing this measurement and “throwing away” the result will leave the system in the state  $|0\rangle$  with probability  $|\alpha|^2$  and in the state  $|1\rangle$  with probability  $|\beta|^2$ . To describe this *mixture* of possible states the *density matrix* formalism proved to be very useful: we write

$$\rho = |\alpha|^2|0\rangle\langle 0| + |\beta|^2|1\rangle\langle 1| = \begin{pmatrix} |\alpha|^2 & 0 \\ 0 & |\beta|^2 \end{pmatrix}$$

Another way we can think about density matrices is to imagine that we have a (big) quantum system and can access only part of it. To describe the quantum state of the accessible part (call it  $A$ ), we have to average over the non-accessible degrees of freedom of the system (part  $B$ ). This is done by performing a complete measurement on system  $B$  (mentally) and “throwing away” the outcomes (because we do not have access to them). Let us give the example of a state of 2 qubits  $|\psi\rangle_{AB} = \alpha|00\rangle + \beta|11\rangle$  where we only have access to the first qubit (part  $A$ ). If we (mentally) measure system  $B$  in the computational basis, we obtain the density matrix from Eq. (14).

Let us proceed to the more general description of the statics and dynamics of open quantum systems, described by mixed states:

**States:** States in an  $N$ -dimensional Hilbert space  $\mathcal{H}_N$  are given by density matrices  $\rho$  such that:

- $\rho$  is hermitian:  $\rho^\dagger = \rho$
- $\rho$  is positive:  $\forall |\psi\rangle \in \mathcal{H}_N \quad \langle \psi | \rho | \psi \rangle \geq 0$ , which is equivalent to  $\lambda_i \geq 0$ , where  $\lambda_i$  are the eigenvalues of  $\rho$  (this can be viewed as a statement about the positivity of probabilities of the pure states in the mixture).
- $\rho$  has trace 1 (this corresponds to the normalization of probabilities)

Pure states  $|\psi\rangle$  of the system are associated with the density matrix  $\rho_{\text{pure}} = |\psi\rangle\langle\psi|$ . A general mixed state is diagonalizable and can be written in its spectral decomposition as

$$\rho = \sum_k p_k |\psi_k\rangle\langle\psi_k|$$

Note that there are in general many other ways to write  $\rho$  in the above form if we allow for non-orthogonal states in the decomposition. Each such decomposition  $\{q_k, |\phi_k\rangle\}$  is called an *ensemble realization* of  $\rho$ . The ambiguity in the decomposition of  $\rho$  manifests some loss of information, in the sense that the probabilistic mixture  $\rho$  could have arisen in a multitude of ways.

**Dynamics:** To describe the evolution of an open system – and thus of decoherence – we will immerse it into a closed system. The evolution of a closed system is described by a unitary transformation, which translates to an effective dynamics of the open system governed by completely positive (and trace-preserving) maps. Loosely speaking, these are maps that in  $\mathcal{H}_A$  take density matrices to density matrices, with the additional property that if we extend the map to bigger spaces  $\mathcal{H}_{AB}$  by applying the map on  $A$  and the identity map on  $B$ , then they still take density matrices to density matrices. More precisely, an operator map  $\Lambda$  is completely positive if  $(I \otimes \Lambda)(\rho) \geq 0$  whenever  $\rho \geq 0$ .

The important point here is that according to *Kraus' Representation Theorem* [Kra83] every completely positive trace preserving map can be written as

$$\rho \rightarrow \sum_{\mu} M_{\mu} \rho M_{\mu}^{\dagger} \quad \text{with} \quad \sum_{\mu} M_{\mu}^{\dagger} M_{\mu} = I \quad (14)$$

where the  $M_{\mu}$  are  $N$ -by- $N$  matrices ( $N$  being the dimension of the Hilbert space). In particular this describes both the Hamiltonian and the Markovian dynamics, though in general it is often tedious to derive the form of the  $M_{\mu}$  from the  $\mathbf{S}_{\alpha}$  of the Hamiltonian picture (Eq. (12)). Note that contrary to the case of unitary evolution, general open system dynamics is not *reversible*.

### B.3. Markovian Picture

Another very powerful formalism to describe decoherence is the approach of *master equations*. *Markovian quantum dynamics* describes processes resulting from the interaction with a Markovian environment in the so called Born-Markov approximation. The main objective is to describe the time-evolution of an open system with a differential equation – the *Master equation* – which properly describes non-unitary behavior.

In fact it is not a priori obvious that there needs to be a differential equation that describes decoherence. Such a description will be possible only if the evolution of the quantum system will be local in time (*Markovian*), i.e. that the density operator  $\rho(t + dt)$  is completely determined by  $\rho(t)$ . This is usually not the case because the bath retains a memory of the state of  $\rho$  at previous times for a while and can transfer it back to the system.

To obtain the Master equation in the Born-Markov approximation a common approach is to start with the Hamiltonian description Eq. (11) and use time-dependent perturbation theory (i.e. an expansion into time-series) with careful truncation (cf. [Car93]).

A more axiomatic way, followed by Lindblad [Lin76, AL87], is to establish the most general linear equation for density matrices. More precisely, by assuming that (i) the evolution of the system density matrix is a one-parameter semigroup, (ii) the system density matrix retains the properties of a density matrix including “complete positivity”, and (iii) the system and bath density matrices are initially decoupled, Lindblad [Lin76] has shown that the most general evolution of the system density matrix  $\rho_S(t)$  (in a Hilbert space of dimension  $N$ ) is governed by the master equation

$$\begin{aligned} \frac{d\rho}{dt} = \mathbf{L}[\rho] &= -i[\mathbf{H}_S, \rho] + \frac{1}{2} \sum_{\alpha, \beta=1}^M a_{\alpha\beta} \left( [\mathbf{F}_{\alpha}, \rho \mathbf{F}_{\beta}^{\dagger}] + [\mathbf{F}_{\alpha} \rho, \mathbf{F}_{\beta}^{\dagger}] \right) \\ &= -i[\mathbf{H}_S, \rho] + \frac{1}{2} \sum_{\alpha, \beta=1}^M a_{\alpha\beta} \mathbf{L}_{\alpha, \beta}[\rho]. \end{aligned} \quad (15)$$

Here  $\mathbf{H}_S$  is the system Hamiltonian generating unitary evolution plus possible additional terms due to the interaction with the bath – usually referred to as

*Lamb-shift* –; the operators  $\mathbf{F}_\alpha$  constitute a basis for the  $M$ -dimensional space of all bounded operators acting on  $\mathcal{H}_S$ <sup>8</sup>, and  $a_{\alpha\beta}$  are the elements of a positive semi-definite Hermitian matrix. We refer to the matrix  $a_{\alpha\beta}$  as the *GKS matrix*.

Every such process described by Eq. (15) corresponds to some interaction which, if applied for a duration  $t$ , induces a quantum operation  $\mathcal{E}_t$ . The class of quantum operations  $\mathcal{E}_t$  forms a Markovian semigroup, such that

$$\mathcal{E}_s \mathcal{E}_t = \mathcal{E}_{s+t}.$$

Here  $\mathcal{E}_s \mathcal{E}_t$  denotes composition of the operations, i.e.,  $\mathcal{E}_s \circ \mathcal{E}_t$ . Each Markovian semigroup in turn describes the dynamics resulting from some interaction with a Markovian environment in the Born approximation.

Note that the Operator Sum Representation also describes Markovian dynamics, though it is in practice often difficult to derive the  $M_\mu$  (Eq. (14)) from the  $\mathbf{F}_\alpha$  of the Markovian picture (Eq. (15)).

To make our description of Markovian quantum dynamics concrete, we present some important examples of qubit noise processes<sup>9</sup>. We choose the basis  $\{F_\alpha\}$  to be the normalized Pauli operators  $\frac{1}{\sqrt{2}}\{\sigma_x, \sigma_y, \sigma_z\}$ , and we write the density matrix of a qubit as

$$\rho = \begin{pmatrix} \rho_{00} & \rho_{01} \\ \rho_{10} & \rho_{11} \end{pmatrix}.$$

The first process, *phase damping*, acts on a qubit as

$$\mathcal{E}_t^{\text{PD}}(\rho) = \begin{pmatrix} \rho_{00} & e^{-\gamma t} \rho_{01} \\ e^{-\gamma t} \rho_{10} & \rho_{11} \end{pmatrix},$$

where  $\gamma$  is a decay constant and  $t$  is the duration of the process. The generator has a GKS matrix with  $a_{33}^{\text{PD}} = \frac{\gamma}{2}$  and all other  $a_{\alpha\beta}^{\text{PD}} = 0$ . The second example is the *depolarizing channel*, which acts on a qubit as

$$\mathcal{E}_t^{\text{DEP}}(\rho) = \begin{pmatrix} \frac{1+e^{-\tilde{\gamma}t}(\rho_{00}-\rho_{11})}{2} & e^{-\tilde{\gamma}t} \rho_{01} \\ e^{-\tilde{\gamma}t} \rho_{10} & \frac{1+e^{-\tilde{\gamma}t}(\rho_{11}-\rho_{00})}{2} \end{pmatrix}.$$

Its GKS matrix has the nonzero elements  $a_{11}^{\text{DEP}} = a_{22}^{\text{DEP}} = a_{33}^{\text{DEP}} = \tilde{\gamma}/4$ . Our final example is *amplitude damping*, which acts on a qubit as

$$\mathcal{E}_t^{\text{AD}}(\rho) = \begin{pmatrix} \rho_{00} + (1 - e^{-\Gamma t})\rho_{11} & e^{-\Gamma t/2} \rho_{01} \\ e^{-\Gamma t/2} \rho_{10} & e^{-\Gamma t} \rho_{11} \end{pmatrix}.$$

The GKS matrix  $a_{\alpha\beta}^{\text{AD}}$  is given by

$$\frac{\Gamma}{4} \begin{pmatrix} 1 & -i & 0 \\ i & 1 & 0 \\ 0 & 0 & 0 \end{pmatrix}. \quad (16)$$

<sup>8</sup>they are often called the *Lindblad operators* or the *quantum jump operators*

<sup>9</sup>For a review of these processes and their relevance to quantum information theory, see [NC00]; [Pre98a].

## Appendix C. The Error-model

The underlying key assumption for efficient usage of quantum error-correcting codes is the *independent error model*. Intuitively, if a noise process acts independently on the different qubits in the code, then provided the noise is sufficiently weak, error-correction should improve the storage fidelity of the encoded over the unencoded state.

Mathematically, the assumption of independent errors can be retraced in each of the decoherence pictures introduced in Sec. B. In the Hamiltonian picture we can rewrite Eq. (13) as

$$\mathbf{H}_I = \sum_{i=1}^K \sum_{\alpha=x,y,z} \sum_k \sigma_i^\alpha \otimes \mathbf{B}_{ik}^\alpha,$$

where  $\mathbf{B}_{ik}^z \equiv \tilde{\mathbf{B}}_k^z$  and  $\mathbf{B}_{ik}^x, \mathbf{B}_{ik}^y$  are appropriate linear combinations of  $\tilde{\mathbf{B}}_k^+$  and  $\tilde{\mathbf{B}}_k^-$ :

$$\begin{aligned} \mathbf{B}_{ik}^x &= \frac{1}{2} \left( g_{ik}^- \tilde{\mathbf{B}}_k^- + g_{ik}^+ \tilde{\mathbf{B}}_k^+ \right) \\ \mathbf{B}_{ik}^y &= \frac{i}{2} \left( g_{ik}^- \tilde{\mathbf{B}}_k^- - g_{ik}^+ \tilde{\mathbf{B}}_k^+ \right) \end{aligned}$$

i.e. all system components can be expressed in terms of tensor products of the single qubit *Pauli matrices*. If we expand the evolution to first order in time and assume that the error-rates  $g_{ik}$  are independent we will get an operator sum representation (OSR) (cf. Eq. (14)) where each term is a linear combination of the Pauli matrices (see [LBW99] for a recent derivation). In the Markovian formulation of noise (cf. Eq. (15)) the independent error model assumes that each of the  $\mathbf{F}_\alpha$  affects only one of the qubits and that the  $\mathbf{F}_\alpha$  are not correlated. Higher order correlations are taken into account by using a code that is suitably constructed for the particular error-model. Therefore the theory of QECCs has focused on searching for codes that make quantum information robust against 1, 2, ... or more erroneous qubits, as this is the most reasonable model when one assumes spatially separated qubits with their own local environments. *Detection and correction procedures must then be implemented at a rate higher than the intrinsic error rate.*

From the linear decomposition of the error operators in the OSR or the master equation it follows that QECC-schemes need to be able to correct only a discrete set of errors, namely those generated by the Pauli-group<sup>10</sup>. Intuitively we can imagine that the error process acting on one qubit puts the quantum state into a superposition of one of the four possible discrete errors ( $I_2, \sigma_{x,y,z}$ ) and the error-detection and correction procedure collapses the state into one of these errors and then corrects as needed. This intuition can be made formal [NC00, KL97]: it is possible to decompose the the operators  $M_\mu$  that appear in Eq. (14) into a basis of tensor products of the Pauli matrices. It can then be seen, when deriving the

<sup>10</sup>In the context of error-correction the Pauli matrices  $\sigma_{x,y,z}$  are often denoted by  $\mathbf{X}, \mathbf{Y}, \mathbf{Z}$  respectively.

OSR representation from the Hamiltonian picture, that to first order in the noise rate the noise process gives terms with a single non-identity matrix (single qubit error). The core message is again that quantum codes need to account only for a discrete *linear basis* of all possible errors.

## Appendix D. Stabilizer Codes

Stabilizer codes, also known as *additive* codes, are an important subclass of quantum codes. The stabilizer formalism provides an insightful tool to quantum codes and fault-tolerant operations. It was developed by Gottesman in 1996 [Got97a, Got97c]. We will not outline the full formalism here but rather describe only the key elements. A full treatment can be found in [Got97b].

The powerful idea behind the stabilizer formalism is to look at the set of group elements that *stabilize* a certain code and to work with this stabilizer instead of directly with the code. In the framework of QECCs, the stabilizer permits on the one hand to identify the errors the code can detect and correct. It also links quantum codes to the theory of classical error correcting codes in a transparent fashion. On the other hand it also allows one to find a set of universal, fault-tolerant gates.

An operator  $\mathbf{S}$  is said to stabilize a code  $\mathcal{C}$  if

$$|\Psi\rangle \in \mathcal{C} \quad \text{iff} \quad \mathbf{S}|\Psi\rangle = |\Psi\rangle \quad \forall \mathbf{S} \in \mathcal{S}. \quad (17)$$

The set of operators  $\{\mathbf{S}\}$  form a group  $\mathcal{S}$ , known as the stabilizer of the code [Got97c]. Clearly,  $\mathcal{S}$  is closed under multiplication. In the theory of QECC the underlying group is the Pauli-group, the stabilizers are subgroups of the Pauli-group (tensor products of  $\mathbf{I}, \mathbf{X}, \mathbf{Y}, \mathbf{Z}$ ). Since any two elements of the Pauli group either commute or anti-commute, the stabilizer, in this case is always *Abelian*. The code is thus the common eigenspace of the stabilizer elements with eigenvalue 1. *Additive* codes are completely characterized by their stabilizer  $\mathcal{S}$ . The stabilizer  $\mathcal{S}$  can be given by a set of generators which span the stabilizer group via multiplication.

We define the *centralizer* of  $\mathcal{S}$  to be the set of elements  $e$  in the Pauli group that commute with every element in  $\mathcal{S}$ , i.e.  $e\mathbf{S} = \mathbf{S}e$  for all  $\mathbf{S} \in \mathcal{S}$ . In case of the Pauli group it coincides with the *normalizer* of  $\mathcal{S}$  – the set of elements  $E$  in the Pauli-group with  $E\mathbf{S}E^\dagger \in \mathcal{S}$  for all  $\mathbf{S} \in \mathcal{S}$ . We will denote it by  $N(\mathcal{S})$  and call it normalizer throughout. Note that the normalizer contains the stabilizer  $\mathcal{S}$  itself.

Recall that in the theory of QECCs the error process  $\mathcal{E}$  can be expanded in terms of the error basis  $\mathbf{E}$  which is a subgroup of the Pauli group. In particular  $\mathbf{E}_\alpha \in \mathbf{E}$  either commutes or anti-commutes with elements in the stabilizer. This allows us to recast the QECC-condition Eq. (7) in the stabilizer formalism as follows:

*QECC-conditions:* A quantum code  $\mathcal{C}$  with stabilizer  $\mathcal{S}$  is an  $\mathcal{E}$ -correcting QECC if for all  $\mathbf{E}_\alpha, \mathbf{E}_\beta \in \mathbf{E}$  one of the following holds:

- (1) There is an  $\mathbf{S} \in \mathcal{S}$  that anti-commutes with  $\mathbf{E}_\alpha^\dagger \mathbf{E}_\beta$
- (2)  $\mathbf{E}_\alpha^\dagger \mathbf{E}_\beta \in \mathcal{S}$ .

This clearly implies the QECC conditions Eq. (7), since in the case of (1)  $\langle \Psi_i | \mathbf{E}_\alpha^\dagger \mathbf{E}_\beta | \Psi_j \rangle = \langle \Psi_i | \mathbf{E}_\alpha^\dagger \mathbf{E}_\beta \mathbf{S} | \Psi_j \rangle = -\langle \Psi_i | \mathbf{S} \mathbf{E}_\alpha^\dagger \mathbf{E}_\beta | \Psi_j \rangle = 0$  and in the case of (2)  $\langle \Psi_i | \mathbf{E}_\alpha^\dagger \mathbf{E}_\beta | \Psi_j \rangle = \langle \Psi_i | \Psi_j \rangle = \delta_{ij}$ . In particular this implies that the matrix element  $c_{\alpha\beta}$  is either 0 in the case of (1) or 1 in the case of (2). Conditions (1) and (2) can be reformulated succinctly as:  $\mathbf{E}_\alpha^\dagger \mathbf{E}_\beta \notin N(\mathcal{S}) - \mathcal{S}$ .

The nine bit Shor code in Eq. (5) is a stabilizer code. The set of its stabilizers is generated by

$$\begin{array}{cccccc} Z_1 Z_2 & Z_2 Z_3 & Z_4 Z_5 & Z_5 Z_6 & Z_7 Z_8 & Z_8 Z_9 \\ X_1 X_2 X_3 X_4 X_5 X_6 & X_1 X_2 X_3 X_7 X_8 X_9 & X_4 X_5 X_6 X_7 X_8 X_9 & & & \end{array}$$

Note that these generators correspond to the measurements to detect bit flip (the  $Z$  generators) and phase flip (the  $X$  generators) errors. Indeed, for instance a bit flip error on the first qubit anticommutes with  $Z_1 Z_2$ .

The generators for the stabilizer of the Steane code in Eq. (9) on the 7 qubits are the following:

$$\begin{array}{cc} IIIZZZZ & IIXXXX \\ IZZIIZZ & IXXIIXX \\ ZIZIZIZ & XIXIXIX. \end{array}$$

Note how the positions of the  $Z$  and  $X$  correspond to the parity check matrix  $H$  in Eq. (8). The fact that the code is self dual is seen in the symmetry between the  $Z$  and the  $X$ . Note that the change of basis from  $|0\rangle, |1\rangle$  to the  $|\pm\rangle$  basis, which is implemented by a conjugation with the Hadamard transform  $H$  on each bit, transforms all  $Z$  into  $X$  and vice versa ( $HXH = Z$  and  $HZH = X$ ).

The smallest possible quantum code to protect against single qubit errors, the 5-qubit code [LMPZ96], has the following (shift invariant) stabilizer

$$\begin{array}{c} XZZXI \\ IXZZX \\ XIXZZ \\ ZXIXZ. \end{array}$$

The stabilizer formalism allows to derive fault-tolerant computation in a convenient way. A key ingredient are encoded gates that transform encoded states, without decoding them, which would expose them to noise without protection. For universal quantum computation it is sufficient to show how to implement a universal *discrete* set of gates fault-tolerantly.

The key insight to fault-tolerant gates is that these encoded gates should only take encoded states to valid encoded states, without leaving the code-space. For

an encoded gate  $G$  this means that after application of  $G$  to a state stabilized by all elements of  $\mathcal{S}$  the resulting state must still be stabilized by  $\mathcal{S}$  (see Eq. (17))

$$G|\Psi\rangle \in \mathcal{C} \quad \leftrightarrow \quad SG|\Psi\rangle = GS|\Psi\rangle \quad (18)$$

or in other words over the code-space  $G$  commutes with all elements of  $\mathcal{S}$ . In the case of QECCs and the Pauli group this means that  $G$  is in the *normalizer*  $N(\mathcal{S})$  of  $\mathcal{S}$ .

The normalizer allows one to easily identify encoded logical operations on the code. It can be shown that for large classes of stabilizer codes a universal gate-set can be implemented either because the encoded gates are *transversal*, i.e. they affect only one qubit per block, or in connection with state-preparation of special states and measurement.

To fault-tolerantly *measure* on encoded states ancilla-state are employed in a procedure like the following<sup>11</sup>: Suppose we wish to measure the encoded qubit in the encoded computational basis. The ancilla is prepared in the state  $|0_L\rangle$ . Then we perform an *encoded CNOT* from the encoded qubit to be measured to the ancilla. We then measure the ancilla state in the computational basis, which gives us a non-destructive measurement of the encoded qubit in the encoded computational basis which is tolerant of possible errors in the encoded qubit. To prevent possible uncontrolled error-propagation caused by an incorrectly prepared ancilla, we prepare multiple  $|0_L\rangle$ -ancillas and apply *CNOT*'s between the DFS state to be measured and each ancilla. Together with majority voting this provides a fault-tolerant method for measuring  $\bar{Z}$  [Got97a].

The stabilizer formalism also provides an easy framework for fault-tolerant encoded state preparation and decoding, as it turns out that only transversal measurements in the Pauli-Z-basis are needed for both. For a detailed account of fault-tolerant computation with stabilizer codes see Gottesman [Got97b].

## Appendix E. Noise model for Decoherence-Free Subsystems

To derive the model of *collective* noise that applies to decoherence-free subsystems, we will work with the Hamiltonian picture (see App. B.1), following [ZR97]. We use the interaction Hamiltonian Eq. (13). *Collective decoherence* is the case where the coupling constants do not depend on the qubit, i.e.  $g_{i\mathbf{k}}^\alpha = g_{\mathbf{k}}^\alpha$ . This allows to rewrite the Hamiltonian in terms of the operators

$$S_\alpha = \sum_{i=1}^n \sigma_\alpha^i \quad (19)$$

as

$$H = \omega_0 S_z + \sum_{\mathbf{k}} \omega_{\mathbf{k}} b_{\mathbf{k}}^\dagger b_{\mathbf{k}} + \sum_{\alpha=\pm,z} S_\alpha \otimes \sum_{\mathbf{k}} g_{\mathbf{k}}^\alpha \tilde{\mathbf{B}}_{\mathbf{k}}^\alpha + h.c.$$

<sup>11</sup>This procedure may differ from case to case, here we only give an example for illustration.

The crucial observation is now that if we start the system in a common eigenstate with the same eigenvalue of all the  $S_\alpha$  with the bath in an eigenstate of  $H_B$  then the evolution will be completely *decoupled*. The condition for decoherence-free subspaces (DFS) is

$$S_\alpha|\Psi\rangle = c_\alpha|\Psi\rangle \quad \forall|\Psi\rangle \in DFS. \quad (20)$$

Dynamical symmetry allows for unitary evolution of a subspace while the remaining part of the Hilbert space gets strongly entangled with the environment. This is true for arbitrary coupling strength. The form of noise where all three  $S_\alpha$ ,  $\alpha \in \{x, y, z\}$ , come into play is now called *strong collective decoherence*, if there is only coupling to one of the  $S_\alpha$  the noise is called *weak collective decoherence*.

It is also possible to study collective noise in the Markovian picture (see App. B.3). We use Eq. (15), where  $\mathbf{L}_D$  gives the non-unitary ‘‘coupling term’’<sup>12</sup>. The decoherence-free condition  $\mathbf{L}_D[\rho] = 0$  implies that

$$\mathbf{F}_\alpha|\Psi\rangle = c_\alpha|\Psi\rangle \quad \forall|\Psi\rangle \in DFS.$$

As before the decoherence-free states are common eigenstates of the operators  $\mathbf{F}_\alpha$ . In case of collective decoherence (symmetry of all the qubits), the  $\mathbf{F}_\alpha$  are exactly the  $S_\alpha$  of Eq. (19), and it is possible to show that the unitary term of the Master-equation does not affect the DFS to first order.

This line of reasoning can be generalized to decoherence-free *subsystems*. The  $S_\alpha$  act on the system space. We can study the irreducible representations of this action and identify irreducible subspaces. For each irreducible representation there will be one or several irreducible subspaces on which the  $S_\alpha$  act in the same way. The one dimensional subspaces will only get a phase factor, they correspond to the decoherence-free subspaces of Eq. (20). But the other subspaces are not lost for our purposes. Any irreducible subspace can be used to encode information, because the action of the noise operators  $S_\alpha$  will keep the state within the subspace. Even though the state will change, its subspace will identify the encoded information. The number of irreducible subspaces corresponding to the same irreducible representation gives the number of different code words we can use.

The irreducible representations corresponding to the operators associated with strong collective decoherence (Eq. (19)) have been studied widely in physics, as they correspond to the *angular momentum* operators.

In the case of two qubits there is a single common eigenstate of the  $S_\alpha$ ,  $\alpha \in \{x, y, z\}$ , the singlet state

$$|\Phi\rangle = \frac{1}{\sqrt{2}}(|0\rangle|1\rangle - |1\rangle|0\rangle).$$

For three qubits there is no one-dimensional irreducible representation of the  $S_\alpha$ , but there are two (identical) two-dimensional irreducibles subspaces into which

---

<sup>12</sup>Note that the coupling of a system with an environment might also change the unitary part of the evolution of  $-i[\mathbf{H}, \rho]$  by introducing an additional term to the system Hamiltonian, called the *Lamb-shift*.

we can encode as

$$|0\rangle_{\text{code}} = \begin{cases} \frac{1}{\sqrt{2}}(|010\rangle - |100\rangle) \\ \frac{1}{\sqrt{2}}(|011\rangle - |101\rangle) \end{cases} \quad |1\rangle_{\text{code}} = \begin{cases} \frac{1}{\sqrt{6}}(-2|001\rangle + |010\rangle + |100\rangle) \\ \frac{1}{\sqrt{6}}(2|110\rangle - |101\rangle - |011\rangle) \end{cases} .$$

Increasing the number of qubits the number of identical irreducible subspaces grows favorably, so that it is possible to encode at a good rate. For more references on this and the theory of fault-tolerant computation on such systems, see Sec. A.

## References

- [AB97] D. Aharonov and M. Ben-Or. Fault-tolerant quantum computation with constant error. In *Proceedings of 29th Annual ACM Symposium on Theory of Computing (STOC)*, page 46, New York, NY, 1997. ACM.
- [AGP05] P. Aliferis, D. Gottesman, and J. Preskill. Quantum accuracy threshold for concatenated distance-3 codes, 2005. lanl-report quant-ph/0504218.
- [AL87] R. Alicki and K. Lendi. *Quantum Dynamical Semigroups and Applications*. Number 286 in Lecture Notes in Physics. Springer-Verlag, Berlin, 1987.
- [ALZ05] R. Alicki, D.A. Lidar, and P. Zanardi. Are the assumptions of fault-tolerant quantum error correction internally consistent?, 2005. lanl-report quant-ph/0506201.
- [AvDK<sup>+</sup>04] D. Aharonov, W. van Dam, J. Kempe, Z. Landau, S. Lloyd, and O. Regev. Adiabatic quantum computation is equivalent to standard quantum computation. In *Proc. 45th Annual IEEE Symp. on Foundations of Computer Science (FOCS)*, 2004.
- [Bac01] D. Bacon. Decoherence, control, and symmetry in quantum computers, 2001. Ph.D. thesis, University of California, Berkeley.
- [BDSW96] C.H. Bennett, D.P. DiVincenzo, J.A. Smolin, and W.K. Wootters. Mixed state entanglement and quantum error correction. *Phys. Rev. A*, 54:3824, 1996.
- [BKLW00] D. Bacon, J. Kempe, D.A. Lidar, and K.B. Whaley. Universal fault-tolerant computation on decoherence free subspaces. *Phys. Rev. Lett.*, 85:1758–1761, 2000.
- [BLW99] D. Bacon, D.A. Lidar, and K.B. Whaley. Robustness of decoherence-free subspaces for quantum computation. *Phys. Rev. A*, 60:1944, 1999.
- [BR01] H.J. Briegel and R. Raussendorf. A one-way quantum computer. *Phys. Rev. Lett.*, 86:5188, 2001.
- [Car93] H. Carmichael. *An Open Systems Approach to Quantum Optics*. Number m18 in Lecture notes in physics. Springer-Verlag, Berlin, 1993.
- [CFP02] A. Childs, E. Farhi, and J. Preskill. Robustness of adiabatic quantum computation. *Phys. Rev. A*, 65:012322, 2002.
- [CL83] A.O Caldeira and A.J. Leggett. Quantum tunneling in a dissipative system. *Ann. of Phys.*, 149(2):374–456, 1983.
- [CRSS98] A.R. Calderbank, E.M. Rains, P.W. Shor, and N.J.A. Sloane. Quantum error correction via codes over GF(4). *IEEE Trans. Inf. Th.*, 44:1369, 1998.

- [CS96] A.R. Calderbank and P.W. Shor. Good quantum error correcting codes exist. *Phys. Rev. A*, 54:1098–1105, 1996.
- [Dav76] E.B. Davies. *Quantum theory of open systems*. Academic Press, London, 1976.
- [DBK<sup>+</sup>00] D. P. DiVincenzo, D. Bacon, J. Kempe, G. Burkard, and K. B. Whaley. Universal quantum computation with the exchange interaction. *Nature*, 408:339, 2000.
- [DG98] L.-M Duan and G.-C. Guo. Reducing decoherence in quantum-computer memory with all quantum bits coupling to the same environment. *Phys. Rev. A*, 57:737, 1998.
- [Die82] D. Dieks. Communication by electron-paramagnetic-resonance devices. *Phys. Lett.*, 92A:271, 1982.
- [DiV95] D. P. DiVincenzo. Two-bit gates are universal for quantum computation. *Phys. Rev. A*, 51(2):1015–1022, 1995.
- [FGG<sup>+</sup>01] E. Farhi, J. Goldstone, S. Gutmann, J. Lapan, A. Lundgren, and D. Preda. A quantum adiabatic evolution algorithm applied to random instances of an NP-complete problem. *Science*, (5516):472–476, 2001.
- [FKLW01] M.H. Freedman, A. Kitaev, M. Larsen, and Z. Wang. Topological quantum computation. LANL preprint quant-ph/0101025, 2001.
- [FKSS04] Jesse Fern, Julia Kempe, Slobodan Simic, and Shankar Sastry. Fault-tolerant quantum computation - a dynamical systems approach, 2004. quant-ph/0409084.
- [Got97a] D. Gottesman. Class of quantum error-correcting codes saturating the quantum hamming bound. *Phys. Rev. A*, 54:1862, 1997.
- [Got97b] D. Gottesman. *Stabilizer codes and quantum error correction*. PhD thesis, California Institute of Technology, Pasadena, CA, 1997.
- [Got97c] D. Gottesman. Theory of fault-tolerant quantum computation. *Phys. Rev. A*, 57:127, 1997.
- [Got05] D. Gottesman. Quantum error correction and fault-tolerance, 2005.
- [Kal05] G. Kalai. Thoughts on noise and quantum computation, 2005. lanl-report quant-ph/0508095.
- [KBLW01] J. Kempe, D. Bacon, D.A. Lidar, and K.B. Whaley. Theory of decoherence-free fault-tolerant universal quantum computation. *Phys. Rev. A*, 63:042307, 2001.
- [Kem01] J. Kempe. *Universal Noiseless Computation: Mathematical Theory and Applications*. PhD thesis, University of California, Berkeley, 2001.
- [Kit97] A.Yu. Kitaev. Quantum computations: Algorithms and error corrections. *Russian Math. Surveys*, 52:1191–1249, 1997.
- [Kit03] A.Y. Kitaev. Fault-tolerant quantum computation by anyons. *Ann. of Phys.*, (303):2–30, 2003.
- [KL96] E. Knill and R. Laflamme. Concatenated quantum codes, 1996. LANL preprint quant-ph/9608012.
- [KL97] E. Knill and R. Laflamme. Theory of quantum error-correcting codes. *Phys. Rev. A*, 55:900, 1997.

- [KLV00] E. Knill, R. Laflamme, and L. Viola. Theory of quantum error correction for general noise. *Phys. Rev. Lett.*, 84:2525, 2000.
- [KLZ96] E. Knill, R. Laflamme, and W. H. Zurek. Accuracy threshold for quantum computation. Technical report, Quantum Physics e-Print archive, 1996. <http://xxx.lanl.gov/abs/quant-ph/9611025>.
- [KLZ98] E. Knill, R. Laflamme, and W. Zurek. Resilient quantum computation. *Science*, 279:342–345, 1998.
- [Kni04] E. Knill. Fault-tolerant postselected quantum computation: Threshold analysis, 2004.
- [Kni05] E. Knill. Quantum computing with realistically noisy devices. *Nature*, 434:39–44, 2005.
- [Kra83] K. Kraus. *States, Effects and Operations*. Fundamental Notions of Quantum Theory. Academic, Berlin, 1983.
- [KSV02] A.Y. Kitaev, A.H. Shen, and M.N. Vyalyi. *Classical and Quantum Computation*. Number 47 in Graduate Series in Mathematics. AMS, Providence, RI, 2002.
- [Lan95] R. Landauer. Is quantum mechanics useful? *Phil. Tran, Roy. Soc. Lond.*, 353:367, 1995.
- [LBW99] D.A. Lidar, D. Bacon, and K.B. Whaley. Concatenating decoherence free subspaces with quantum error correcting codes. *Phys. Rev. Lett.*, 82:4556, 1999.
- [LCD<sup>+</sup>87] A.J. Leggett, S. Charkavarty, A.T. Dorsey, M.P.A. Fisher, A. Garg, and W. Zwerger. Dynamics of the dissipative two-state system. *Rev. Mod. Phys.*, 59(1):1–85, 1987.
- [LCW98] D.A. Lidar, I.L. Chuang, and K.B. Whaley. Decoherence free subspaces for quantum computation. *Phys. Rev. Lett.*, 81:2594, 1998.
- [Lin76] G. Lindblad. On the generators of quantum dynamical semigroups. *Commun. Math. Phys.*, 48:119, 1976.
- [LMPZ96] R. Laflamme, C. Miquel, J.P. Paz, and W.H. Zurek. Perfect quantum error correction code. *Phys. Rev. Lett.*, 77:198, 1996.
- [LW03] D.A. Lidar and K.B. Whaley. *Lecture Notes in Physics*, volume 622, chapter Decoherence-Free Subspaces and Subsystems, pages 83–120. Springer, Berlin, 2003.
- [NC00] M.A. Nielsen and I.L. Chuang. *Quantum Computation and Quantum Information*. Cambridge University Press, Cambridge, UK, 2000.
- [ND05] M.A. Nielsen and C.M. Dawson. Fault-tolerant quantum computation with cluster states. *Phys. Rev. A*, 71:042323, 2005.
- [Neu56] J. von Neumann. Probabilistic logics and the synthesis of reliable organisms from unreliable components. In *Automata Studies*, pages 329–378, Princeton, NJ, 1956. Princeton University Press.
- [Pre98a] J. Preskill. Quantum information and computation, lecture notes. <http://www.theory.caltech.edu/people/preskill/ph229/>, 1998.
- [Pre98b] J. Preskill. Reliable quantum computers. *Proc. R. Soc. A*, 454:385–410, 1998.

- [Pre99] J. Preskill. Fault-tolerant quantum computation. In T.P. Spiller H.K. Lo, S. Popescu, editor, *Introduction to quantum computation*, page 213, Singapore, 1999. World Scientific.
- [PSE96] G. Palma, K. Suominen, and A. Ekert. Quantum computers and dissipation. *Proc. Roy. Soc. London Ser. A*, 452:567, 1996.
- [Rei05] B. Reichardt. Threshold for the distance three steane quantum code, 2005. lanl-report quant-ph/0509203.
- [SBFH05] S. H. Simon, N.E. Bonesteel, M.H. Freedman, and N. Petrovic and L. Hor-mozi. Topological quantum computing with only one mobile quasiparticle, 2005. lanl-archive quant-ph/0509175.
- [Sho94] P.W. Shor. Algorithms for quantum computation: Discrete log and factor-ing. In *Proceedings of the 35th Annual Symposium on the Foundations of Computer Science*, pages 124–134, Los Alamitos, CA, 1994. IEEE Computer Society.
- [Sho95] P.W. Shor. Scheme for reducing decoherence in quantum memory. *Phys. Rev. A*, 52:2493–2496, 1995.
- [Sho96] P.W. Shor. Fault-tolerant quantum computation. In *Proceedings of the 37th Symposium on Foundations of Computing*, pages 56–65, Los Alamitos, CA, 1996. IEEE Computer Society Press.
- [Ste96a] A. Steane. Multiple particle interference and quantum error correction. *Proc. Roy. Soc. London*, 452:2551–2577, 1996.
- [Ste96b] A.M. Steane. Error correcting codes in quantum theory. *Phys. Rev. Lett.*, 77:793, 1996.
- [Ste97] A.M. Steane. Active stabilisation, quantum computation and quantum state synthesis. *Phys. Rev. Lett.*, 78:2252–2255, 1997.
- [Ste99] A.M. Steane. Quantum error correction. In S. Popescu H.K. Lo and T.P. Spiller, editors, *Introduction to Quantum Computation and Information*, page 184. World Scientific, Singapore, 1999.
- [Ste01] A.M. Steane. *Decoherence and its implications in quantum computation and information transfer*, chapter Quantum Computing and Error Correction, pages 284–298. IOS Press, Amsterdam, 2001.
- [Ste03] A.M. Steane. Overhead and noise threshold of fault-tolerant quantum error correction. *Phys. Rev. A*, 68:042322, 2003.
- [TB05] B. M. Terhal and G. Burkard. Fault-tolerant quantum computation for local non-markovian noise. *Phys. Rev. A*, 71:012336, 2005.
- [Unr95] W.G. Unruh. Maintaining coherence in quantum computers. *Phys. Rev. A*, 51:992–997, 1995.
- [VKL99] L. Viola, E. Knill, and S. Lloyd. Dynamical decoupling of open quantum systems. *Phys. Rev. Lett.*, 82:2417, 1999.
- [WZ82] W. Wootters and W. Zurek. A single quantum cannot be cloned. *Nature*, 299:802, 1982.
- [Zan97] P. Zanardi. Dissipative dynamics in a quantum register. *Phys. Rev. A*, 56:4445, 1997.

- [Zan98] P. Zanardi. Dissipation and decoherence in a quantum register. *Phys. Rev. A*, 57:3276, 1998.
- [ZR97] P. Zanardi and M. Rasetti. Error avoiding quantum codes. *Mod. Phys. Lett. B*, 11:1085, 1997.
- [Zur91] W.H. Zurek. Decoherence and the transition from quantum to classical. *Phys. Today*, Oktober:36–44, 1991.

Julia Kempe  
CNRS & LRI  
Laboratoire de Recherche Informatique  
Bât. 490, Université de Paris-Sud  
91405 Orsay Cedex  
France  
e-mail: [kempe@lri.fr](mailto:kempe@lri.fr)

# Decoherence of a Quantum Bit Circuit

Grégoire Ithier, François Nguyen, Eddy Collin,  
Nicolas Boulant, Phil J. Meeson, Philippe Joyez,  
Denis Vion and Daniel Estève

**Abstract.** Solid state quantum bit circuits (qubits) are candidates for the implementation of quantum processors, which can in principle perform some computational tasks beyond reach of classical sequential processors. Decoherence is there a key issue since electrical circuits are more prone to decoherence than microscopic objects such as atoms. We introduce the different families of solid state qubits, which are either based on single particle states in semiconductor nanostructures, or on global quantum states of superconducting Josephson circuits. We treat more in detail the Cooper pair box Josephson circuit, and the quantronium circuit derived from it. In this device, a decoupling strategy of the circuit from the outside circuitry allows to improve quantum coherence. We expose results obtained on the manipulation of the qubit state in the quantronium. We develop a general framework for understanding decoherence in qubit circuits, and show how coherence time measurements allow to characterize noise sources coup.

## 1. Why solid state quantum bit circuits ?

These notes provide an introduction to the solid state quantum electrical circuits developed during recent years, following recent propositions for quantum machines. If no quantum-classical frontier indeed exists between the microscopic world and the macroscopic one, quantum machines could indeed take advantage of the richness of quantum physics for performing specific tasks more efficiently than classical ones. Although no quantum machine has been operated yet, probing quantum mechanics with collective variables involving a large number of underlying microscopic degrees of freedom is already an important goal. As expected, decoherence plays there an important role. We present here the systematic investigation carried out on the quantronium circuit developed by our team.

## 2. Towards quantum machines

Very interesting propositions for truly quantum machines, in which state variables are ruled by quantum mechanics, appeared in the domain of processors after Deutsch and Josza showed that the concept of algorithmic complexity is hardware dependent. It was shown that a simple set of unitary operations on an ensemble of coupled two level systems, called quantum bits (qubits), is sufficient to perform some specific computing tasks in a smaller number of algorithmic steps than with a classical processor [1]. Quantum algorithms furthermore solve some mathematical tasks presently considered as intractable, such as the factorization of large numbers, exponentially faster than classical algorithms operated on sequential Von Neumann computers. Solid state quantum bit circuits are a new type of electronic circuits that aim at implementing quantum bits and quantum processors.

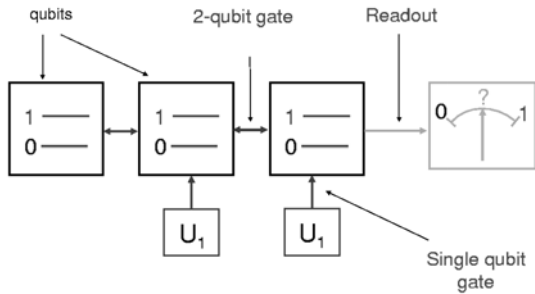


FIGURE 1. A quantum processor consists of an array of qubits. Logic operations are performed by controlling the single and two qubit Hamiltonians. (*Quantronics group*).

A sketch of a quantum processor is shown in Fig. 1. Each qubit is controlled independently, so that any unitary operation can be applied to it. Qubits are coupled in a controlled way so that all the two qubit gate operations required by algorithms can be performed. A two-qubit gate is universal when, combined with a subset of single qubit gates, it allows implementation of any unitary evolution[1]. For instance, the control-not gate (C-NOT), which applies a not operation on qubit 2 when qubit 1 is in state 1, is universal.

### 2.1. Criteria required for qubits

Not all two level systems are suitable for implementing qubits. A series of points, summarized by DiVicenzo, need to be addressed (see chapter 7 in[1]):

- 1) The level spectrum should be sufficiently anharmonic to provide a good two level system.
- 2) An operation corresponding to a ‘reset’ is needed.

- 3) The quantum coherence time must be sufficient for the implementation of quantum error correction codes. This requirement is extremely demanding: less than one error in  $10^4$  gate operations in the most optimistic case.
- 4) The qubits must be of a scalable design with a universal set of gates.
- 5) A high fidelity readout method is needed.

## 2.2. Qubit implementation: Atoms and ions versus electrical circuits

On the experimental side, implementing a quantum processor fulfilling these criteria is a formidable task [2]. The activity has been focused on the operation of simple systems, with at most a few qubits. Two main roads have been followed. Microscopic quantum systems like atoms[3] and ions[4] have been considered. Their main advantage is their excellent quantum coherence, but their scalability is questionable. The most advanced qubit implementation is based on ions in linear traps, coupled to their longitudinal motion [4] and addressed optically.

Solid state electrical circuits have attracted a large interest because they are considered as more versatile and more easily scalable, although reaching the quantum regime is extremely difficult. In this course, we provide a simple presentation of solid state qubits (see refs. [5, 6, 7, 8] for further reading on solid state qubit circuits).

## 2.3. Solid state electrical qubit circuits

Two main strategies based on quantum states of either single particles or of a whole circuit, have been followed for making solid-state electrical qubits.

In the first strategy, the quantum states are nuclear spin states, single electron spin states, or single electron orbital states. The advantage of using microscopic states is that their quantum behaviour has already been probed and can be excellent at low temperature. The main drawback is that qubit operations are difficult to perform since single particles are not easily controlled and read out.

The second strategy has been developed in superconducting circuits based on Josephson junctions, which form a kind of artificial atoms. Their Hamiltonian can be tailored almost at will, and a direct electrical readout can be incorporated in the circuit. On the other hand, these artificial atoms are less quantum than natural ones and spin degrees of freedom.

## 3. Qubits based on semiconductor structures

Different types of quantum states suitable for making qubits can be found in semiconductor nanostructures, as described below. Two families can be distinguished: the first one being based on quantum states of nuclear spins, or of localized electrons, while the second one is based on propagating electronic states (flying qubits).

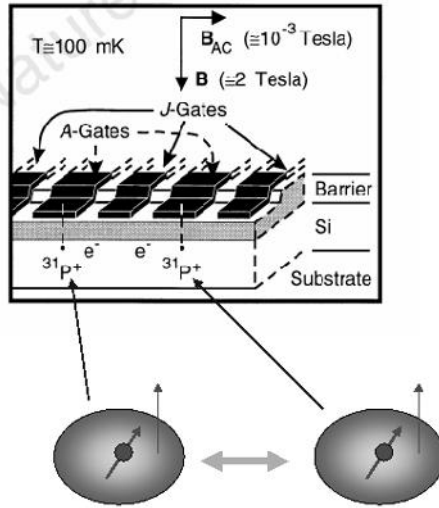


FIGURE 2. Kane's proposal: nuclear spins of phosphorus impurities form the qubits. The control is provided by the hyperfine interaction with a bound electron around each impurity. Each qubit is controlled by applying a voltage to an A gate electrode that displaces slightly the wavefunction of the bound electron, and thus modifies the hyperfine interaction. The two qubit operations are performed using the J gates, which control the exchange interaction between neighboring bound electrons, and thus the interaction between the qubits. (Picture taken from [9].) (Quantronics group).

### 3.1. Kane's proposal: nuclear spins of P impurities in silicon

Kane's proposal, sketched in Fig. 2, is based on the  $S=1/2$  nuclear spins of  $P^{31}$  impurities in silicon [9]. The qubits are controlled through the hyperfine interaction between the nucleus of the  $P^{31}$  impurity and the bound electron around it. The transition frequency of each qubit is determined by the magnetic field applied to it, and by its hyperfine coupling controlled by a gate voltage (A gates). The exchange interaction between the electrons mediates an effective interactions between the qubits, which can be also controlled by a gate voltage (J gate). Single qubit gates would be performed by using resonant pulses, like in NMR, while two qubit gates would be performed using the J gates. The readout would be performed by transferring the information on the qubit state to the charge of a quantum dot, which would then be read using an electrometer. The feasibility of this seducing proposal still has to be demonstrated.

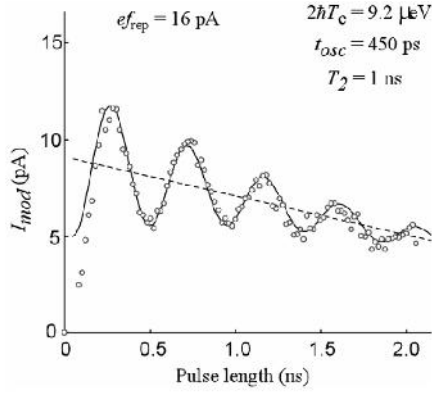


FIGURE 3. Coherent oscillations of a single electron inside a double dot structure, as a function of the duration of a dc pulse applied to the transport voltage. These oscillations are revealed by the average current when the pulse is repeated at a large rate (*Picture taken from Hayashi et al. [10].*) (*Quantronics group*).

### 3.2. Charge states in quantum dots

Although the occupation of a quantum dot by a single electron is not expected to provide an excellent qubit because the electron strongly interacts with electric fields, coherent oscillations in a semiconductor qubit circuit [10] were observed by measuring the transport current in a double dot, as shown in Fig. 3. Recently, a coherence time of the order of 200 ns was achieved in a similar double dot structure, using a single electron transistor (SET) for the qubit readout. [11].

### 3.3. Electron spins in quantum dots

Using electron spins for the qubits is attractive because the spin is weakly coupled to the other degrees of freedom of the circuit, and because the spin state can be transferred to a charge state for the purpose of readout (see [12] and refs. therein). The device shown in Fig. 4 is a double dot in which the exchange interaction between the single electrons in the dots is controlled by the central gate voltage. The readout is performed by monitoring the charge of the dot with a quantum point contact transistor close to it: first, the dot gate voltage is changed so that an up spin electron stays in the dot, while a down spin electron leaves it. In that case, another up spin electron from the reservoir can enter the dot. The detection of changes in the dot charge then provides a single shot efficient measurement of the qubit state [12].

Another setup based on a similar double-dot structure, was recently proposed [13]. In this new scheme, the qubit is encoded in the spin of two electron states with one electron charge in each dot. These spin states are the singlet  $S$  state and the triplet  $T$  state  $m = 0$ . Coherent qubit manipulation was achieved by

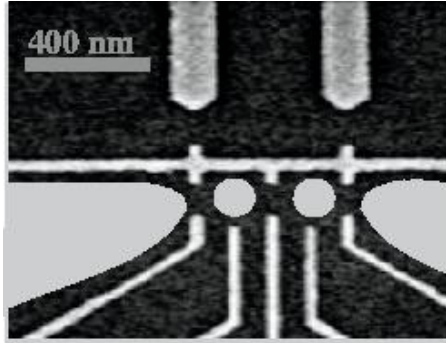


FIGURE 4. Scanning Electron Micrograph of a double dot implementing two qubits. The qubits are based on the spin of a single electron in the ground state of each dot (disks). (*Courtesy of Lieven Vandersypen, T.U. Delft.*) (*Quantronics group*).

controlling the exchange interaction between the two dots. Although the coherence time was limited at about 10 ns due to the magnetic field produced by the nuclei in the substrate, coherent signals were recovered at times  $1 \mu\text{s}$  using echo methods, like in NMR.

### 3.4. Flying qubits

Propagating electron states have also been proposed for implementing qubits. Propagating states in wires with a small number of conduction channels have been considered, but edge states in Quantum hall Effect structures seem to offer a better solution [5] because of their long phase coherence time at low temperature. Qubit states could then be encoded using electrons propagating in opposite directions, along the opposite sides of the wires.

## 4. Superconducting qubit circuits

The interest of using the quantum states of a whole circuit for implementing qubits is to benefit from the wide range of Hamiltonians that can be obtained when inductors and capacitors are combined with Josephson junctions, which provide the anharmonicity required for making two level systems. Josephson qubit circuits can be considered as artificial macroscopic atoms, whose properties can be tailored. Their Hamiltonian can be controlled by applying electric or magnetic fields, and bias currents.

### 4.1. Hamiltonian of Josephson circuits

When branch variables are chosen, the contribution to the Hamiltonian of a Josephson element in a given branch is:

$$h(\theta) = -E_J \cos(\theta),$$

where  $\theta$  is the superconducting phase difference across the junction,  $E_J = I_0\varphi_0$  the Josephson energy, with  $I_0$  the critical current of the junction, and  $\varphi_0 = \hbar/2e$ . The phase  $\theta$  is the conjugate of the number  $N$  of Cooper pairs passed across the junction. The full Hamiltonian is then obtained by adding the electromagnetic terms to the Josephson terms [14, 15]. Any junction in a circuit is characterized by the fluctuations of  $\theta$  and of  $N$ . Often, the circuit junctions are either in the phase or number regimes, characterized by small and large fluctuations of the phase, respectively. Qubit circuits can be classified according to the regime to which they belong. The main types of superconducting qubit circuits can be classified along a phase to charge axis, as shown in Fig. 5.

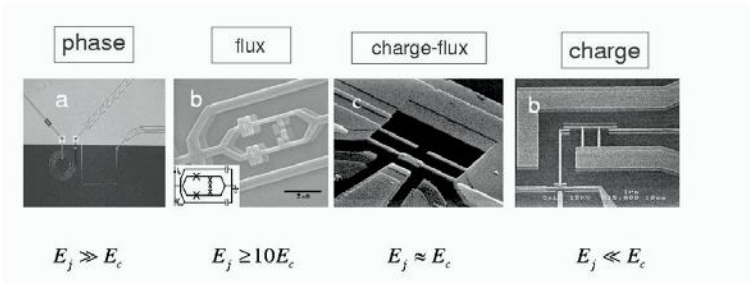


FIGURE 5. Left: A Cooper-pair box consists of a small superconducting island connected by a Josephson junction to a superconducting reservoir, and charge biased by a gate capacitance connected to a voltage source. Right: schematic circuit. The Josephson coupling allows the exchange of Cooper pairs. The phase of the superconducting island and the number of extra Cooper pairs inside are conjugated variables. (*Quantronics group*).

The phase qubit [16] developed at NIST (Boulder) consists of a Josephson junction in a flux biased loop, and the Josephson potential has two wells. The qubit states are two quantized levels in the first potential well, and the readout is performed by resonantly inducing the transfer to the second well, using a monitoring SQUID to detect it.

The flux qubit [17, 18] developed at T.U. Delft consists of three junctions in a loop, placed in the phase regime. Its Hamiltonian is controlled by the flux threading the loop. The flux qubit can be coupled in different ways to a readout SQUID. This circuit is in the phase regime.

The quantronium circuit [19, 20, 8, 21], developed at CEA-Saclay is operated in the intermediate charge-phase regime. The Cooper pair box [23], operated in the charge regime at NEC, is the first qubit circuit for which coherent control of the quantum state was achieved [22]. A detailed description of all Josephson qubits, with extensive references to other works, is given in [6, 7, 8].

## 4.2. The Cooper pair box

The single Cooper pair box [8] consists of a single junction connected to a voltage source across a small gate capacitor, as shown in Fig. 6. Its Hamiltonian writes:

$$\hat{H}(N_g) = E_C(\hat{N} - N_g)^2 - E_J \cos \hat{\theta} \quad (1)$$

where  $E_C = (2e)^2/2C_\Sigma$  is the charging energy of a cooper pair in the island, and  $N_g = C_g V_g/(2e)$  the reduced gate charge with  $V_g$  the gate voltage. The operators  $\hat{N}$  and  $\hat{\theta}$  obey the commutation relation  $[\hat{\theta}, \hat{N}] = i$ . The energy spectrum can be analytically determined, and is  $2e$  periodic with the gate charge. When  $E_J \ll E_C$ , and at  $N_g \equiv 1/2 \text{ mod } [1]$ , the qubit states are simply symmetric and antisymmetric combinations of successive  $|N\rangle$  states.

The most direct way to probe the Cooper pair box is to measure the island charge. After the measurement of the island charge in the ground state [23] with an electrometer based on a Single Electron Transistor (SET) [24], the first Josephson qubit experiment was performed by monitoring the current through an extra junction connected on one side to the box island and on the other side to a voltage source [22]. A charge readout of a Cooper pair box [25] using a rf-SET [26], and a single-shot high fidelity sample and hold readout [27] were later obtained. Finally, a Cooper pair box embedded in a resonant microwave cavity, similar to an atom in a cavity [3], was recently operated [28].

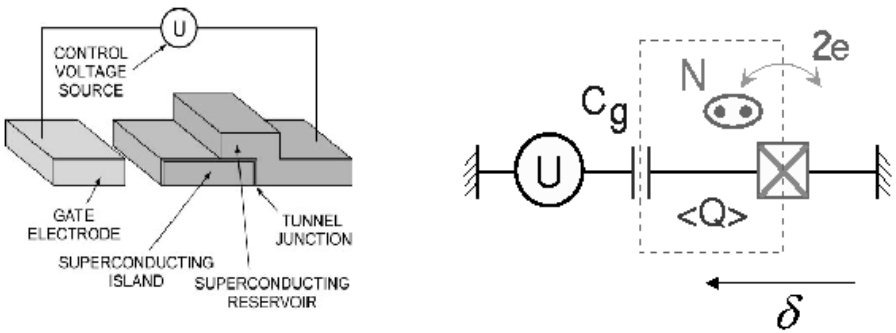


FIGURE 6. The Cooper pair box consists of a small superconducting island connected to a superconducting reservoir, by a Josephson junction (crossed square in the electrical scheme), and biased by a gate capacitor. The Josephson coupling allows the exchange of Cooper pairs between the island and the reservoir. The island phase and the extra number of Cooper pairs in the island are conjugated variables. (*Quantronics group*).

### 4.3. How to maintain quantum coherence?

When the readout circuit measures the qubit, its backaction results in full qubit decoherence during the time needed to get the outcome, and even faster if the readout efficiency is below the quantum limit. In order to reduce decoherence, the readout circuit should thus be switched off when the qubit is operated, and switched on just at readout time. Before explaining a possible strategy to circumvent this problem, we expose the basic concepts underlying decoherence in qubit circuits.

The interaction between a qubit and the degrees of freedom of its environment entangles both parties. This entanglement takes a simple form in the weak coupling regime, which is usually the case in qubit circuits[29]. The control parameters of the qubit Hamiltonian ( such as  $N_g$  for the Cooper pair box), are in fact dynamical variables of the qubit environment, which can fluctuate.

### 4.4. Qubit-environment coupling Hamiltonian

We call  $\lambda$  the set of control variables entering the Hamiltonian of a qubit. At a given working point  $\lambda_0$ , the qubit space is analogous to a fictitious spin 1/2 with  $\sigma_z$  eigenstates  $|0\rangle$  and  $|1\rangle$ . Using the Pauli matrix representation of spin operators, the expansion of the Hamiltonian around  $\lambda_0$  yields the coupling Hamiltonian:

$$\hat{H}_X = -1/2 \left( \vec{D}_\lambda \cdot \vec{\sigma} \right) \left( \hat{\lambda} - \lambda_0 \right) \quad (2)$$

where  $\vec{D}_\lambda \cdot \vec{\sigma}$  is the restriction of  $-2\partial\widehat{H}/\partial\lambda$  to the  $\{|0\rangle, |1\rangle\}$  space. This coupling Hamiltonian determines the qubit evolution when a control parameter is varied, and thus the coupling to decoherence noise sources.

In the weak coupling regime, the fluctuations of the qubit environment are characterized by the spectral density:

$$S_{\lambda_0}(\omega) = \frac{1}{2\pi} \int_{-\infty}^{+\infty} d\tau \left\langle \left( \hat{\lambda}(t) - \lambda_0 \right) \left( \hat{\lambda}(t + \tau) - \lambda_0 \right) \right\rangle \exp(-i\omega\tau) . \quad (3)$$

This spectral density is defined for positive and negative  $\omega$ 's, proportional to the number of environmental modes that can absorb and emit a quantum  $\hbar\omega$ , respectively. In the case of the Cooper pair box, the fluctuations of the gate charge  $N_g$  arise from the impedance of the biasing circuitry and from microscopic charge fluctuators in the vicinity of the box island[8, 21].

### 4.5. Relaxation

The decay of the diagonal part of the density matrix in the eigenstate basis  $\{|0\rangle, |1\rangle\}$  involves  $|1\rangle \rightarrow |0\rangle$  qubit transitions, with the energy transferred to the environment. Such an event resets the qubit in its ground state. The decay is exponential, with a rate:

$$\Gamma_1 = \frac{\pi}{2} \left( \frac{D_{\lambda,\perp}}{\hbar} \right)^2 S_{\lambda_0}(\omega_{01}) . \quad (4)$$

The symbol  $\perp$  indicates that only transverse fluctuations at positive frequency  $\omega_{01}$  induce downward transitions. Upward transitions, which involve  $S_{\lambda_0}(-\omega_{01})$ , occur at a negligible rate for experiments performed at temperatures  $k_B T \ll \hbar\omega_{01}$ , provided the environment is at thermal equilibrium. The relaxation time is thus  $T_1 = 1/\Gamma_1$ .

#### 4.6. Decoherence= relaxation + dephasing

When a coherent superposition  $a|0\rangle + b|1\rangle$  is prepared, the amplitudes  $a$  and  $b$  evolve in time, and the non diagonal part of the density matrix oscillates at the qubit frequency  $\omega_{01}$ . The precise definition of decoherence is the decay of this part of the density matrix. There are two distinct contributions to this decay. Relaxation contributes to decoherence by an exponential damping factor with a rate  $\Gamma_1/2$ , but another process, called dephasing, often dominates. When the qubit frequency  $\Omega_{01}$  fluctuates, an extra phase factor  $\exp[i\Delta\varphi(t)]$  with  $\Delta\varphi(t) = \frac{D_{\lambda,z}}{\hbar} \int_0^t (\widehat{\lambda}(t') - \lambda_0) dt'$  builds up between both amplitudes, the coupling coefficient  $D_{\lambda,z}$  being:

$$D_{\lambda,z} = \langle 0 | \widehat{\partial H / \partial \lambda} | 0 \rangle - \langle 1 | \widehat{\partial H / \partial \lambda} | 1 \rangle = \hbar \partial \omega_{01} / \partial \lambda .$$

Dephasing thus involves longitudinal fluctuations, and contributes to decoherence by the factor:

$$f_X(t) = \langle \exp[i\Delta\varphi(t)] \rangle . \quad (5)$$

This dephasing factor  $f_X(t)$  is not necessarily exponential. When  $D_{\lambda,z} \neq 0$ , and assuming a gaussian process for  $(\widehat{\lambda}(t') - \lambda_0)$ , one finds using a semi-classical approach:

$$f_X(t) = \exp \left[ -\frac{t^2}{2} \left( \frac{D_{\lambda,z}}{\hbar} \right)^2 \int_{-\infty}^{+\infty} d\omega S_{\lambda_0}(\omega) \text{sinc}^2 \left( \frac{\omega t}{2} \right) \right] , \quad (6)$$

which is justified by a full quantum treatment of the coupling to a bath of harmonic oscillators justifies using the quantum spectral density in the above expression [21, 29].

#### 4.7. The optimal working point strategy

The above considerations on decoherence yield the following requirements for the working point of a qubit:

- In order to minimize the relaxation, the coefficients  $D_{\lambda,\perp}$  should be small, and ideally  $D_{\lambda,\perp} = 0$ .
- In order to minimize dephasing, the coefficients  $D_{\lambda,z} \propto \partial \Omega_{01} / \partial \lambda$  should be small. The optimal case is when the transition frequency is stationary with respect to all control parameters:  $D_{\lambda,z} = 0$ . At such optimal points, the qubit is decoupled to first order from its environment and from the readout circuitry. This means that the two qubit states cannot be discriminated at an optimal point. One must therefore depart in some way from the optimal point in order to perform the readout.

## 5. The quantronium circuit

The optimal working point strategy was first applied to the Cooper pair box, with the quantronium circuit [19, 20, 8].

The quantronium circuit, shown in Fig. 7, is derived from the Cooper pair box. The box Josephson junction is split into two junctions with respective Josephson energies  $E_J(1 \pm d)/2$ , with  $d \in [0, 1]$  a small asymmetry coefficient. The reason for splitting the junction into two halves is to form a loop that can be biased by a magnetic flux  $\Phi$ . A third junction is inserted in the loop for the purpose of performing the readout of the qubit. A split box has two degrees of freedom, which can be chosen as the island phase  $\hat{\theta}$  and the phase difference  $\hat{\delta}$  across the two box junctions.

The phase difference  $\hat{\delta}$  in the split-box Hamiltonian is related to the phase difference across the readout junction by the relation  $\hat{\delta} = \hat{\gamma} + \Phi/\phi_0$ , where the phase  $\hat{\gamma}$  is the phase of the readout junction. Except at readout time, when the qubit gets entangled with the readout junction,  $\hat{\delta}$  can be considered as an almost classical parameter. The Hamiltonian of the split box alone, which depends on the two control parameters  $N_g$  and  $\delta$ , writes:

$$\hat{H} = E_C(\hat{N} - N_g)^2 - E_J \cos\left(\frac{\hat{\delta}}{2}\right) \cos(\hat{\theta}) + dE_J \sin\left(\frac{\hat{\delta}}{2}\right) \sin(\hat{\theta}). \quad (7)$$

The corresponding energy levels can be calculated as a function of the control parameters [21]. The variations of the qubit transition frequency with the control parameters are shown in Fig. 7. Different optimal points where all derivatives  $\partial\Omega_{01}/\partial\lambda_i$  vanish are present.

The loop current operator provides a new variable to probe the qubit:

$$\hat{I}(N_g, \delta) = (-2e) \left( -\frac{1}{\hbar} \frac{\partial \hat{H}}{\partial \delta} \right).$$

The average loop current  $\langle i_k \rangle$  in state  $|k\rangle$  obeys a generalized Josephson relation:  $\langle i_k(N_g, \delta) \rangle = \langle k | \hat{I} | k \rangle = \frac{1}{\varphi_0} \partial E_k(N_g, \delta) / \partial \delta$ . The difference between the loop currents of the two qubit states is  $\Delta i_{10} = \langle i_1 \rangle - \langle i_0 \rangle = 2e \partial \omega_{10} / \partial \delta$ . As expected, the difference  $\Delta i_{10}$  vanishes at an optimal point.

### 5.1. Relaxation and dephasing in the quantronium

The split box is coupled to noise sources that affect the gate charge  $N_g$  and the phase  $\delta$  [8, 21]. The coupling to these noise sources  $D_{\lambda,\perp}$  and  $D_{\lambda,z}$  for relaxation and dephasing are obtained from the definition 2.

The coupling vector  $D_{\lambda,\perp}$  for relaxation is:

$$D_{\lambda,\perp} = \left\{ 4E_C \left| \langle 0 | \hat{N} | 1 \rangle \right|, 2\varphi_0 \left| \langle 0 | \hat{I} | 1 \rangle \right| \right\}.$$

Relaxation can thus proceed through the charge and phase ports, but the phase port does not contribute to relaxation at  $N_g = 1/2$  when the asymmetry

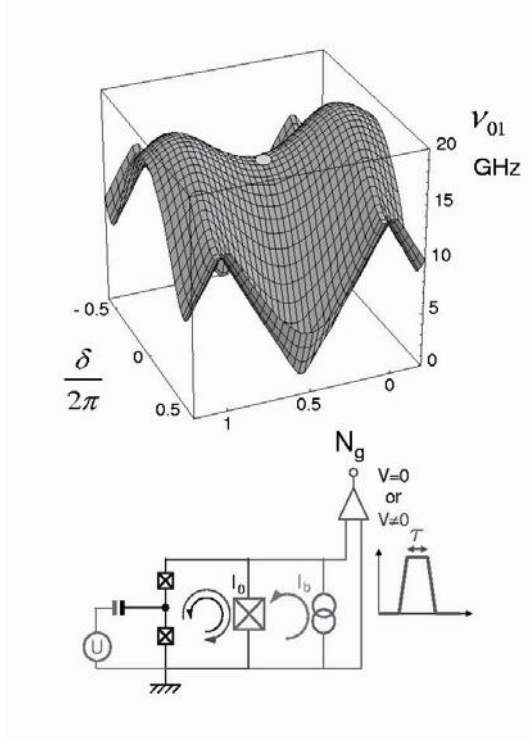


FIGURE 7. Bottom: Schematic circuit of the quantonium qubit circuit. The quantonium consists of a readout junction inserted in the loop of a split-junction Cooper pair box. When a trapezoidal current pulse is applied, the readout junction switches to the voltage state with a larger probability for state  $|1\rangle$  than for state  $|0\rangle$ . Top: Calculated transition frequency as a function of the control parameters  $N_g$  and  $\delta$  for the parameters  $E_J = 0.86 k_B K$ ,  $E_C = 0.68 k_B K$ . The optimal point used in the experiments is the saddle point ( $N_g = 1/2, \delta = 0$ ). (*Quantronics group*).

factor  $d$  vanishes. Precise balancing of the box junctions is thus important in the quantonium.

The coupling vector for dephasing is directly related to the derivatives of the transition frequency:

$$D_{\lambda,z} = \hbar (\partial\omega_{01}/\partial N_g, \partial\omega_{01}/\partial\delta).$$

The charge noise arises from the noise in the gate bias circuit and from the background charge noise due to microscopic fluctuators in the vicinity of the box tunnel junctions. These noises have a  $1/f$  spectral density at low frequency.

## 5.2. Readout of the quantronium

The readout junction can be used in different ways in order to discriminate the qubit states.

**5.2.1. Switching readout.** The simplest method consists in using the readout junction to perform a measurement of the loop current after adiabatically moving away from the optimal point. For this purpose, a trapezoidal readout pulse with a peak value slightly below the readout junction critical current is applied to the circuit (see fig. 7). Since this bias current adds to the loop current in the readout junction, the switching of the readout junction to a finite voltage state can be induced with a large probability for state  $|1\rangle$  and with a small probability for state  $|0\rangle$ . This switching method is in principle a single shot readout. It has been applied to the quantronium [20] and to the flux qubit [18], with a switching probability difference up to 40% and 70%, respectively. The lack of fidelity is attributed to spurious relaxation during the readout bias current pulse. This switching method does not allow for a subsequent readout and is thus not quantum non demolition (QND).

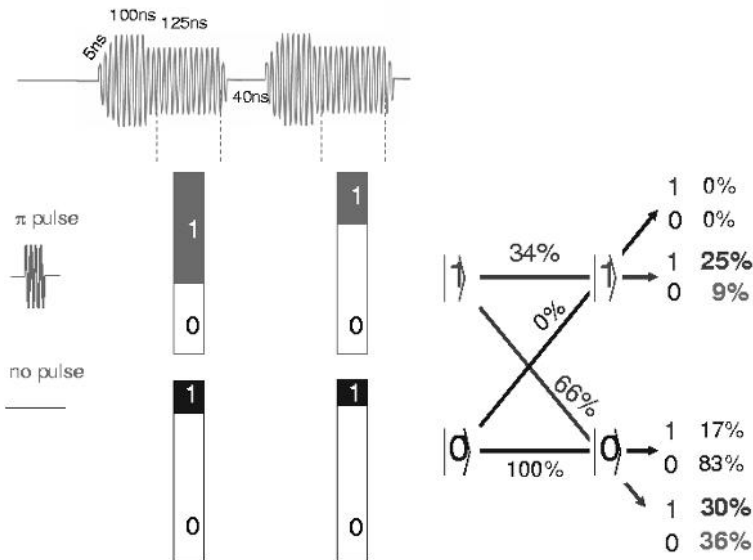


FIGURE 8. The statistics of successive readout outcomes, performed in the ground state and in the excited state of the qubit, give access to the QND fraction of the ac readout method developed for the quantronium. In this experiment, the readout fidelity and the QND fraction are rather low in the excited state of the qubit. (*Quantronics group*).

**5.2.2. AC methods for QND readout.** Recently, microwave methods measuring the phase of a microwave signal reflected or transmitted by the circuit have been proposed for different superconducting qubits in order to attempt a non destructive QND readout. In general, with these rf methods, the working point stays, on average, at the optimal point, and undergoes small amplitude oscillations at a frequency different from the qubit frequency. Avoiding relaxation when moving far away from the optimal point might furthermore improve the readout fidelity. Such methods have been proposed for the flux qubit [30], the quantronium [31, 32], and the Cooper pair box [28, 33]. In the quantronium, The qubit slightly modifies the inductance of the whole circuit [32], with opposite changes for the two qubit states. This change is inferred from the phase of the reflected signal, taking benefit of the non-linear resonance of the readout junction [31]. We have probed the QND character of this Josephson Bifurcation Amplifier (JBA) readout [32, 34] by comparing the outcomes of two successive readouts, as shown in Fig. 8. We found that the readout is only partly QND, and induces relaxation. Like in the case of the switching readout, spurious relaxation limits readout performances.

## 6. Coherent control of the qubit

Coherent control of a qubit is performed by driving the control parameters of the Hamiltonian. Although an adiabatic evolution is possible, most of experiments have been performed with hard pulses.

In the dc-pulse method [22], a sudden change of the Hamiltonian is performed. The qubit state does not in principle evolve during the change, but evolves afterwards with the new Hamiltonian during the pulse duration. This simple method requires extremely short pulse rise-times.

In the resonant pulse method, a control parameter is varied sinusoidally at the qubit frequency. When the gate voltage of a Cooper pair box is modulated by a resonant microwave pulse with amplitude  $\delta N_G$ , the Hamiltonian 2 contains a term  $h(t) = -2E_C \langle 0 | \widehat{N} | 1 \rangle \sigma_X$ , which induces Rabi precession at the frequency

$$\omega_R = 4E_C \delta N_G / \hbar \left| \langle 0 | \widehat{N} | 1 \rangle \right|.$$

As described in Fig. 9, the fictitious spin representing the qubit rotates around an axis located in the equatorial plane of the Bloch sphere, at an angle given by the phase of the microwave pulse. A single resonant pulse with duration  $\tau$  induces a rotation by an angle  $\omega_R \tau$ , which manifests itself by oscillations of the switching probability, as shown in Fig. 9. When the pulse is not resonant, the detuning adds a  $z$  component to the rotation vector.

### 6.1. NMR-like control of a qubit

More complex manipulations inspired from NMR [35, 36, 37] have been performed in order to implement single qubit gates, and to probe decoherence processes [38, 39].

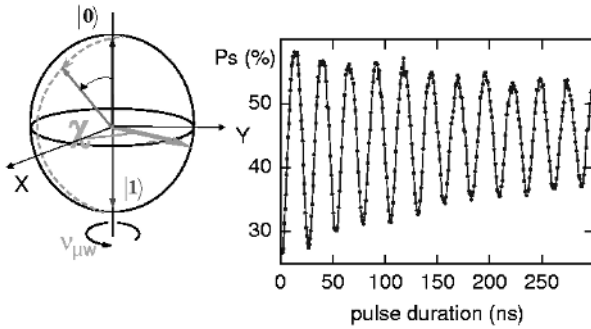


FIGURE 9. Left: Rabi precession of the qubit state represented on the Bloch sphere in the rotating frame during a resonant microwave pulse; Right: Rabi oscillations of the switching probability with the pulse duration. (*Quantronics group*).

Three sequential rotations around two orthogonal axes, for instance the  $x$  and  $y$  axes on the Bloch sphere, allow to perform any unitary operation on a qubit. It is thus important to test whether or not two subsequent rotations combine as predicted, which is shown in Fig. 10. The issue of gate robustness is also extremely

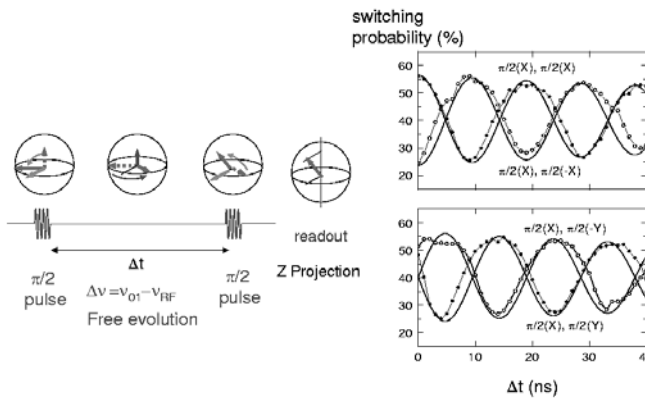


FIGURE 10. Switching probability after two  $\pi/2$  pulses around two orthogonal axes, as a function of the delay between the pulses. The phase of the oscillating signal at the detuning frequency 50 MHz varies as predicted for the different combinations of rotation axes. The solid lines are theoretical fits. (*Taken from [39]. (Quantronics group)*).

important because the needs of quantum computing are extremely demanding. In NMR, composite pulse methods have been developed in order to make transformations less sensitive to pulse imperfections [36, 37, 40]. In these methods, a single pulse is replaced by a series of pulses that yield the same target operation, but with a decreased sensitivity to pulse imperfections. In the case of frequency detuning, a particular sequence named CORPSE (Compensation for Off-Resonance with a Pulse Sequence) has proved to be extremely efficient [40]. This sequence was probed in the quantronium for a  $\pi$  rotation around the  $X$  axis [39].

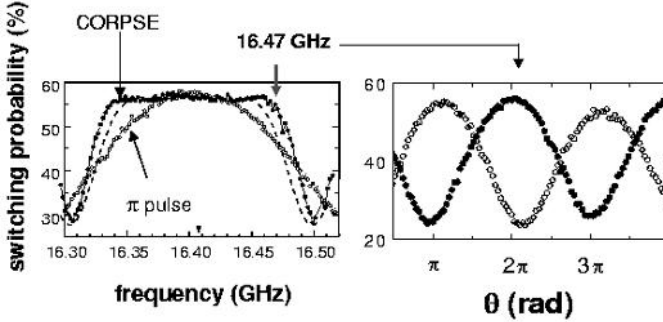


FIGURE 11. Left: switching probability after a single  $\pi$  pulse (open symbols) and after a Corpse pulse corresponding to the same rotation (full symbols), as a function of frequency. The broad maximum for the CORPSE pulse proves the robustness respectively to frequency variations. Right: switching probability after a rotation by an angle  $\theta$  around the  $-X$  axis (open symbols), and after a subsequent CORPSE pulse (full symbols). The phase opposition between the two patterns indicates that the Corpse pulse works for any initial state. (*Quantronics group*).

## 7. Probing qubit coherence

We discuss now decoherence during the free evolution of the qubit, and during its driven evolution. Decoherence induces the decay of the qubit density matrix elements, both in the lab and rotating frames. As explained in section 4.6, decoherence is characterized by relaxation, affecting the diagonal and off diagonal parts of the density matrix, and by dephasing, which affects only its off diagonal part. Detailed explanations can be found in [41].

### 7.1. Relaxation

Relaxation is readily obtained from the decay of the signal after a  $\pi$  pulse. The relaxation time in the quantronium ranges from a few hundreds of nanoseconds

up to a few microseconds. These relaxation times are shorter than those calculated from the coupling to the external circuit using an estimated value for the asymmetry factor  $d$ . Excessive relaxation is found in all Josephson qubits, and could be attributed to the coupling with spurious microscopic two level systems, as suggested in [42].

## 7.2. Decoherence during free evolution

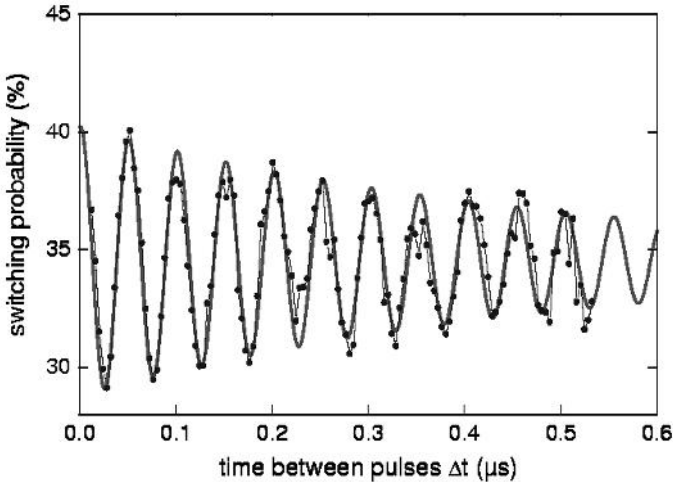


FIGURE 12. Ramsey fringe experiment on a quantronium sample at the optimal point. Two  $\pi/2$  microwave pulses slightly out of resonance and separated by a time delay  $t$  are applied to the gate. The oscillations of the switching probability (dots) at the detuning frequency probe decoherence. In this experiment, the coherence time was  $500\text{ ns}$ , as estimated from an exponentially decaying cosine fit (full line). For the quantronium, Coherence times have been measured in the range  $200 - 500\text{ ns}$ . (*Quantronics group*).

The most direct way to probe decoherence is to perform a Ramsey fringe experiment, as shown in Fig. 12, using two  $\pi/2$  pulses slightly out of resonance. The first pulse creates a superposition of states, with an off diagonal density matrix. After a period of free evolution, during which decoherence takes place, a second pulse transforms part of the off-diagonal terms of the density matrix into a longitudinal term, which is measured by the subsequent readout pulse. The decay of the obtained oscillations at the detuning frequency characterize decoherence. This experiment was first performed in atomic physics, and it corresponds to the free induction decay (FID) in NMR. When the decay is not exponential, we define the coherence time as the time corresponding to a decay factor  $\exp(-1)$ . Other more sophisticated pulse methods have been developed to probe coherence. When the

operating point is moved away from the optimal point at which decoherence is weak during a fraction of the delay between the two pulses of a Ramsey sequence, the signal gives access to decoherence at this new working point.

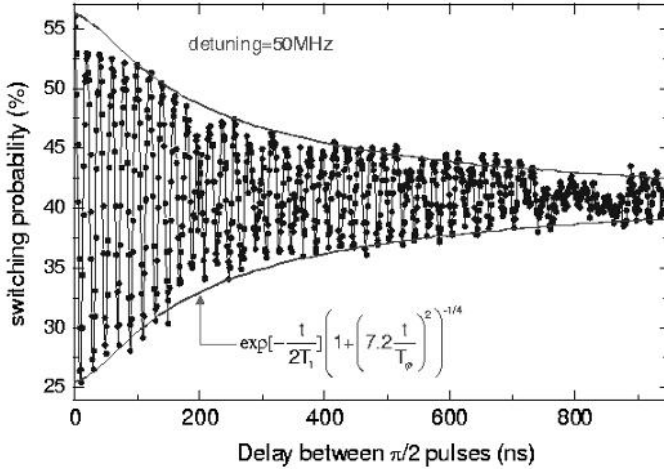


FIGURE 13. Symbols: Switching probability after a Ramsey two pulse sequence, as a function of the delay between pulses. The envelope is the best fit obtained with the static approximation. (*Qnantronics group*).

In order to better characterize decoherence, a series of experiments has been performed on the same sample whose decay of Ramsey interferences is shown in Fig. 13. This decay is not exponential, as expected from the so-called 'static' model [41] which assumes that frequency fluctuations responsible for dephasing are almost static on the time scale of each Ramsey pulse sequence. Other more sophisticated pulse methods have been developed to probe coherence [41]. When the operating point is moved away from the optimal point at which decoherence is weak during a fraction of the delay between the two pulses of a Ramsey sequence, the signal gives access to decoherence at this new working point. The interest of this 'detuning' method is to perform qubit manipulations at the optimal working point without being hindered by decoherence. When the coherence time is too short for time domain experiments, the lineshape, which is the Fourier transform of the Ramsey signal, gives access to the coherence time. Coherence times obtained with all these methods on a single sample away from the optimal point in the charge and phase directions are indicated by full symbols in Fig. 14.

It is possible to shed further light on the decoherence processes and to fight them using the echo technique well known in NMR [35]. An echo sequence is a two  $\pi/2$  pulse Ramsey sequence with a  $\pi$  pulse in the middle, which causes the phase accumulated during the second half to be subtracted from the phase accumulated during the first half. When the noise-source producing the frequency fluctuation is static on the time scale of the pulse sequence, the echo does not decay. The observed echo decay times, indicated by open disks in Fig. 14, thus set constraints on the spectral density of the noise sources. In particular, these data indicate that the charge noise is significantly smaller than expected from the low frequency  $1/f$  spectrum. Bang-bang suppression of dephasing, which generalizes the echo technique, could fight decoherence more efficiently [43].

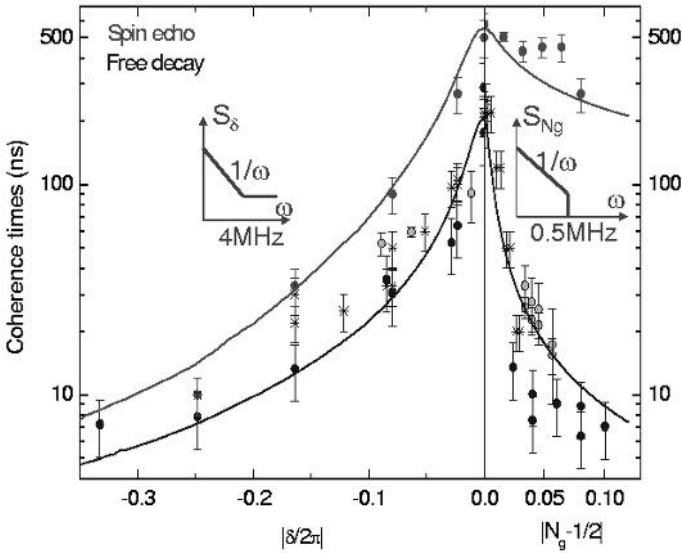


FIGURE 14. Coherence times  $T_2$  and  $T_{Echo}$  in a quantronium sample extracted from the decay of free evolution signals. The full and dashed lines are calculated using the the spectral densities depicted by the bottom graphs for the phase noise (left) and for the charge noise (right), respectively. (*Quantronics group*).

### 7.3. Decoherence during driven evolution

During driven evolution, the density matrix is best defined using the eigenstate basis in the rotating frame. On resonance, these eigenstates are the states  $|X\rangle$  and  $|-X\rangle$  on the Bloch sphere. As in the laboratory frame, the decay of the density matrix involves relaxation and dephasing. The measurement of the relaxation time can be performed using the so-called spin locking technique in NMR [35], which

allows one to measure the qubit polarization after the preparation of the state  $|X\rangle$ . The coherence time during driven evolution is easily obtained from Rabi oscillations. Indeed, the initial state  $|0\rangle$  is a coherent superposition of the eigenstates during driven evolution:  $|0\rangle = (|X\rangle + |-X\rangle)/\sqrt{2}$ .

The Rabi signal measured after a pulse of duration  $t$  thus probes decoherence during driven evolution. The corresponding coherence time is longer than the coherence time during free evolution because the driving field quenches the effect of the low frequency fluctuations that dominate dephasing during free evolution.

## 8. Qubit coupling schemes

### 8.1. First experimental results

Single qubit control and readout has been achieved for several Josephson qubits. Although the control accuracy and readout fidelity do not yet meet the requirements for quantum computing, the demonstration on such 'working' qubits of logic gates is now a main goal. Presently, only a few experiments have been performed on coupled qubits. A logic  $C - NOT$  gate was operated in 2003 on charge qubits [44], but without single shot readout. The correlations between coupled phase qubits were measured recently using a single-shot readout [45]. In this experiment, a fixed coupling between two phase qubits with the same resonance frequency is implemented with a capacitor as shown in Fig. 15. Starting from state  $|10\rangle$ , the probabilities to obtain states  $|10\rangle$  and  $|01\rangle$  are then anticorrelated, as expected for a swapping interaction. The entanglement between two coupled qubits should however be investigated with better accuracy in order to probe the violation of Bell inequalities predicted by quantum mechanics. Only such an experiment could indeed test if collective degrees of freedom do obey quantum mechanics, and whether or not the entanglement decays as predicted from the known decoherence processes. We now discuss the different types of coupling schemes.

### 8.2. Tunable versus fixed couplings

In a processor, single qubit operations have to be supplemented with two qubit logic gate operations. During a logic gate operation, the coupling between the two qubits has to be controlled with great accuracy. For most solid state qubits, there is however no simple way to switch and to control the coupling. In the case of the superconducting qubits, controllable coupling circuits have been proposed [47], but fixed coupling Hamiltonians have been mostly considered and operated: capacitive coupling for phase, charge-phase and charge qubits, and inductive coupling for flux qubits. It is nevertheless possible to use a constant coupling Hamiltonian provided that the effective qubit-qubit interaction is controlled by other parameters. We now discuss all these coupling schemes.

The first demonstration of a logic gate was performed using a fixed Hamiltonian. The system used consisted of two Cooper pair boxes with their islands

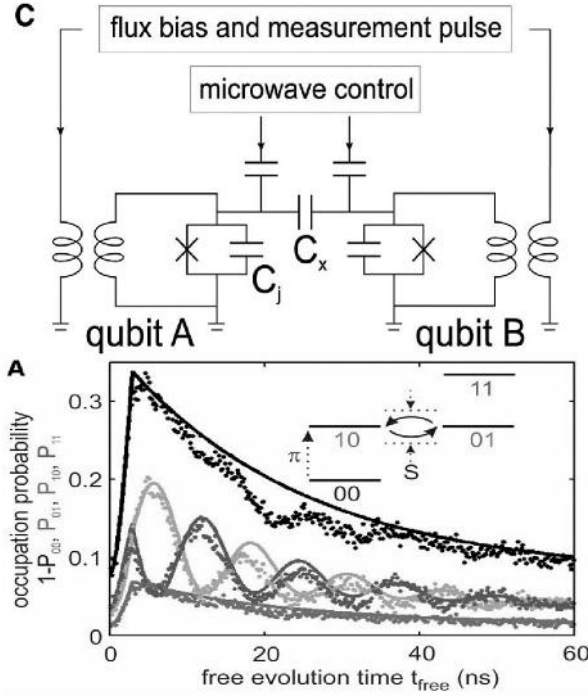


FIGURE 15. Two phase qubits are capacitively coupled and measured simultaneously after a free evolution time. The anticorrelation between the probabilities  $P_{01}$  and  $P_{10}$  demonstrate the swapping induced by the interaction (taken from [45]). (*Quantronics group*).

connected by a capacitance  $C_C$ . The coupling Hamiltonian is

$$H_{cc} = -E_{CC}(\hat{N}_1 - N_{G1})(\hat{N}_2 - N_{G2}) \quad (8)$$

where  $E_{CC} = -E_{C1}E_{C2}C_C/(2e)^2$  is the coupling energy, smaller than the charging energy of the Cooper pair boxes. This Hamiltonian corresponds to changing the gate charges by  $(E_{CC}/2E_{C1})/(\hat{N}_2 - N_{G2})$  for qubit 1, and by  $(E_{CC}/2E_{C2})/(\hat{N}_1 - N_{G1})$  for qubit 2. The correlations between the two qubits predicted for this Hamiltonian have been probed, and a C-NOT logic gate was operated with this circuit[44].

In the uncoupled eigenstate basis, The Hamiltonian (8) contains both longitudinal terms of type  $\hat{\sigma}_{Z1}\hat{\sigma}_{Z2}$  and transverse terms of type  $\hat{\sigma}_{X1}\hat{\sigma}_{X2}$ . At the double optimal point  $N_{G1} = N_{G2} = 1/2$ ,  $\delta_1 = \delta_2 = 0$ , the Hamiltonian (8) is

however purely transverse  $H_{CC} = \hbar\Omega_C \hat{\sigma}_{X1} \hat{\sigma}_{X2}$ , with  $\Omega_C = E_{CC}/\hbar \left| \langle 0_1 | \hat{N}_1 | 1_1 \rangle \right| \left| \langle 0_2 | \hat{N}_2 | 1_2 \rangle \right|$ . When the two qubits have the same resonance frequency  $\omega_{01}$ , and when  $\Omega_C \ll \omega_{01}$ , the non-secular terms in  $H_{CC}$  that do not commute with the single qubit Hamiltonian are ineffective, and the effective Hamiltonian reduces to:

$$H_{CC}^{\text{sec}} = (\hbar\Omega_C) (\hat{\sigma}_{+1} \hat{\sigma}_{-2} + \hat{\sigma}_{-1} \hat{\sigma}_{+2}) . \quad (9)$$

The evolution of the two qubits corresponds to swapping them periodically. More precisely, a swap operation is obtained at time  $\pi/\Omega_C$ . This gate is called *ISWAP* because of extra factors  $i$ :

$$\begin{aligned} \text{ISWAP} |00\rangle &= |00\rangle; \quad \text{ISWAP} |10\rangle = -i |01\rangle; \\ \text{ISWAP} |01\rangle &= -i |10\rangle; \quad \text{ISWAP} |11\rangle = |11\rangle. \end{aligned}$$

At time  $\pi/4\Omega_C$ , the evolution operator corresponds to the gate  $\sqrt{\text{ISWAP}}$ , which is universal.

### 8.3. Control of the interaction mediated by a fixed Hamiltonian

The control of the qubit-qubit interaction mediated by a fixed Hamiltonian depends on the form of this Hamiltonian.

For a coupling of the form 9, the effective interaction can be controlled by varying the qubit frequencies since the qubits are affected only when their frequency difference is smaller than  $\Omega_C$ . This tuning strategy was recently applied to capacitively coupled phase qubits, in which the qubit frequency is directly controlled by the bias current of the junctions [7]. The correlations predicted by quantum mechanics between the readouts of the two qubits were observed [45]. The tuning strategy would be also well suited for coupling many qubits together through an oscillator [29]. The virtual exchange of photons between each qubit and the oscillator indeed yields a coupling of the form 9, which is efficient only when the two qubits are tuned. This coupling scheme yields truly scalable designs, whereas most of other schemes are limited to 1D qubit arrays, with nearest neighbor couplings. The coupling between a qubit and a resonator has already been demonstrated for the charge and flux qubits [46, 28].

Another method proposed recently consists in maintaining the qubits out of resonance, but in reaching an equivalent resonance condition in the presence of resonant microwave pulses applied to each one [48]. This method is based on a well known NMR protocol that aims at placing two different spin species 'on speaking terms'. In this scheme, the energy difference between the two qubits is exchanged with the microwave fields.

## 9. Conclusions and perspectives

Many solid state qubits have been proposed, and several of them have already demonstrated coherent evolution.

For semiconductor qubits, the coherent transfer of an electron between two dots has been demonstrated, and other promising designs are under investigation.

For superconducting qubits, single qubit control, single-shot readout, and a two-qubit logic gate have been achieved. Methods inspired from NMR have been applied to qubit manipulation in order to improve manipulation robustness, and to probe decoherence processes. However, the lack of an efficient readout scheme and of robust two qubit gates still hinders the development of the field. New QND readout schemes are presently investigated in order to reach a higher readout fidelity. New qubit gates have been proposed, but none of them is as robust as classical gates used in ordinary classical processors. Currently, the coherence time, the readout fidelity, and the gate accuracy are insufficient to envision quantum computing. But how far from this goal are solid state qubits?

In order to use quantum error correcting codes, an error rate of the order of  $10^{-4}$  for each logic gate operation is required. Presently, the gate error rates can be estimated at about a few % for single qubit gates, and at about 20% at best for two qubit gates. The present solid state qubits thus miss the goal by many orders of magnitude. When decoherence and readout errors are taken into account, quantum computing appears even more unrealistic. This is not, however, a reason to give up because conceptual and technical breakthroughs can be expected in this rather new field, and because no fundamental objection has been found. One should not forget that, in physics, everything which is possible is eventually done. Furthermore, quantum circuits provide new research directions in which fundamental questions on quantum mechanics can be addressed. The extension of quantum entanglement out of the microscopic world, and the location and nature of the frontier between quantum and classical worlds, are two of these essential issues. For instance, the accurate measurement of the correlations between two coupled qubits would indeed probe whether or not the collective variables of qubit circuits do follow quantum mechanics.

Our feeling is that, whatever the motivation, complex quantum systems and quantum machines are a fascinating field worth the effort.

**Acknowledgments.** We acknowledge all the members of the Quantronics group, and the help of the Qlab team at Yale. We acknowledge the support of the Eurosqip project.

## References

- [1] M.A. Nielsen and I.L. Chuang, " *Quantum Computation and Quantum Information*" (Cambridge University Press, Cambridge, 2000).
- [2] *Quantum Coherence and Information Processing* , edited by D. Estève, J.M. Raymond and J. Dalibard (Elsevier, 2004).
- [3] S. Haroche, course 2 in ref. 2; M. Brune, course 3 in ref. 2.
- [4] R. Blatt, H. Häffner, C.F. Ross, C. Becher and F. Schmidt-Kaler, course 5 in ref. 2; D.J. Wineland, course 6 in ref. 2.
- [5] C. Glattli, course 11 in ref. 2.
- [6] M.H. Devoret and J. Martinis, course 12 in ref. 2.

- [7] J. Martinis, course 13 in ref. 2.
- [8] D. Vion, course 14 in ref. 2.
- [9] B. E. Kane, *Nature* **393** (1998), 133 .
- [10] T. Hayashi, T. Fujisawa, H. D. Cheong, Y. H. Jeong and Y. Hirayama, *Phys. Rev. Lett.* **91** (2003), 226804.
- [11] J. Gorman, D.G. Hasko and D.A. Williams, *Phys. Rev. Lett.* **95** (2005), 090502.
- [12] J. M. Elzerman, R. Hanson, L. H. Willems van Beveren, B. Witkamp, J. S. Greidanus, R. N. Schouten, S. De Franceschi, S. Tarucha, L. M. K. Vandersypen and L.P. Kouwenhoven, *Quantum Dots: a Doorway to Nanoscale Physics*, in *Series: Lecture Notes in Physics*, **667**, Heiss, WD. (Ed.), (2005), and refs. therein.
- [13] A. C. Johnson, J. R. Petta, J. M. Taylor, A. Yacoby, M. D. Lukin, C. M. Marcus, M. P. Hanson, A. C. Gossard, *Nature* **435** (2005), 925.
- [14] M.H. Devoret, in " *Quantum Fluctuations*", S. Reynaud, E. Giacobino, J. Zinn-Justin, eds. (Elsevier, Amsterdam, 1996), p.351.
- [15] Guido Burkard, Roger H. Koch and David P. DiVincenzo, *Phys. Rev. B* **69** (2004), 064503.
- [16] J. M. Martinis, S. Nam, J. Aumentado and C. Urbina, *Phys. Rev. Lett.* **89** (2002), 117901.
- [17] J. E. Mooij, T. P. Orlando, L. Levitov, Lin Tian, Caspar H. van der Wal and Seth Lloyd, *Science* **285** (1999), 1036.
- [18] I. Chiorescu, Y. Nakamura, C. J. P. M. Harmans and J. E. Mooij, *Science* **299** (2003), 1869.
- [19] A. Cottet, D. Vion, P. Joyez, P. Aassime, D. Estève and M.H. Devoret, *Physica C* **367** (2002), 197.
- [20] D. Vion *et al.*, *Science* **296** (2002), 886.
- [21] A. Cottet, *Implementation of a quantum bit in a superconducting circuit*, PhD thesis, Université Paris VI, (2002); [www-drecam.cea.fr/drecam/spec/Pres/Quantro/](http://www-drecam.cea.fr/drecam/spec/Pres/Quantro/) .
- [22] Y. Nakamura, Yu. A. Pashkin and J. S. Tsai, *Nature* **398** (1999), 786.
- [23] V. Bouchiat, D. Vion, P. Joyez, D. Estève and M.H. Devoret, *Physica Scripta* **76** (1998), 165; V. Bouchiat, PhD thesis, Université Paris VI, (1997), [www-drecam.cea.fr/drecam/spec/Pres/Quantro/](http://www-drecam.cea.fr/drecam/spec/Pres/Quantro/) .
- [24] *Single Charge Tunneling*, edited by H. Grabert and M. H. Devoret (Plenum Press, New York, 1992).
- [25] T. Duty, D. Gunnarsson, K. Bladh and P. Delsing, *Phys. Rev. B* **69** (2004), 140503.
- [26] R.J. Schoelkopf *et al.*, *Science* **280** (1998), 1238.
- [27] O. Astafiev, Yu. A. Pashkin, Y. Nakamura, T. Yamamoto and J. S. Tsai, *Phys. Rev. Lett.* **93** (2004), 267007.
- [28] A. Wallraff, D. Schuster,-I.; A. Blais; L. Frunzio; R.-S. Huang,- J. Majer, S. Kumar, S.M.Girvin, R.J. Schoelkopf, *Nature* **431** (2004), 162; and p. 591 in ref. 2.
- [29] Y. Makhlin, G. Schön and A. Shnirman, *Rev. Mod. Phy* **73** (2001), 357.
- [30] A. Lupascu, .J.M.Verwijs, R.N. Schouten, C.J.P.M. Harmans and J.E. Mooij, *Phys. Rev. Lett.* **93** (2004), 177006.

- [31] I. Siddiqi, R. Vijay, F. Pierre, C. M. Wilson, M. Metcalfe, C. Rigetti, L. Frunzio, R.J. Schoelkopf, M. H. Devoret, D. Vion and D. Estève, *Phys. Rev. Lett.* **94** (2005), 027005.
- [32] I. Siddiqi, R. Vijay, F. Pierre, C. M. Wilson, M. Metcalfe, C. Rigetti, L. Frunzio and M. H. Devoret, *Phys. Rev. Lett.* **93** (2004), 207002.
- [33] Mika A. Sillanpää, Leif Roschier and Pertti J. Hakonen, *Phys. Rev. Lett.* **93** (2004), 066805x.
- [34] I. Siddiqi et al., *Cond-Mat* 0507548. **93** (2004), 207002.
- [35] C.P. Slichter, *Principles of Magnetic Resonance*, Springer-Verlag (3rd ed: 1990).
- [36] J. Jones, course 10 in ref. 2.
- [37] L.M.K. Vandersypen and I.L. Chuang, *quant-ph/0404064*.
- [38] D. Vion *et al.*, *Fortschritte der Physik* **51** (2003), 462.
- [39] E. Collin, G. Ithier, A. Aassime, P. Joyez, D. Vion and D. Estève, *Phys. Rev. Lett.* **93** (2004), 157005.
- [40] H.K. Cummins, G. Llewellyn and J.A. Jones, *Phys. Rev. A* **67** (2003), 042308.
- [41] G. Ithier et al., *Phys. Rev. B.* **72** (2005), 134519.
- [42] K. B. Cooper, Matthias Steffen, R. McDermott, R. W. Simmonds, Seongshik Oh, D. A. Hite, D. P. Pappas and John M. Martinis, *Phys. Rev. Lett.* **93** (2004), 180401.
- [43] G. Falci, A. D'Arrigo, A. Mastellone and E. Paladino, *Phys. Rev. A* **70** (2004), 040101; H. Gutmann, F.K. Wilhelm, W.M. Kaminsky and S. Lloyd, *Quantum Information Processing* **3** (2004), 247.
- [44] T. Yamamoto et al., *Nature* **425** (2003), 941, and Yu. Pashkin *et al.*, *Nature* **421** (2003), 823.
- [45] R. McDermott, R. W. Simmonds, Matthias Steffen, K. B. Cooper, K. Cicak, K. D. Osborn, Seongshik Oh, D. P. Pappas and John M. Martinis, *Science* **307** (2005), 1299.
- [46] I. Chiorescu, P. Bertet, K. Semba, Y. Nakamura, C. J. P. M. Harmans and J. E. Mooij, *Nature* **431** (2004), 159.
- [47] J. Q. You, Y. Nakamura and F. Nori, *Phys. Rev. B* **71** (2005), 024532; J. Lantz, M. Wallquist, V. S. Shumeiko and G. Wendin, *Phys. Rev. B* **70** (2004), 140507.
- [48] C. Rigetti, A. Blais and M. H. Devoret *Phys. Rev. Lett.* **94** (2005), 240502.

Grégoire Ithier, François Nguyen, Eddy Collin,  
Nicolas Boulant, Phil J. Meeson, Philippe Joyez,  
Denis Vion and Daniel Estève

Quantronics

SPEC, CEA-Saclay

F-91191 Gif-sur-Yvette

e-mail: gregoire.ithier@rhul.ac.uk, francois.nguyen@cea.fr  
eddy.collin@grenoble.cnrs.fr, nboulant@cea.fr  
phil.meeson@rhul.ac.uk, pjoyez@dsm-mail.cea.fr  
denis.vion@cea.fr, daniel.esteve@cea.fr

# Roots and Fruits of Decoherence

H. Dieter Zeh

**Abstract.** The concept of decoherence is defined, and discussed in a historical context. This is illustrated by some of its essential consequences which may be relevant for the interpretation of quantum theory. Various aspects of the formalism are also reviewed for this purpose.

## 1. Definition of concepts

The concept of decoherence has become quite popular during the last two decades. However, while its observable consequences have now been clearly confirmed experimentally [1, 2] (see also contributions to this seminar), some misunderstandings regarding its meaning seem to persist in the literature. The phenomenon itself obviously does not depend on any particular interpretation of quantum theory, but its relevance for them may vary considerably [3, 4]. I am indeed surprised about the indifference of most physicists regarding the potential consequences of decoherence in this respect, since this concept arose as a by-product of arguments favoring either a collapse of the wave function as part of its dynamics, or an Everett-type interpretation. In contrast to the Copenhagen interpretation, which insists on fundamental classical concepts, both these interpretations regard the wave function as a complete and universal representation of reality (cf. [5]).

So let me first emphasize that by decoherence I do neither just mean the disappearance of spatial interference fringes in the statistical distribution of measurement results, nor do I claim that decoherence without additional assumptions is able to solve the infamous measurement problem by *explaining* the stochastic nature of measurements on the basis of a universal Schrödinger equation. Rather, I mean no more (and no less) than the *dynamical delocalization of quantum mechanical superpositions*, which are defined in an abstract Hilbert space with a local basis (given by particle positions and/or spatial fields, for example). The ultimate nature of this Hilbert space basis (the stage for a universal wave function) can only be found in a unifying TOE (theory of everything).

Dislocalization arises through the formation of entanglement of any system under consideration (with states  $\phi$ ) with another one, such as its unavoidable environment (described by states  $\Phi$ ). This is often achieved by means of a von-Neumann type “measurement” interaction

$$\left(\sum c_i \phi_i\right) \Phi_0 \rightarrow \sum c_i \phi_i \Phi_i \quad , \quad (1)$$

which would represent a logical *controlled-not* operation in the case  $i = 1, 2$  and  $\Phi_0 = \Phi_1$ . Ideal measurements, that is, those without recoil or change of the state  $\phi_i$ , define “pure decoherence”. After the interaction, these superpositions still *exist*, even though they *are not there* any more [6, 7]. The difference between these two traditionally equivalent phrases reflects the essential character of nonlocal quantum reality. I am indeed convinced that the importance of decoherence was overlooked for the first 60 years of quantum theory precisely because entanglement was regarded just as an aspect of quantum mechanical methods of calculation rather than of physical reality.

Dislocalization of superpositions may be reversible (“virtual”) or irreversible in practice (“real” decoherence). In the first case it would either allow the complete relocalization of the superposition (“recoherence”), or at least its reconstruction (the “quantum erasure” of measurement results). The distinction according to the reversibility or irreversibility of decoherence *explains* also the virtual versus real nature of other “quantum events”, such as radioactive decay, particle creation, or excitation. For example, decayed systems remain in a superposition with their undecayed sources until partial waves corresponding to different decay times are decohered from one another. (This has the dynamical consequence of giving rise to an *exact* exponential decay law – see the contribution by Erich Joos to these proceedings.) In contrast to recoherence (complete reversal of the dislocalization), quantum erasure is compatible with the irreversible and non-unitary dynamics of open systems – related to a local entropy decrease at the cost of an entropy increase in the environment [8].

According to (1), dislocalization of superpositions requires a distortion of the environment  $\Phi$  by the system  $\phi$  rather than a distortion of the system by the environment (such as by classical “noise”). This leads to the important consequence that decoherence in quantum computers cannot be error-corrected for in the usual manner by means of redundant information storage. Adding extra physical quantum bits to achieve redundancy, as it would be appropriate to correct spin or phase flips *in the system*, would in general even raise the quantum computer’s vulnerability against decoherence – for the same reason as the increased size of an object normally strengthens its classicality. (Error correction codes proposed in the literature for this purpose are based on the presumption of decoherence-free auxiliary qubits, which may not be very realistic.)

In special situations, decoherence may be observed as a disappearance of spatial interference fringes. Only for mass points, or center of mass positions of extended objects, are wave functions isomorphic to *spatial* waves, and only after

position measurements with many equivalently prepared objects do they form a *statistical distribution*. The interference pattern could then conceivably also have been obscured by a slightly varying preparation procedure (for example due to uncontrollable “noise”), while decoherence according to Equ. (1) affects *individual* quantum states. Because of the latter’s nonlocality it leads locally to a reduced density matrix that describes formally an *apparent ensemble* of states (thus *not* presuming it). The conceptually important difference between true and apparent ensembles was clearly pointed out by Bernard d’Espagnat [9] when he distinguished between proper and improper mixtures. In the case of virtual (reversible) decoherence, this difference can be observed as recoherence (relocalization of the superposition) – impossible for a proper mixture.

Superpositions thus define pure states, which characterize *individual* properties that are not present in their formal components. For example, the superposition of two different spinor states is again an individual spinor state (up or down with respect to another direction); the superposition of a  $K$ -meson and its antiparticle defines a new particle ( $K_{long}$  or  $K_{short}$ ); that of a continuum of positions (in the form of a plane wave) defines a certain “momentum” (wave number). Similarly, a superposition of products of the spin states of two particles (even at different places) by means of Clebsch-Gordon coefficients defines an individual state of total spin, while each particle is then in an “improper mixture” because of its virtual decoherence by the other one. Under unitary transformations (described by a Schrödinger equation) these total states remain pure and can never become ensembles that might represent different measurement outcomes. However, unitary decoherence may irreversibly lead to *apparent* ensembles (improper mixtures) for local systems, which would precisely explain the required ensembles of measurement outcomes if they were genuine (proper). This consequence can hardly be an unrelated accident!

## 2. Roots in nuclear physics

Nuclear physics provides some nice examples of many-particle systems which are nonetheless clearly microscopic (found in energy eigenstates). While I was involved in low energy nuclear physics during the sixties, I became irritated by some methods which were quite successfully used. One of them, called the time-dependent Hartree-Fock approximation, describes “stationary” states of heavy nuclei by means of time-dependent determinants of single-nucleon wave functions. But how can the mathematical solution of a static equation  $H\psi = E\psi$  know about a concept of time? Similarly, certain deformed nuclei were often described by means of a time-dependent “cranking model” in order to calculate an effective moment of inertia, or to reproduce a Coriolis type coupling between collective rotational states and individual nucleons. However, both parameters characterize the spectra of static energy eigenstates! It turned out that time is here used as a

misleading tool to describe *static superpositions* of one-parametric continua of different determinants in order to construct quantum states for their corresponding collective degrees of freedom (vibrations or rotations around one axis, for example).

For other collective modes, more than one parameter may be required. General rotations, for example, have to be represented by a non-Abelian symmetry group characterized by three Euler angles. Superpositions then assume the form

$$\Psi = \int d\Omega f(\phi, \theta, \chi) U(\phi, \theta, \chi) \Phi(\mathbf{r}_1, \dots, \mathbf{r}_n) \quad , \quad (2)$$

where  $U(\phi, \theta, \chi)$  is the unitary transformation describing a rotation and  $d\Omega$  the volume element in this space, while  $\Phi$  is a deformed determinant or other “model wave function”. There are many other cases where entanglement is classically circumscribed in terms of a time-dependent jargon. Well known is the picture of “vacuum fluctuations” – used to characterize a static state of entangled quantum fields.

If a variational procedure

$$\delta \langle \Phi | (H - E) | \Phi \rangle = 0 \quad , \quad (3)$$

with determinants  $\Phi$  consisting of single nucleon wave functions  $\phi_i$ , leads to a deformed solution (as it happens for many heavy nuclei), one must first conclude that  $\Phi$  can *not* be an approximation to the correct solution of  $H\psi = E\psi$ , since it is far from being an angular momentum eigenstate. However, using the degeneracy of these “wrong” solutions under rotations, one may consider their superposition (2) as the next best step. Simultaneous variation of the single-particle wave functions in  $\Phi$  and the superposition amplitudes  $f(\phi, \theta, \chi)$  then leads to angular momentum eigenstates and rotational spectra, including Coriolis effects for the single particle motion [10].

The superposition (2) may be regarded as being “dislocalized” over all nucleons in such a way that they are all strongly entangled with one another. A *strong* symmetry violation of the model wave function  $\Phi$  may be defined by the quasi-orthogonality of slightly different orientations,

$$\langle \Phi | U(\phi, \theta, \chi) | \Phi \rangle \approx 0 \quad \text{for} \quad U \neq 1 \quad , \quad (4)$$

as though the collective orientation were an observable, and  $f(\phi, \theta, \chi)$  therefore the corresponding wave function. In a similar way, phonon degrees of freedom arise in solid bodies. This strong violation of rotational symmetry does not require a “needle limit” of strong *geometric* asymmetry: it is a collective effect of many slightly asymmetric single-particle wave functions (subsystems). For product wave functions  $\Phi = \prod_i \phi_i(\mathbf{r}_i)$ , for example, one would get

$$\begin{aligned} \langle \Phi | U(\phi, \theta, \chi) | \Phi \rangle &= \prod_i \langle \phi_i | U(\phi, \theta, \chi) | \phi_i \rangle \\ &= \prod_i (1 - \epsilon_i) \approx \prod_i \exp(-\epsilon_i) = \exp\left(-\sum_i \epsilon_i\right) \quad . \end{aligned} \quad (5)$$

(For nucleons, their indistinguishability reduces this result somewhat, and may let nuclei behave as a superfluid.) This quasi-orthogonality is very similar to decoherence, which is often achieved by means of a product of inner products of many environmental subsystems (such as many scattered particles) [6]. In lowest approximation of the strong symmetry violation, each nucleon then “feels” only the deformed (apparently oriented) self-consistent potential produced by the others. While there is no *absolute* orientation in this case of rotational symmetry of the exact Hamiltonian, the latter’s dependence on inertial frames allows the nucleons in higher order also to experience a Coriolis-type coupling with the collective angular momentum.

So one may say that the individual nucleons “observe” an apparent asymmetry in spite of the symmetric global superposition of all orientations. However, a similar superposition of different pointer positions occurs in a quantum measurement that is described by von Neumann’s unitary interaction (1). This analogy led me to the weird speculation about a nucleus that is big enough to contain a complex subsystem which may resemble a registration device or even a conscious observer. It/she/he would then become entangled with its/her/his “relative world”, such as with a definite orientation. Does the dynamical consequence described above then indicate a way to solve the measurement problem? If the nucleons in the deformed nucleus dynamically feel a definite orientation in spite of the global superposition, would an internal observer then not similarly have to become “aware of” a certain measurement result?

This picture was also my first attempt towards a (non-relativistic) quantum cosmology – a kind of Everett interpretation as I later discovered. When I learned about the static Wheeler-DeWitt quantum universe, described by an equation  $H\psi = 0$ , it also helped me to understand the concept of time that emerges therein (cf. [11] and Sect. 6.2.2 of Ref. [8]). In contrast to a macroscopic body, a nucleus in an energy eigenstate represents a closed quantum “universe”. However, it was absolutely impossible at that time to discuss these ideas with colleagues, or even to publish them. An influential Heidelberg Nobel prize winner frankly informed me that any further activities on this subject would end my academic career!

Macroscopic objects are never found in energy eigenstates, but rather in states of certain (usually time-dependent) orientations or positions. Therefore, it was generally concluded that “quantum theory is not made for macroscopic objects” or even the universe. According to Niels Bohr, macroscopic systems have to be described in terms of *presumed* classical (or “every-day”) concepts – even though they would have to obey the uncertainty relations.

### 3. The quantum-to-classical transition

Much has been written about the quantum-to-classical transition (cf. [12, 7] and Zurek’s contribution to these proceedings). It is evidently crucial for a theory that describes reality exclusively in terms of quantum states, while it would be of no

more than secondary importance (such as for explaining the absence of interference patterns in scattering experiments) if classical concepts were *presumed* for a probabilistic interpretation from the beginning. I could never accept such a fundamental divide between quantum and classical concepts. So one has to understand the different *appearance* of atoms, nuclei and small molecules on the one hand, and macroscopic objects on the other. If both are described quantum mechanically, their energy spectra differ quantitatively. For example, rotational states of macroscopic objects are very dense. As a consequence, they cannot resist entanglement with their environment even in the case of very weak interactions. Their reduced density matrices must then always represent “mixed states”, while the locality of these interactions leads to the vanishing of non-diagonal elements preferentially in the position or “pointer” representation. This is now called decoherence.

Although this term came up more than ten years later (probably it was first used in talks given by Gell-Mann and Hartle at the end of the eighties, preceding their publication of 1993 [13]), I pointed out in a number of papers (see [14, 15]) that this disappearance of certain non-diagonal elements of the density matrix explains superselection rules, which were often postulated as fundamental restrictions of the superposition principle (for example in axiomatic foundations of quantum theory). They were assumed to hold for specific properties, such as electric charge, as well as for “classical observables”, although the axioms did not define a precise boundary between quantum and classical concepts.

In these early papers you will not even find the word “entanglement” – simply because this concept was so rarely used at that time that I did not know this English translation of Schrödinger’s *Verschränkung*. So I referred to it as “quantum correlations”. Remember that even Schrödinger, in his famous paper of 1935 [16], regarded *Verschränkung* as a mysterious probability relation (which would have to characterize ensembles rather than individual states), since he was convinced that reality has to be defined in space and time.

However, what I had in mind went beyond what is now called decoherence, since it was inspired by the above mentioned picture of an observer inside a closed quantum system. An external observer, who is *part of the environment* of the observed object, becomes entangled, too, with the property he is observing – just as the observer within the deformed nucleus is entangled with its orientation. He is thus part of a much bigger “nucleus” (or closed system): the quantum universe. So he “feels”, or can be aware, only of a definite value of the property he has measured (or separately of different values in different “Everett worlds”). All you have to assume is that his *various* quantum states which may exist as factor states in these *components* of the global wave function are the true carriers of awareness. This is even plausible from a quite conventional point of view, since these decohered component states, which are a consequence of the Schrödinger equation, possess all properties required to define observers, such as complexity and dynamical stability (memory). Indeed, these states are the same ones that would arise in appropriate collapse theories if they were, according to von Neumann’s motivation, constructed in order to re-establish a psycho-physical parallelism, but I do not see why a

modification of the dynamics that eliminates all “other” components from reality should be required.

A genuine collapse that was simply *triggered* by irreversible decoherence (as recently suggested in a very clever way by Roland Omnès [17]) would not lead to any observable consequences, while other models should either be experimentally confirmed or refuted. As long as they are *not* confirmed, it is just a matter of taste whether you apply Occam’s razor to the facts (by inventing new dynamical laws to cut off what you cannot see) or to the laws (by leaving the Schrödinger equation unchanged) – although this choice must clearly have *cosmological* consequences (such as a symmetric superposition of many different asymmetric “worlds” that might have been essential, that is, not yet decohered, during early stages of the universe).

For me the most important fruit of decoherence (that is, of a universal entanglement) is the fact that no classical concepts are required any more on a fundamental level. There is then also no need for a fundamental concept of “observables”, which would assume *certain* values only upon measurement – see Chap. 4, and for uncertainty relations then restricting such values. The Fourier theorem for the wave function explains this “uncertainty” in a natural way – well known for classical radio waves, which are themselves real and certain. When Bohr and Heisenberg insisted that the uncertainty relations go beyond the Fourier theorem, they were apparently thinking of *spatial* wave functions only (thus neglecting entangled states).

For microscopic objects which can be sufficiently isolated, the experimental physicist has a choice between mutually exclusive (“conjugate”) measurements, while macroscopic properties are decohered by their unavoidable environment in a *general and specific* manner. This explains their classical appearance. The corresponding quasi-classical basis in Hilbert space then *appears* as a classical configuration space, while the conventional “quantization” procedure may be regarded as the re-introduction of these lost superpositions into the (approximately valid) classical theory. Similarly, the classical world appears local to us, since nonlocal entanglement becomes immediately uncontrollable: it is decohered.

In order to illustrate the difference between this and the Copenhagen interpretation, let me quote from a recent publication by Ulfbeck and Aage Bohr from Copenhagen regarding the nature of *quantum events*. They write [18]: “No event takes place in the source itself as a precursor of the click in the counter . . .”. Hence, there is no decay event in the atom, for example! So far I agree; this conclusion, which is in contrast to earlier interpretations of quantum theory, is enforced by experiments which use reflected decay fragments to demonstrate recoherence (state vector revival) or interference with partial waves resulting from later decay times. In order to appreciate this important change in the Copenhagen interpretation, one may compare the *new* version with Pauli’s claim from the fifties that “the appearance of a certain position or momentum *of a particle* is a creation outside the laws of nature” (my italics), which clearly refers to the creation of particle properties. Ulfbeck and Bohr then continue their sentence of above: “. . . where

the wave function loses its meaning.” Here I strongly disagree. After all, it is precisely the arising uncontrollable entanglement with the environment, described by a global wave function, which explains decoherence. These authors are correct, though, when placing the creation of (apparent, I would add) stochastic “events” in the apparatus, where the dislocalization of the relevant superposition becomes irreversible FAPP (for all practical purposes), thus creating an *apparent* ensemble of quasi-classical wave packets. The dishonesty of the Copenhagen interpretation consists in switching concepts on demand and regarding the (genuine or apparent) collapse as a “normal increase of information” – as though the wave function represented no more than an ensemble of *possible* physical states. However, this is ruled out by observed state vector revival phenomena.

Of course, you may *pragmatically* use classical concepts *as though* they were fundamental – even when studying decoherence as a phenomenon. One cannot expect practicing physicists always to argue in terms of a universal wave function. But they may keep in mind that there *is* a consistent description (thus representing a “quantum reality”) underlying their classical terminology. Similarly, a high-energy physicist uses the concepts of momentum and energy to describe the objects in his laboratory, although he knows that they are no more than limited descriptions of the objective relativistic concept of “momenergy”. Fortunately, there are other fruits of decoherence in the form of observable phenomena which demonstrate decoherence in action [1, 2]. Nonetheless, the derivability in principle of classical (such as particle) concepts undermines the motivation for the Heisenberg picture as well as for Bohm’s quantum mechanics, for example.

#### 4. Quantum mechanics without observables<sup>1</sup>

In quantum theory, measurements are traditionally described by means of “observables”, which in the Heisenberg picture are assumed to replace classical *variables*, and therefore have to carry the dynamical time dependence. They are formally represented by hermitean operators, and introduced in addition to the concepts of quantum states and their dynamics as a fundamental and independent ingredient of quantum theory. However, even though often forming the starting point of a formal quantization procedure, this ingredient may not be separately required if physical states are universally described by general quantum states (superpositions in an appropriate basis of states) and their dynamics. This interpretation, to be further explained below, would comply with John Bell’s quest for a theory in terms of “beables” rather than observables [19]. It was for this reason that his preference shifted from Bohm’s theory to collapse models (where wave functions are assumed to completely describe *reality*) during his last years. (Another reason was his antipathy against the “extravagance” – as he called it – of the multiplicity of Everett worlds, which appears in the form of myriads of empty components as well in Bohm’s never collapsing wave function.)

---

<sup>1</sup> This chapter is based on Sect. 2.2 of [7]. It may be skipped for a quick reading.

Let  $|\alpha\rangle$  be an arbitrary quantum state of a local system (perhaps experimentally prepared by means of a “filter” – see below). The *phenomenological* probability for finding this system in another quantum state  $|n\rangle$ , say, after an appropriate measurement, is given by means of their inner product,  $p_n = |\langle n | \alpha \rangle|^2$ , where both state vectors are assumed to be normalized. This transition of state may either correspond to a collapse or a branching of the wave function – though here neglecting the states of the apparatus and the environment. The state  $|n\rangle$  represents here a specific measurement. In a position measurement, for example, the number  $n$  has to be replaced with the continuous coordinates  $x, y, z$ , leading to the “improper” Hilbert states  $|\mathbf{r}\rangle$ . Measurements are called “of the first kind” or “ideal” if the system will again be found in the state  $|n\rangle$  (except for a phase factor) whenever the measurement is immediately repeated. *Preparations* of states can be regarded as measurements which *select* a certain subset of outcomes for further measurements.  $n$ -preparations are therefore also called  $n$ -filters, since all “not- $n$ ” results are thereby excluded from the subsequent experiment proper. The above probabilities can be written in the form  $p_n = \langle \alpha | P_n | \alpha \rangle$ , with a special “observable”  $P_n := |n\rangle\langle n|$ , which is thus *derived* from the kinematical concept of quantum *states* by using their (phenomenological) probabilistic dynamics during measurements, rather than being introduced as a fundamental concept.

Instead of these special “ $n$  or not- $n$  measurements” (for fixed  $n$ ), one can also perform more general “ $n_1$  or  $n_2$  or ... measurements”, with all  $n_i$ ’s mutually exclusive ( $\langle n_i | n_j \rangle = \delta_{ij}$ ). If the states forming such a set  $\{|n\rangle\}$  are pure and exhaustive (that is, complete,  $\sum P_n = 1$ ), they represent a basis of the corresponding Hilbert space. By introducing an arbitrary “measurement scale”  $a_n$ , one may construct *general* observables

$$A = \sum |n\rangle a_n \langle n| \quad , \quad (6)$$

which permit the definition of “expectation values”

$$\langle \alpha | A | \alpha \rangle = \sum p_n a_n \quad . \quad (7)$$

In the special case of a yes-no measurement, one has  $a_n = \delta_{nn_0}$ , and expectation values become probabilities. Finding the state  $|n\rangle$  during a measurement is then also expressed as “finding the value  $a_n$  of an observable”. A uniquely invertible change of scale,  $b_n = f(a_n)$ , describes the *same* physical measurement; for position measurements of a particle it would simply represent a coordinate transformation. Even a measurement of the particle’s potential energy  $V$  is equivalent to an (incomplete) position measurement if the function  $V(\mathbf{r})$  is *given*.

According to this definition, quantum expectation values must not be understood as mean values in an ensemble that represents ignorance about the precise state. Rather, they have to be interpreted as resulting from the probabilities for *potentially arising* quantum states  $|n\rangle$  – regardless of the interpretation of this stochastic process. If the set  $\{|n\rangle\}$  of such potential states forms a basis, any state  $|\alpha\rangle$  can be represented as a superposition  $|\alpha\rangle = \sum c_n |n\rangle$ . In general, it neither

forms an  $n_0$ -state nor any not- $n_0$  state. Its dependence on the complex coefficients  $c_n$  requires that states which differ from one another by a numerical factor must be different “in reality”. This is true even though they represent the same “ray” in Hilbert space and cannot, according to the measurement postulate, be distinguished operationally. The states  $|n_1\rangle + |n_2\rangle$  and  $|n_1\rangle - |n_2\rangle$  could not be physically different from another if  $|n_2\rangle$  and  $-|n_2\rangle$  were the *same* state. While operationally indistinguishable in the state  $\pm|n_2\rangle$  itself, any numerical factor – such as a phase factor – would become relevant in the case of recoherence. (Only a *global* factor would thus be “redundant”.) For this reason, projection operators  $|n\rangle\langle n|$  are insufficient to characterize quantum states.

The expansion coefficients  $c_n$  relating physically meaningful states – for example those describing different spin directions or different versions of the K-meson – have in principle to be determined (relative to one another) by appropriate experiments. However, they can often be derived from a previously known (or conjectured) classical Hamiltonian theory by means of “quantization rules”. In this case, the classical configurations  $q$  (such as particle positions or field variables) are *postulated* to parametrize a basis in Hilbert space,  $\{|q\rangle\}$ , while the canonical momenta  $p$  parametrize another one,  $\{|p\rangle\}$ . Their corresponding observables,

$$Q = \int dq |q\rangle q \langle q| \quad \text{and} \quad P = \int dp |p\rangle p \langle p| \quad , \quad (8)$$

are then required to obey commutation relations in analogy to the classical Poisson brackets. In this way, they form an important *tool* for constructing and interpreting the specific Hilbert space of quantum states. These commutators essentially determine the unitary transformation  $\langle p | q \rangle$  (e.g. as a Fourier transform  $e^{ipq}$ ) – thus more than what could be defined by means of the projection operators  $|q\rangle\langle q|$  and  $|p\rangle\langle p|$ . This algebraic procedure is mathematically very elegant and appealing, since the Poisson brackets and commutators may represent generalized symmetry transformations. However, the *concept* of observables (which form the algebra) can be derived from the more fundamental one of state vectors and their inner products, as described above.

Physical states are assumed to vary in time in accordance with a dynamical law – in quantum mechanics of the form  $i\partial_t|\alpha\rangle = H|\alpha\rangle$ . In contrast, a measurement device is usually defined regardless of time. This must then also hold for the observable representing it, or for its eigenbasis  $\{|n\rangle\}$ . The probabilities  $p_n(t) = |\langle n | \alpha(t) \rangle|^2$  will therefore vary with time according to the time-dependence of the physical states  $|\alpha\rangle$ . It is well known that this (Schrödinger) time dependence is formally equivalent to the (inverse) time dependence of observables (or the reference states  $|n\rangle$ ). Since observables “correspond” to classical *variables*, this time dependence appeared suggestive in the Heisenberg–Born–Jordan algebraic approach to quantum theory. However, the absence of *dynamical states*  $|\alpha(t)\rangle$  from this Heisenberg picture, a consequence of insisting on *classical* kinematical concepts, leads to paradoxes and conceptual inconsistencies (complementarity, dualism, quantum logic, quantum information, negative probabilities, and all that).

The transition to a Heisenberg picture essentially breaks down for open systems, which cannot obey a Schrödinger equation.

An environment-induced superselection rule means that certain superpositions are highly unstable against decoherence. It is then impossible in practice to construct measurement devices for them. This *empirical* situation has led some physicists to *deny the existence* of these superpositions and their corresponding observables – either by postulate or by formal manipulations of dubious interpretation, often including infinities or non-separable Hilbert spaces.

While *any* basis  $\{|n\rangle\}$  in Hilbert space defines formal probabilities,  $p_n = |\langle n|\alpha\rangle|^2$ , only a basis consisting of states that are not immediately destroyed by decoherence defines “realizable observables”. Since the latter usually form a genuine subset of *all* formal observables (diagonalizable operators), they must contain a nontrivial “center” in algebraic terms. It consists of those which commute with all the rest. Observables forming the center may be regarded as “classical”, since they can be measured simultaneously with *all* realizable ones. In the algebraic approach to quantum theory, this center appears as part of its axiomatic structure [20]. However, since the condition of decoherence has to be considered quantitatively (and may even vary to some extent with the specific nature of the environment), this algebraic classification remains an approximate and dynamically emerging scheme.

These “classical” observables thus characterize the subspaces into which superpositions decohere. Hence, even if the superposition of a right-handed and a left-handed chiral molecule, say, *could* be prepared by means of an appropriate (very fast) measurement of the first kind, it would be destroyed before the measurement may be repeated for a test. In contrast, the chiral states of all individual molecules in a bag of sugar are “robust” in a normal environment, and thus retain this property *individually* over time intervals which by far exceed thermal relaxation times. This stability may even be increased by the quantum Zeno effect (see [21] for a consistent and exhaustive discussion). Therefore, chirality does not only appear classical in these cases, but also as an approximate constant of the motion that has to be taken into account for defining canonical ensembles in thermodynamics.

The above-used description of measurements of the first kind by means of probabilities for transitions  $|\alpha\rangle \rightarrow |n\rangle$  (or, for that matter, by corresponding observables) is phenomenological. However, measurements should be described *dynamically* as interactions between the measured system and the measurement device. The observable (that is, the measurement basis) should thus be derived from the corresponding interaction Hamiltonian and the initial state of the device. As shown by von Neumann, this interaction must be diagonal with respect to the measurement basis (see (1) and [22]). Its diagonal subsystem matrix elements are operators acting on the quantum state of the device in such a way that the “pointer” evolves into a position appropriate for being read,  $|n\rangle|\Phi_0\rangle \rightarrow |n\rangle|\Phi_n\rangle$ . Here, the first ket refers to the system, the second one to the device. The states  $|\Phi_n\rangle$ , representing different pointer positions, must approximately be mutually orthogonal, and “classical” in the explained sense.

Because of the dynamical version of the superposition principle, an initial superposition  $\sum c_n |n\rangle$  does *not* lead to definite pointer positions (with their empirically observed frequencies). If decoherence is neglected, one obtains their *entangled superposition*  $\sum c_n |n\rangle |\Phi_n\rangle$ , that is, a state that is different from all potential measurement outcomes  $|n\rangle |\Phi_n\rangle$ . This dilemma represents the “quantum measurement problem”. Von Neumann’s interaction is nonetheless regarded as the first step of a measurement (a “pre-measurement”). Yet, a collapse still seems to be required – now in the measurement device rather than in the microscopic system. Because of the entanglement between system and apparatus, it would then affect the total system. (Some authors seem to have taken the phenomenological collapse in the *microscopic system* by itself too literally, and therefore disregarded the state of the measurement device in their measurement theory. Such an approach is based on the assumption that quantum states always exist for all systems. This would be in conflict with quantum nonlocality, even though it may be in accordance with early interpretations of the quantum formalism.)

If, in a certain measurement, a whole subset of states  $|n\rangle$  leads to the same pointer position  $|\Phi_{n_0}\rangle$ , these states can not be distinguished by this measurement. According to von Neumann’s interaction, the pointer state  $|\Phi_{n_0}\rangle$  will now be correlated with the *projection* of the initial state onto the subspace spanned by this subset. A corresponding *collapse* was therefore formally postulated by Lüders [23] as a generalization of von Neumann’s “first intervention” (as he called the collapse dynamics).

In this sense, the interaction with an appropriate measuring device *defines* an observable. The formal time dependence of observables according to the Heisenberg picture would then describe a time dependence of the states diagonalizing the interaction Hamiltonian, such that, paradoxically, the device would be assumed to be dynamically controlled by the Hamiltonian of the system.

The question whether a certain formal observable (that is, a diagonalizable operator) can be *physically realized* can only be answered by taking into account the unavoidable environment. A macroscopic measurement device is *always* assumed to decohere into its macroscopic pointer states. However, as mentioned in Chapter 3, environment-induced decoherence by itself does not solve the measurement problem, since the “pointer states”  $|\Phi_n\rangle$  may be defined to include the total environment (the “rest of the world”). Identifying the thus arising global superposition with an *ensemble* of states (represented by a statistical operator  $\rho$ ) that leads to the same expectation values  $\langle A \rangle = \text{tr}(A\rho)$  for a *limited* set of observables  $\{A\}$  would beg the question. This merely operational argument is nonetheless often found in the literature.

## 5. Rules versus tools

As the Everett interpretation describes a “branching quantum world”, which mimics a collapsing wave function to the internal observer, the question is often raised

for the precise *rules* of this branching – similar to the dynamical rules for a collapse. Such collapse rules would have to define the individual branches (or the “pointer states”) as well as their dynamical probabilities. In contrast, decoherence describes the branching by means of the Schrödinger equation as a dislocalization of initially local superpositions in such a way that the latter become gradually inaccessible to any local observer. Decoherence neither defines nor explains this ultimate (conscious) observer. While the branching is ultimately justified by the *observer’s* locality, the dislocalization itself is an *objective* dynamical process – in particular occurring in measurement devices.

This unitary dynamical process causes the non-diagonal elements of the reduced density matrices of all dynamically involved local systems (such as those forming a chain of interactions which lead to an observation) to vanish very fast. These *indicators* of dislocalized superpositions are therefore often used to *define* decoherence. However, subsystems and their density matrices are no more than convenient conceptual tools, useful because of the locality of all interactions and the causal structure of our world (based on cosmic initial conditions that are responsible for the arrow of time [8]). In contradistinction to a nonlocal superposition, the concept of a density matrix *presumes* the probability interpretation. The degree of diagonalization of the reduced density matrices would depend on the precise choice and boundaries of subsystems, but this is irrelevant for a sufficient definition of “macroscopically distinct” global branches FAPP. Decoherence may thus be called a *collapse without a collapse*.

While a genuine collapse theory would have to postulate (as part of the dynamical law) probabilities for its various *possible* outcomes, in an Everett world *all* branches are assumed to remain in existence. One can then meaningfully argue only about *frequencies* of outcomes (such as spots on a screen) in *series* of measurements that were performed in our branch. Graham was able to show more than thirty years ago [24] that all those very abundant (by number) “maverick Everett worlds” which do not possess frequencies in accordance with the Born probabilities possess a norm that vanishes with increasing size of the series. While their exclusion is nonetheless *not* a trivial assumption, the norm plays here a similar rôle as phase space does in classical statistical physics: it is dynamically conserved under the Schrödinger equation, and thus an appropriate measure of probability.

## 6. Nonlocality

Let me continue with another reminiscence from the “dark ages of decoherence” (that ended not before Wojciech Zurek had published his first papers on this subject in the Physical Review [22]). After I had completed the manuscript for my first paper on what is now called decoherence [14], the only well known physicist who responded to it in a positive way for a long time was Eugene Wigner. He helped me to get it published, and he also arranged for an invitation to a conference on

the foundations of quantum theory to be held in Varenna in 1970, organized by Bernard d'Espagnat [25].

When I arrived at Varenna, I found the participants (John Bell included) in hot debates about the first experimental results regarding the Bell inequalities, which had been published a few years before [26]. I had never heard of them, but I could not quite share the general excitement, since I was already entirely convinced that entanglement (and hence nonlocality) was a well founded property of quantum states, which in my opinion described reality rather than probability correlations. So I concluded that everybody would now soon agree.

Obviously I was far too optimistic. Some physicists are searching for loopholes in the experiments which confirm the violation of these inequalities until today – even though all experimental results were precisely predicted by quantum theory. Others (perhaps still the majority) are interpreting nonlocality as a “spooky action at a distance”, which would have to affect tacitly presumed local quantities or events (such as described by classical concepts). I cannot see anything but prejudice (once shared by Einstein and Schrödinger!) in such an assumption about reality. It is amazing that even Bohm, who did assume the nonlocal wave function to be real, added classical concepts to describe another (local) reality, which would have to include the local observer, and for which the wave function acts as no more than a pilot wave.

It appears strange, too, that certain “measures of entanglement” that have recently been much in use [27] measure only reversible or *usable* entanglement, while quite incorrectly regarding irreversible entanglement (decoherence) as “noise” or “distortion”. It is certainly not an accident that this position appears related to Ulfbeck and Bohr’s above-mentioned statement. The observable consequences of Eq. (1) demonstrate that quantum measurements can *not* be regarded as describing a “mere increase of information” – even in the absence of any recoil. Quantum measurement interactions produce *real* nonlocal entanglement.

If reality is accepted to be *kinematically* nonlocal, you also don’t need any “spooky teleportation” in order to explain certain experiments that appear particularly attractive to science fiction authors. In all these experiments you have to *prepare in advance* a nonlocal (entangled) state that contains, in one of its components, precisely what is later claimed to be ported already at its final position. For example, in such a setting two spinors have to be prepared in the form of a Bell state

$$\begin{aligned} & | \uparrow \rangle_A | \downarrow \rangle_B - | \downarrow \rangle_A | \uparrow \rangle_B \\ & = | \rightarrow \rangle_A | \leftarrow \rangle_B - | \leftarrow \rangle_A | \rightarrow \rangle_B = \dots \quad , \end{aligned} \quad (9)$$

where  $A$  and  $B$  refer to Alice’s and Bob’s place, respectively. Nothing has to be ported any more when Alice, say, follows the usual “teleportation” procedure to perform the measurement of another (local) Bell state that includes her spinor of (9) and the one to be ported. Because of the “real” (irreversible) decoherence of the nonlocal superposition (9) caused by this measurement, this *initial* Bell state becomes an apparent ensemble, such that the entanglement it represents

*appears* to be a statistical correlation from the point of view of all local observers (such as Bob). His apparently incomplete information may then be “completed” by apparently classical means (Alice sending a message to Bob). In quantum terms, this “information transfer” means that Bob and his spin, too, become consistent members of the (partly irreversible) global entanglement (see Joos’s Sect. 3.4.2 of [7]). This is then experienced by Bob (in all his arising branches) as a collapse of the wave function. If the relativistic universal Hamiltonian is local (an integral over a spatial Hamiltonian density), it becomes obvious from this unitary treatment that there can be no superluminal influence. Quantum nonlocality is therefore compatible with the *dynamical locality* of quantum fields that is often referred to as “relativistic causality”.

Alice assumes here the rôle of Wigner’s well known “friend”, who performs a measurement without immediately telling the former the outcome (so when is the collapse?). If Pauli’s remark of Chap. 5 were right, though, something like telekinesis “outside the laws of nature” would indeed have to create the measurement result at Bob’s place in the case of an initial nonlocal Bell state. The term “quantum information” instead of entanglement is therefore quite misleading: entanglement must be part of quantum reality – even though it may often become indistinguishable from a statistical correlation in practice.

Alice would need a similar initial Bell-type superposition of the kind

$$|CK\rangle_A|noCK\rangle_B - |noCK\rangle_A|CK\rangle_B \quad (10)$$

in order to “beam” Captain Kirk (CK) from her to Bob’s place, provided he *could* be shielded against decoherence until she either “measures” his absence at her place or else sends Bob a message to perform a unitary transformation that leads to  $|CK\rangle$ . (This hypothetical isolation of (10) would indeed permit the existence of a local Schrödinger cat state  $|CK\rangle \pm |noCK\rangle$ .) However, the Captain Kirk who is then found at Bob’s place could not be one who knows what happened at Alice’s place *after* the preparation of the initial Bell state. You would need a tremendously more complex entangled state, that had to contain *all possibilities* as part of its nonlocal quantum reality, in order to decide later *what* to beam. The term “quantum teleportation” drastically misleads the public and should in my opinion not be used by serious scientists. There is enough genuine weirdness that quantum theory has to offer!

In practice, most nonlocal states (except for entanglement between very weakly interacting subsystems, such as photons or neutral spins) would immediately be irreversibly destroyed (that is, become uncontrollable) by decoherence. The apparent locality of our classical world is therefore the consequence of its drastic nonlocality: classical “facts” (or events) *appear* to be local, although they arise precisely by the dislocalization of superpositions. Hypothetical local (classical) variables which have not been measured are then often regarded as “counterfactuals” (but not rejected as potential concepts even though they *would* contradict

experimental results!), while the nonlocal concepts (superpositions) which successfully describe all these irreversible processes dynamically are simply dismissed as “not conceivably representing reality”.

## 7. Information loss (paradox?)

The collapse of the wave function (without observing the outcome) or any other *indeterministic* process would represent a dynamical information loss, since a pure state is transformed into an ensemble of possible states (described by a proper mixture, for example). The dislocalization of quantum mechanical superpositions, on the other hand, leads to an *apparent* information loss, since the relevant phase relations merely become irrelevant for all practical purposes of local observers. I will now argue that the “information loss paradox of black holes” (Hawking’s lost bet) is precisely based on this decoherence (or otherwise on the collapse of the wave function), and *not* a specific property of black holes.

For a better understanding one may first consider irreversible processes in classical mechanics, such as Boltzmann’s molecular collisions (see Chap. 9). Since they are based on deterministic dynamics (in analogy to quantum unitarity), *ensemble entropy* is here conserved. However, collisions lead to the formation of uncontrollable statistical correlations, which are irrelevant FAPP in the future. (They are important, though, for the correct backward dynamics because of the specific cosmic initial condition that has to be assumed for this Universe.) This apparent loss (namely, the dislocalization) of *information* in this classical case affects *physical entropy*, since this entropy concept disregards *by definition* the arising uncontrollable correlations [8]. It is defined as an extensive (additive) quantity, usually in terms of “representative ensembles” characterizing the local macroscopic variables, while microscopic (the *real*) states – including those of subsystems – are objectively determined in principle by the global initial conditions because of the presumed classical mechanical laws. In contrast, quantum mechanical subsystems possess non-vanishing objective entropy (described by improper mixtures) even for a completely defined global state.

In general relativity (GR), “information” may disappear when physical objects fall onto a spacetime singularity, but in classical physics the real state of external matter would still exist and remain determined. In contrast, for *quantum* mechanics on a classical spacetime, the information loss would have to include all existing entanglement with external matter, thus transforming the latter’s improper mixture into a proper one. This conclusion seems to remain true when the black hole disappears by means of Hawking radiation, and this has been regarded as a paradox, since it would violate unitarity.

One may consider the spacetime geometry of a black hole in Kruskal-type coordinates (see Figure 1). Simultaneities used by external observers in asymptotically flat spacetime (such as Minkowski time coordinates in the black hole’s rest system) can here be continued towards the center of the spherical black hole in

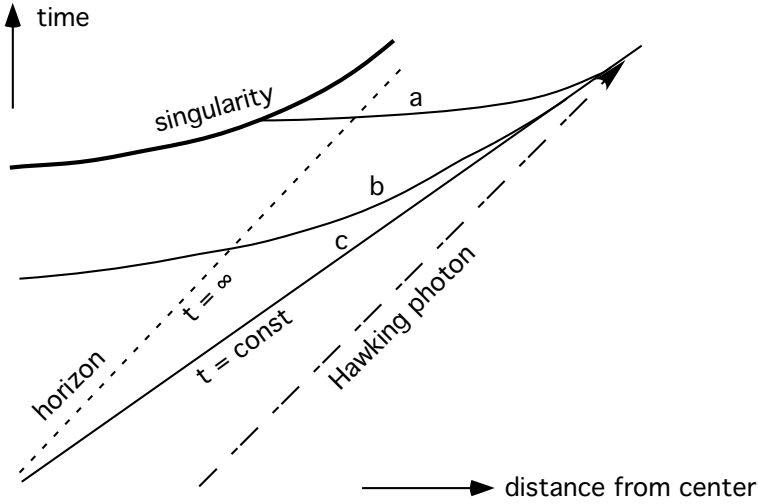


FIGURE 1. Various simultaneities for a spherical black hole in a Kruskal type diagram: (a) hitting the singularity, (b) entering the regular interior region only, (c) completely remaining outside (Schwarzschild time coordinate  $t$ ). Light cones open everywhere at  $\pm 45^\circ$  around the vertical time axis in this diagram, while lengths are strongly distorted. Schwarzschild time is appropriate in particular for posing external boundary conditions. The angle between the horizon and the line  $t = \text{const}$  can here be arbitrarily changed by a passive time translation. This includes the (apparently close) vicinity of the horizon, which can thus be arbitrarily “blown up” in the diagram – thus transforming *any* Schwarzschild time into the horizontal line  $t = 0$ , for example.

different arbitrary ways. If everywhere chosen according to the Schwarzschild time coordinate  $t$ , for example, they would never intersect the horizon, but this choice does *not* affect the density matrix representing the region far from the horizon (far right in the Figure). The information loss noticed by an external observer can therefore not be *caused* by the singularity – no matter how long he waits. Not even the horizon ever enters his past, and thus never becomes a “fact” for him, while the Hawking radiation which he may observe would originate earlier in Schwarzschild time than the horizon. Because of the singular time dilation, the close vicinity of the horizon can causally affect only the very distant future, since superluminal effects are excluded in spite of quantum nonlocality (cf. Chap. 6).

On the other hand, a macroscopic black hole is permanently affected by various kinds of decoherence [28] – most importantly by means of its retarded radiation. So this quantum radiation must be highly entangled with the remaining black hole, and therefore with all radiation that is emitted later [29]. If usable

information about the black hole is stored in the external world (such as in the form of emitted light), it defines separate Everett branches. While the unitary dynamics determines the later global quantum state uniquely, it does *not* determine an observer's branch: the present state of an observer will have *many* successors in the future. Any confirmation of the black hole's unitary dynamics would thus require the complete recovery of coherence, including the recombination of Everett worlds – just as it would be required to demonstrate unitarity for *all* macroscopic objects. In practice, their evolution is irreversible. This means that the answer to Hawking's bet has nothing specifically to do with black holes [30].

The spacetime metric with its event horizons and singularities may be assumed to be “real and certain” only in classical GR. In quantum gravity, even the spacetime geometry on which simultaneities are to be defined has to be replaced by an entangled quantum state of matter and geometry [31, 11]. *All* macroscopic properties are thereby decohered and have to be associated with separate Everett worlds. The Wheeler-DeWitt wave function  $\Psi^{[3G, \phi_{matter}]}$  (or its generalization to unified theories), which describes their global superposition, defines “probability amplitudes” on *all* simultaneities (not just on those forming one geometro-dynamic history, that is, a specific foliation of spacetime).

This timeless wave function has to obey certain *timeless* boundary conditions; it cannot distinguish between past and future singularities [32]. For example, these conditions may exclude local singularities (or those with non-vanishing Weyl tensor), or just any entanglement between them and regular regions. This would strongly affect the wave function on all spatial geometries which intersect a black hole horizon, and induce effects corresponding to apparent final conditions. The WKB approximation, which allows quasi-classical spacetime (hence proper times) to *emerge* by means of the process of decoherence, may then completely break down in such regions of configuration space [33], while the classical spacetime diagram of Figure 1 would lose its meaning close to the horizon.

However, this need *not* affect quasi-classical solutions restricted to Schwarzschild simultaneities (the external part of the black hole). In particular, Bekenstein's black hole entropy is a *general* result derived in this region, that cannot be used to confirm *specific* models of quantum gravity, such as string theory.

## 8. Dynamics of entanglement

The entangled state of any two quantum systems, if assumed to be pure, can always be written as a single sum in the *Schmidt canonical form* [34]

$$\psi = \sum_i \sqrt{p_i} \phi_i \Phi_i \quad , \quad (11)$$

where the states  $\phi_i$  and  $\Phi_i$  forming the two bases are *determined* (up to linear combinations between degenerate coefficients) by the total state  $\psi$ . The coefficients can be chosen real and positive by an appropriate choice of phases for the states forming the Schmidt bases, and have therefore been written in the form  $\sqrt{p_i}$ .

In contrast to Equ. (1), the states  $\Phi_i$  are now assumed to be orthogonal: the expansion (11) is thus in general different from the right hand side of (1). This Schmidt representation determines the reduced density matrices in their diagonal form

$$\begin{aligned}\rho_\phi &= \sum_i |\phi_i\rangle p_i \langle \phi_i| \quad , \\ \rho_\Phi &= \sum_i |\Phi_i\rangle p_i \langle \Phi_i| \quad .\end{aligned}\tag{12}$$

Since all systems must be assumed to be entangled with their environments, the second system has in principle always to be understood as the “rest of the universe” in order to represent a realistic situation.

If the total state  $\psi$  depends on time, the bases  $\phi_i$  and  $\Phi_i$  and the coefficients  $\sqrt{p_i}$  must carry a separate time dependence, which is determined, too, by that of the global state  $\psi(t)$ . It can be explicitly described [15] by

$$\begin{aligned}\frac{d\sqrt{p_i}}{dt} &= Im \sum_j \sqrt{p_i} \langle ii | H | jj \rangle \\ i \frac{d\phi_i}{dt} &= \sum_{j \neq i} (p_i - p_j)^{-1} \sum_m \sqrt{p_m} [\sqrt{p_i} \langle ji | H | mm \rangle - \sqrt{p_i} \langle mm | H | ij \rangle] \phi_j \\ i \frac{d\Phi_i}{dt} &= \sum_{j \neq i} (p_i - p_j)^{-1} \sum_m \sqrt{p_m} [\sqrt{p_i} \langle ij | H | mm \rangle - \sqrt{p_i} \langle mm | H | ji \rangle] \Phi_j \\ &\quad + \sqrt{p_i} Re \sum_m \sqrt{p_m} \langle ii | H | mm \rangle \Phi_i \quad .\end{aligned}\tag{13}$$

The asymmetry between the two subsystems described by  $\phi$  and  $\Phi$  is here due to an asymmetric phase convention. It could be avoided by a different choice [35].

In classical physics, subsystems would evolve deterministically, controlled by time-dependent Hamiltonians which would depend on the state of the other system (thus forming coupled deterministic dynamics). This classical picture of time-dependent Hamiltonians is often, not very consistently, used also in quantum mechanics – for example in the form of perturbing “kicks” instead of genuine quantum interactions. However, an effective Hamiltonian depending on the state of the environment would require a separately existing state of this environment. In contrast, Eqs. (13) define highly nontrivial (not practically usable) nonunitary subsystem dynamics. For this reason, the “probabilities”  $p_i$  and the entropy  $\sum p_i \ln p_i$  defined by them must usually change in time. In particular, initially separating systems will become entangled.

Although Eqs. (13) define a continuous evolution separately for each term of the Schmidt representation, this dynamics seems to be singular whenever two diagonal elements  $p_i$  of the density matrix become equal. Closer inspection of the dynamics reveals that two eigenvalues coming close repel each other (unless the corresponding matrix elements of the Hamiltonian vanish exactly), and therefore never intersect as functions of time (see Figure 2). Thereby, the quasi-singular

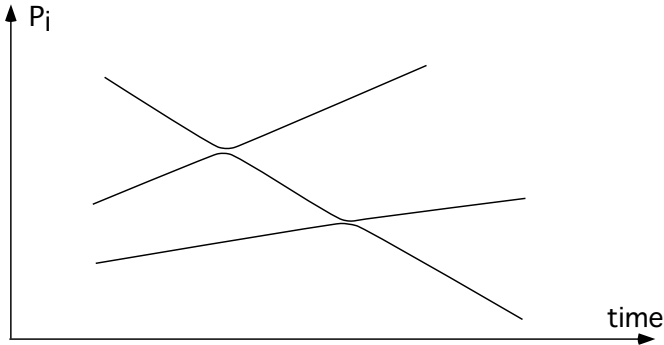


FIGURE 2. Trajectories of different probabilities  $p_i(t)$  repel each other, while their corresponding factorizing Schmidt components interchange their identity (including all memories). Causal histories of Schmidt components thus intersect in this diagram, although they never touch. This effect may also be regarded as a pure artifact of the Schmidt representation.

dynamics (13) of the states forces the latter to interchange their identity within a very short time. In other words: degenerate probabilities (such as in exact Bell states!) can never occur, while the formal continuity of Schmidt components in Figure 2 is entirely unphysical (not representing any preserved identity of states). Subsystem density matrices are *not* affected by this phenomenon, since the resonance terms are a consequence of the ambiguity of their degenerate eigenstates. The non-unitary dynamics of entangled density matrices can implicitly (that is, depending on the solutions of (13)) be written as [36]

$$\begin{aligned}
 i \frac{d\rho_\Phi}{dt} &:= i \frac{d \sum p_i \Phi_i \Phi_i^*}{dt} \\
 &= \sum_{i,j} (\sqrt{p_i} \langle ij | H | \psi \rangle - \sqrt{p_j} \langle \psi | H | ji \rangle) \Phi_i \Phi_j^* \quad . \quad (14)
 \end{aligned}$$

Initially separating (factorizing) states are of special interest for the process of decoherence. While this assumption enforces an initial degeneracy to exist between all vanishing probabilities, the initial component with  $p_0 = 1$  would at least quadratically depend on time because of the time reversal symmetry of the global Schrödinger equation. In this small-times approximation its precise form can be derived by means of perturbation theory as

$$p_0(t) \approx 1 - t^2 A \quad , \quad (15)$$

where the quantity

$$A = \sum_{j \neq 0, m \neq 0} |\langle jm | H | 00 \rangle|^2 \quad (16)$$

has been called a *deseperation parameter*. It measures the arising entanglement (that is, the growing deviation from separating states). Index pairs  $jm$  here refer to product states  $\phi_j\Phi_m$ . Note that  $A$  is different from the quantity

$$B = \sum_{jm \neq 00} |\langle jm|H|00\rangle|^2 \geq A \quad , \quad (17)$$

which measures the *total* change of the global state in this approximation (including the “classical” change characterizing a time-dependent product). If the environment and the interaction Hamiltonian  $H$  are given, the deseperation parameter  $A$  can be used to estimate the robustness of certain states against decoherence. For example, coupled harmonic oscillators turn out to be robust when in coherent states (such as in states describing classical fields), while their energy eigenstates (such as photon number eigenstates) are unstable against decoherence [15] (a result that was later confirmed in [37]).

## 9. Irreversibility

The dynamics of entanglement, derived from a global Schrödinger equation and discussed in the preceding chapter, is time reversal invariant. An asymmetry may be introduced by assuming *initially* separating states, for example by using Equ. (15) exclusively for  $t > 0$ . However, if one of the two systems is indeed the “rest of the universe”, this assumption can be exact only once (such as at the big bang), although similar assumptions may then *approximately* apply later, too, in particular for dynamically autonomous Everett components after they have branched off (or, alternatively, after a time-asymmetric collapse).

A similar situation of special initial conditions is known to be required for irreversible processes in general. For example, Boltzmann collisions are assumed to affect initially uncorrelated single particle distributions (defined in  $\mu$ -space), although correlations must have built up ever since the big bang. The point here is that these correlations remain irrelevant in the future because of the chaotic nature of these classical systems and the enormous lengths of their Poincaré recurrence times – reflecting a very large information capacity of correlations. Decoherence produced by scattering of photons or molecules [6] is analogous to Boltzmann’s entropy production by means of molecular collisions, while coupled oscillators, which have often been used to study decoherence [38], may be useful because of their analytical solutions, but are known to possess pathological properties: they are not *mixing* in a thermodynamical sense if treated as closed systems. Similar arguments apply to systems consisting of interacting spins, which may better be regarded as representing *virtual* decoherence – in strong contrast to systems which would classically show chaotic behavior [39].

In quantum theory, reversibility would not even hold in principle in the case of a genuine stochastic collapse of the wave function. If the Schrödinger equation is instead assumed to be universally exact, recoherence of different Everett branches would have to be taken into account in order to facilitate reversibility. This can

be excluded FAPP (just as the reversal of any other macroscopic arrow of time), and it is therefore neglected in the usual description of phenomena by means of irreversible master equations, for example.

This general mechanism of irreversible dynamics was elegantly formulated by Zwanzig [40] by means of idempotent operators  $P$  acting either on classical statistical probability distributions or on density matrices  $\rho$ . These “Zwanzig projectors” need neither be linear nor hermitean. They are chosen to formalize the neglect of an appropriate kind of “irrelevant information”. Idempotence ( $P^2 = P$ ) means that throwing away the same information twice at the same time does not add anything to doing it once. One should keep in mind, however, that density matrices usually represent improper mixtures, such that a dynamically applied Zwanzig projection includes collapse dynamics, while it would merely represent dynamical mixing for statistical distributions.

A linear Zwanzig projection is given by tracing out the environment,

$$\rho_{\text{rel}} = P_{\text{sub}}\rho = \rho^{(\phi)} = \text{Trace}_{\Phi}\rho \quad , \quad (18)$$

while a nonlinear one may merely neglect correlations between the two subsystems,

$$\rho_{\text{rel}} = P_{\text{sep}}\rho = \rho^{(\phi)}\rho^{(\Phi)} = \text{Trace}_{\Phi}\rho \text{Trace}_{\phi}\rho \quad . \quad (19)$$

There are many other applications of this very general concept, which can also be regarded as a *generalized coarse graining*. For example, one may just neglect quantum correlations (entanglement), while leaving all classical correlations intact. As another example, Boltzmann’s *Stoßzahlansatz* neglects dynamically all arising statistical correlations between particles.

Zwanzig projectors are useful, in particular, since they often allow the formulation of an effective (approximately autonomous) dynamics for  $\rho_{\text{rel}}$ . This requires the special initial, but approximately maintained, condition  $\rho_{\text{irrel}} \approx 0$ , which may lead to a master equation of the form

$$\frac{d\rho_{\text{rel}}}{dt} = -G_{\text{rel}}\rho_{\text{rel}} \quad , \quad (20)$$

applicable in the forward direction of time.  $G_{\text{rel}}$  must be a positive operator, acting on the density matrix, in order to describe an entropy increase (loss of information). The entropy is here defined by

$$S = -k_B \text{Trace}[\rho_{\text{rel}} \ln \rho_{\text{rel}}] \quad . \quad (21)$$

This dynamics is schematically depicted in Figure 3 (cf. Chap. 3 of [8]), where relevant information is permanently lost to the “irrelevant channel”. For the Zwanzig projector  $P_{\text{sep}}$  this process describes the production of entropy by means of decoherence, while for  $P_{\text{sub}}$  it would include an information transfer from the system to the environment (that is, an entropy transfer from the environment to the system – usually attributed to heat or noise). The “doorway channel” in this picture describes irrelevant degrees of freedom which can directly interact with the relevant channel. In the case of entanglement, it corresponds to virtual decoherence. Note, however, that, for these quantum Zwanzig projectors,  $\rho_{\text{rel}}$  includes an apparent

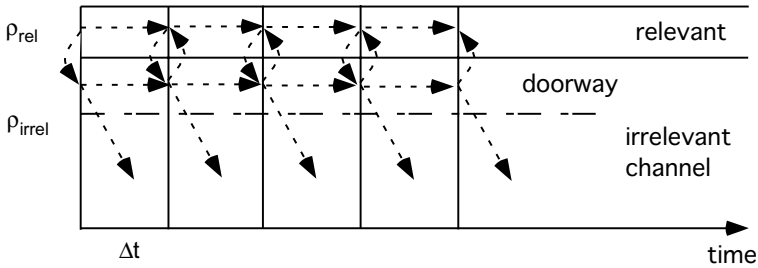


FIGURE 3. Propagation of “information” contained in the statistical distribution or density matrix  $\rho$  for the case  $\rho_{irrel}(t = 0) = 0$ . It propagates through two coupled “channels” (relevant and irrelevant – see also Figs. 3.2–3.4 of [8]). Intervals  $\Delta t$  characterize steps of integration for the coupling  $PH(1 - P) + (1 - P)HP$  in the interaction representation. The entropy, defined in terms of  $\rho_{rel}$ , grows irreversibly FAPP if relevant information disappears into the irrelevant channel for very long Poncaré times (usually by far exceeding the age of the universe). This may allow the formulation of master equations for  $\rho_{rel}$ . If the irrelevant channel describes entanglement, the irreversible loss represents real decoherence, while the “doorway channel”, which is part of the irrelevant channel, corresponds to virtual decoherence.

(improper) ensemble of different Everett “worlds”, since their superposition has been dislocalized (become irrelevant to local observers). This means that the formal entropy  $S[\rho_{rel}]$  contains not only physical entropy, but also the “entropy of lacking information” about the outcomes of all measurements or spontaneous symmetry breakings. Physical entropy is defined as a *function* of these macroscopic quantities. Definite macroscopic (classical) histories in quantum mechanical description are thus based on a collapse or branching of the wave function, while classically they merely require the *selection of subensembles*, which represent incomplete information (“ignorance”) about the real physical states. Such a selection is required in order to describe individual macroscopic histories whenever microscopic causes have macroscopic effects. In quantum theory, this “selection” corresponds to a genuine quantum measurement.

Explicit models for the irreversible process of decoherence and their consequences are discussed in the accompanying paper by Erich Joos.

## 10. Concluding remarks

To conclude, let me emphasize that the concept of decoherence does not contain any new physical laws or assumptions beyond the established framework of quantum theory. Rather, it is a consequence of the universal application of quantum concepts (superpositions) and their unitary dynamics.

However, a consistent interpretation of this theory in accordance with the observed world requires a *novel and nontrivial identification of observers* with appropriate quantum states of local systems which exist only in certain, dynamically autonomous *components* of the global wave function. Accordingly, it is the observer who “splits” indeterministically – not the (quantum) world.

This interpretation is an attempt to replace the “pragmatic irrationalism” that is common in quantum theory textbooks (complementarity, dualism, uncertainty etc.) by a consistent application of those concepts which are actually, and without restriction or exception *successfully*, used when the theory is applied.

**Acknowledgements:** I wish to thank Erich Joos and Claus Kiefer for their collaboration over many years, for their persisting interest in the subject, and for their critical comments on the manuscript of this contribution.

## References

- [1] M. Brune, E. Hagley, J. Dreyer, X. Maître, Y. Moali, C. Wunderlich, J.M. Raimond, and S. Haroche, *Phys. Rev. Lett.* **77** (1996), 4887.
- [2] M. Arndt, O. Nairz, J. Vos-Andreae, C. Keller, G. van der Zouw, and A. Zeilinger, *Nature* **401** (1999), 680 .
- [3] M. Schlosshauer, *Rev. Mod. Phys.* **76** (2004), 1267 ; *Ann. Phys. (N.Y.)*, to be published – quant-ph/0506199.
- [4] G. Bacciagaluppi, <http://plato.stanford.edu/entries/qm-decoherence/>.
- [5] H.D. Zeh in: *Science and Ultimate Reality*, J.D. Barrow, P.C.W. Davies, and C.L. Harper, eds. (Cambridge UP 2004) – quant-ph/0204088.
- [6] E. Joos and H.D. Zeh, *Z. Phys.* **B59** (1985), 223 .
- [7] E. Joos, H.D. Zeh, C. Kiefer, D. Giulini, J. Kupsch, and I.-O. Stamatescu, *Decoherence and the Appearance of a Classical World in Quantum Theory*, 2nd edn. (Springer, Berlin 2003).
- [8] H.D. Zeh, *The Physical Basis of the Direction of Time*, 4th edn. (Springer, Berlin 2001); see also [www.time-direction.de](http://www.time-direction.de).
- [9] B. d’Espagnat, in: *Preludes in theoretical physics*, A. De-Shalit, H. Feshbach, and L. van Hove, eds. (North-Holland, Amsterdam 1966).
- [10] H.D. Zeh, *Z. Phys.* **202** (1967), 38 ; see also Chap. 9 of [7].
- [11] H.D. Zeh, *Phys. Lett.* **A116** (1986), 9 ; **A126** (1988), 311 .
- [12] W.H. Zurek, *Phys. Today* **44** (Oct.) (1991), 36 .
- [13] M. Gell-Mann and J.B. Hartle, *Phys. Rev.* **D47** (1993), 3345 .

- [14] H.D. Zeh, *Found. Phys.* **1** (1970), 69 .
- [15] O. Kübler and H.D. Zeh, *Ann. Phys. (N.Y.)* **76** (1973), 405 .
- [16] E. Schrödinger, *Proc. Cambridge Phil. Soc.* **31** (1935), 555 .
- [17] R. Omnès, *Phys. Rev.* **D 71** (2005), 065011 – quant-ph/0411201.
- [18] O. Ulfbeck and A. Bohr, *Found. Phys.* **31** (2001), 757 .
- [19] J.S. Bell, *Speakable and Unspeakable in Quantum Mechanics* (Cambridge UP 1987).
- [20] J.M. Jauch, *Foundations of Quantum Mechanics* (Addison Wesley, Reading Mass. 1968).
- [21] E. Joos, *Phys. Rev.* **D29** (1984), 1626 ; see also Chap. 3 of [7].
- [22] W.H. Zurek, *Phys. Rev.* **D24** (1981), 1516 ; dto. **D26** (1982), 1862.
- [23] G. Lüders, *Ann. Phys. (Leipzig)* **8** (1951), 322 .
- [24] N. Graham, *The Everett Interpretation of Quantum Mechanics* (Univ. North Carolina, Chapel Hill 1970).
- [25] B. d’Espagnat, ed., *Foundations of Quantum Mechanics* (49th Enrico Fermi School, Varenna), (Academic Press, New York 1971).
- [26] J.S. Bell, *Physics* **1** (1964), 195 .
- [27] A. Peres, *Phys. Rev. Lett.* **77** (1996), 1413 ; V. Vedral, M.B. Plenio, M.A. Rippin, and P.L. Knight, *Phys. Rev. Lett.* **78** (1997), 2275.
- [28] J.-G. Demers, and C. Kiefer, *Phys. Rev.* **D53** (1996), 7050 .
- [29] D.N. Page, *Phys. Rev. Lett.* **44** (1980), 301 .
- [30] H.D. Zeh, *Phys. Lett.* **A 347** (2005), 1 – gr-qc/0507051; C. Kiefer, gr-qc/0508120.
- [31] E. Joos, *Phys. Lett.* **A116** (1986), 6 .
- [32] H.D. Zeh, in: *Physical Origins of the Asymmetry of Time*, J.J. Halliwell, J. Perez-Mercader, and W.H. Zurek, eds. (Cambridge UP 1994).
- [33] C. Kiefer and H.D. Zeh, *Phys. Rev.* **D51** (1995), 4145 ; C. Kiefer, *Quantum Gravity*, (Clarendon Press, Oxford 2004).
- [34] E. Schmidt, *Math. Annalen* **63** (1907), 433 .
- [35] Ph. Pearle, *Int. J. Theor. Phys.* **18** (1979), 489 .
- [36] H.D. Zeh, *Found. Phys.* **3** (1973), 109 – quant-ph/0306151.
- [37] W.H. Zurek, S. Habib, and J.P. Paz, *Phys. Rev. Lett.* **70** (1993), 1187.
- [38] A.O. Caldeira and A.J. Leggett, *Physica* **121A** (1983 ), 587.
- [39] W.H. Zurek and J.P. Paz, *Phys. Rev. Lett.* **72** (1994), 2508 ; *Nuovo Cim.*, **110B** (1995), 611 .
- [40] R. Zwanzig, *Boulder Lectures in Theoretical Physics* **3** (1960), 106.

H. Dieter Zeh  
 Universität Heidelberg  
 Gaiberger Str. 38  
 D-69151 Waldhilsbach  
 Germany  
 e-mail: zeh@urz.uni-heidelberg.de

# Dynamical Consequences of Strong Entanglement

Erich Joos

**Abstract.** The concept of motion in quantum theory is reviewed from a didactical point of view. A unitary evolution according to a Schrödinger equation has very different properties compared to motion in classical physics. If the phase relations defining unitary dynamics are destroyed or unavailable, motion becomes impossible (Zeno effect). The most important mechanism is delocalization of phase relations (decoherence), arising from coupling of a quantum system to its environment. Macroscopic systems are not frozen, although strong decoherence is important to derive quasi-classical motion within the quantum framework. These two apparently conflicting consequences of strong decoherence are analyzed and compared.

## 1. Introduction

It seems to be widely accepted by now that non-classical states of macroscopic objects can never show up in the laboratory or elsewhere since they are unstable against decoherence. This explains superselection rules, that is, kinematical restrictions in the space of all quantum states allowed by the superposition principle. The observation that macroscopic objects are under “continuous observation” by their natural environment paved the way for our current understanding of the quantum-to-classical transition [1].

Since in a consistent quantum treatment macro-objects are obviously to be considered as open systems, their dynamics can longer follow a Schrödinger equation. This alone invalidates the textbook “derivations” of the classical limit via Ehrenfest theorems. Instead, one has to study the consequences of strong measurement-like interaction of the considered system with its environment. The resulting entanglement not only superselects certain states, which are then called “classical” by definition, but also leads to dynamical consequences. Very simple arguments seem to show that strong decoherence, that is, strong entanglement, leads to slowing down of the dynamics of *any* system. However, the objects in our

macroscopic world obviously *are moving* and there seems to be no “Zeno effect”. How this puzzle can be solved will be discussed in the following sections.

## 2. The quantum Zeno effect

The quantum Zeno effect was discovered independently by several authors when studying the properties of decay probabilities in quantum theory. The now popular term “quantum Zeno effect” was introduced by Misra and Sudarshan [2].

Let a system be described by some “undecayed” state  $|\Psi(0)\rangle = |u\rangle$  at some initial time  $t = 0$ . The probability  $P(t)$  to find it again in this “undecayed” state at a later time  $t$  is

$$P(t) = |\langle u | e^{-iHt} | u \rangle|^2 \quad (1)$$

where  $H$  is the Hamiltonian of the system. For small times we can expand  $P(t)$ , yielding

$$P(t) = 1 - (\Delta H)^2 t^2 + O(t^4) \quad (2)$$

with

$$(\Delta H)^2 = \langle u | H^2 | u \rangle - \langle u | H | u \rangle^2. \quad (3)$$

The important feature to notice here is the *quadratic* time dependence of the survival probability. This may be compared with the usual exponential decay law

$$P(t) = \exp(-\Gamma t), \quad (4)$$

which leads to a *linear* time dependence for small times,

$$P(t) = 1 - \Gamma t + \dots \quad (5)$$

This raises the question, how these two differing results can be made compatible. Both look fundamental, but they obviously contradict each other. This conflict can be made even stronger, when we consider the case of repeated measurements in a short time interval.

Suppose we repeat the measurement  $N$  times during the interval  $[0, t]$ . Then the non-decay (survival) probability according to Equ. (2) is

$$P_N(t) \approx \left[ 1 - (\Delta H)^2 \left( \frac{t}{N} \right)^2 \right]^N > P(t), \quad (6)$$

which for large  $N$  gives

$$P_N(t) = 1 - (\Delta H)^2 \frac{t^2}{N} + \dots \xrightarrow{N \rightarrow \infty} 1. \quad (7)$$

This is the Zeno effect: Sufficiently dense measurements should halt any motion!

There is no Zeno effect if the system decays according to the exponential decay (4) law, since in this case trivially

$$P_N(t) = \left( \exp \left( -\Gamma \frac{t}{N} \right) \right)^N = \exp(-\Gamma t) = P(t). \quad (8)$$

The conclusion is that any system showing a quadratic short-time behavior is very sensitive to measurements, whereas an exponentially decaying system does not care about whether its decay status is measured or not, that is, it behaves classically in this respect.

If a system is governed by the Schrödinger equation, as used in Equ. (1), the transition probability for small times *must* start quadratically, hence the exponential decay law can only be an approximation for larger times.<sup>1</sup> What happens in the limit of “continuous” observation? The Zeno argument seems to show that there will be no motion at all!

To gain a better understanding of what is going on here, I will discuss in the following why motion is slowed down by measurements. In addition, the measurement process itself will be described by a unitary evolution following the Schrödinger equation as the fundamental law of motion for quantum states. It will turn out, that the Zeno effect can be understood as a unitary dynamical process and the collapse of the wave function is not required.

### 3. Interference, Motion and Measurement in Quantum Theory

Why does measurement slow down motion in quantum theory, but not in classical physics? The reason can be traced back to the very nature of quantum evolution. Quantum dynamics is unitary and can be viewed as a rotation in Hilbert space, see Fig. 1. If the Hamiltonian describes a direct unitary transition between two

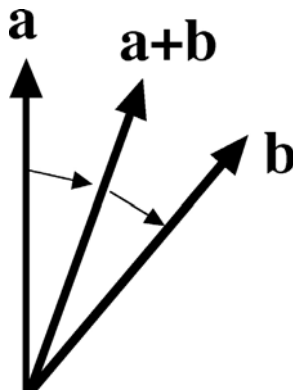


FIGURE 1. Evolution in quantum theory can be viewed as a rotation connecting an initial state  $|a\rangle$  with a final state  $|b\rangle$ . For direct transitions, at intermediate times superpositions such as  $|a\rangle + |b\rangle$  (neglecting normalization) are required for undisturbed motion.

<sup>1</sup>There is a certain irony in this situation, since – at least in popular accounts – exponential (“random”) decay is used as a major argument that classical physics has to be replaced by a new (quantum) theory. But there is no strictly exponential decay law in quantum theory.

states  $|a\rangle$  and  $|b\rangle$ , the system has to go through a sequence of superposition states  $\alpha(t)|a\rangle + \beta(t)|b\rangle$ . An essential feature of such a superpositions is the presence of interference (coherence). As is well known, such a superposition has properties which none of its components has – it is an entirely new state.<sup>2</sup> Unitary evolution from  $|a\rangle$  to  $|b\rangle$  requires all the phase relations contained in the intermediate states  $\alpha|a\rangle + \beta|b\rangle$ . Phase relations are destroyed by measurements, so it is not surprising that motion becomes impossible in quantum theory if coherence is completely absent!

As an example consider the evolution of a two-state system from an initial state  $|1\rangle$  as a two-step process connecting times 0,  $t$ , and  $2t$ , as shown in Fig. 2. If

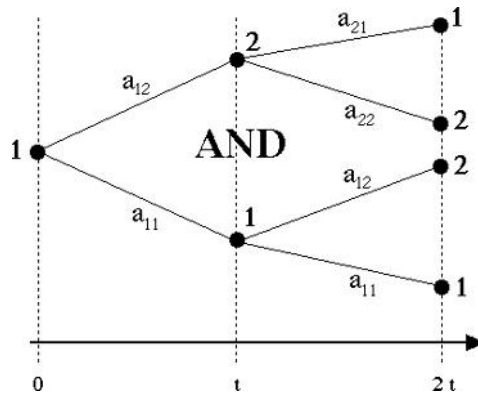


FIGURE 2. Evolution of a two-state system away from initial state  $|1\rangle$ . The amplitude (and therefore the probability) of state  $|2\rangle$  at time  $2t$  depends on the phases contained in the superposition of  $|1\rangle$  and  $|2\rangle$  at the intermediate time  $t$ , as in a double-slit experiment.

$a_{ij}$  are transition amplitudes (calculated from the Schrödinger equation) we have the chain

$$\begin{aligned}
 t = 0 : & \quad |1\rangle \\
 & \longrightarrow a_{11} |1\rangle + a_{12} |2\rangle \\
 & \longrightarrow (a_{11}^2 + a_{12}a_{21}) |1\rangle + (a_{12}a_{22} + a_{11}a_{12}) |2\rangle .
 \end{aligned} \tag{9}$$

The final probability for state  $|2\rangle$  at time  $2t$  is then

$$P_2 = |a_{12}a_{22} + a_{11}a_{12}|^2 . \tag{10}$$

To study the Zeno effect we are interested in the behavior of  $P_2$  for small times. In this limit it is given by

$$P_2 \approx |V|^2 (2t)^2 \quad \text{with} \quad V = \langle 1|H|2\rangle . \tag{11}$$

---

<sup>2</sup>This is the reason why stochastic models for quantum evolution are unsuccessful: A superposition cannot be replaced by an ensemble of its components.

Clearly the value for  $P_2$  depends essentially on the presence of interference terms. In a sense unitary evolution is an ongoing double- (or multi-)slit experiment (without ever reaching the screen)!<sup>3</sup>

Now compare this evolution with the same process, when a measurement is made at the intermediate time  $t$ . This measurement may either be described by a collapse producing an ensemble (that is, resulting in  $|1\rangle$  or  $|2\rangle$ ), or dynamically by coupling to another degree of freedom. In the latter case an entangled state

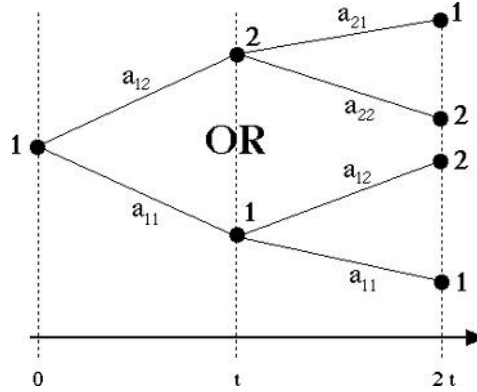


FIGURE 3. Evolution of a two-state system with measurement. The probability for state  $|2\rangle$  at time  $2t$  results solely from the transition probabilities to intermediate states at time  $t$ . The loss of phase relations leads to a decrease of the total transition probability.

containing the system and the measuring device  $|\Phi\rangle$  (or, generally, the system's environment) ensues (more on this in the next section). The equations now look like

$$\begin{aligned}
 t = 0 : & \quad |1\rangle |\Phi\rangle \\
 \longrightarrow & \quad (a_{11} |1\rangle + a_{12} |2\rangle) |\Phi\rangle \\
 \longrightarrow & \quad a_{11} |1\rangle |\Phi_1\rangle + a_{12} |2\rangle |\Phi_2\rangle \\
 \longrightarrow & \quad (a_{11}^2 |\Phi_1\rangle + a_{12} a_{21} |\Phi_2\rangle) |1\rangle + (a_{12} a_{22} |\Phi_1\rangle + a_{11} a_{12} |\Phi_2\rangle) |2\rangle
 \end{aligned} \tag{12}$$

(the third line describes the new measurement step) and the transition probability is given by

$$\begin{aligned}
 P_2 &= |a_{12} a_{22}|^2 + |a_{11} a_{12}|^2 \\
 &\approx \frac{1}{2} |V|^2 (2t)^2.
 \end{aligned} \tag{13}$$

<sup>3</sup>Obviously, the above model is nothing more than a very primitive version of the path-integral formalism.

Since the interference terms are missing, we lose half of the probability! Clearly then, if we divide the time interval not in two but into  $N$  steps the transition probability is reduced by a factor  $1/N$ : the Zeno effect. This reduction is a sole consequence of entanglement without any “disturbance” of the measured system, since the measurement is assumed ideal in this model. No coherence, no motion!

The Zeno effect can also be seen more formally from the von Neumann equation for the density matrix. If coherence is absent in a certain basis, the density matrix is diagonal, i.e.,

$$\rho_{nm} = \rho_{nn}\delta_{nm}. \quad (14)$$

But then no evolution is possible, since the von Neumann equation immediately yields

$$\frac{d}{dt}\rho_{nn} = \sum_k (H_{nk}\rho_{kn} - \rho_{nk}H_{kn}) \equiv 0. \quad (15)$$

#### 4. Measurement as a Dynamical Process: Decoherence

To further analyze the Zeno effect I will consider a specific model for measurements of an  $N$ -state system. As a preparation, let me shortly review the dynamical description of a measurement process. In a dynamical description of measurement, the well-known loss of interference during measurement follows from a certain kind of interaction between a system and its environment.

Following von Neumann, consider an interaction between an  $N$ -state system and a “measurement device” in the form

$$|n\rangle |\Phi_0\rangle \longrightarrow \exp(-iHT) |n\rangle |\Phi_0\rangle = |n\rangle |\Phi_n\rangle \quad (16)$$

where  $|n\rangle$  are the system states to be discriminated by the measurement device and  $|\Phi_n\rangle$  are “pointer states” telling which state of the system has been found.  $H$  is an appropriate interaction leading after the completion of the measurement (at time  $T$ ) to orthogonal states of the measuring device. Since in Equ. (16) the system state is not changed, this measurement is called “ideal” (recoil-free). A general initial state of the system will – via the superposition principle – lead to an entangled state,

$$\left( \sum_n c_n |n\rangle \right) |\Phi_0\rangle \longrightarrow \sum_n c_n |n\rangle |\Phi_n\rangle. \quad (17)$$

This correlated state is still pure and does therefore *not* represent an ensemble of measurement results (therefore such a model alone does not solve the measurement problem of quantum theory). The important point is that the phase relations between different  $n$  are *delocalized* into the larger system and are no longer available at the system alone. Therefore the system *appears* to be in one of the states  $|n\rangle$ ,

formally described by the diagonalization of its density matrix,

$$\begin{aligned}
 \rho &= \sum_{n,m} c_m^* c_n |n\rangle \langle m| \\
 &\rightarrow \sum_{n,m} c_m^* c_n \langle \Phi_m | \Phi_n \rangle |n\rangle \langle m| \\
 &= \sum_n |c_n|^2 |n\rangle \langle n|,
 \end{aligned} \tag{18}$$

where the last line is valid if the pointer (or environmental) states are orthogonal,  $\langle \Phi_m | \Phi_n \rangle = 0$ .

Any measurement-like interaction will therefore produce an apparent ensemble of system states. This process is now usually called “decoherence” [1]. Note that the origin of this effect is *not* a disturbance of the system. Quite to the contrary: the system states  $|n\rangle$  remain unchanged, but they “disturb” (change) the environment!

## 5. Strong Decoherence of a Two-State System

As a first application of the von-Neumann measurement model let us look at an explicit scheme for a two-state system with Hamiltonian

$$\begin{aligned}
 H &= H_0 + H_{\text{int}} \\
 &= V(|1\rangle \langle 2| + |2\rangle \langle 1|) + E|2\rangle \langle 2| \\
 &\quad + \gamma \hat{p}(|1\rangle \langle 1| - |2\rangle \langle 2|).
 \end{aligned} \tag{19}$$

The momentum operator  $\hat{p}$  in  $H_{\text{int}}$  (last line) leads to a shift of a pointer wavefunction  $\Phi(x)$  “to the right” or “to the left”, depending on the state of the measured system,  $\gamma$  represents a measure of the strength of this interaction. Because of the special structure of the Hamiltonian this interaction is recoil-free. This model can be solved exactly and shows the expected damped oscillations. In view of the Zeno effect we are mostly interested in the limit of strong coupling. Here the solutions (calculated in perturbation theory) show two interesting features, as displayed in Figs. 4 and 5 [3]. First, the transition probability from  $|1\rangle$  to  $|2\rangle$  depends in a complicated way on the coupling strength, but for large coupling it always decreases with increasing interaction. This is the expected Zeno behavior.

If we look at the time dependence of the transition probability, we see the quadratic behavior for very small times (as is required by the general theorem Equ. (2)), but soon the transition probability grows linearly, as in an exponentially decaying system (the rate, however, depends on the coupling strength).

A realization of the quantum Zeno effect has been achieved in an experiment [4] where the two-state system is represented in the form of an atomic transition, while the measurement process is realized by coupling to a third state which emits fluorescence radiation, see. Fig. 6.

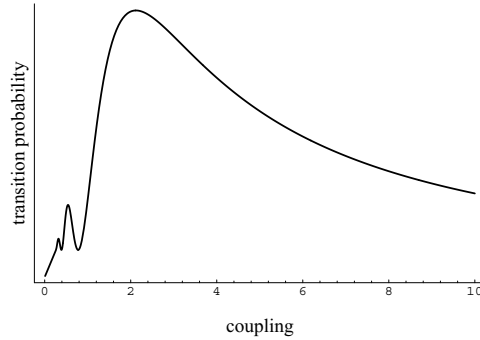


FIGURE 4. Transition probability as a function of the coupling strength in a two-state model. For strong coupling, transitions are always damped (Zeno effect).

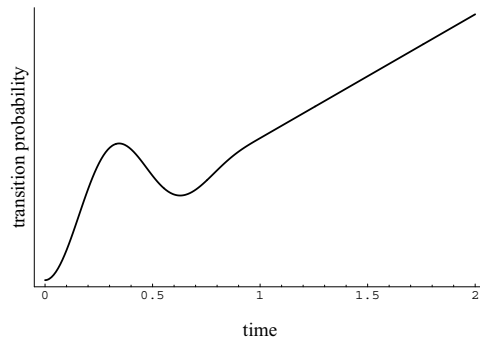


FIGURE 5. Transition probability as a function of time. If the measurement can be considered complete (here at  $t \approx 1$ ), the transition probability grows linearly (constant transition rates)

The Zeno effect also shows up in a curious way in a recent proposal of “interaction-free measurement”.

Early ideas about “negative result” or “interaction-free” measurements [5] can be combined with the Zeno mechanism [6]. One of these schemes is exemplified in Fig. 7. If a horizontally polarized photon is sent through  $N$  polarization rotators (or repeatedly through the same one), each of which rotates the polarization by an angle  $\Delta\Theta = \frac{\pi}{2N}$ , the photon ends up with vertical polarization. In this case the probability to find horizontal polarization would be zero,

$$P_H = 0. \quad (20)$$

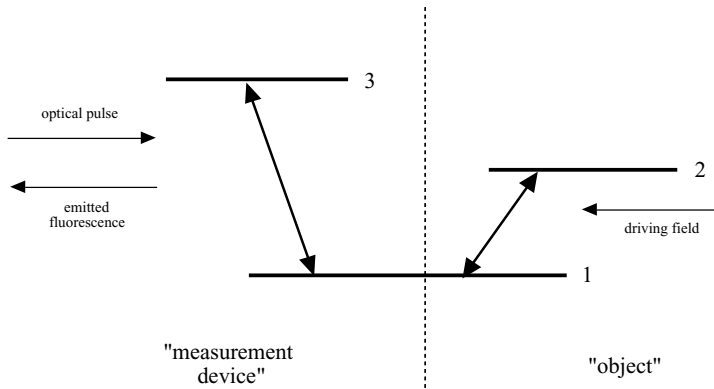


FIGURE 6. Zeno experiment in atomic physics [4]. The two-state system under repeated observation is represented by a transition between states  $|1\rangle$  and  $|2\rangle$ . Measurement is accomplished through an optical pulse leading to fluorescence from level  $|3\rangle$  if the state  $|1\rangle$  is present.

If this evolution is interrupted by a horizontal polarizer (absorber) the probability of transmission is (similar to Eqs. (6) and (7)) given by

$$P'_H = \cos^{2N} \Delta\Theta = \cos^{2N} \frac{\pi}{2N} \approx 1 - \frac{\pi^2}{4N} \longrightarrow 1. \quad (21)$$

To implement this idea, a photon is injected into the setup shown in Fig. 7 and goes  $N$  times through the rectangular path, as indicated. The initial polarization is rotated at R by an angle  $\Delta\Theta = \frac{\pi}{2N}$  on each passage. In the absence of the absorbing object, the polarizing beam splitters, making up a Mach-Zehnder interferometer, are adjusted to have no effect. That is, the vertical component V is coherently recombined with the horizontal one (H) at the second beamsplitter to reproduce the rotated state of polarization. If, however, the “bomb” is present, the vertical component is absorbed at each step. After  $N$  cycles, the photon is now still horizontally polarized, thereby indicating the presence of the object with probability near one, or has been absorbed (with arbitrarily small probability). For details of experimental setups see [7].

One should be aware of the fact that the term “interaction-free” is seriously misleading since the Zeno mechanism is a consequence of *strong* interaction. Part of this conceptual confusion is related to the classical particle pictures often used in the interpretation of interference experiments, in particular “negative-result measurements”.



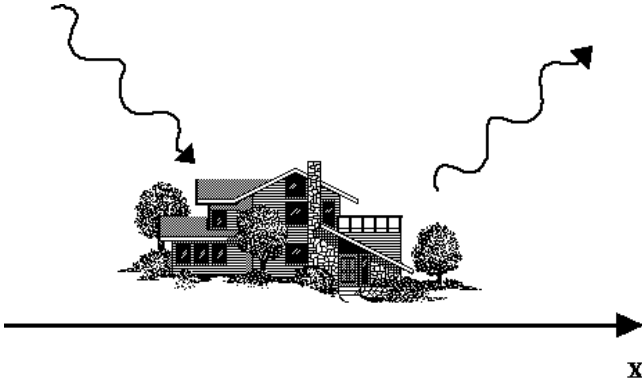


FIGURE 8. Macroscopic objects can never be considered as isolated from their natural environment. Irreversible scattering processes lead to ever-increasing entanglement.

extreme situations, for example, a dust particle scattering only cosmic background radiation. For small distances, interference is damped according to

$$\rho(x, x', t) = \rho(x, x', 0) \exp[-\Lambda t(x - x')^2] \quad (22)$$

with a “localization rate”  $\Lambda$  given by

$$\Lambda = \frac{k^2 N v \sigma_{eff}}{V}. \quad (23)$$

Here  $k$  is the wave vector of the scattered particle,  $Nv/V$  the incoming flux and  $\sigma_{eff}$  of the order of the total cross section. Some typical numbers are shown in the table.

The above equations are valid in the limit of small wavelengths,  $k|x - x'| \ll 1$ , comprising the effect of many individually ineffective scattering processes. The typical decoherence timescale according to Equ. (22) is  $t_{dec} \approx \frac{1}{\Lambda|x - x'|^2}$ . In the opposite limit  $k|x - x'| \gg 1$ , already a single scattering event destroys coherence. The decoherence timescale is then given by the scattering rate (that is,  $t_{dec} \approx \frac{V}{Nv\sigma_{tot}} \approx \frac{k^2}{\Lambda}$ ). A quantitative test of the quantum theory of spatial decoherence ([9], [10]) has been achieved in interference experiments with large molecules [11].

The equation of motion of, say, a dust particle, is then no longer the von Neumann-Schrödinger equation, but contains an additional scattering term (compare Equ. (22)),

$$i \frac{\partial \rho(x, x', t)}{\partial t} = \frac{1}{2m} \left( \frac{\partial^2}{\partial x'^2} - \frac{\partial^2}{\partial x^2} \right) \rho - i\Lambda(x - x')^2 \rho. \quad (24)$$

If one analyzes the solutions of this equation, one finds that, for example, the Ehrenfest theorems for mean position and momentum are still valid: The motion

	$a = 10^{-3}$ cm dust particle	$a = 10^{-5}$ cm dust particle	$a = 10^{-6}$ cm large molecule
Cosmic background radiation	$10^6$	$10^{-6}$	$10^{-12}$
300 K photons	$10^{19}$	$10^{12}$	$10^6$
Sunlight (on earth)	$10^{21}$	$10^{17}$	$10^{13}$
Air molecules	$10^{36}$	$10^{32}$	$10^{30}$
Laboratory vacuum ( $10^6$ particles/cm <sup>3</sup> )	$10^{23}$	$10^{19}$	$10^{17}$

TABLE 1. Localization rate  $\Lambda$  in  $\text{cm}^{-2}\text{s}^{-1}$  for three sizes of “dust particles” and various types of scattering processes according to (23). This quantity measures how fast interference between different positions disappears for distances smaller than the wavelength of the scattered particles, following Equ. (22). For large distances, decoherence rates are just given by scattering rates, and are thus independent of  $x - x'$ .

is *not* damped, although coherence between different positions is destroyed. There is no Zeno effect.

The above equation of motion is a special case of more general equations which are studied under the topic “Quantum Brownian Motion”. In addition to decoherence, these models include friction effects. A simple example is [12]

$$\begin{aligned}
 i\frac{\partial\rho(x, x', t)}{\partial t} &= \left[ \frac{1}{2m} \left( \frac{\partial^2}{\partial x'^2} - \frac{\partial^2}{\partial x^2} \right) \right. \\
 &\quad \left. - i\Lambda(x - x')^2 \right. \\
 &\quad \left. + i\frac{\gamma}{2}(x - x') \left( \frac{\partial}{\partial x'} - \frac{\partial}{\partial x} \right) \right] \rho(x, x', t) \quad (25)
 \end{aligned}$$

where

$$\Lambda = m\gamma k_B T. \quad (26)$$

This model represents the environment as a bath of harmonic oscillators (with temperature  $T$ ), coupled to the mass point under consideration. The three lines in Equ. (24) describe free motion, decoherence, and friction (damping constant  $\gamma$ ), respectively.

In typical macroscopic situations, decoherence is much more important than friction. The ratio of decoherence to relaxation rate can be estimated as

$$\frac{\text{decoherence rate}}{\text{relaxation rate}} \approx mk_B T (\Delta x)^2 = \left( \frac{\Delta x}{\lambda_{th}} \right)^2, \quad (27)$$

where  $\lambda_{th}$  is the thermal deBroglie wavelength of the macroscopic body. This ratio has the enormous value of about  $10^{40}$  for a macroscopic situation ( $m=1$  g,  $\Delta x = 1$  cm) [13].

We can conclude from these models that

- Newton’s reversible laws of motion can be derived (to a very good approximation) from strong *irreversible* decoherence.
- The appearance of classical objects has its origin in low-entropy condition in the early universe and the unique features of quantum nonlocality.
- Decoherence works *much* faster than friction in macroscopic situations.
- Although coherence is strongly suppressed, no Zeno effect (slowing down of motion) appears.

## 6.2. Rate equations

The exponential decay law  $P(t) = \exp(-\lambda t)$  mentioned at the beginning is a special case of a general rate equation with transition rates  $A_{\alpha\beta}$ ,

$$\frac{d}{dt}P_\alpha = \sum_\beta A_{\alpha\beta}P_\beta = \sum_{\beta \neq \alpha} (A_{\alpha\beta}P_\beta - A_{\beta\alpha}P_\alpha). \quad (28)$$

Its quantum analogue, describing the dynamics of “occupation probabilities” is usually called the “Pauli equation”,

$$\frac{d}{dt}\rho_{\alpha\alpha} = \sum_\beta A_{\alpha\beta}\rho_{\beta\beta}. \quad (29)$$

An obvious feature of (29) is that interference terms do not play any dynamical role. On the other hand, this cannot be true exactly, since then the von Neumann equation would lead to Zeno freezing,

$$\frac{d}{dt}\rho_{\alpha\alpha} = \sum_\beta (H_{\alpha\beta}\rho_{\beta\alpha} - \rho_{\alpha\beta}H_{\beta\alpha}) \equiv 0. \quad (30)$$

To further analyze these matters let us assume that the properties  $\alpha$  in the rate equation are macroscopic in the sense that they are *continuously observed by the environment*. The microscopic characterization is in the following assumed to be given entirely by energy, further degeneracies are neglected for simplicity. The macroscopic feature  $\alpha$  is measured by a “pointer” as in the two-state Zeno model above, see Fig. 9. The Hamiltonian then reads [3]

$$\begin{aligned} H &= \sum_{\alpha E} E |\alpha E\rangle \langle \alpha E| + \sum_{\alpha E \neq \alpha' E'} V_{\alpha E, \alpha' E'} |\alpha E\rangle \langle \alpha' E'| \\ &+ \sum_{\alpha E} \gamma(\alpha) \hat{p} |\alpha E\rangle \langle \alpha E|. \end{aligned} \quad (31)$$

As in the previous two-state model, the last line represents the (recoil-free) coupling to the “pointer”.

Since we are interested in the limit of strong coupling to the pointer, we calculate the transition probability from property  $\alpha_0$  to another one,  $\alpha$ , in lowest order perturbation theory. Starting from

$$|\Psi(0)\rangle = |\alpha_0 E_0\rangle |\Phi\rangle, \quad (32)$$

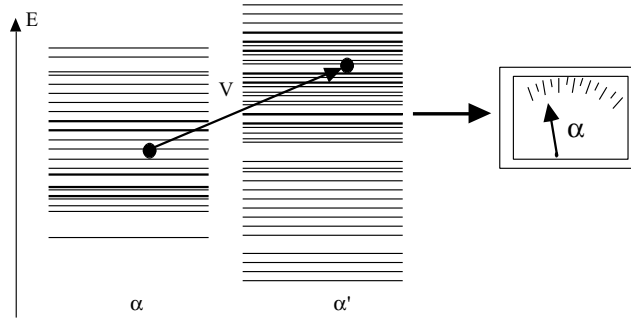


FIGURE 9. Transitions between groups of states are monitored by a pointer. The symbolic measurement device in the figure represents the interaction with the environment (which may or may not contain an experimental setup). Transition probabilities often follow Fermi's Golden rule (rates governed by transition matrix elements  $V$  and level densities at resonance energy), but may be influenced by the presence of the environment monitoring certain features  $\alpha$  of initial or final states.

where  $\Phi$  is the pointer state, the transition probability is

$$P_{\alpha E} = 4 \int dp |V_{\alpha E, \alpha_0 E_0}|^2 |\Phi(p)|^2 \frac{\sin^2(E - E_0 + \gamma(\alpha)p)t/2}{(E - E_0 + \gamma(\alpha)p)^2} \quad (33)$$

(assuming  $\gamma(\alpha_0) = 0$  for simplicity). This expression shows a familiar resonance factor, but now we have new resonances for each value of  $p$  with weight  $|\Phi(p)|^2$ , shifted from  $E = E_0$  to a new value  $E = E_0 - \gamma(\alpha)p$ . Summing over many states with property  $\alpha$  gives

$$P_{\alpha} \approx 2\pi t \int dE \frac{\sigma_{\alpha}(E) |V_{\alpha E, \alpha_0 E_0}|^2}{\gamma(\alpha)} \left| \Phi \left( \frac{E - E_0}{\gamma(\alpha)} \right) \right|^2. \quad (34)$$

Three limiting cases can be extracted from this expression (see also Fig. 10).

- Case 1: *Zeno limit*: For large coupling  $\gamma(\alpha)$  we have

$$P_{\alpha} \approx \frac{2\pi t}{\gamma(\alpha)} \int dE \sigma |V|^2(E) |\Phi(0)|^2 \sim \frac{1}{\gamma(\alpha)}. \quad (35)$$

Transitions are suppressed as expected.

- Case 2: *Golden Rule limit*: For small coupling, transition rates become independent of  $\gamma$  and the usual result is recovered,

$$P_{\alpha} = 2\pi t \sigma_{\alpha}(E_0) |V(E_0)|^2. \quad (36)$$

- Case 3: *“Anti-Zeno effect”*: If the contributions from each transition are comparable, that is, if  $\sigma |V|^2 \approx \text{const.}$  in the relevant interval  $[E_{\min}, E_{\max}]$  then it is easy to see that we have a smooth transition from the Zeno region to

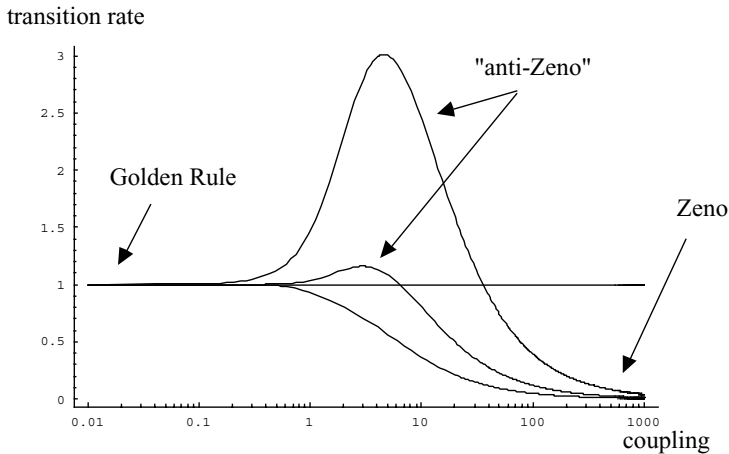


FIGURE 10. Continuous coupling to a pointer changes the transition rate from an initial state  $|\alpha_0 E_0\rangle$  to a group of final states in various ways. For small coupling we find the standard Golden rule result (here normalized to unity). Increasing the coupling to the measuring agent may in some cases increase the transition probability by shifting the effective resonance frequency to regions with higher level density or larger transition matrix elements (anti-Zeno effect). Strong interaction always leads to decreasing transition rates (Zeno effect).

the Golden Rule limit. If this is not the case, it can happen that in the intermediate range transition probabilities are *enhanced* above the Golden rule value. This is occasionally called “anti-Zeno effect”.

## 7. Summary

We have seen that unitary evolution depends decisively on interference between components of the wave function. If phase relations are lost, evolution is hindered. This leads finally to the Zeno freezing of motion. No coherence, no motion.

The destruction of phase relations can be understood as phase *de-localization* arising from *unitary* quantum evolution, if the interaction of a system with its environment is taken into account. In this way, the Zeno effect can be completely understood as a dynamical effect. No collapse of the wave function is required, but only quantum nonlocality.

Many-state systems can escape Zeno freezing. This is important for the properties of our experienced macroscopic world, but also for common “quantum” features such as radioactive decay, which happens whether or not a counter is setup

to observe the decay. (In fact, in most cases Nature herself provides the necessary “counters”.)

Systems with only a few degrees of freedom are very sensitive to quantum entanglement and can therefore never escape the Zeno effect if they are interacting with other systems. Zeno freezing can thus be used to delineate the borderline between classical and quantum objects.

## References

- [1] E. Joos, H.D. Zeh, C. Kiefer, D. Giulini, J. Kupsch, and I.-O. Stamatescu, *Decoherence and the Appearance of a Classical World in Quantum Theory*. 2<sup>nd</sup> edition (Springer, Berlin 2003).
- [2] B. Misra and E.C.G. Sudarshan, *Journal of Math. Phys.* **18** (1977), 756.
- [3] E. Joos, *Phys. Rev.* **D29** (1984), 1626.
- [4] W.M. Itano, D.J. Heinzen, J.J. Bollinger, and D.J. Wineland, *Phys. Rev.* **A41** (1990), 2295 .
- [5] A.C. Elitzur and L. Vaidman, *Found. Phys.* **23** (1993), 987 .
- [6] C.H. Bennett, *Nature* **371** (1994), 479 .
- [7] P.G. Kwiat, A.G. White, J.R. Mitchell, O. Nairz, G. Weihs, H. Weinfurter, and A. Zeilinger, *Phys. Rev. Lett.* **83** (1999), 4725 .
- [8] H.D. Zeh, *Found. Phys.* **1** (1970), 69.
- [9] E. Joos and H.D. Zeh, *Z. Phys.* **B59** (1985), 223.
- [10] K. Hornberger and E. Sipe, *Phys. Rev.* **A68** (2003), 012105.
- [11] L. Hackermüller, K. Hornberger, B. Brezger, A. Zeilinger and M. Arndt, *Nature* **427** (2004), 711.
- [12] A.O. Caldeira and A.J. Leggett, *Physica* **121A** (1983), 587.
- [13] W.H. Zurek in: *Frontiers in Nonequilibrium Statistical Physics*, ed. by G.T. Moore and M.T. Scully (Plenum, New York, 1986).

Erich Joos  
Rosenweg 2  
D-22869 Schenefeld  
Germany  
e-mail: [physics@erichjoos.de](mailto:physics@erichjoos.de)